Numerical Studies on Surplus Electrons in Polar Media.

By

Ian C. Carmichael

Submitted in the Autumn of 1974 in partial fulfilment of the requirements for the degree of Doctor of Philosophy.

Chemistry Department,
University of Glasgow,
GLASGOW G12 8QQ
Scotland.

ProQuest LLC.
789 East Eisenhower Parkway
P.O. Box 1346
Ann Arbor, MI 48106 – 1346

Abstract

Accurate numerical solutions of the polarized cavity and semicontinuum models for excess electrons in polar media are derived.

Part I presents the results of a numerical investigation of similar models for the surplus electron in crystalline solids. Here, the existence of a few analytical and numerical solutions affords an excellent check on the accuracy and efficiency of the presently-used finite-difference technique. In addition, the extent of amelioration produced in approximate variational treatments is disclosed. Some relevant theory is developed.

In Part II the numerical technique is used in a thorough-going study of polarized cavity and semicontinuum models, within both the adiabatic and scf formulations, for the excess single-electron species. The considerable improvements effected on existing one-parameter variational approaches is demonstrated and several results are called into question. In particular the scf treatment of the polarized cavity model for the hydrated electron is shown to be inadequate. This refutes a recent, variationally-based claim to the contrary. In the realm of semicontinuum theories it is shown that the presently used parameterizations do, on accurate solution, no longer give concurrence with experimental data. While this could be renewed for any given observation by a more appropriate selection of variables, deviations will generally remain in the other predictions. It is shown to be unlikely that transitions to higher excited states contribute much to the observed band width, which the present treatments based on a single 1s - 2p transition badly underestimate.

Localized dielectron species form the subject of Part III. The numerical solution technique is carried through on similar levels of approximation in an attempt to resolve recent contradictory statements

as to the dissociative stability of the ammoniated dielectron made by the alternative formulations of the semicontinuum model. The disparity remains. The introduction of a second solvation shell is effected in an attempt to reduce the computational differences of the models used, but to no avail. The adiabatic treatment prefers two singly-solvated species while an scf scheme favours a trapped dielectron. Absorption at doubly-charged sites is shown to be of doubtful importance in the observed spectrum.

Clearly some major alterations in the present models are necessary.

The contradiction has now been removed. More recent calculations have revealed that, within the semicontinuum model, the adiabatic approximation also favours stable dielectrons.

Acknowledgments

I am grateful to the members of the Theoretical group at Glasgow for their many assistances. In particular, I thank Brian Webster for his initiation of this study and his continued inspiration and Ronald Stewart for an introduction to the power of the numerical method. I am greatly indebted to Barbara who preared the bulk of the manuscript.

I thank the Science Research Council for three years of financial support.

Table of Contents.

SUMMARY of the thesis, "Numerical Studies on Surplus Electrons in Polar Media", submitted by Ian C. Carmichael as partial fulfilment of the requirements for the degree of Doctor of Philosophy.

To date theoretical investigations into the structure and properties of localized surplus electron states in polar media have proceeded in terms of models, which necessarily approximate, usually somewhat crudely, an inherently complex reality. In evaluating the worth of such models, it is important to determine to what extent the essential physical content of the situation has been included. This is answered by a comparison of the derived model predictions with a body of experimental data.

One crucial difficulty has been overlooked. In the development of the theory of excess electrons in polar liquids, ices and glasses, the properties of the simple model potentials postulated have, generally, only been obtained in an approximate manner. Thus, one must also how accurately the solution technique reflects the properties of the model. This, for the most part, has been neglected.

In the present work this latter question is obviated. An accurate finite-difference method has been employed to determine the exact predictions of the simple theories, currently fashionable in the above field. Several hopefully established results are thus challenged.

In Part I, the accuracy and efficiency of the present numerical solution technique is thoroughly tested in the related field of colour centres in crystalline solids. Here, the existence of exact analytical, accurate numerical and variational

solution of models on a similar approximation level provides an excellent area of comparison. Some relevant theory is also developed.

In Part II the numerical technique is used in an extensive study of both polarized cavity and semicontinuum models, within both the adiabatic and self-consistent field formulations, for the excess single-electron species. A considerable improvement effected on existing one-parameter variational approaches is demonstrated and several results are called into question. In particular the scf treatment of the polarized cavity model for the hydrtaed electron is shown to be inadequate. This refutes a recent, variationally-based claim to the contrary. In the realm of semicontinuum theories it is shown that the presently used parameterizations do, on accurate solution, no longer give concurrence with experimental data. While this could be renewed for any given observation by a more appropriate selection of variables, deviations will generally remain in the other predictions. It is demonstrated to be unlikely that transitions to higher excited states contribute significantly to the observed band-width, which the present treatments, based on a single 1s-2p transition, badly underestimate.

Localized dielectron species form the subject of Part III. The numerical solution technique is carried through on similar levels of approximation in an attempt to resolve recent contradictory statements as to the dissociative stability of the ammoniated dielectron made by the alternative formulations of the semicontinuum model. The disparity remains. The introduction of a second solvation shell is effected in an attempt to reduce the computational differences of the models employed, but to no avail. The adiabatic treatment prefers two separate singly-solvated

species, while an scf scheme favours the trapped dielectron. Absorption at doubly-charged sites is shown to be of doubtful importance in the observed spectrum. Clearly some major alterations in the current models are necessary.

PART I

Surplus Electrons in Crystalline Solids.

SECTION 1

Introduction.

a) A great many studies, both experimental and theoretical, performed with the intention of elucidating the structure and properties of colour centres have involved an investigation of the F-centre in alkali halides.

The quite spectacular colouration of crystals containing F-centres obviously provided some incentive for the early experimental work. The alkali halides have occupied a very fundamental position throughout the development of the theory of solids and the F-centre, comprising an electron trapped at a negative-ion vacancy, is perhaps the simplest strong-force imperfection occuring in these crystals; hence the attractiveness to the theoretician.

By far the majority of the data discussed here derive from this prototype colour centre. Attention is almost exclusively devoted to the computation of the associated optical properties, to the complete neglect of magnetic effects. The latter, however, are recognized as being of the utmost importance in determining the detailed structure of such centres, particularly through the techniques of electron-paramagnetic and electron-nuclear double resonance spectroscopy. Indeed the final confirmation of the now accepted model of the F-centre, mooted by de Boer[52], as long ago as 1937, was obtained by the endor experiments of Feher[51]. However, the models considered here are inherently unsuitable for the computation of such quantities as are required for the prediction of magnetic resonance results.

The presence of F-centres is evidenced by a strong, broad, bell-shaped absorption band in the visible region, the perfect alkali

halides possessing such a wide band-gap as to be conveniently transparent in this spectral domain. Typically, the bands are a few tenths of an eV wide and are peaked somewhere between two and five eV. Data from Gebhardt and Kuhnert[24] for KBr give the absorption peak as $E(a) = 2.06$ eV at a temperature of 4K and a full-width at half-maximum of $W(a) = 0.16$ eV. Increasing the temperature broadens the band and causes a red shift of the peak position without any marked change in the total oscillator strength. An even broader emission band, considerably Stokes shifted, is also observed. In KBr, again at 4K it has a width $W(e) = 0.22$ eV and a maximum at $E(e) = 1.14$ eV. It is affected by temperature in a similar fashion. One perplexing observation is the length of the luminescent lifetime of the excited state involved in this band, being about two orders of magnitude longer than that in analogous transitions in isolated atomic systems.

The photoconductivity threshold associated with the F-band occurs in KBr at 4K around $I_T = 2.2$ eV [53] and in addition to optical ionization processes, thermal activation energies of $\varepsilon_t(0) = 1.8$ eV and $\varepsilon_t(1) = 0.13$ eV for the ground and relaxed excited state respectively have been measured in this salt.

These then are the characteristic properties which the models outlined in the subsequent sections have attempted to reproduce.

b) Choice of Models.

From amongst the plethora of conceptual approaches previously employed in efforts to elucidate the electronic structure of colour-centres, two were selected for detailed study. They will be termed the polarized cavity model and, its refinement, the semicontinuum model. In the literature of the field the latter term has usually been used to encompass both descriptions. It has been reserved here, however, for models which involve to some extent, a consideration of the discrete structure of the bulk medium.

Similar levels of approximation pervade theoretical attempts to understand the structure of excess electron states in non-crystalline media, which form the bulk of this work. The above choice, therefore, allowed experience to be gained in handling the characteristic computational techniques and, more importantly, provided many simple model potentials where the effectiveness of a numerical method of solution could be essayed against extant variational ones. In addition a few analytical solutions of such problems have been achieved, which permitted direct corroboration of numerical results.

Before discussing these models, several essential preliminaries must be presented.

c) The Born-Oppenheimer Approximation.

In this section a justification for the adiabatic separation of the nuclear lattice motion from that of the bound electrons is presented in a form suitable for the later attempted separation of the electron coordinates of the surplus species.

Consider a crystalline medium. If $\underline{R}_I$ denotes the set of nuclear coordinates and $\underline{r}_i$ those of the electrons, the total crystal Hamiltonian may be written as

$$H_T = T_I + T_i + V(\underline{R}_I, \underline{r}_i), \tag{1}$$

where T_I is the kinetic energy operator for all the nuclei, T_i is the same for the electrons and V represents the potential energy of their interactions.

If the nuclei are held fixed at $\underline{R}$, the corresponding Hamiltonian becomes

$$H^o = T_i + V(\underline{R}, \underline{r}_i) \ . \tag{2}$$

Assuming the eigenvalues, $E_n(R)$, and the eigenfunctions, $u_{n,\underline{R}}(r)$, where n represents the set of electronic quantum numbers, of the related Schrodinger equation

$$H^o \, u_{n,\underline{R}}(\underline{r}) = E_n(\underline{R}) \, u_{n,\underline{R}}(\underline{r}) \tag{3}$$

are known, then a solution of the Schrodinger equation for the total crystal,

$$H_T \, W_N(\underline{R}, \underline{r}) = E_N \, W_N(\underline{R}, \underline{r}) \tag{4}$$

may be sought in the form

$$W_N(\underline{R}, \underline{r}) = \sum_n U_{nN}(\underline{R}) \, u_{n,\underline{R}}(\underline{r}) \ , \tag{5}$$

where N represents the set of nuclear quantum numbers.

If the $\underline{R}$-dependence of $u_{n,\underline{R}}$ is weak, Seitz[1] has shown that the nuclear functions approximately satisfy

$$\left[T_I + E_n(\underline{R})\right] U_{nN}(\underline{R}) = E_N \, U_{nN}(\underline{R}) \tag{6}$$

which is the goal of the present derivation. However, to prepare the

way for subsequent developments, a different approach is presented here.

Expanding W as indicated in (5) and substituting in the total Schrodinger (4) yields

$$(T_I + H^o)\, \Sigma_n U_{nN}(\underline{R})\, u_{n,\underline{R}}(\underline{r}) = E_N\, \Sigma_n U_{nN}(\underline{R})\, u_{n,\underline{R}}(\underline{r}). \qquad (7)$$

Multiplying from the left by one of the u's, $u_{m,\underline{R}}(\underline{r})$ say, integrating over the electronic coordinates $\underline{r}$ and noting the orthonormality of the u's results in

$$\int u_{m,\underline{R}}(\underline{r})\, T_I\, \Sigma_n U_{nN}(\underline{R})\, u_{n,\underline{R}}(\underline{r})\, d\underline{r} + (E_n(\underline{R}) - E_N)\, U_{mN}(\underline{R}) = 0. \qquad (8)$$

The first term involves the operator T_I which is (9), the sum being over all 3J nuclear coordinates

$$T_I = \Sigma_J h^2 \,/\, 2M_J\, \nabla_J^2 \,. \qquad (9)$$

This term may be written

$$\int u_{m,\underline{R}}(\underline{r})\, \Sigma_{n,J} h^2 \,/\, 2M_J \Big[2\, \nabla_J u_{n,\underline{R}}(\underline{r}) \cdot \nabla_J U_{nN}(\underline{R}) + U_{nN}(\underline{R})\, \nabla_J^2\, u_{n,\underline{R}}(\underline{r}) + u_{n,\underline{R}}(\underline{r})\, \nabla_J^2\, U_{nN}(\underline{R})\, d\underline{r}. \Big]$$

Replacing $p_J = -ih\, \nabla_J$ the momentum operator reduces this to

$$T_I\, U_{nN}(\underline{R}) + \Sigma_{n,J}\ \ 1/M_J\, (A_{mn}^{J}\, p_J + B_{mn}^{JJ})\ \ U_{nN}(\underline{R}) \,,$$

where

$$A_{mn}^{J} = \int u_{m,\underline{R}}(\underline{r})\, p_J\, u_{n,\underline{R}}(\underline{r})\, d\underline{r}$$

and

$$B_{mn}^{JJ} = \tfrac{1}{2} \int u_{m,\underline{R}}(\underline{r})\, p_J \cdot p_J\, u_{n,\underline{R}}(\underline{r})\, d\underline{r} \,.$$

When n = m

$$A_{mm}^{J} = -i/2\ d/dr_J \int u_{m,\underline{R}}^2(\underline{r})\, d\underline{r}$$

which, since the u's can be normalized to unity for each value of $\underline{R}$, is equal to zero. Similarly

$$B_{mm}^{JJ} = \tfrac{1}{2} \int (du_{m,\underline{R}}(\underline{r}) \,/\, dr_J)^2\, d\underline{r}$$

which must be either equal or greater than zero.

The equation of motion of the nuclei is finally

$$(T_I + V_m(\underline{R}) - E_N)\, U_{mN}(\underline{R}) = -\Sigma (n \neq m)\, C_{mn} U_{mN}(\underline{R}) \qquad (10)$$

where

$$V_m(\underline{R}) = E_m(\underline{R}) + \Sigma_J \, 1/M_J \, B^{JJ}_{mm}$$

which is the effective potential for nuclear motion, and

$$C_{mn} = \Sigma_J \, 1/M_J \, (A^J_{mn} \, P_J + B^{JJ}_{mn}) \, .$$

The adiabatic or Born-Oppenheimer approximation asserts that since M_J is a nuclear mass, the RHS of (10) may be neglected leaving, as before,

$$(T_I + E_m(\underline{R}) - E_N) \, U_{mN} = 0 \, . \qquad (11)$$

The nuclei, then, respond only to the average position of the electrons, depending only on the eigenstate u. These electronic states depend adiabatically, through $E_n(\underline{R})$, on the lattice motion.

Having effectively uncoupled the electronic motion from the lattice vibrations, there still remains a many-electron problem. Attempts to reduce this further to a one-electron problem must be in the direction of accurately separating the motion of the excess, comparatively weakly-bound electrons from that of those tightly held in the ion-cores. Assuming these ion-cores are unpolarizable and treating both the trapped and core electrons on an equal basis by allowing each to respond only to the average coulomb field of the other forms the Hartree approximation. Introducing specific exchange interactions among the electrons yields the Hartree-Fock method, which will now be discussed

d) The Hartree-Fock Approximation.

The Hartree-Fock (HF) electronic Hamiltonian is

$$H_{HF} = \Sigma_i f_i + \tfrac{1}{2} \Sigma_{i,j} g_{ij}$$

where

$$f_i = -\tfrac{1}{2}\nabla_i^2 - \Sigma_N Z_N / r_i \ ,$$

the sum being over all the nuclei, and

$$g_{ij} = |\underline{r}_i - \underline{r}_j|^{-1} \qquad i \neq j$$
$$0 \qquad i = j$$

The corresponding eigenfunction is taken to be an antisymmetrized product

$$U(r_1 \ldots . r_{c+t}) = \left[(c+t)!\right]^{-\frac{1}{2}} \Sigma_P (-1)^P \underline{P}\ u_1(1)\ u_2(2) \ldots . u_{c+t}(c+t)$$

where $u_i(j)$ is the i^{th} one-electron orbital occupied by the j^{th} electron c is the number of core electrons, t of those trapped and $\underline{P}$ is the usual antisymmetrizer.

Substitution of this form of wave-function into the appropriate Schrodinger equation and minimizing the eigenvalue with respect to variations in the single particle functions, u, while constraining these to be orthonormal results in the Hartree-Fock equations for each u_i ;

$$f_i\ u_i + \Sigma_j \left[(u_j|g_{ij}|u_j)u_i(i) - (u_j|g_{ij}|u_i)U_j(i)\right] = E_i\ u_i(i) \ .$$

To solve these, even for the perfect crystal, recourse has to be made to several drastic assumptions.

The ion-core orbitals are assumed unaffected by the presence of the vacancy and the electron. These functions are then replaced by the free-ion orbitals x_i, between which all overlaps are neglected. The interaction of a core-electron with nuclei other than its "parent" is approximated by the Madelung energy leading to

$$f_1\ u_1(1) + \Sigma_j \left[(x_j|g_{1j}|x_j)u_1(1) - (x_j|g_{1j}|u_1)x_j(1)\right] = E_1\ u_1(1)$$

for the equation of motion of an excess electron. Unfortunately it is computationally difficult to enforce the core-electrons to experience

the average field of the trapped particles, since the excited free-ion orbitals, due to their spatial extent, certainly do not provide good representations of those in even the perfect crystal. However a simple model system reveals how the HF treatment describes these polarization effects.

Consider a crystal represented as a continuous medium, characterized by high and low frequency permittivities k_{op} and k_{st} respectively, in which there is one spherically symmetric trapping centre. The potential of an electron at the centre is a sum of the trapping potential, $V(r)$, and that due to the polarization of the surrounding medium. The periodic potential produced by the ion-cores is assumed eliminated by the effective mass approximation discussed below. Since $V(r)$ is assumed constant in time, it contributes an amount, E_v, to the radial component of the field acting on the electron, considered as a test-charge mapping the field, which is diminished by the static polarization of the medium;

$$E_v(r) = -k_{st}^{-1}\, dV(r) / dr \qquad (12)$$

If the charge distribution of the electron, represented by a radial wave-function $P_i(r)$, normalized such that $\int P_i^2(r)\, dr = 1$, is described by $p(r) = \int_0^r P_i^2(s)\, ds$, then it contributes an amount

$$E_p(r) = -p(r) / k_{st}\, r^2 + p(r) / r^2 \qquad (13)$$

to this component of the field. The latter term is included since the instantaneous field experienced by the electron is being sought and since the core-electrons respond only to its average position. The total potential experienced by the excess electron in the HF approach is

$$V_{HF}(r) = -k_{st}^{-1}\, V(r) - \delta f_i(r) \qquad (14)$$

where $\delta = (1 - k_{st}^{-1})$ and $f_i(r) = Y_o(i,i;r) / r$. The Y_k's having been previously defined by Hartree[2] as

$$Y_k(i,i;r) = r^{-k} \int_0^r P_i(s)\, P_j(s)\, s^k\, ds + r^{k+1} \int_r^\infty P_i(s)\, P_j(s)\, s^{-k-1}\, ds$$

Written in this way, (14) conceals the fact that the polarization potential comprises two distinct components viz.

$$\delta f_i(r) = \beta f_i(r) + \gamma f_i(r)$$

where $\beta = (k_{op}^{-1} - k_{st}^{-1})$ and $\gamma = (1 - k_{op}^{-1})$. The first is due to inertial ion-displacement polarization and the second, to optical, core-electronic polarization. It is important that the latter contribution is state-dependent, responding instantly to changes in the excess electron wavefunction.

If the motion, characterized by an angular frequency w, of the trapped electron sets up a field

$$E_t = E_o + E_1 \exp(iwt) + \exp(-iwt) \qquad (15)$$

at the ion-cores, then it will produce a polarization[3] proportional to

$$1/(w_c + w) + 1/(w_c - w) . \qquad (16)$$

When discussing ion-displacement polarization hw_c corresponds to the energy of a quantum of vibrational motion. w_c is therefore much smaller than w, which implies that only the first term of (15) is important and that the ions experience the average field of the excess electron. If optical polarization is sought, comparison of a typical band-gap for crystalline insulators, ($\sim$ 10 eV) with a typical binding energy for an additional electron ($\sim$ 3 eV) suggests that perhaps w may be neglected with respect to w_c. This allows the bound core-electrons to respond to the instantaneous position of the trapped species and generates the quasi-adiabatic (QA) approximation. A return to the HF approach may also be effected by neglecting the second term of (16) since w_c and w are both large and very little polarization will be produced.

Clearly cognizance of the difference in response times of these polarization effects, which forms the basis of the low and high frequency dielectric functions measured in the bulk crystal, will be of prime importance in investigating the energy level structure of a colour centre.

e) The Quasi-Adiabatic Approximation.

The development of the QA approach may be carried through identically to that of the Born-Oppenheimer approximation previously discussed, the trapped electron coordinates replacing those of the nuclei, with one important difference.

In the RHS of (10), M_j, previously a large nuclear mass, thus this term can not be immediately discarded. An indirect justification of its neglect may, however, be attempted.[4] M_j is an electronic mass.

When the excess electron is outwith the ion-core, $u_{n,\underline{R}}(\underline{r})$ (the core-electron function) will remain more or less orthogonal to $u_{m,\underline{R}'}(\underline{r})$ assuming that the ions are not very polarizable. The integral

$$I = \int u_{m,\underline{R}}(\underline{r})\, u_{n,\underline{R}'}(\underline{r})\, d\underline{r}$$

will vanish if $\underline{R} = \underline{R}'$ of course, but if $\underline{R} \neq \underline{R}'$ it may be expanded in a power series in $(\underline{R} - \underline{R}')$ giving, for the first few terms

$$I = \int u_{m,\underline{R}}(\underline{r})\, d\underline{r} + i \Sigma_a (\underline{R}'-\underline{R})_a A^a_{mn} - \Sigma_{b,a} (\underline{R}'-\underline{R})_b\, (\underline{R}'-\underline{R})_a\, B^{ab}_{mn} \qquad (17)$$

where A and B are as previously defined. The first term of (17) vanishes as stated above and if it is accepted that I is small, since u will only respond slightly to changes in the instantaneous position of the excess electron, then the remainder of the RHS of (17) may be set equal to zero reducing the equation of motion of the trapped electron to

$$(T_I + E_n(\underline{R}) - E_T)\, U_{nN}(\underline{R}) = 0$$

where T_I is now the kinetic energy operator of the excess electron, $\underline{R}$ forms a set of its coordinates and N are the associated quantum numbers. While this may be plausible well outside the ion-cores it will certainly break down in the vicinity of a nucleus. Three major considerations invalidate the reduction in this area. Firstly since $B^{aa}_{mn} \neq 0$, $V_m(\underline{R})$ can not generally be replaced by $E_n(\underline{R})$ and similarly $C_{mn}(n \neq m)$ cannot be neglected. Lastly exchange interactions between the trapped and core electrons, which have been neglected in setting up the trial wave func-

tion W (no antisymmetry included) are bound to be extremely important.

Again employing the simple model used to illustrate the HF potential experienced by the trapped electron

$$E_v(r) = -k_{st}^{-1}\, dV(r) / dr$$

as before, but,

$$E_p(r) = -p(r) / k_{st}\, r^2 - p(r) / k_{op}\, r^2 \qquad (18)$$

the latter term accounting for the following of the motion of the trapped electron by those of the ion-cores.

The total potential acting on the electron is

$$V_{QA}(r) = -k_{st}^{-1}\, V(r) - \beta f_r(r) \qquad (19)$$

Note that f_r must be computed from the relaxed state function, no matter the electronic configuration under consideration; making this a state-independent potential. Since the polarization term approaches $-\beta / r$ for large r then, until relaxation of the nuclear configuration takes place, the QA potential (19) will support an infinity of bound states[5].

f) The Effective - Mass Formalism.

Consider a perfect crystal of volume V containing N unit cells. Assuming, for simplicity, one atom per unit cell, Bloch functions, b^o, may be developed such that

$$b^o_n(\underline{k},\underline{r}) = \exp(i\underline{k}\cdot\underline{r})\, u_{n,k}(\underline{r})$$

where u is periodic in the direct lattice, satisfy

$$H_T\, b^o_n(\underline{k},\underline{r}) = E_n(\underline{k})\, b^o_n(\underline{k},\underline{r}) \qquad (21)$$

for each energy band, n. H_T is again the perfect crystal Hamiltonian. The b^o's form a complete set provided one sums over n and $\underline{k}$; thus

$$\int b^o_n(\underline{k},\underline{r})\, b^o_{n'}(\underline{k}',\underline{r})\, d\underline{r} = \delta_{nn'}\, \delta_{kk'}$$

where the integration is over the crystal volume.

Localized functions, the Wannier functions, a^o, may be defined as the fourier transforms of these Bloch functions

$$a^o_n(\underline{r}-\underline{s}) = N^{-\frac{1}{2}} \Sigma_{\underline{k}} \exp(-i\underline{k}\cdot\underline{s})\, b^o_n(\underline{k},\underline{r}) \qquad (22)$$

where $\underline{s}$ is the position vector of the atom in the s^{th} unit cell. This Wannier function is localized on the s^{th} cell since its components, through the exponential term, add constructively in the cell but interfere elsewhere. The relation (22) may, of course, be inverted to give

$$b^o_n(\underline{k},\underline{r}) = N^{-\frac{1}{2}} \Sigma_{\underline{s}} \exp(i\underline{k}\cdot\underline{s})\, a^o_n(\underline{r}-\underline{s})$$

and the Wannier functions may similarly be shown to form a complete orthonormal set, provided one sums over all bands, n; thus

$$\int a^o_n(\underline{r}-\underline{s})\, a^o_{n'}(\underline{r}-\underline{s}')\, d\underline{r} = \delta_{nn'}\, \delta_{ss'}$$

where the integral is over V.

The Wannier functions are not eigenfunctions of the crystal Hamiltonian since

$$\begin{aligned} H_T\, a^o_n(\underline{r}-\underline{s}) &= N^{-\frac{1}{2}} \Sigma_{\underline{k}} \exp(-i\underline{k}\cdot\underline{s})\, E_n(\underline{k})\, b^o_n(\underline{k},\underline{r}) \\ &= N^{-1} \Sigma_{\underline{k},\underline{s}'} E_n(\underline{k}) \exp\left[i\underline{k}\cdot(\underline{s}'-\underline{s})\right] a_n(\underline{r}-\underline{s}') \\ &= \Sigma_{\underline{s}'} A_n(\underline{s}'-\underline{s})\, a^o_n(\underline{r}-\underline{s}') , \end{aligned} \qquad (23)$$

but they may be expanded in terms of the other functions from the same band, the coefficients in the expansion, the A's being the fourier trans-

form of the band energy

$$A_n(\underline{s}-\underline{s}') = N^{-1} \Sigma_{\underline{k}} E_n(\underline{k}) \exp\left[i\underline{k}\cdot(\underline{s}-\underline{s}')\right]$$
$$= \int a_n^o(\underline{r}-\underline{s})\, H_r\, a_n^o(\underline{r}-\underline{s}')\, d\underline{r} \qquad (24)$$

The relation (24) may also be inverted to give

$$E_n(\underline{k}) = \Sigma_{\underline{s}} A_n(\underline{s}) \exp(-i\underline{k}\cdot\underline{s}) \qquad (25)$$

Colour centres, however, do not exist in perfect crystals. A localized perturbation $V^P(\underline{r})$ must be introduced into the crystal destroying the periodicity. The perturbed Hamiltonian is

$$H^P = H_T + V^P(\underline{r})$$

and Bloch-like eigenfunctions may be developed such that

$$H^P\, b_n(\underline{l},\underline{r}) = E_n(\underline{l})\, b_n(\underline{l},\underline{r}) \qquad (26)$$

where $\underline{l}$ is now an intraband quantum number. Since the b^o's and a^o's form complete sets they may be used to provide an expansion for the perturbed eigenfunction, e.g.

$$b_n(\underline{l},\underline{r}) = \Sigma_m \Sigma_{\underline{s}} F_{nm}(\underline{l},\underline{s})\, a_m^o(\underline{r}-\underline{s}) \qquad (27)$$

provided, again, this is a many-band expansion.

The first step in evaluating the coefficents F_{nm} is to substitute the expansion (27) into the non-periodic Hamiltonian (26), multiply through from the left by $a_{m'}^o(\underline{r}-\underline{t})$ and integrate over the crystal value. This yields

$$\Sigma_m \Sigma_s \left[A_{m'}(\underline{t}-\underline{s})\, \delta_{m',m} + V^P_{m',m}(\underline{t},\underline{s})\right] F_{nm}(\underline{l},\underline{s}) = E_n(\underline{l})\, F_{nm}(\underline{l},\underline{t}) \qquad (28)$$

where

$$V^P_{m',m}(\underline{t},\underline{s}) = \int a_{m'}^o(\underline{r}-\underline{t})\, V^P(\underline{r})\, a_m^o(\underline{r}-\underline{s})\, d\underline{r}$$

is the matrix element of the perturbing potential. This represents an N x N set of coupled difference equations for the coefficients, F, and is the Koster-Slater[6] method for determining the wave-functions in non-periodic systems.

These difference equations in the discrete functions $F(\underline{s})$ may be converted into differential equations for the continuous functions $F(\underline{r})$, ($\underline{r}$ represents an arbitrary vector in direct space while

$\underline{s}$, $\underline{t}$ are position vectors of cells in the direct lattice). To see this first consider the operator $\exp(-i\underline{t}\ \ )$ operating on some arbitrary function $x(\underline{r})$

$$\exp(-i\underline{t}\cdot\nabla)\, x(\underline{r}) = x(\underline{r}) - \underline{t}\cdot\nabla x(\underline{r}) + \tfrac{1}{2}(\underline{t}\cdot\nabla)\,(\underline{t}\cdot\nabla x(\underline{r})) + \ldots.$$

which is simply the Taylor series of expansion for $x(\underline{r}-\underline{t})$. Thus the operator is equivalent to a translation operator and

$$\exp(-i\underline{t}\cdot\nabla)\, x(\underline{r}) = x(\underline{r}-\underline{t}) \qquad (29)$$

Consider also the first term of the difference equations (28) namely

$$\Sigma_{m,\underline{s}} A_{m'}(\underline{t}-\underline{s})\, \delta_{m',m}\, F_{nm'}(\underline{l},\underline{s})$$

Setting $\underline{s}' = \underline{t}-\underline{s}$ and including the delta function gives

$$\begin{aligned}
&\Sigma_{\underline{s}'} A_{m'}(\underline{s}')\, F_{nm'}(\underline{l},\underline{t}-\underline{s}') \\
&= \Sigma_{\underline{s}'} A_{m'}(\underline{s}')\, \exp(-\underline{s}'\cdot\nabla)\, F_{nm'}(\underline{l},\underline{t}) \\
&= \Sigma_{\underline{s}'} A_{m'}(\underline{s}')\, \exp(-s'\cdot\nabla)\, F_{nm'}(\underline{l},\underline{r})_{\underline{t}}
\end{aligned}$$

The function $F(\underline{t})$ has been replaced by the continuous function $F(\underline{r})$ such that $F(\underline{t}) = F(\underline{r})$ when $\underline{r} = \underline{t}$. Finally replacing the sum over the A's by its fourier transform

$$= E_{m'}(-i\nabla)\, F_{nm'}(\underline{l},\underline{r})$$

where the quasi-momentum $\underline{k}$ has been formally replaced by the operator $-i\nabla$. This transforms the difference equations (28) into

$$E_{m'}(-i\nabla)\, F_{nm'}(\underline{l},\underline{r}) + \Sigma_{m,\underline{s}} V^{p}_{m',m}(\underline{t},\underline{s})\, F_{nm}(\underline{l},\underline{r}) = E_n(\underline{l})\, F_{nm'}(\underline{l},\underline{r}) \qquad (30)$$

A rigorous solution of these equations requires the knowledge of the a^{o}_{n}'s of all bands which enter into the expansion (27) of b, the generalized Bloch function. In addition one must know the variation with $\underline{k}$ of the energy of all these bands. Clearly approximations must be resorted to.

In the colour centre problems dealt with in this work, the perturbation is a negative ion vacancy. At a distance of several lattice-spacings from this vacancy, in the so-called one-band region, the following approximation may be expected to be justifiable

$$V^{P}_{m',m}(\underline{t},\underline{s}) = V^{P}(\underline{r})\,\delta_{mm'}\,\delta_{\underline{t},\underline{s}} \qquad (31)$$

resulting in a differential equation for the F's

$$E_m(-i\nabla) + V^{P}(\underline{r})\;F_{nm}(\underline{l},\underline{r}) = E_n(\underline{l})\;F_{nm}(\underline{l},\underline{r}). \qquad (32)$$

The perturbation $V^{P}(\underline{r})$, with its origin at $\underline{r} = \underline{t}$ being, at such distance from $\underline{t}$, too weak to induce interband transition. Thus the generalized Bloch function (27), which is an eigenfunction of the perturbed Hamiltonian may be written simply as

$$b_n(\underline{l},\underline{r}) = \Sigma_{\underline{s}} F_{nm}(\underline{l},\underline{s})\; a^{o}_{m}(\underline{r}-\underline{s}), \qquad (33)$$

a one-band expansion.

Markham[7], who analyzes the problem in a manner similar to this presentation, following Smith[8], now reduces the operator $E(-i\;\;)$ to a simple form by considering an expansion of $E_m(\underline{k})$ about a local turning point, $\underline{k}_m$, in $\underline{k}$-space: viz.

$$E_m(\underline{k}) = E_m(\underline{k}_m) + \tfrac{1}{2}\Big[\nabla_{\underline{k}}\cdot\nabla_{\underline{k}}E_m(\underline{k})\Big]_{\underline{k}_m}(\underline{k}-\underline{k}_m)^2 + \ldots.$$

Substitution of this into the differential equation (32) leads to a "Schrodinger" type equation for the F's with the electronic mass replaced by a tensorial effective mass, m*, given by

$$(m^*)^{-1} = h^{-2}\;\nabla_{\underline{k}}\cdot\nabla_{\underline{k}}E_m(\underline{k})$$

The amplitude function, F, may be replaced by a normalized function, f, given by

$$f_{nm}(\underline{l},\underline{r}) = (V\,/\,N)^{\frac{1}{2}}\;F_{nm}(\underline{l},\underline{r})\;\exp(-i\underline{k}_m\,\underline{r})$$

such that the expansion (32) is

$$\begin{aligned} b_n(\underline{l},\underline{r}) &= (N\,/\,V)^{\frac{1}{2}}\;\Sigma_{\underline{s}} f_{nm}(\underline{l},\underline{r})\;\exp(i\underline{k}_m\cdot\underline{r})\;a^{o}_{m}(\underline{r}-\underline{s}) \\ &= (N\,/\,V)^{\frac{1}{2}}\;\Sigma_{\underline{k}} g_{nm}(\underline{l},\underline{k})\;b^{o}_{m}(\underline{k},\underline{r}) \qquad (34) \end{aligned}$$

where $$g_{nm}(\underline{l},\underline{k}) = N^{-\frac{1}{2}}\;\Sigma_{\underline{s}}\exp\Big[i(\underline{k}_m-\underline{k})\cdot\underline{s}\Big]\;f_{nm}(\underline{l},\underline{s})$$

which may be inverted to give

$$f_{nm}(\underline{l},\underline{r}) = N^{-\frac{1}{2}}\;\Sigma_{\underline{k}} g_{nm}(\underline{l},\underline{k})\Big[\exp\,-i(\underline{k}_m-\underline{k})\cdot\underline{r}\Big]$$

where $f(\underline{r})$ is again the value of the function at $\underline{r} = \underline{s}$. If the main contribution to b_n comes from around $\underline{k} = \underline{k}_m$ then

$$b_n(\underline{l},\underline{r}) = V^{-\frac{1}{2}}\;b^{o}_{n}(\underline{k}_m,\underline{r})\;f_{nm}(\underline{l},\underline{r})\;. \qquad (35)$$

In this effective-mass approximation, then, the impurity wave-function may be written as a simple product of the Bloch function of the lowest point in the conduction band (the nearest local minimum) and the smooth "envelope" function $f(\underline{r})$. It will therefore be approximately orthogonal to the ion-core for large r since the Bloch functions are automatically orthogonal to such states and the envelope function will, in this region, be a slowly decaying function of r, approximately constant over the cones.

While the formalism provides a legitimate theory for shallow traps with extended electronic orbits it cannot be expected to handle the deep, sharply localized component of the potential associated with the missing ions in excess electron colour centre problems. The reduction of the potential (31) will be invalidated and one is forced to deal with the complete many-band expansion (27) for small r.

A more rigorous treatment of the deep trap problem is provided by the one-dimensional work of Kohn and Onffroy[9] who, using generalized Wannier functions $a_{n,\underline{s}}(\underline{r}-\underline{s})$, the subscripted $\underline{s}$ allowing the functions to vary from site to site, expand the generalized Bloch function

$$b_n(\underline{l},\underline{r}) = \sum_{\underline{s}} G_{nn}(\underline{l},\underline{s})\, a_{n,\underline{s}}(\underline{r}-\underline{s})$$

in a single band expansion, analogous to (27) for perfect crystals. The G_{nn} are no longer plane waves as were the F_{nm} and they will differ from band to band as suggested by the additional subscripted n.

They have shown that the functions a_n approach the same asymptotic limit as the a_n^o of the perfect crystal. In particular they need only differ from the a_n^o in the many-band region. This, coupled with the facts that the G_{nn} can be obtained from a similar set of difference equations to those occurring in the Koster-Slater method but involving rigorously only one band and that one need only know the $a_{n,\underline{s}}$ alone, (not necessarily the energy surface) makes this method,

when treated by the variational approach suggested by Kohn[10], much more attractive for a self-consistent solution of the deep trap problem, provided one can overcome the problems outlined by des Cloizeaux[11] in converting the asymptotic behaviour argument to three dimensions.

Alternatively one may use the Koster-Slater technique for large $\underline{r}$ by writing an effective Hamiltonian for the excess electron as

$$H = p^2 / 2m + \sum_{\underline{s}}{}' V_L(\underline{r}-\underline{s}) + V_P(\underline{r})$$

where the sum over the lattice potential excludes a contribution from the ion at the origin (since it's not there) and V_P describes the total polarization effects. Following Fowler[12] one adds $V_L(\underline{r})$ to this sum and replaces the result as

$$H_i = p^2 / 2m^* + V_P(\underline{r}) - V_L(\underline{r}) \qquad (36)$$

the introduction of the effective mass having removed the periodic potential. As before it is convenient to choose this as the (scalar) mass at the bottom of the conduction band.

For small $\underline{r}$ such an approach cannot be valid and attempts to allow for the breakdown of the effective mass approximation in this region lead to a consideration of polarized cavity models.

Section 2

Polarized Cavity Models.

a) Centred on the lattice site of the missing anion, of charge Z_o say, associated with the colour centre, a spherical void of radius R is introduced into the crystal.

Outwith this cavity the excess electron function, ψ_i, is assumed to be obtainable by the foregoing effective mass method, the potential due to the ionic defect decaying as $-Z_v e / 4\pi k_o k_e r$ for large r. $Z_v = -Z_o$ and k_e is an effective relative permittivity which accounts for the partial screening of the apparent vacancy charge by the presence of the electron and its polarization effects on the continuous medium. The Schrodinger equation is written in terms of m*, the (assumed scalar) effective mass at the bottom of the conduction band, and solved for the envelope function $f(\underline{r})$. This is then multiplied by the Bloch function associated with the conduction band minimum, as discussed above, to give ψ_i.

Inside the void ψ_i is obtained directly as a solution of a Schrodinger equation in which the true electronic mass appears and the eigenvalues of which are adjusted by an amount -X, X being the electron affinity of the crystal, to relocate the zero of energy at the lowest point of the conduction band rather than the vacuum zero. These solutions are then constrained to obey the quantum-mechanical continuity conditions across the fictitious cavity-crystal boundary.

Consider a charge of magnitude q distributed with spherical symmetry about the centre, O, of such a hole in a crystal. The bulk crystalline medium, extending from R to infinity is again characterized by high and low frequency relative permittivities k_{op} and k_{st} respectively.

At distances r, greater than R, the electric displacement $\underline{D}$ due to this charge distribution is

$$\underline{D}(\underline{r}) = (q / 4\pi r^3)\, \underline{r}$$

while the associated electric field is

$$\underline{E}(\underline{r}) = (q / 4\pi k_o\, k_r\, r^3)\, \underline{r} \qquad (37)$$

where k_o is the permittivity of free space and k_r is one of k_{op} or k_{st} as discussed below. Since the medium is proposed to be both linear and isotropic

$$\begin{aligned}\underline{P}(\underline{r}) &= \underline{D}(\underline{r}) - k_o\, \underline{E}(\underline{r}) \\ &= (1 - k_r^{-1})\, (q / 4\pi r^3)\, \underline{r}\end{aligned}$$

describes the polarization field which induces a surface charge distribution of

$$C_P = -P_r(R) = (1 - k_r^{-1})\, (q / 4\pi R^2)$$

on the walls of the cavity. $P_r(R)$ is the value of the radial component of the polarization at $\underline{r} = R$. This, in turn, produces a potential

$$V_P = -(1 - k_r^{-1})\, (q / 4\pi k_o\, R) \qquad (38)$$

at the centre of the cavity.

The total work required to bring a charge q from infinity into this cavity is therefore

$$\begin{aligned}W_P &= -\int_o^q (1 - k_r^{-1})\, (q / 4\pi k_o\, R)\, dq \\ &= \tfrac{1}{2}\, q^2\, (1 - k_r^{-1}) / 4\pi k_o\, R \qquad (39)\end{aligned}$$

provided the process is performed infinitely slowly (i.e. adiabatically). The colour centre comprises an electron trapped by an anionic vacancy. At the centre of this vacancy the potential experienced by this electron has two major components. Firstly, the Madelung term

$$V_M = Z_v\, a_M / 4\pi k_o\, a$$

where a_M is the Madelung constant of the crystal structure and a is the nearest neighbour distance in the perfect crystal. This represents the potential of all the other ions in the crystal regarded as unpolarizable point charges and provides the main contribution to the well depth; for

example, about 7 to 10 eV for F-centres in alkali halides. The ions are, however, not only polarizable, in that their core-electrons are capable of being distorted by the effective vacancy charge but also in the imperfect crystal they will suffer a displacement from their perfect lattice sites. One way to take this into account is the Jost cavity model[13] outline above, which leads (38) to a polarization potential of

$$V_P = -Z_v \left(1 - k_r^{-1}\right) / 4\pi k_o R_v \qquad (40)$$

at the centre of the hole of radius R_v assumed to be formed on the removal of the anion. The apposite values of k_r and R_v are given by the calculations of Mott and Littleton[14]. Holdings the ions fixed ($k_r = k_{op}$) Mott and Littleton find the field acting on the distant ions from (37) and calculate the induced dipole moment at each site. This induced moment contributes to the field acting on an ion neighbouring the vacancy and, along with that due to the polarizing charge and that due to moments similarly induced on the other nearest neighbour ions, provides an effective field polarizing the ion. The contribution from these nearest neighbours is then combined with the sum from all the other induced moments to give the total polarization potential at the centre of the vacancy. This value is set equal to (40) and a value of $R_v = R_{ML}$, the Mott-Littleton radius, determined. This rigid lattice work has been extended by Hunter, Rittner and du Pre[15], who list extensive accurate results involving as many as eight discrete layers surrounding the cavity.

The calculation becomes much more involved when the ions are allowed to move and Mott and Littleton give results only for NaCl where R_{ML} has been reduced from the rigid lattice value of .95a to .75a and the induced potential correspondingly increased from 3 to 6 eV. This indicates that the energies associated with ionic readjustments are of the correct order of magnitude to explain the Stokes shift observed

on emission; the value for the F-centre in NaCl being about 1.8 eV.[16]

b) Contributions to the Polarization.

The polarization potential should include contributions from the interaction of both the apparent stationary vacancy charge and the mobile electronic charge with the optical (i.e. core-electronic) distortions and the inertial (i.e. bulk-ionic) displacements. The effective fixed charge produces, through interaction with the optical polarization, a potential energy at the centre of the cavity of

$$W^v_{op}(0) = \gamma Z_v^2 / 4\pi k_o R_v \qquad (41)$$

and of $$W^v_{st}(0) = \beta Z_v^2 / 4\pi k_o R_v ,$$

via the inertial effect. The net vacancy-polarization energy is then

$$W^v_{pol}(0) = \delta Z_v^2 / 4\pi k_o R_v .$$

Outside the vacancy the polarization will screen the apparent charge resulting in

$$W^v(r) = -Z_v^2 / 4\pi k_o k_{st} r \qquad (42)$$

Treating the excess electron as a point charge and introducing it, by means of an infinitely slow process, into the cavity yields a contribution to the potential energy which may also be separated as

$$W^e_{op}(0) = -\tfrac{1}{2} e^2 \gamma / 4\pi k_o R_v \qquad (43)$$

and $$W^e_{st}(0) = -\tfrac{1}{2} e^2 \beta / 4\pi k_o R_v$$

Since the trapped electron charge distribution is not confined to the cavity a more careful calculation of these terms is necessary. The HF method discussed in Section 2c yields

$$W^e_{op}(0)_{HF} = -e^2 \gamma f_i(R_v) / 4\pi k_o \qquad (44)$$

$$W^e_{st}(0)_{HF} = -e^2 \beta f_r(R_v) / 4\pi k_o$$

f_r stands for the potential due to the relaxed state, i.e. that state in equilibrium with the nuclear configuration. f_i represents the contribution from the instantaneous electronic state. Within the QA approximation (Section 2.e) the optical component will provide no net potential energy; the medium electrons being able to respond to the instan-

taneous position of the surplus electron. Therefore,

$$W^{e}_{op}(0)_{QA} = 0 \ ,$$

while the inertial polarization remains identical to the HF value. Outside the cavity the HF and QA methods will yield modified coulomb tails identical to the electronic part of (14) and (19) respectively.

c) Fowler's Application of Haken's Theory.

An alternative approach has been distilled by Fowler[12] from Haken's theory of Wannier excitons. Fowler stresses that the nature of the potential outside the vacancy can best be represented by a spatially dependent relative permittivity, $k_e(r)$, such that

$$V(r) = -eZ_v / 4\pi k_o \, k_e(r) \, r \ , \qquad (45a)$$

where k_e varies between k_{op} and k_{st} depending on the compactness of the electronic state under consideration. Treating the anionic defect as a hole of infinite mass, the interaction with the excess electron is given, for large r, by

$$V(r) = -Z_v / 4\pi k_o \, k_{st} \, r + \tfrac{1}{2} Z_v \, \beta \, \exp(-vr) + \exp(-2r / a) \ / 4\pi k_o \qquad (45b)$$

where $v^2 = 2m^*w \ / h$ and w is the frequency of the longitudinal optical phonon for the crystal. Handling the self-energies of the vacancy and electron in a consistent manner requires the replacement of the second members of (41) and (43) by

$$V^v_{st}(0) = Z_v^2 \, \beta \, / 4\pi k_o \, a \qquad (46)$$

and

$$V^e_{st}(0) = -\tfrac{1}{2} e^2 \, \beta \, v \, / 4\pi k_o$$

respectively.

d) Potentials Investigated.

The simplest potential form investigated arises in the point-charge description (43) through the neglect of any inertial contribution. Making the further simplification of setting $R = a$, Zahrt and Lin[17] achieved an analytical solution of the radial Schrodinger equation derived from the resulting potential form

$$V(r) = \begin{cases} V_M + \tfrac{1}{2}\,\gamma\, Z_v / 4\pi k_o\, a - x & r < a \\ - Z_v / 4\pi k_o\, k_{op}\, r & r \geqslant a \end{cases} \qquad (47)$$

Markham[18] has suggested that the self-energy due to optical polarization should be augmented by a similar term representing the work necessary to remove the surplus electron from a void of radius R_e when it is assumed to be in the conduction band before localization. Setting $R_e = R_v$ (and reverting to $R_v = a$) yields the original potential utilized by Tibbs[19], namely

$$V(r) = \begin{cases} V_M + Z_v\,\gamma / 4\pi k_o\, R_v - X & r < R_v \\ - Z_v / 4\pi k_o\, k_{op}\, r & r \geqslant R_v \end{cases} \qquad (48)$$

However, such an energy term will be redundant in that this effect will already be included in any measurement of the electron affinity of the crystal.

Maintaining the artificial correction but omitting the electron affinity leads to the well treated variationally by Simpson[20]

$$V(r) = \begin{cases} V_M + Z_v\,\gamma / 4\pi k_o\, R_v & r < R_v \\ - Z_v / 4\pi k_o\, k_{st}\, r - \beta\, e\, f_r(r) / 4\pi k_o & r \geqslant R_v \end{cases} \qquad (49)$$

This approach reintroduces the energy due to inertial displacements at least outwith the cavity and, importantly, indicates the necessity of obtaining a solution self-consistent in the excess electron wave function in this region. Simpson's method, along with that of Zahrt and Lin, makes no mention of the effective mass approximation or of the necessity of solving two different Schrodinger equations, one on either side of the boundary.

Perhaps the most complete formulation of the polarized cavity model in these simple terms is found in the work of Krumhansl and Schwartz[21] as reported by Gourary and Adrian[4]. The inertial effects are reintroduced inside the cavity also and the self-energy of the electron with respect to the polarization is expressed in one of two forms. Working within the QA approximation leads to

$$V(r)_{QA} = V_M + \delta Z_v / 4\pi k_o R_v - \tfrac{1}{2}\gamma e / 4\pi k_o R_v - \beta e f_r(R_v) / 4\pi k_o - X \qquad r < R$$
$$-Z_v / 4\pi k_o k_{st} r - \beta e f_r(r) / 4\pi k_o \qquad r > R \,, \tag{50}$$

while the HF approach gives

$$V(r)_{HF} = V_M + \delta Z_v / 4\pi k_o R_v - \gamma e f_i(R_v) / 4\pi k_o) - \beta e f_r(R_v) / 4\pi k_o - X \qquad r < R$$
$$-Z_v / 4\pi k_o k_{st} r - \beta e f_r(r) /4\pi k_o \qquad r > R \,. \tag{51}$$

In this work, as in the original Tibbs potential, the lattice potential, V_L, is also included outside R_v and a solution in this region found in terms of a product of an envelope function and a Bloch function and the effective mass. However, it has been shown by Dexter[22] and Krumhansl[23] that the expectation value of any slowly varying function of r will be independent of the form of the Bloch function. A further approximation, assuming this function is constant by neglecting the rapid fluctuations near the nuclei, is therefore customary.

While previous workers, whose results are presented in the following section, have neglected some of the polarization terms, the components included, whether by way of the simple Mott-Littleton method or by the more refined Haken theory, by no means provide a rigorous description of the potential experienced by the surplus electron. Clearly a definitive theory of polarization effects within this cavity model has yet to be presented.

e) Results and Discussion.

An excellent check on the accuracy of the solutions derived by the present numerical technique is provided by a comparison with the results of Zahrt and Lin[17] using the simple potential form (47). Their analytical solution of the appropriate radial Schrodinger equation was achieved by matching the spherical Bessel functions $j_\lambda(\alpha r)$ of order λ and argument $\alpha = \left[2(E-V)\right]^{\frac{1}{2}}$ obtained within the cavity to the Whittaker functions, representing the solutions for $r>R$, at the cavity-crystal boundary. The derived energy levels for several alkali halide F- centres are listed, together with the necessary input data and the numerically obtained results, in Table I.1.

The values given by the numerical method differ only marginally from those of Zahrt and Lin; the 1s energy is 0.3% to 0.5% lower while the 2p energy improves by up to 0.8%. No systematic improvement on the analytical approach is expected and the slight discrepancies observed here are not supposed significant. They may be attributed to the different methods involved in defining the cavity radius.

Clearly the finite-difference scheme employed here is capable of reproducing the correct energy values to any required degree of accuracy. The calculated transition energies associated with this simple potential approach the peak value of the optical absorption band with remarkable consistency.

Considerably more interesting is the amelioration in the wave function expected, concomitant with a lowering of the energy level, when the numerical solutions are set beside those obtained by recourse to the variation theorem, particularly if the latter approach has employed inflexible one-parameter trial functions.

Simpson[20] has used just such a variational method to solve the Schrodinger equation incorporating the potential presented in (49). Selecting a void of radius 5.0 au to represent the F-centre in NaCl,

Simpson calculates a well depth of -.22 au. If the wave- functions of the two lowest electronic states are assumed to be representible by single exponentials i.e.

$$P_{1s}(r) = N_1 \; r \; \exp(-cr)$$

and

$$P_{2p}(r) = N_2 \; r^2 \; \exp(-dr), \qquad (52)$$

the N_i being normalization factors, this potential is seen to support a 1s level of about -3.0 eV and a 2p energy of -1.0 eV. It is important to notice that both these states are in equilibrium with the relaxed nuclear configuration of the bulk lattice, as are those derived numerically and listed for comparison in Table I.2. The 1s variational properties tabulated were secured using the rather more flexible trial function

$$P_{1s}'(r) = N_1' \; r \; (1+ar) \; \exp(-ar)$$

which, with an optimum value for a of 0.52 au^{-1}, produces a 7% improvement in the 1s energy. The numerical function is seen to afford a further 5% lowering of this energy.

Figure I.1 depicts these functions together with their 2p counterparts; the variational excited state function plotted has an exponent of d = 0.36 au^{-1}. The reason for the energy lowering is evident. The numerical 1s function is somewhat more compact, indicating that even the more flexible single- exponential wave- function does not provide a suitablerepresentation of the charge distribution in the vicinity of the relatively deep, flat- bottomed potential well. This important point will be further evidenced throughout this work. The 16% amelioration of the variational 2p energy may be ascribed to the same cause.

The optical excitation energy is derived by considering a "vertical" transition in that the potential tail is assumed to be governed by the inertial polarization created by the ground state

charge distribution for some time after excitation. Within the accuracy available to Simpson's method, he was unable to distinguish the energy of this unrelaxed excited state from that pertaining when the nuclei have adjusted to accommodate the 2p distribution. The vertically obtained state is computed here at -1.216 eV yielding a transition energy of 2.156 eV which is in reasonable agreement with the peak of the experimental absorption band at 2.770 eV[24]. The oscillator strength associated with the transition was calculated to be 0.938 by means of the dipole velocity formula (52).

For a transition between an initial state of energy E_i described by a wave-function ψ_i and a final state E_j, represented by ψ_j, with degeneracy g_j, the dipole velocity formulation of the oscillator strength is

$$f_{vel} = \tfrac{2}{3} h^2 g_j |E_j - E_i|^{-1} N_{ji}^2 \qquad (52)$$

where $N_{ji} = I / m + J / m^*$

and $I = \int \psi_j (-\partial/\partial z) \psi_i \, dv; r < R$

and J is the same integral over the volume enclosed by $R < r < \infty$. The dipole length form of the oscillator strength of this same transition is somewhat less sensitive to the precise nature of the wave functions and is

$$f_{len} = \tfrac{2}{3} h^{-2} g_j |E_j - E_i| M_{ji}^2 \qquad (53)$$

where $M_{ji} = mk + m^*L$

and $K = \int \psi_j(z) \psi_i \, dv$ for $r < R$ and L is again the value of this integral for $r > R$. A comparison of the values of f_{vel} and f_{len} computed from the electronic energies and wave functions as presented above affords a useful test as to how accurately the derived functions represent the exact solutions of the particular model Schrodinger equation under study. The closer the ratio $t = f_{vel} / f_{len}$ to unity, the better the approximate solutions.

The values displayed in Table I.3 indicate that the numerical

solutions approach the exact solutions very closely. The oscillator strengths associated with the variational solution of the cavity model have been calculated assuming that no significant change occurs in the excited state charge distribution on lattice relaxation as suggested by Simpson and borne out by the numerical wave-functions.

The medium polarization energy,U, is computed from

$$U = \tfrac{1}{2}\ \beta \int_R^\infty P_i(r)\ f_i(r)\ P_i(r)\ dr \qquad (54)$$

which has been corrected from Simpson's treatment (see e.g. Lehovec[25]). It represents the energy given up by the medium in the process of thermally removing the electron from the excited state. The value computed here, 0.668 eV, therefore places the thermal activation energy at .498 eV, much higher than the experimental value of .074eV in NaCl[26].

It is also interesting to examine the corresponding improvements obtained in a case where attempting to fit an exponential function to the true solution should result in no great error. Such is the interstitial ion model discussed by Simpson and procured from the foregoing potential by allowing the cavity to collapse to zero radius. As can be seen from Table I.2 a meagre energy increase of 2% occurs with the present technique and, as Figure I.2 shows, the numerical and single-exponential functions are quite similar. In agreement with these observations Simpson achieved no discernible amelioration in the 1s level on employing a double-exponential function;

$$P_{1s}(r) = N\left[\exp(-ar) + \exp(-br)\right]$$

to represent the ground state charge distribution. No data are presented in Table I.3 on the oscillator strengths in this model since Simpson has not calculated the energy of the 'vertical' 2p state. The numerical solution reveals that a substantial change in the 2p level -.620eV to -.448 eV accompanies lattice relaxation. It is, therefore, not possible to use the relaxed state exponent, .36 au^{-1} to describe the optically attained state. The numerical results presented, however, show that

again an excellent solution has been found.

An extensive investigation of the optical properties of F-centres in alkali halides, within the framework of Simpson's cavity model, has been carried through by Smith[27]. Table I.4 presents a few of his results for comparison with the corresponding values obtained in this work. It should be noted, however, that Smith's original variational 2p results were in error and those tabulated are due to R. Gilbert as quoted in Markham (see ref. 18, p. 321).

The numerical 1s energies show about a 2-3% improvement while a dramatic 14-16% lowering of the 2p levels occurs. This indicates the need for also introducing more flexibility into the trial function chosen to represent the 2p state of such comparatively deep, potential wells.

Again this method is seen to yield transition energies which are in substantial agreement with the experimental values. Krumhansl and Schwartz[21] have suggested an entirely different perturbation theory approach to the solution of Simpsom-type potentials. The problem they actually tackled was more complex in two respects. Firstly, while in the original Simpson model, only the walls of the potential well needed to be self-consistent with the excess electron wave-function, even in the adiabatic formulation of Krumhansl and Schwartz's potential (50) both the walls and the well depth must be determined self-consistently. In addition they reintroduced the effective mass approximation outwith the void and solved for an envelope function which was then multiplied by the usual Bloch function. For $r < R$ a zero-order problem is chosen which neglects the contribution to the potential which is wave-function dependent. This problem is solved analytically in terms of products of spherical Bessel functions with spherical harmonics in a similar fashion to the original work of Tibbs and also that of Zahrt and Lin

mentioned previously. For $r > R$ a more complicated choice of zero-order equation, together with the neglect of terms involving the radial derivative of the Bloch function and the constraint $m^* = m$ leads to a solution in the form of products of spherical harmonics with decaying exponentials. Matching these solutions and their derivatives at $r = R$ leads to an eigenvalue equation which is solved numerically to give the zero-order functions and energies. These energies are then corrected to account for the presence of the self-consistent terms by first-order perturbation theory.

A typical calculation for NaCl yields a zero-order energy $E_o(1s) = -4.10$ eV which is corrected to $E_1(1s) = -3.85$ eV and $E_o(2p) = -1.77$ eV which gives $E_1(2p) = -1.44$ eV as the energy correct to first order. Numerical calculations involving a similar potential expression result in a 1s energy of 64.04 eV and a transition energy of 2.45 eV with an oscillator strength of 0.98. Fowler[12] solved the same potential form variationally using trial functions $P_{1s}(r) = N_1\ r\ (1+ar)\ \exp(-ar)$ and $P_{2p}(r) = N_2\ r^2\ \exp(-br)$ which, with optimized exponents $a = .56au^{-1}$ and $b = .42au^{-1}$ gave a 1s level at -3.87 eV and a transition energy of 2.80 eV with a strength of around unity. One important difference in Fowler's treatment is the use of an effective mass of $m^* = 0.6\ m_e$. This, together with slight discrepancies in the values of the relative permittivities assumed, precludes the possibility of a direct comparison with the perturbation scheme. However a similarly parameterized model when solved numerically yielded $E(1s) = -4.02$ eV, an improvement of just under 4%, $E(2p) = -1.32$ eV, a much larger (15%) lowering and the functions compared in Figure I.3 with those obtained variationally. A more flexible representation of the 2p function is again obviously required.

It should also be noticed that this potential again supports energy levels, the transition between which offers a fair estimate of

the peak of the experimental absorption band. Clearly any model comprising a well of depth about the Madelung energy and of width about the nearest-neighbour spacing will yield a reasonable transition energy. The most naive and incomplete of the potentials studied, that of Zahrt and Lin, gives perhaps the most consistent overall fit of the computed to the observed absorption energies. This quantity certainly does not provide a sensitive test of a model's worth. The very existence of such a well-obeyed Mollwo-Ivey[28] plot for F-centres in absorption makes this assertion unsurprising.

Attempts to similarly correlate the emission energies to an inverse power of the nearest-neighbour spacing have largely failed.[16,29] It might therefore be inferred that a satisfactory description of the emission properties of colour centres would constitute a better criterion for model testing. None of the above models approach even a qualitative estimate of the emission energy. Zahrt and Lin's potential does not allow for lattice relaxation. Simpson's cavity model gives almost no change in the excited state function on relaxation. Krumhansl and Schwartz's approach predicts emission energies of 2.01 eV in NaCl and 1.89 eV in KCl which badly underestimate the observed Stokes shift.

In an endeavour to resolve this inadequacy, Fowler[12] has investigated the important suggestion that the electronic states involved in the transition might undergo marked changes on nuclear relaxation; in particular that the relaxed excited state may be extremely diffuse. The relaxation is expressed by allowing the nearest-neighbour ions to move radially and by adjusting the behaviour of the potential tail through the incorporation of an effective relative permittivity as in equation (45a). With a k_e of 4.2, a 10% outward motion of the adjacent cations and a concomitant 10% cavity expansion, Fowler predicts an emission energy of 1.24 eV in NaCl, the relaxed 2p state being only

f) Conclusion.

The polarized cavity models, in this limit, offer qualitative guidance on the effect of changes in such parameters as the well-depth, well-width, effective dielectric constant and effective mass. They are of limited assistance in indicating the direct expression of the physical content of the situation. Making the well-depth less negative, increasing k_e and decreasing m^* all allow percolation of the ground and excited state functions out into the medium.

These statements are illustrated in Table I.5 where the results are listed for the purely empirical potential

$$V(r) = V_o \qquad r < R$$
$$= -1 / 4\pi k_o k_e r \qquad r > R,$$

solved variationally by Smith and Spinolo[30] and numerically by Fowler, Calabrese and Smith[31] with parameters opposite to RbCl on absorption (cols. 1,3,5) and NaCl on emmission (cols. 4,5). The results derived by the present technique, also listed (cols. 3,5) are once again seen to be in excellent agreement with other accurate solutions.

Section 3

Semicontinuum Models.

a) The distinguishing feature of the semicontinuum models lies in their recognition of some extent of discrete structure in the bulk crystalline medium outside the void. Fowler's suggestion[12] of local lattice dilation on emission initiated work in this direction but it was left to Bennett[31] to carry through a calculation which predicted, by an energy minimization technique, the amount of distortion to be expected for a given charge distribution of the surplus electron.

By the usual appeal to the Born- Oppenheimer Approximation the single-particle Hamiltonian for the colour centre is split into a term determined by the excess electron coordinates, which depends parametrically on the nuclear displacements x_i from the perfect crystal equilibrium, and a term which is independent of the electronic coordinates and represents the lattice energy.

The absorption process at the colour centre is viewed as promotion of the trapped electron from a relaxed ground state described by a function $f_o^*(x_o)$, x_o being the lattice distortion necessary to accommodate this relaxed state, to a quasistationary state $f_1(x_o)$ which, by the assumption of a Franck- Condon principle, experiences the same crystal potential as the initial state. After a time, about 10^{-10} sec, considered long with respect to electronic processes, the nuclear framework adjusts to the excited state charge distribution which may now be expressed as $f_1^*(x_1)$. Again following Fowler f_1^* is assumed, in general, to differ substantially from the unrelaxed state f_1.

One possible mechanism of energy loss from this excited state $f_1^*(x_1)$ is radiative decay into an unrelaxed ground state represented by the function $f_o(x_1)$ with the emission process again constrained to

be vertical.

Bennett's formulation of these ideas within a semicontinuum theory involves potentials similar to those discussed in the polarized cavity problem with some modifications as presented in Section c.

There remains the task of computing the change in lattice energy due to the readjustments in the medium following the replacement of an anion by an electron.

b) The Medium Rearrangement Energy.

The ionic lattice is treated classically. If U_{ij} is the interaction energy between two ions of charge Z_i and Z_j respectively at a separation $r_{ij} = \underline{r}_i - \underline{r}_j$ then,

$$U_{ij} = Z_i Z_j / 4\pi k_o r_{ij} - C_{ij} / r_{ij}^6 - C_{ij} / r_{ij}^8 + X_{rep}(r_{ij}) \quad (55)$$

where C and C^1 are the van der Waals constants and x_{rep} represents the repulsive interactions. The van der Waals terms are small[32] and are ignored in Bennett's treatment. This leaves the lattice energy as a simple sum with an electrostatic contribution, E_e, and a repulsive part, E_r. Therefore

$$E_L = E_e + E_r$$

where $$E_e = (4\pi k_o)^{-1} \sum_{i,j}(i<j)\ Z_i Z_j \left| \underline{r}_i - \underline{r}_j \right|^{-1}$$

and $$E_r = \sum_{i,j}(i<j)\ x_{rep}(r_{ij})$$

Employing the empirical Born- Mayer exponential expression for the unknown form of the repulsive energy term gives

$$X_{rep}(r_{ij}) = b\ B_{ij}\ \exp(R_i / s)\ \exp(R_j / s)\ \exp(-r_{ij} / s)$$

where R_n is the radius of the n^{th} ion, B_{ij} is the Pauling factor for ions i and j and s is a "hardness parameter".[33] b may be determined by writing the cohesive energy, $\underline{E}$, of the crystal as

$$\underline{E}(\underline{r}) = \sum_{i,j}(i<j)\ U_{ij} + U_o$$

where U_o is the zero point energy, differentiating this with respect to r and setting the result at r=a, the perfect crystal spacing, equal to zero. Viz.

$$\left[\partial \underline{E}(r) / \partial r\right]_{r=a} = 0$$

Creating a vacancy of charge Z_v by removing the anion at $\underline{r}_o$ and allowing no subsequent displacement of the neighboring ions requires an energy

$$\Delta E_L = \Delta E_e + \Delta E_r$$

where $$\Delta E_e = Z_v \sum_{j \neq o} Z_j \left| \underline{r}_j \right|^{-1}$$

and $$\Delta E_r = -\sum_{j=o} X_{rep}(r_j)$$

The n nearest neighbour ions are then allowed to move radially to new sites $\underline{r}_i^1 = \underline{r}_i\ (1-x)$ for $1 < i < n$. The concommitant change in electrostatic lattice energy may be expressed as a sum of four terms. Firstly there is a change in electrostatic energy when a defect cation (i.e. a nearest neighbour ion) moves in the background of the perfect point-ion lattice potential

$$4\pi k_o\ \Delta E_a = n\ Z_1 \sum_{j\neq i} Z_j \left[|\underline{r}_1' - \underline{r}_j|^{-1} - |\underline{r}_1 - \underline{r}_j|^{-1} \right] \qquad (56)$$

Then there is the change in energy when one defect ion moves in the potential of the remaining n-1 defect ions

$$4\pi k_o\ \Delta E_b = -n\ Z_i \sum_{j\neq o,1}(j<n)\ Z_j \left[|\underline{r}_1' - \underline{r}_j|^{-1} - |\underline{r}_1' - \underline{r}_j|^{-1} \right] \qquad (57)$$

The effect of all n defect ions moving radially is given by

$$4\pi k_o\ \Delta E_c = \sum_{i\neq o}(i<n) \sum_{j\neq o}(j<n)\ (i<j)\ Z_i Z_j\ (|\underline{r}_i' - \underline{r}_j'| - |\underline{r}_i - \underline{r}_j|) \qquad (58)$$

Lastly there is an alteration in the interaction energy between the effective vacancy charge and the defect ions given by

$$4\pi k_o\ \Delta E_d = Z_v \sum_{j\neq o}(j<n)\ Z_j \left[|\underline{r}_j'|^{-1} - |\underline{r}_j|^{-1} \right] \qquad (59)$$

These terms are evaluated rigorously except for ΔE_a which involves an infinite summation. It is expanded in a power series in x

$$4\pi k_o\ \Delta E_a = -n / a\ (c_4 x^4 + c_6 x^6 + c_8 x^8 + \ldots) \qquad (60)$$

where the c_i are the lattice sums discussed in appendix B.

By considering the excess electron as a point charge Bennett has illustrated the necessity of including second nearest neighbours in the formulation of the repulsive interaction to prevent cavity collapse, at least in those crystals containing multiply charged vacancies. For consistency this incorporation is maintained in all the centres studied here. The total energy E_T, the sum of the medium rearrangement energy, E_L, and the electronic energy is plotted as a function of distortion, x, and the relaxed state is assumed sustained by a potential described by the distortion at this curve's minimum.

c) The Semicontinuum Potential.

The potential experienced by the electron in the semicontinuum treatment is constructed in a manner similar to that employed with the polarized cavity model. The one major difference lies in the amendment of the spherically symmetric portion of the point-ion potential from its former value, the Madelung energy, $V_o = V_M$, to

$$4\pi k_o V_o = -Z_v \left[a_M / a + \sum_i N_i Z_i \, x(i) / i\, a\, (1-x(i)) \right] \qquad (61)$$

where N_i is the number of ions of charge Z_i is the i^{th} shell centred on the vacancy, which are assumed to be displaced by an amount $x(i)$ from their perfect crystal positions. Only the first shell will be treated as discrete here, the summation then merely encompasses the cations adjacent to the defect.

Outside the well Fowler's extension of the Maken theory presented in equation (45b) is again used.

The five different semicontinuum models investigated by Bennett differ in their treatments of the polarization potential seen by the addition electron. Maintaining his amended notation[34] the SP(QA) model includes the inertial polarization as given by the Haken theory in equation (46), as does the model labelled SP(HF); they differ in their treatment of optical effects, the former includes Krumhansl and Schwartz's quasi-adiabatic potential (50), the latter the Hartree-Fock potential (51) of these authors.

Bennett has found "subtle difficulties" in calculating the bound states of such potentials. The major problem on absorption is a drastic overestimation of the ionic polarization developed during the transition through the use of the Haken theory. The relaxed ground state function may be assumed to be reasonably compact and any ionic polarization other than that treated explicitly in the motion of the nearest-neighbour ions must be negligible for a univalent defect. The electron distribution will almost completely shield the effective

charge outwith the first shell. This is contrary to the computational results.

To discuss the situation in multiply charged defects Bennett arbitrarily separates the total charge into an "uncompensated" component Z_v-e; i.e. the lowest possible value of the effective charge assuming complete shielding and a "compensated" contribution which is modified by the distribution of the surplus electron; i.e. ranges from zero for complete shielding to +e in the limit of an extremely diffuse trapped electron distribution. The Haken theory description of the external potential is scrapped but the use of an effective dielectric constant, k_e, is maintained. The uncompensated charge produces a potential due to ionic polarization of

$$V_{st,u}(r) = -\beta(Z_v-e) / 4\pi k_o r$$

and due to electronic polarization of

$$V_{op,u}(r) = -(Z_v-e) / 4\pi k_o k_e r.$$

The partially compensated charge produces a potential due to inertial effects of

$$V_{st,c}(r) = -e (k_e^{-1}-k_{op}^{-1}) / 4\pi k_o r$$

which is employed only for states involved in the emission process. For absorptive transitions, to resolve the above-mentioned difficulty, it is simply set equal to zero. Optical polarization effects of this part of the change are described by

$$V_{op,c}(r) = -e / 4\pi k_o k_{op} r.$$

Setting the inertial self-energy of the centre (vacancy plus electron) equal to zero, i.e. neglecting $V_{st}(r)$ for $r < R$, and incorporating the above alterations secures the models termed $SP(QA_1)$ and $SP(HF_1)$ depending on the description of the optical polarization inside the cavity.

One further modification was investigated by Bennett and involves the reintroduction of V_{st} within the cavity when considering

emission states only, in terms of the Haken theory and the inclusion of a functionally similar form of the potential due to electronic polarization, modelled after the work of Toyozawa.[35] Wood and Opik[36] have written this contribution as

$$U_{op}(r) = e\, Z_v \,/\, 4\pi k_o\, r\left[1 - \gamma\left\{1 - \tfrac{1}{2}\left(\exp(-R_e r) + \exp(-R_h r)\right)\right\}\right] \qquad (61)$$

for $r \quad R$. R_e and R_h are the radii of fictitious cavities associated with the electron and the vacancy respectively. Here $R_e = R_h = R_v$. The corresponding self-energy term within the cavity is

$$U_{op} = -\tfrac{1}{2}\gamma \,/\, 4\pi k_o\, R\,(Z_v^2 + e^2) \qquad (62)$$

Supplementing these with the terms due to the inertial effects estimated above leads to Bennett's $SP(ET_1)$ model. It is important that the value of X, the energy zero correction included inside the cavity, should not contain, in this model, the self-energy of the electron due to optical polarization. This would result in a double counting of this term since equation (62) is an attempt to allow for it.

d) The Lifetime of the Excited State.

In seeking a sensitive test of the model's worth the emission energies mooted previously unfortunately are also inadequate. Each of Bennett's models produces a sensible Stokes shift, as indeed do several other completely different formulations; e.g. the extended-ion approach of Wood[37] and the polaron model of Wang.[38]

The stimulating results obtained by Swank and Brown[39,26] which revealed the unexpectedly long radiative lifetime associated with F- centre luminescence provide an experimental measurement which should offer a satisfactory challenge to the theoretician. These values which were previously assumed to be about 10^{-8} seconds, as in atoms, turned out to be two orders of magnitudes longer. Before presenting the computational efforts directed towards the evaluation of this quantity it is necessary to digress to outline the theory of optical processes in solids.

These results are by no means an experimental artefact having been since reproduced by many workers (eg. Watts and Noble[4]) with completely different apparatus.

e) Optical Processes in Atoms and Solids.

Consider an isolated atom which is found in the state u_i of energy E_i with unit probability. Bombarding this atom with a monochromatic unpolarized beam of N photons per unit volume, each of energy E, is supposed to induce transitions to a level u_f, again considered a discrete solution of the time-independent Schrodinger equation for the atom, of energy E_f.

If only electric-dipole transitions are allowed and processes non-linear in N are neglected (i.e. a small photon flux is assumed) then the probability of an absorptive transition per unit time is

$$W_{if} = \left\{4\pi^2 e^2 / (4\pi k_o)\, 3\hbar\right\} E_{if}\, N \left|\underline{r}_{if}\right|^2 \delta(E_{if} - E) \qquad (63)$$

where the transition energy E_{if} is $E_f - E_i$ and the dipole matrix element $\underline{r}_{if} = \sum_e \int u_f^* \underline{r}_e u_i \, dv$, the summation being over all electrons. In general, the states i and f involved in the process may be degenerate when this element must be summed over the components of both states and divided by the initial state degeneracy.[40] This procedure will be assumed understood and the form presented above will be carried throughout the analysis for simplicity.

Associated with this probability there may be defined an absorption cross-section, S_{if}, which is the transition probability divided by the photon flux and integrated over the energy delta function to give

$$\begin{aligned} S_{if} &= \left\{4\pi^2 e^2 / (4\pi k_o)\, 3\hbar c\right\} E_{if} \left|\underline{r}_{if}\right|^2 \\ &= \left\{2\hbar\pi^2 e^2 / (4\pi k_o)\, mc\right\} f_{if} \end{aligned} \qquad (64)$$

on introducing the dimensionless oscillator strength f_{if} for the transition

$$f_{if} = (2m / 3\hbar^2)\, E_{if} \left|\underline{r}_{if}\right|^2$$

The radiation flux may also cause induced emission from the state u_f and this, the spontaneous emission also possible and the induced absorption already mentioned are most readily interrelated by the

Einstein A and B coefficients.

For induced absorption

$$B_{if} = \left\{ \pi e^2 / (4\pi k_o)\, m \right\} f_{if} / E_{if}$$

for spontaneous emission,

$$A_{if} = \left\{ 2e^2 / (4\pi k_o)\, mc^3\hbar^2 \right\} f_{fi}\, E_{fi}^2$$

and for induced emission,

$$B_{fi} = \left\{ \pi e^2 / (4\pi k_o)\, m \right\} f_{fi} / E_{if}$$

Since, for an isolated atom, $E_{if} = E_{fi}$ and $f_{if} = f_{fi}$ the following relationships hold.

$$B_{if} = B_{fi} \tag{65}$$

and

$$A_{fi} = (2E_{fi}^3 / \pi c^3\hbar^2)\, B_{fi} \tag{66}$$

The spontaneous emission coefficient, A, may be expressed as a reciprocal lifetime

$$A_{fi} = t_{fi}^{-1}$$

where the radiative lifetime of the excited state is

$$t_{fi} = \left\{ (4\pi k_o)\, mc^3\hbar^2 / 2e^2 \right\} E_{fi}^{-2}\, f_{fi}^{-1} \tag{67}$$

A simple relationship may be formed between this and the previously defined absorption cross-section

$$t_{fi}\, S_{if} = \hbar^3 \pi^2 c^2 / E_{fi}^2 \tag{68}$$

which, for strongly allowed transitions, with oscillator strengths of the order of unity, gives a lifetime of about 10^{-8} seconds.

Though the general theory of optical processes at a colour-centre in a solid may proceed along lines similar to those developed above, the various effects of the surrounding medium must be carefully considered.

The energy density of the radiation field will be reduced by a factor of $n^{-2}(E)$ where n is the refractive index of the crystal for a photon of energy E. The speed of light in the medium is reduced from its free-space value to $c / n(E)$. The electron field associated with

the radiation, which is the perturbation producing the observed absorption will, at the centre, be generally different from the average field in the medium E_o. Since the transition probability is proportional to the square of the local perturbation field this effect will produce a correction factor of $(E_e / E_o)^2$, the "squared- effective field" ratio (E_e is the effective field right at the centre). It is expected to vary from unity for a very diffuse centre to a value, roughly estimable by the Lorentz local field

$$E_e = \tfrac{1}{3} \left\{ n^2(E) + 2 \right\} E_o$$

for very compact centres. Fowler has estimated that, for the centres considered here, the ratio will generally lie between 1 and 2.

As evidenced by the Stokes shift, $E_{if} = E_{fi}$, the medium has a considerable effect on the centre and, in general, it cannot be expected that the dipole matrix elements for absorption and emission will be equal; i.e.

$$\underline{r}_{if} \neq \underline{r}_{fi}$$

More formally, the states involved in the transition will depend on (medium) nuclear as well as electronic coordinates. In the framework of the Born- Oppenheimer Approximation these states may be written as products of an electronic function $u_{n,\underline{R}}(\underline{r})$ and a nuclear wave function $U_{nN}(\underline{R})$, n and N representing sets of electronic and nuclear quantum numbers respectively; $\underline{r}$ and $\underline{R}$ representing the repective coordinates as previously.

Thus, labelling the initial state E_{iI} and assigning to the final state an energy of E_{fF} gives a transition energy

$$E_{iI,fF} = E_{fF} - E_{iI}$$

which has an oscillator strength of

$$f_{iI,fF} = (2m / 3\hbar^2)\, E_{iI,fF} \left| \underline{r}_{iI,fF} \right|^2$$

where

$$\underline{r}_{iI,fF} = \int u^*_{i,\underline{R}}(\underline{r})\, U^*_{iI}(\underline{R})\, \underline{r}\, u_{f,\underline{R}}(\underline{r})\, U_{fF}(R)\, d\underline{r}\, d\underline{R}$$

defining $\underline{r}_{if}(\underline{R})$ as $\int u^*_{i,\underline{R}}(\underline{r})\ \underline{r}\ u_{f,\underline{R}}(\underline{r})\ dr$ gives

$$\underline{r}_{iI,fF} = \int U^*_{iI}(\underline{R})\ U_{fF}(\underline{R})\ d\underline{R} \qquad (69)$$

In general, sharp transitions between such discrete states are not observed (except, for example, the zero-phonon lines). Instead experiment reveals a broad band which represents the sum of many such transitions. Following Lax[41] a thermal average over the initial nuclear states, I, is combined with a simple summation over the final vibrational states, F_1, to give a broad-band oscillator strength

$$f_{if} = \mathrm{av}_I \sum_F f_{iI,fF}$$

Assuming that the matrix element $\underline{r}_{if}(\underline{R})$ is largely independent of $\underline{R}$, so that it may be replaced by some average value at $\underline{R}_o$ say, the equilibrium nuclear configuration with no great error (the Condon approximation), then

$$f_{if} = (2m / 3\hbar^2)\ \underline{r}_{if}(\underline{R}_o)^2\ \mathrm{av}_I \sum_F E_{iI,fF}\ S(R)\ S(R')$$

where $$S(R) = \int U^*_{iI}(R)\ U_{fF}(R)\ d\underline{R}$$

If, in addition, the transition energy is replaced by some average value E_{if}, the average of the sum over the integrals involving the vibrational functions will collapse to unity and the oscillator strength will be given simply by

$$f_{if} = (2m / 3\hbar^2)\ E_{if}\ \underline{r}_{if}(\underline{R}_o)^2 \qquad (70)$$

for an absorption transition and may be written for on emission as

$$f_{fi} = (2m / 3\hbar^2)\ E_{fi}\ \underline{r}_{fi}(\underline{R}'_o)^2 \qquad (71)$$

As discussed in the introduction to this section the value of $\underline{R}_o$ employed for absorption (this value determines the crystal potential) is, in general, much different from that required to describe emissive processes. Thus, the relation between the Einstein emission coefficients, (65), may be generalized to

$$A_{fF,iI} = B_{fF,iI} \left\{ 2n^3(F) / \pi c^3 \hbar^2 \right\} E^3_{fF,iI}$$

which since $$C_{fi} = \mathrm{av}_I \sum_F C_{fF,iI}$$

where C is A or B, yields, on employing the above average energy,

$$A_{fi} = \left\{ 2n^3(E) \,/\, \pi c^3 \hbar^2 \right\} E_{fi}^3 \; B_{fi}, \qquad (72)$$

No relation between the induced coefficients as in (66) can be found.

The absorption cross-section is now expressed as

$$S_{if} = \left\{ E_e(a) \,/\, E_o \right\}^2 \left\{ 2\pi^2 \hbar e^2 \,/\, (4\pi k_o)\; mcn(E_{if}) \right\} f_{if}$$

and the luminescent lifetime of the excited state given by

$$t_{fi} = \left\{ E_o \,/\, E_e(e) \right\}^2 \left\{ (4\pi k_o)\; mc^3 \hbar^2 \,/\, 2e^2 n(E_{fi}) \right\} E_{fi}^{-2} \; f_{fi}^{-1}$$

where $E_e(a)$ and $E_e(e)$ are the effective fields experienced by the centre during absorption and emission respectively.

$$t_{fi} \; S_{fi} = \left\{ E_e(a) \,/\, E_e(e) \right\}^2 \left\{ \pi^2 \hbar^3 c^2 \,/\, n(E_{if})\; n(E_{fi}) \right\} f_{if} \; f_{fi}^{-1} \; E_{fi}^{-2} \qquad (73)$$

Defining $f' = f_{if} \; f_{fi}^{-1}$ and substituting reasonable values for the other parameters yields a radiative lifetime approximately given by

$$t_{fi} = 2f' \times 10^{-8} \text{ seconds} \qquad (74)$$

eg. for the F- centre in NaCl where $S_{if} = .91 \times 10^{-16}$ eVcm^2 assuming a squared-effective field ratio of 2.0 yields

$$t_{fi} = 2.36f' \times 10^{-8} \text{ seconds.}$$

f) Results and Discussion.

Table I.6 lists the input data required for computations within Bennett's semicontinuum models. In addition to the values presented in that table, a knowledge of the lattice sums given in Table 1 of Appendix B is necessary. The Pauling factors B_{ij} are given by the simple formula

$$B_{ij} = 1 + (Z_i / n_i) + (Z_j / n_j)$$

where z_i is the valency of the i^{th} ion which has n_i outer electrons. It should be remembered that the structure of CaF_2 differs from that of the other three crystals, a fact which is reflected in the change in Madelung constant required; for CaF_2 $a_M = 4.071$ while for the NaCl structure $a_M = 1.748$. Notice also that the value of a corresponds, in CaF_2, to the Ca - Ca distance.

The value of the effective dielectric constant to be used in emission calculations is obtained by assuming that the relaxed excited state is characterizable, within the effective mass approximation, as a shallow hydrogen- like level so that the thermal ionization energy of the excited state $\varepsilon_t(1)$ may be equated to the screened hydrogenic energy

$$\varepsilon_t(1) = -\tfrac{1}{2}\, m^* / n^2 k_e^2 ,$$

where n is the principal quantum number associated with that state.

The value of the effective mass in the conduction band, generally obtained experimentally, involves a contribution due to electron-ionic displacement polarization interactions which is not desired here. It is dependent on both the electron-electronic polarization effective mass, m*, which is required and the coupling constant

$$= \left\{ \beta e^2 / (4\pi k_o) \right\} \left\{ m^* / 2\hbar^3 w_e \right\}^{\frac{1}{2}}$$

which indicates the extent of the electron-phonon coupling.

The numbers listed for CaO and CaF_2 have been rather crudely estimated by Bennett along with the corresponding electron affinity, X, values.

Bennett[31] performed variational solutions of the model potentials

given by the incorporation of these parameters using the trial functions

$$P_{1s}(r) = N_1 \; r \; (1+ar) \; \exp(-ar)$$

and

$$P_{2p}(r) = N_2 \; r^2 \; \exp(-br)$$

The optimized results for the SP(HF) model, with parameters for KCL, are displayed in Figure I.5 (absorption) and I.6 (emission) where they are compared with the functions secured by the present technique. The optimum values of the exponents derived by the variation theorem were, for absorption, a = 0.566 au^{-1} and b = 0.424 au^{-1} and, for emission, a = 0.473 au^{-1} and b = 0.088 au^{-1}. The corresponding transition properties are tabulated in Table I.8 along with Bennett's[34] "exact" solution, obtained by numerical solution of the Hartree-Fock-Slater equations resulting in the substitution of the appropriate potential forms into a radial Schrodinger equation.

The variational functions for absorption, Figure I.5, offer rather poor representations of the true charge distributions relevant to the model (assumed given by the present work), a fact which is not wholly brought out by a simple comparison of the mean radii also presented in Table I.8. In particular the 2p state is markedly too diffuse when obtained variationally. This again indicates the need for a more flexible representation of the 2p state in such a deep well. Improving the accuracy of the solution alters the absorption energy by about 10% while having little effect on the emission energy prediction. In accordance with this observation, the numerical and variational functions corresponding to emission states, Figure I.6, are relatively much less disparate.

The present finite-difference method provides numbers only marginally different from Bennett's "exact" values. Achieving such an accurate solution spoils the agreement with the experimental absorption energy and reveals that the apparently correct prediction of a long lifetime by the variational approach was fortuitous.

Also listed in Table I.8 are the SP(HF_1) results which afford but little better an estimate of this highly model-sensitive quantity. One other comparison with the variation method is possible through the computed thermal ionization energies. Variationally Bennett obtains for KCl, within the SP(HF) model, $\varepsilon_t(0)$ = 1.88eV and $E_t(1)$ = 0.14eV while they have been computed at 1.96eV and 0.20eV respectively in this work. Predictions of the peak of the emission band in both models is seen to correspond closely with the experimental value for KCl as shown in Table I.7, along with other measured properties.

Table I.9 contains the results for these model potentials in CaO and CaF_2, taken as representative of the alkaline-earth oxides and flourides respectively. Again the accuracy of the present numerical solutions is borne out by the compatibility with Bennett's "exact" work. The apparent success of the SP(HF) model in matching the absorption peak in CaF_2, when solved variationally is again revealed as fortuitous. The SP(HF_1) results are seen to be in no way superior to the SP(HF) values and neither affords even an order of magnitude estimate of the observed CaO emission band.

The configuration-coordinate diagram presented in Figure I.7 derives from the present numerical solution of the SP(HF_1) model for KCl. It is virtually indistinguishable from that obtained by Bennett[34] in his numerical work. Several points should be noted. As mentioned previously, in the introduction, transitions are assumed to be vertical. The lattice configuration pertaining to a given relaxed state is found at the distortion, x, which yields the minimum in the total energy, E_T. Absorptive transitions involving the curves marked "1s*" and "2p" which are coplanar lead to the broad absorption band of Figure I.8. This figure also includes the emission band coming from transitions between the curves "2p" and "1s" which, while coplanar, do not necessarily contain the plane of the absorption curves.

The minimum in the relaxed ground state is found at a very small inward distortion, 0.08% of the lattice spacing, where the corresponding energy is -4.482 eV. The predicted optical absorption band is peaked at 2.93 eV somewhat higher than experiment and has a half-width of 0.093 eV. The emission curves are seen to be considerably shifted towards the continuum. A large outward relaxation, 9.8%, has occurred in order to accommodate the excited state charge distribution, the energy associated with which is -1.307 eV at this optimum configuration. The half-width of the implied emission band is 0.12 eV and the band maximum is centred at 1.17 eV, very close to the observed value. It is important to notice that the half-widths predicted by this one-coordinate approach are a factor of two below those obtained by experiment. The inability of such treatments, containing only radial breathing modes to reproduce sufficiently wide bands will be met again in the semicontinuum models applying to electrons in polar liquids.

The predictions of the models containing the quasiadiabatic treatment of the optical polarization, SP(QA) and SP(QA_1), are presented in Table I.10. In KCl, while the latter approaches the absorption energy closely, both underestimate the emission energy and fail to forecast the luminescent lifetime by an order of magnitude. The SP(QA) model is badly out for both CaO and CaF_2, the absorption energies in which are reasonably estimated by SP(QA_1) model. Neither model suggests the very small Stokes shift observed in CaO, the former giving a hopeless absorption energy, the latter grossly overestimating it. Comparison with the variational treatment of these model potentials is limited by Bennett's provision of but a few figures for NaCl. E(a), the absorption energy, improves from 1.62 eV to 2.43 eV on numerical solution; still short of the observed peak at 2.77 eV. E(e), the emission energy, goes from 0.63 eV to 0.97 eV happily coinciding with the experimental value. Bennett's variational treatment yields a radiative lifetime of

2.31×10^{-8} seconds (estimated using equation (74)), which is recalculated numerically to be 1.90×10^{-8} seconds in very poor accord with the experimental 10^{-6} seconds.

The configuration coordinate diagram derived in the present work for the SP(QA) model for NaCl is shown if Figure I.9, the corresponding band-shapes are in Figure I.10. Again both numerical techniques arrive at substantially the same numbers.

The general failure of any of these models to predict a sensible lifetime in the alkali-halides, the system for which they seem best adapted, has been interpreted as indicating the presence of some special mechanism which is responsible for producing the unexpected length. Within the framework of these models the most likely suggestion, made by Swank and Brown[45], is that there exists some degree of 2s-2p mixing on lattice relaxation. This suggestion is supported by the fact that these levels approach each other as the lattice relaxes and, at the emission configuration, are almost degenerate. For example, in the $SP(HF_1)$ model for KCl the 2s state at the distortion opposite to absorption lies at -0.44 eV compared with a 2p energy of -1.47 eV. After relaxation the corresponding states at the emission configuration have energies of -1.20 eV and -1.22 eV respectively. This agrees surprisingly well with the results of Stiles et al.[46], who, using the variation of luminescent lifetime with applied electric field, place the 2s level 0.02 eV below the relaxed 2p state. The mixing mechanism, invoked by Bennett in an attempt to forecast the extended lifetime, employs an internal electric field generated by the non-cubic longitudinal optical phonons present. Taking 10^7 V/m as a reasonable estimate of this field, the model predicts strong (60/40) mixing of the 2p and 2s states and a lifetime of 31×10^{-8} seconds, which is a step towards the experimental 57×10^{-8} seconds. None of the other models investigated are able, even with internal fields large enough to cause dielec-

tric breakdown, to yield a lifetime greater than 10^{-7} seconds.

Calculations using the remaining model, $SP(EI_1)$, with the polaron-type optical polarization are so inconsistent with the experimental data for all three types of salt studied that they are not detailed here. By way of an example, the model has 1.25 eV for absorption in KCl and 0.41 eV for the emission band. However, again, the present numerical method and Bennett's work produce very similar numbers, not differing by more than 1%.

g) Conclusion.

The semicontinuum models provide a detailed framework for the computation of optical processes at point defects in crystals. Even with this somewhat limited goal, within the present formulation, they are found to be restricted to F-centres in alkali-halides if some predictive accuracy is desired. Of the models studied here, that termed SP(HF_1), which is theoretically rather unsatisfactory as it involves the ad hoc neglect of some factors, yields perhaps the best overall agreement with experiment in these salts. Other models investigated offer, basically, only qualitative suggestions as to the true values.

It has been amply demonstrated that the present numerical, finite-difference scheme is entirely suitable for deriving highly accurate solutions of the model potentials associated with trapped electron problems.

Tables I

Tables 1-5 have results for polarized cavity models of the F-centre. 1 includes the analytical solution of Zahrt and Lin for the simplest potential studied. 2,3 and 4 are Simpson's cavity and interstitial ion model. 5 is a parameterized potential, R = 4.1 au, V_o = -5.92 eV, k_e = 3.0, for RbCl in absorption and NaCl in emission, R = 5.5 au, V_o = -3.28 eV, k_e = 5.4.

Tables 6-10 are apposite to the semicontinuum treatment. 6 has the necessary input data, 7 the experimental values they are expected to explain. Bennett's SP(HF) and SP(HF_1) models are in 8 for KCl and in 9 for CaO and CaF_2. 10 has the SP(QA) and SP(QA_1) results for all these systems.

Energies are in eV, distances in au, except R_v in Å in 4.

TABLE I.1

SALT	NaCl	KCl	KBr	RbF
a	5.317[e]	5.94	6.24	5.33
k_{op}	2.25[e]	2.13	2.33	1.93
E(1s)	5.245[a]	5.001	4.766	5.449
E(1s)	5.269[n]	5.022	4.791	5.471
E(2p)	2.633[a]	2.816	2.704	2.865
E(2p)	2.657[n]	2.830	2.722	2.891
ΔE	2.62[a]	2.19	2.07	2.58
ΔE	2.612[n]	2.193	2.069	2.580
f	0.995[a]	0.98	-	0.98
f	0.998[n]	0.986	0.979	0.988
ΔE	2.67[e]	2.20	1.97	2.60

a Analytical solution of Zahrt and Lin.

e Parameters employed by Zahrt and Lin.

n Present numerical work

TABLE I.2

	Interstitial ion		Polarized cavity	
$-E(1s)$	1.52^{v}	1.556^{n}	3.2^{v}	3.372^{n}
$-E(2p)$	0.44	0.448	1.0	1.166
$\bar{r}(1s)$	5.75	5.44	4.14	3.94
$\bar{r}(2p)$	18.3	17.42	7.0	6.37
U	-	0.615	0.55	0.668

n Present numerical work.

v Simpson's variational solution.

TABLE I.3

	Polarized cavity		Interstitial ion
ΔE	2.2^{v}	2.156^{n}	0.935^{n}
f_{vel}	0.81	0.938	0.709
f_{len}	1.13	0.938	0.709
t_f	0.72	1.000	1.000

n Present numerical work.

v Simpson's variational results.

TABLE I.4

SALT	NaCl	KCl	KBr
$R_v(\mathring{A})$	2.6	2.6	2.8
$-E(1s)^v$	3.29	2.80	2.63
$-E(1s)^n$	3.345	2.847	2.672
$-E(2p)^v$	1.01	0.85	0.81
$-E(2p)^n$	1.168	0.977	0.951
ΔE^v	2.28	1.95	1.82
ΔE^n	2.177	1.870	1.721

n Present numerical work.

v Smith's variational results.

TABLE I.5

	Absorption states			Emission states	
$-E(1s)$	2.574[v]	2.58[a]	2.591[b]	1.31[a]	1.339[b]
$-E(2p)$	0.493	0.49	0.496	0.148	0.175
$-E(2s)$	-	0.42	0.429	0.152	0.170
$-E(3p)$	0.201	0.20	0.208	0.063	0.069
$\Delta E(1s-2p)$	2.081	2.09	2.095	1.162	1.154
$\Delta E(1s-3p)$	2.373	2.38	2.383	-	-
$\bar{r}(1s)$	-	-	3.754	-	4.935
$\bar{r}(2p)$	-	-	10.457	-	16.960

a Numerical results of Fowler,Calabrese and Smith.

b Present numerical work.

v Variational results of Smith and Spinolo.

TABLE I.6

SALT	KCl	CaO	CaF_2
a	5.93	4.54	10.32
R^+	2.77	2.21	2.21
R^-	3.00	2.55	1.98
s	0.637	0.629	0.546
R_v	5.10	4.00	9.56
k_{op}	2.13	3.28	2.05
k_{st}	4.67	11.76	6.71
k_e	3.88	5.0	4.0
-X	0.022	0.04	0.04
m^*	0.6	1.0	1.0
w_l	3.95	13.07	1.38

TABLE I.7

SALT	NaCl[a]	KCl[a]	CaO	CaF_2
E(a)	2.770	2.313	3.646[b]	3.292[c]
E(e)	0.975	1.215	3.292[b]	
t	100.0	57.0		
f(a)	0.6	0.85		
W(a)	0.255	0.163		
W(e)	0.337	0.261		
$\varepsilon_t(1)$[d]	0.08	0.09		
$\varepsilon_t(0)$[e]	1.94	2.05		

a Fowler in ref. 44, p. 627

b Kemp et al. in ref. 49, p.

c Feltham and Anders in ref. 50

d Markham in ref. 7, p. 82

e Markham in ref. 7, p. 123

TABLE I.8

KCl		SP(HF)		SP(HF_1)	
E(a)	2.78[v]	3.02[a]	2.98[b]	2.97[a]	2.93[b]
E(e)	1.22	1.22	1.20	1.22	1.17
t	83.9	10.9	8.7	19.0	16.2
f(a)	1.05	-	0.91	-	0.63
W(a)	-	-	0.09	-	0.09
W(e)	-	-	0.12	-	0.13
$\bar{r}_{1s}$*(a)	3.74	-	3.51	4.15	4.12
$\bar{r}_{2p}$ (a)	5.81	-	5.07	22.83	20.98
$\bar{r}_{2p}$*(e)	25.91	-	24.33	32.32	30.16
$\bar{r}_{1s}$ (e)	4.12	-	4.01	6.11	6.04

a Bennett's numerical solution.

b Present numerical work.

v Bennett's variational results.

TABLE I.9

CaF_2		SP(HF)		SP(HF_1)	
E(a)	3.265[v]	2.803[a]	2.784[b]	4.598[a]	4.384[b]
E(e)	-	0.735	0.730	0.599	0.592
t	-	0.5	0.47	4.8	4.2
CaO					
E(a)	-	2.041	2.028	4.626	4.589
E(e)	-	0.299	0.307	0.218	0.213
t	-	0.5	0.48	0.3	0.26

a Bennett's numerical solution.

b Present numerical work.

v Bennett's variational results

TABLE I.10

		SP(QA)		$SP(QA_1)$	
	E(a)	1.796[a]	1.784[b]	2.258[a]	2.249[b]
KCl	E(e)	0.707	0.704	0.626	0.623
	t	4.1	4.02	7.6	7.47
	E(a)	-	2.071	3.510	3.495
CaF_2	E(e)	0.544	0.541	0.435	0.433
	t	1.0	1.32	2.6	2.81
	E(a)	0.354	0.360	3.728	3.684
CaO	E(e)	0.327	0.331	0.245	0.243
	t	8.3	8.11	0.8	0.74

a Bennett's numerical solution.

b Present numerical work.

Figures I

Figures 1-4 are functions derived from polarized cavity models of the F-centre. 1 and 2 are relevant to Simpson's cavity and interstitial ion models respectively. 3 and 4 pertain to Fowler's model parameterized for NaCl on absorption and emission respectively.

Figures 5-10 derive from semicontinuum calculations. Bennett's model for KCl on absorption provides 5 and on emission, 6. In all above, variational functions are in full-line. Broken-line is present numerical work. (a) are ground 1s state functions, (b) excited 2p functions. Bennett's SP(HF_1) model gives the configuration coordinate diagram of 7 on numerical solution and also the absorption (full-line) and emission (broken-line) line-shapes in 8. The emission band has been moved 1.6 eV to the blue. 9 has the SP(QA) model numerical results for NaCl and in 10 the computed absorption bands at 298^{o}K (full-line) and 77^{o}K (broken-line) are presented.

Figure I.1

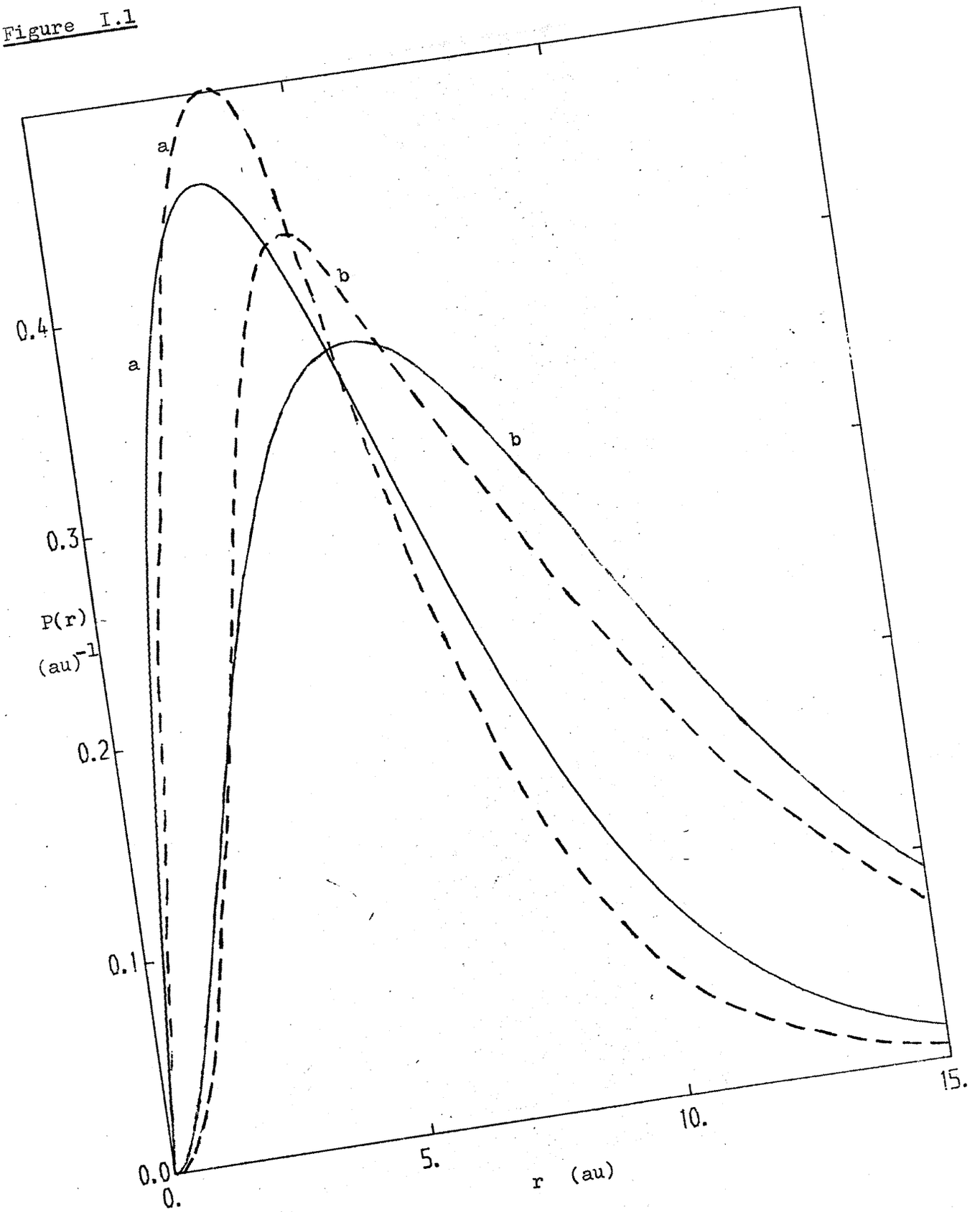

Figure I.2

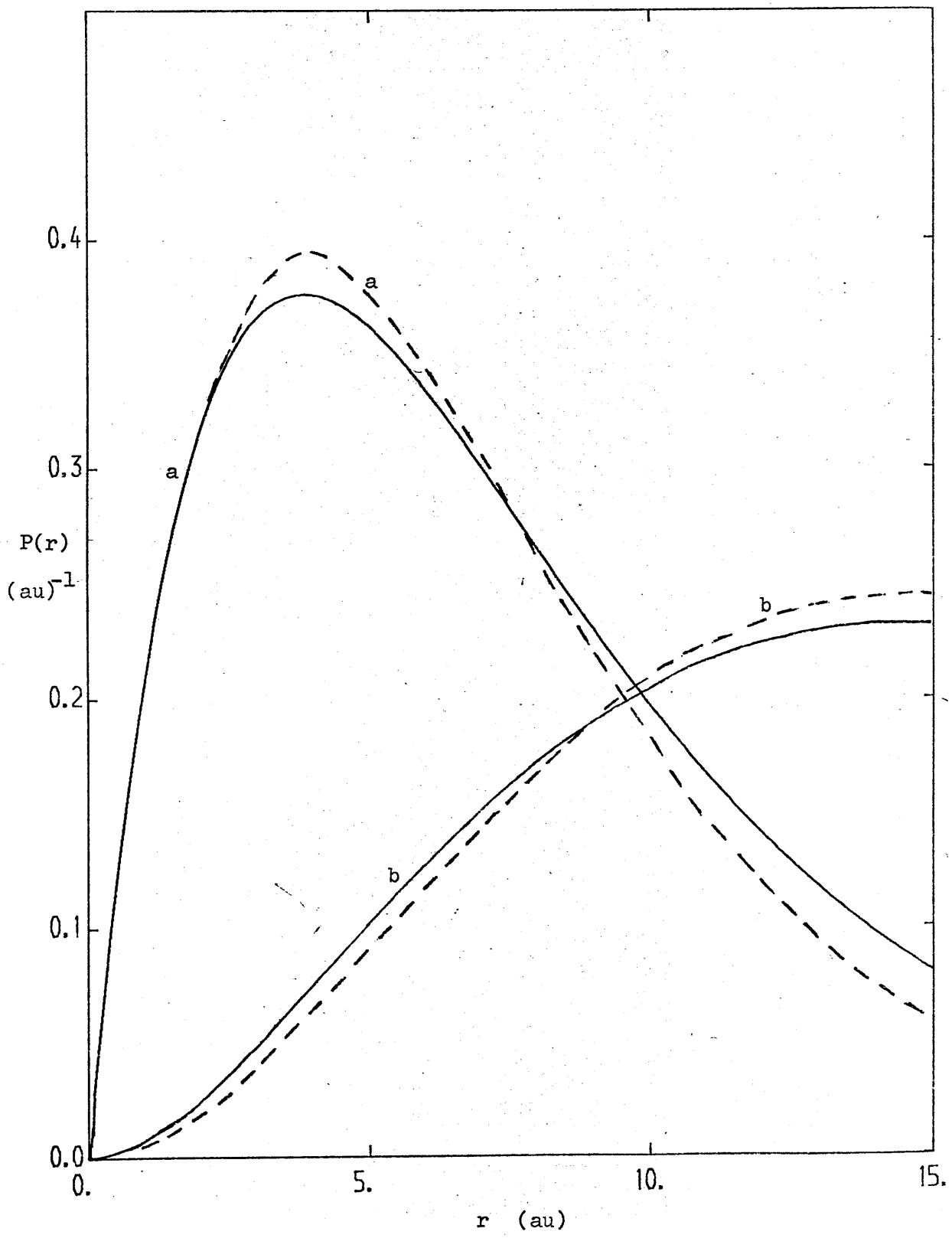

Figure I.3

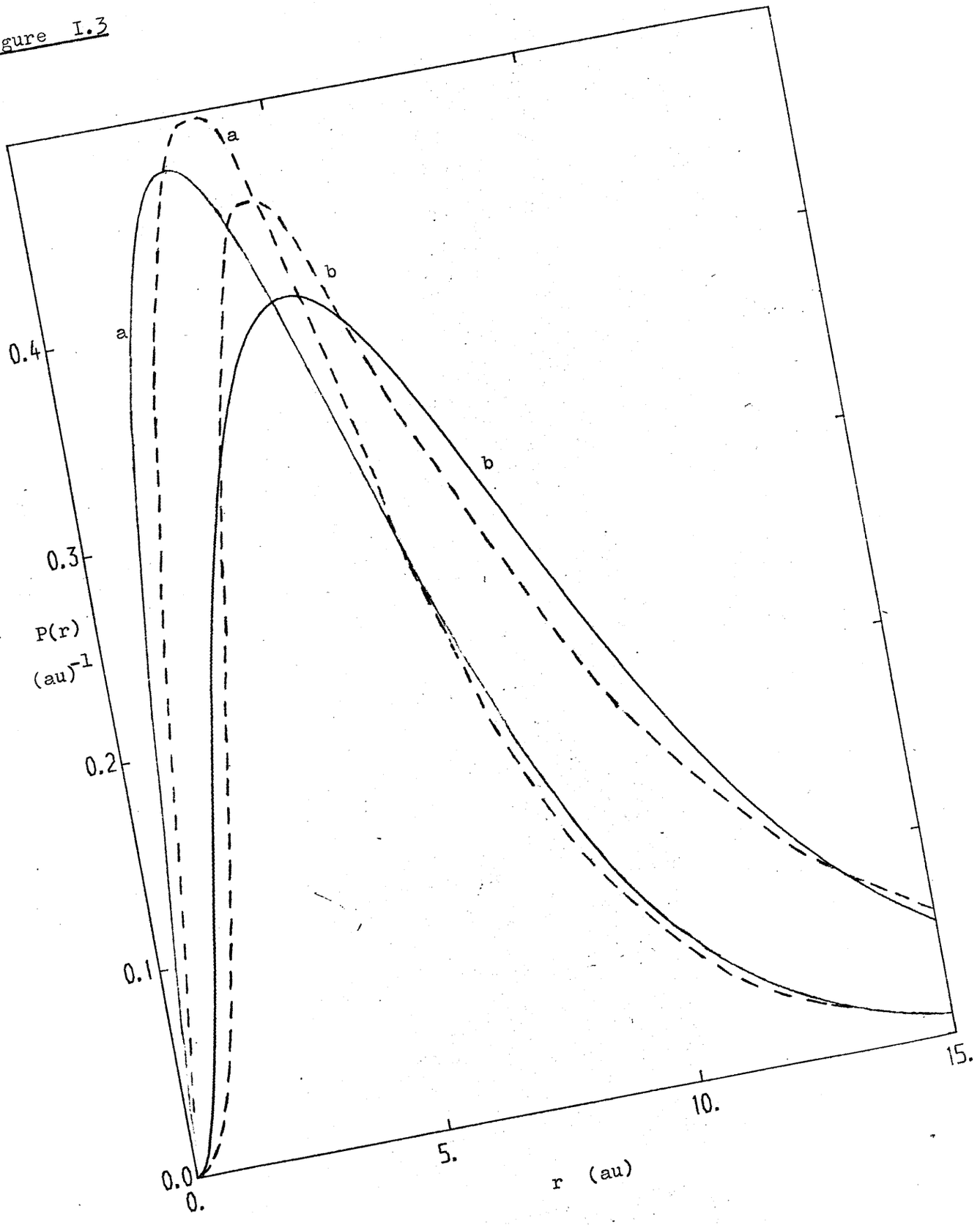

Figure I.4

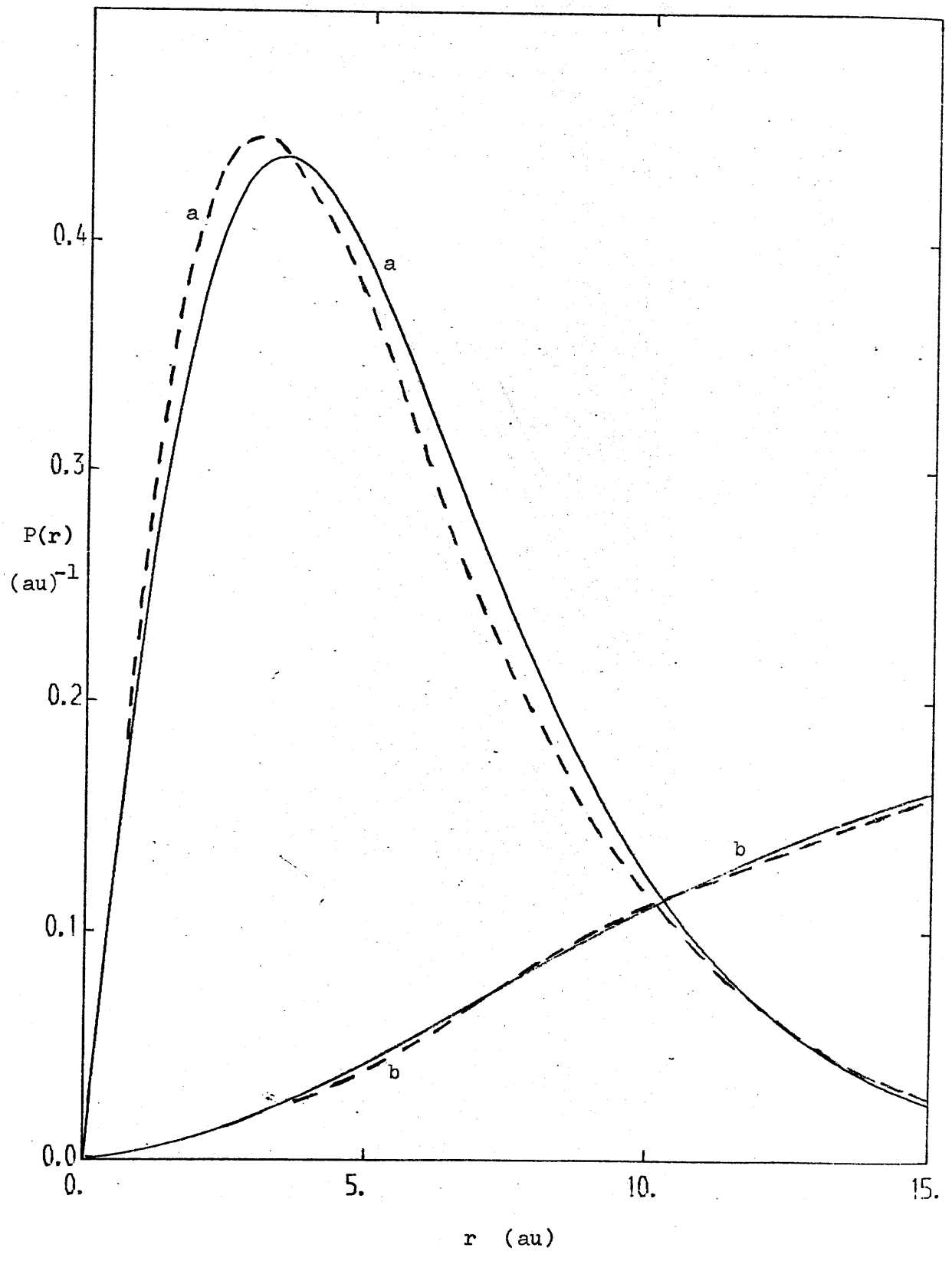

Figure I.5

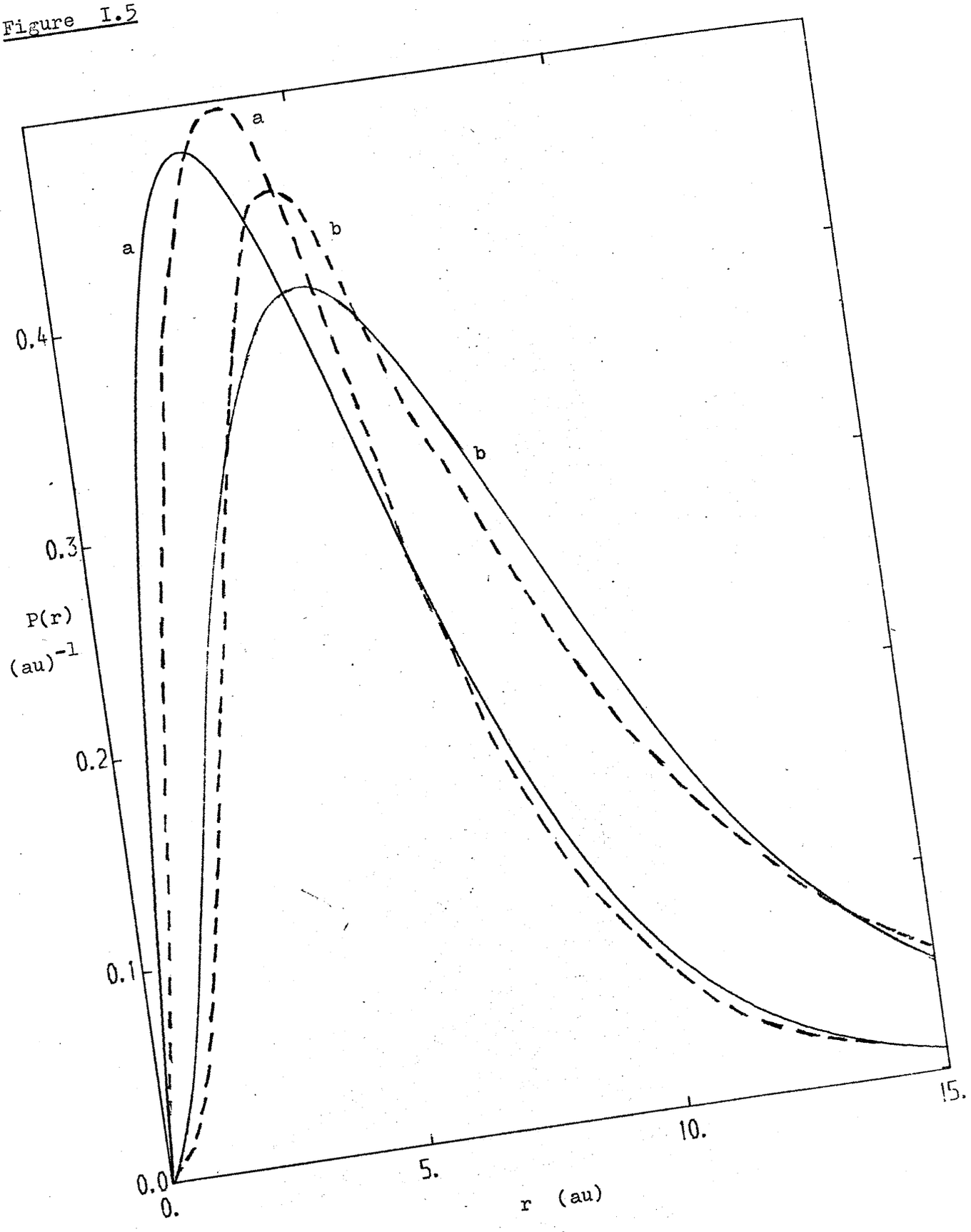

Figure I.6

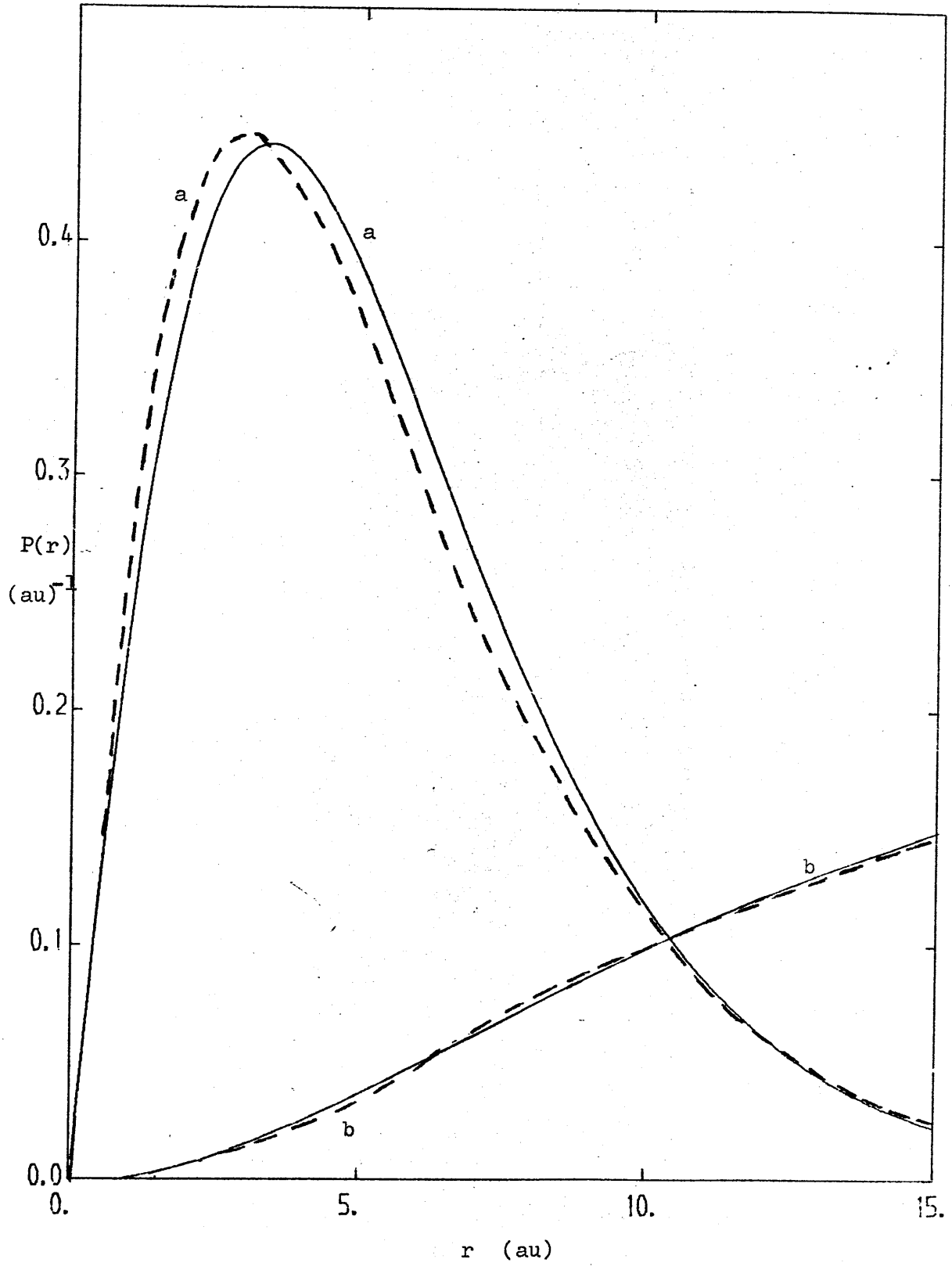

Figure I.7

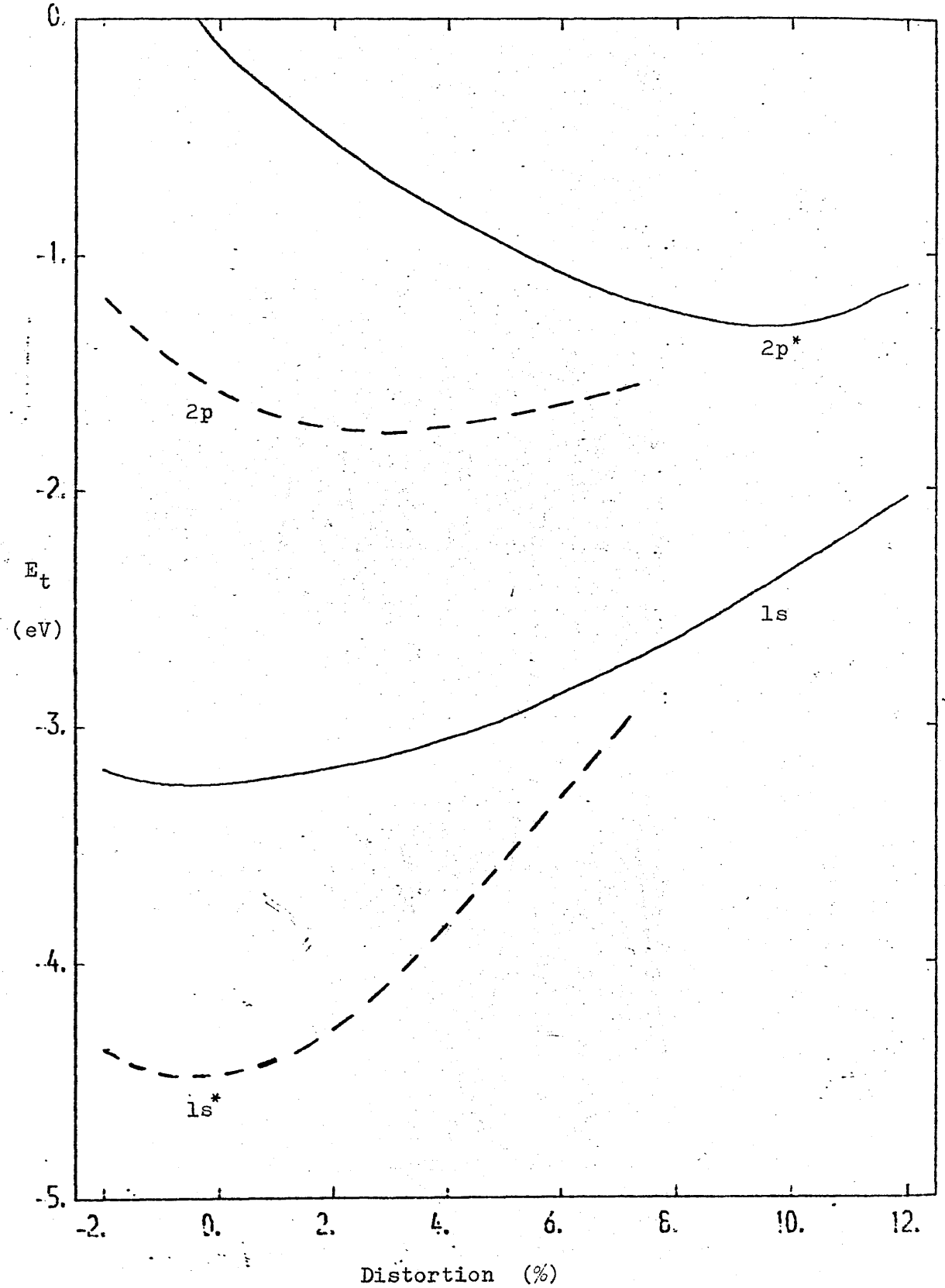

Figure I.8

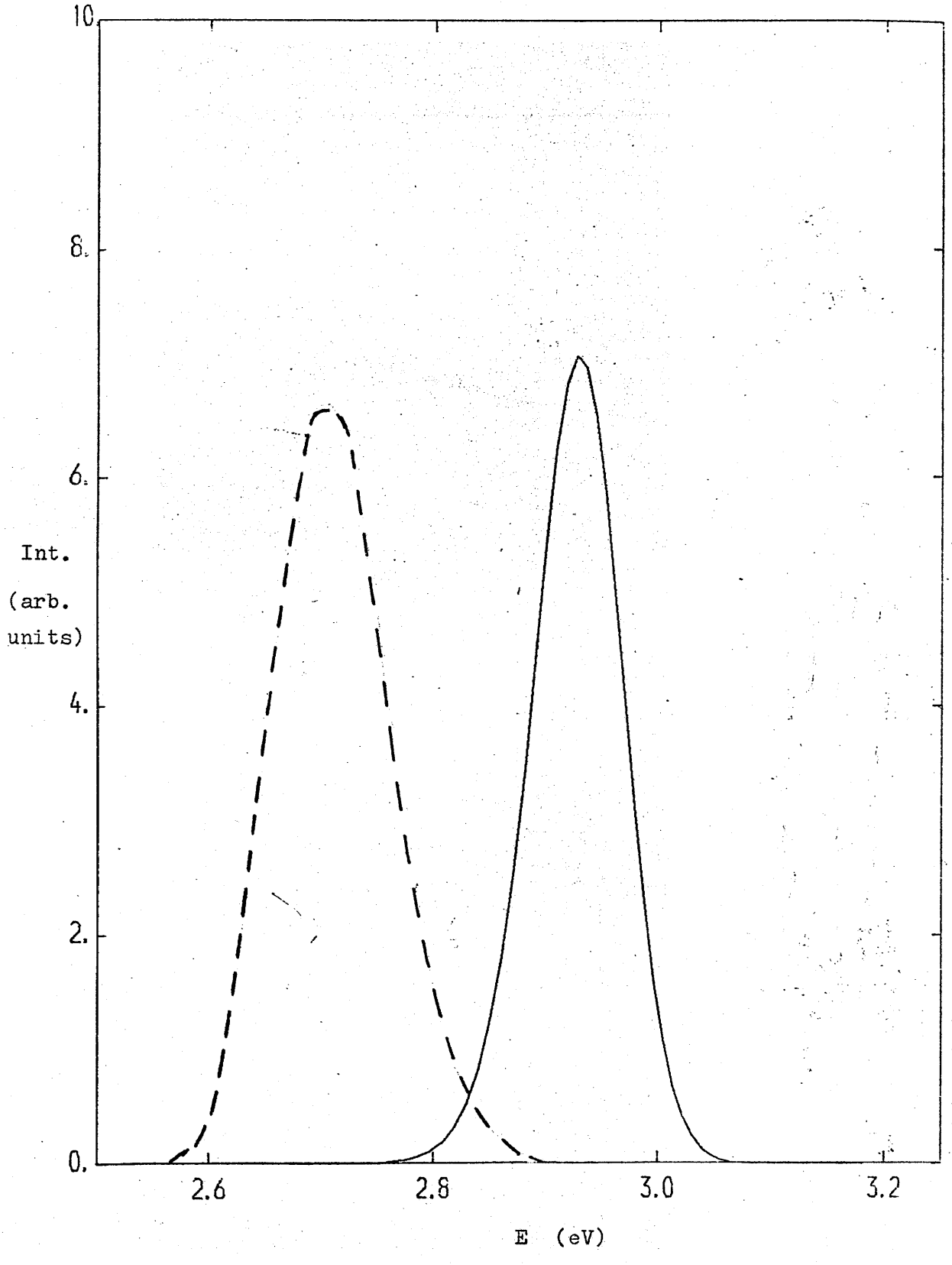

Figure I.9

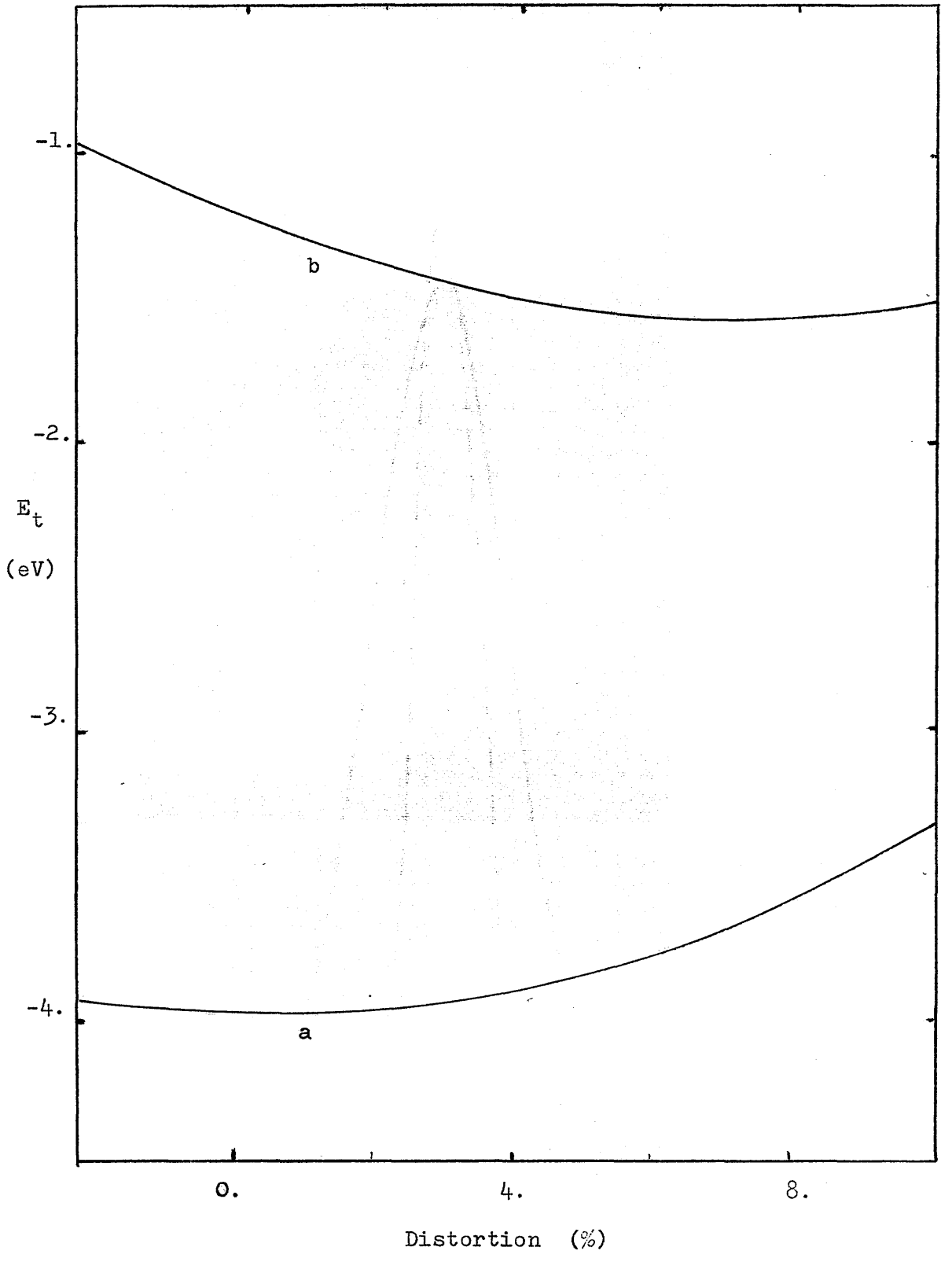

Figure I.10

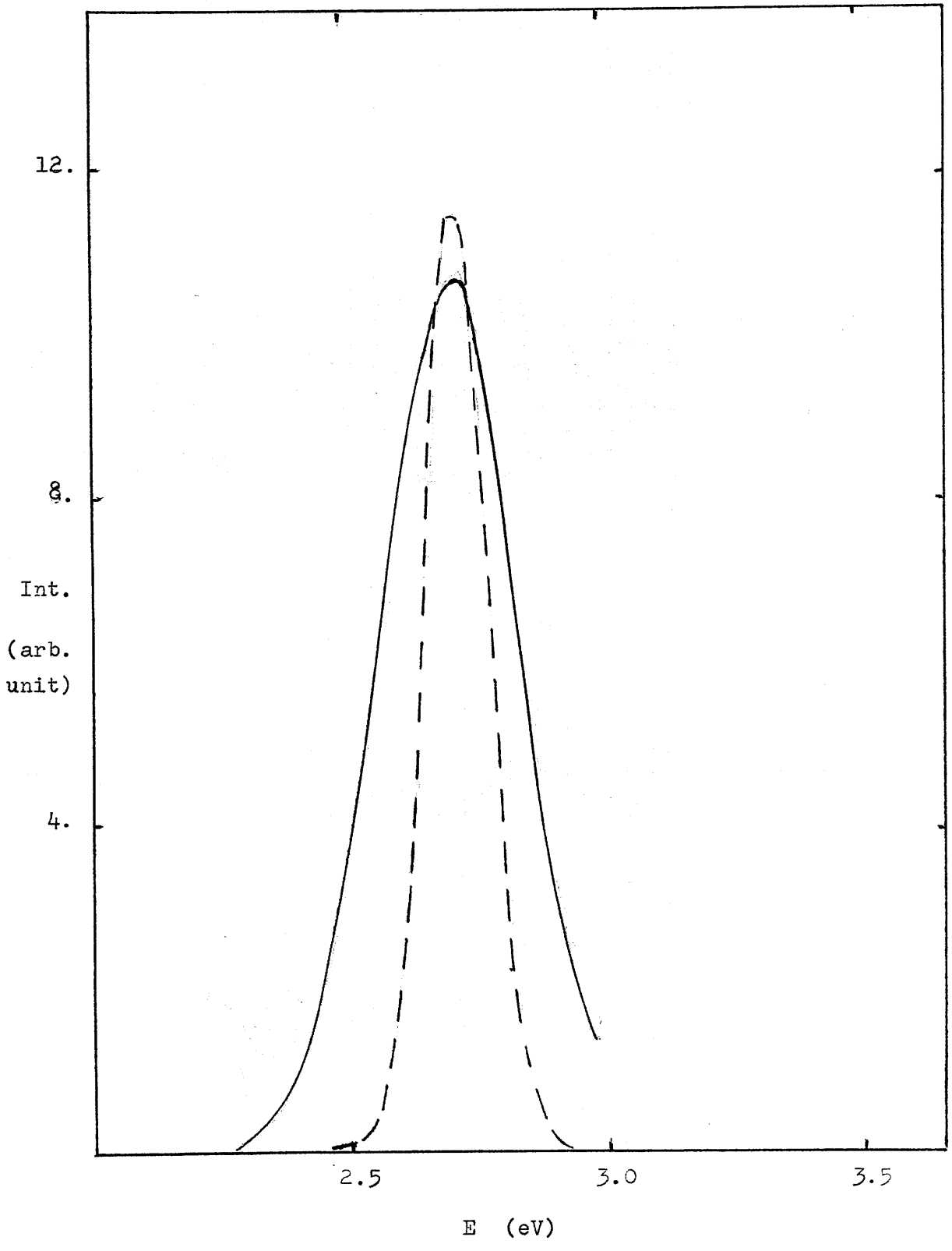

PART II

Surplus Single Electron Species in Polar Media.

Section 1

Introduction.

a) The absorption spectra associated with the presence of excess electrons in polar liquids, ices and glasses are, in many ways, similar to those observed at colour centres in crystalline solids.

They are generally broad unsymmetrical bands peaked either in the visible or near-infra-red, depending on the polarity of the host matrix. Roughly speaking, the more polar the medium the further into the visible lies the observed band maximum. On closer examination of all the available experimental data it would seem that quite significant differences also exist between these species. In particular the absence of such a Raman effect as is observed in F-centres[53,54] and the much narrower line width given by electron magnetic resonance experiments have been noted. However, the optical properties mentioned above do contain striking analogies, a fact which has encouraged very closely related theoretical formulations for discussing the properties of the respective systems to be developed.

A typical band appears in liquid ammonia upon the dissolution of both alkali and alkaline-earth metals. At low concentration it is independent of the nature of the dissolved atomic species and is peaked around 0.8 eV in the near i.r., appearing indefinitely stable. The high energy tail which is a characteristic of trapped electron spectra in polar liquids extends well into the visible and is responsible for the deep blue colour of the solutions. Relatively stable absorption curves are also exhibited in many low-temperature glasses, in alkaline ice and even in pure ice at $4^{o}K$ which have been subjected to, say,

irradiation. All bands shift to the red with increase in temperature and those studied to date exhibit a blue shift under increased

ambient pressure. The temperature and pressure effects on the half-width are not so marked though some confusion appears to exist over this (see, e.g., the three(!) temperature variations of this quantity listed for the ammoniated electron).

With the advent of pulse radiolysis and related ultrafast techniques the capability of observing processes on a sub-microsecond, nanosecond and, most recently, picosecond time-scale has been achieved. Such methods have revealed the presence of transient absorption bands in a vast range of irradiated media from the very polar water, through the less polar alcohols and ethers, to the essentially non-polar hydrocarbons and even in liquid rare gases. These bands have been attributed to the presence of electrons "solvated" in the media. It appears, therefore, that electrons solvate to some degree in all liquids. A steady flow of stimulating observations on the properties of these solvated electrons is continually being reported, offering many substantial challenges to theory.

Theoretical developments presented here, forwarded in efforts to gain insight into the nature of this species, have progressed in a similar fashion to those discussed in Part I with reference to colour centres. Before tracing this development and presenting the current computational results, the properties of several systems which were investigated are detailed. This will serve to outline the goals of the theory and highlight its present deficiencies or at least delimit its domain of validity.

b) The Hydrated Electron.

Hart and Boag[55] were first to observe the transient absorption band in water now known to be characteristic of the hydrated electron. Their results were accomplished by irradiating pure deaerated water with a pulse of 1.8 MeV electrons which produced the band peaked at around 7000 A with a long high-energy tail extending through the visible. Since this initial discovery much refined experimental work has been undertaken on this solvated species and a rather complete documentation of its properties exist. A useful guide to these properties is offered by the book of Hart and Anbar[56].

At a temperature of 298°K the band maximum is observed at 1.73 eV[57] with an extinction coefficient of $1.85 \times 10^{-6} M^{-1} m^{-1}$, the associated oscillator strength being 0.65[57]. The full width at half-maximum is 0.92 eV and the primary yield has been found to be $G(e^-_{aq}) = 2.7$ per 100 eV of radiation energy deposited[58]. Interestingly, this yield has been shown to be independent of pressure over a range from atmospheric up to 6Kbar[59]. The observed effect on the spectrum of this massive pressure increase is merely a 33% depression of the extinction coefficient at the band maximum with a concurrent 32% broadening of the band (measured at the half-height). The oscillator strength remains approximately constant[60]. A slight blue shift with increasing pressure is exhibited by the band maximum, the coefficient being 5.3×10^{-5} eV/bar[61]. The partial molal volume and the cavity volume have been placed at 7 and 10 ml mol^{-1} respectively at a pressure of one atmosphere and a temperature of 302°K and have been shown to be compressible[62].

The effect of temperature over the range 4-90°C has been interpreted[63] by assuming that the primary yield is again unaffected and that the observed decrease in the apparent molar extinction coefficient is due rather to the slight broadening of the band with in-

creasing temperature. Within this range the red shift noted at the band maximum is described by a temperature coefficient of -2.8×10^{-3} eV/deg[63]. It is important to realize that this figure has been obtained at constant pressure.

Of great interest are the recent observations by the application of ultrafast technology which have continually lowered the limit of the experimentally measurable "hydration" time. Hunt and Thomas[64] first showed this to be less than 500 psec. Next Bronskill et al.[65] placed the value below 20 psec then 10 psec[66]. Kenney-Walker and Wallace with a somewhat brave extrapolation of their data suggested 6 psec as the upper limit for the solvation process[67]. Most recently Rentzepis et al. have observed that the "normal" hydrated electron spectrum is present within 4 psec of photoionization of the ferrocyanide ion in aqueous solution, a process which is known to generate quasi-free electrons in this medium. 2 psec after this generation a band is observed in the infra-red, at 1.06 μ, the observation wavelength, which gradually evolves in time, shifting toward higher energies until the normal position is attained. It should be understood that the lifetime of the trapped species in water is very variable, depending in a dramatic fashion on the amount of impurities present which may act as scavengers, e.g. the hydroxyl radical. A typical lifetime is of the order of nanoseconds.

The heat of solvation has been estimated at 1.7 eV[68] but the photoelectric threshold has yet to be determined. However, the important work of Delahay and colleagues on photoelectron emission spectroscopy seems likely to reveal this value. A mobility of about 2×10^{-7} $m^2V^{-1}sec^{-1}$ has been measured[69] which is on a par with the aqueous hydroxide ion. From this figure a diffusion coefficient of around $5 \times 10^{-9} m^2sec^2$ was calculated which indicates the presence of some special diffusion mechanism to account for its motion.

Lastly the epr spectrum was discovered under conditions where the solvated species had a particularly long half-life, of the order of 5 μsec[70]. It was found to be extremely narrow $<$.5 gauss and possess a g-factor of 2.0002 + .0002.

c) Very Dilute Metal Ammonia Solutions.

The properties of these solutions are the subject of the intense investigations presented in the proceedings of the Colloque Weyl Symposia initiated in 1964 by Lepoutre[70-72]. These three collected volumes provide a valuable source of references to an extensive field.

The definition of "very dilute" is taken here to encompass only solutions which are less than 10^{-3}M in metal. Such a limitation is necessary since just above this range of concentration the ideal electrolyte behaviour pattern of a solvated metal positive ion and a solvated negative electron is lost due to some degree of ionic association. Considerable changes in the properties of the solutions are thereby affected. The electrical conductivity drops markedly[73]. The frequency of the absorption maximum, which is concentration independent in the very dilute range, suddenly decreases by about 400cm^{-1} before levelling out again at concentrations of around 10^{-2}M.[74] This is concomitant with a marked increase in the amount of spin-pairing in the solution[75].

Even more dramatic changes in the properties and hence the nature of metal-ammonia solutions may be observed on further increasing the metal concentration. These will not be discussed here but are well documented in the review article by Cohen and Thompson[76], as well as in the above-mentioned proceedings.

The discussion is therefore limited to the very dilute region where the unassociated solvated electron species is assumed responsible for the near infra-red band and the blue colour of the solutions. At 240K the band maximum lies at 0.80 eV and has an apparent molar extinction coefficient of 4.9×10^{6} M^{-1} m^{-1} and an oscillator strength of 0.77[77]. It is therefore an intense band due to an allowed transition. As usual the band moves to the red with temperature increases, the

coefficient being of the order of 10^{-3} eV/deg, while the temperature variation of the half-width has been variously reported as 0.6×10^{-3} eV/deg,[78] 1.6×10^{-3} eV/deg [79] or indeed to be independent of temperature[77].

Increasing the ambient pressure shifts the band to the blue, the pressure coefficient of the band maximum being 3.6×10^{-5} eV/bar.[80] Theoretical models generally picture the electron in a cavity walled by ammonia molecules which can explain the above data. The high pressure studies of Hentz et al.[80] attribute a partial molal volume of 98 ml mol^{-1} to the ammoniated electron and indicate that the cavity is more compressible than that in water. Interestingly, there appears to be a marked decrease in the primary yield with increase in pressure, contrasting the observation in water. Further support for the high degree of solvation expected in this picture comes from the interpretation of the epr spectrum, a single, extremely narrow, less than 0.1 gauss in the liquid state, structureless line with a g-value of 2.0012[81] and has been inferred from viscosity data[82,83].

The absence of a Raman band, expected due to the symmetric breathing mode of such cavities has been noted[84] but several explanations of this immediately suggest themselves, e.g. the over-simplification of this one-coordinate cavity model, smearing by thermal effects, and this presents no insurmountable objections. The N-H infra-red stretching frequency has been observed to shift to lower values in metal-ammonia solutions which may again be attributed to the presence of strongly solvated electrons[85].

Sundry other observations have been made in this concentration region. The heat of solution of the electron has been placed, somewhat crudely, at 1.7 + 0.7 eV by Jortner[86] and the photoelectric threshold has been estimated at 1.6 eV [87]. A more recent suggestion of this quantity is the 1.85 eV given by Delahay[88].

d) Ices.

Eiben and Taub[89] and later Khodzhaev[90] et al. first reported the now characteristic broad asymmetric band due to trapped electrons in crystalline ice generated by irradiation at 77K. It had previously been assumed that this was not a stable species in pure ice, presumably because the very low values of the radiation yield, $G(e^-_{ice})_{77^\circ K} 10^{-4}$ x $G(e^-_{H_2O})_{298^\circ K}$, had hindered its detection. Taub and Eiben[91] subsequently confirmed the assignment of the band, peaked at 6400 A, to trapped electrons in ice and made extensive studies on the species employing a pulse radiolysis method. Kawabata[92] has pursued these investigations in crystalline ice, obtaining substantially better yields of trapped electrons, and therefore facilitating his experiments, by the simple expedient of doping the ice with small (10^{-4}-10^{-2}M) quantities of NH_4F which produced no noticeable effect on the optical spectrum, other than the apparent enhancement in intensity. He was thus able to colour the doped single-crystals of ice quite considerably by γ irradiation at $77^\circ K$.

The absorption band maximum lies at 1.93 eV and the half-width was estimated at about 0.5 eV, much narrower than that due to the electron hydrated in the liquid state. The rate of decrease of the absorption maximum with temperature is also less than in water, the coefficient being -1.2×10^{-3} eV/deg.[91] Recently Kawabata et al.[93] have observed a high-frequency shoulder in the absorption spectrum at about 2.3 eV. Since the spectrum may be assumed to arise from a single type of trapping centre in accordance with the photobleaching behaviour, the quantum efficiency of this process being constant across the entire absorption band, this must be taken to be the first indication of a structured absorption band, illustrating transitions between more than one set of states within the same potential well, in these media.

This is in marked contrast with the findings in the

γ-irradiated alkaline ices investigated by Kevan and coworkers. Here the host ice matrix is doped with about 10M NaOH, say, and is glassy rather than crystalline. The complex absorption band, photobleaching behaviour and decay-rate patterns are taken as indicating the presence of at least two types of traps for electrons. The primary yields are almost as high as in water $G(e_t^-)_{77^oK} = 1.9$ per 100 eV of energy deposited and the molar extinction coefficient at the band maximum is around $2.0 \times 10^6 M^{-1} m^{-1}$. The absorption peak is located at 2.12 eV[94]. The similarity in the shapes of the optical absorption band, which has a half-width of the order of 1.0 eV and an oscillator strength of 0.86(!), and the wavelength dependence of the photocurrent developed on bleaching[95] has led to the suggestion that the observed absorption may be due to transitions directly into the conduction band. However, this behaviour may also be accommodated by postulating a very loosely bound excited state which becomes degenerate with the conduction band during relaxation. The absence of any temperature dependence in the photocurrent profile[96] also supports these suggestions.

e) Theoretical Considerations.

The cavity concept which permeates almost all theoretical studies attempted to explain the foregoing observations on solvated or trapped electrons has its origins in the work of Ogg in the 1940's[97]. Minor improvements on the infinite square well model of Ogg were devised by Lipscomb[98] and Stairs[99] but no mention was made of the crucial importance of polarization effects. Concurrently, an alternative continuum theory involving polarization only had been developed by Pekar[100,101] and coworkers, initially in an endeavor to understand the properties of the F-centre, which had its roots in the early work of Landau[102]. Jortner[103] first accomplished the successful synthesis of these approaches in 1959. A critical review of the detailed historical evolution of the theory to this point has recently been presented[147] and will not be repeated here. However, a discussion of the polarized cavity model as formulated by Jortner and others at a later date is highly pertinent and is presented in the next section.

As is to be discussed, this model has been framed within the same two basic approximate solution techniques as in the corresponding model for colour centres. Analogous refinements to include some discrete structure in the bulk medium have also been pursued in this problem and the resulting semicontinuum models are discussed in Section 3.

Many-electron treatments involving molecular orbital approaches are becoming quite commonplace. Indeed one "ab initio" study concerning the ground state of the ammoniated electron and purporting to contain all the important effects, has been completed by Newton[104]. While this may be indicative of the way the field is developing, consideration here is limited to the above-mentioned one-electron methods.

Previous studies of these polarized cavity and semicontinuum models for excess electrons in polar media have, to date, almost exclusively involved a variational solution technique; the sole exception

being in the work of O'Reilly[105,106]. It was felt necessary to provide a thorough-going numerical investigation of these models to divulge the deficiencies of the previous solution method and again to clearly delimit the region of their applicability.

Section 2

Polarized Cavity Models.

a) As before, see Section I.2, the electron is assumed to be localized in a physical cavity bounded by a continuous isotropic linear medium again characterized by low and high frequency dielectric functions k_{st} and k_{op} respectively. The potential acting on this localized electron due to the polarization of the medium it produces is

$$V(r) = e \,/\, (4\pi k_o) \int_r^\infty \underline{p}_i(\underline{r}') \cdot (\underline{r} - \underline{r}') \,/\, \left|\underline{r} - \underline{r}'\right|^3 d\underline{r}'$$

where $\underline{p}_i(\underline{r}')$ is the polarization responsible for electron trapping. The subscripted i is present to imply that this polarization may be dependent on the instantaneous electronic state i under consideration. Assuming a spherically symmetric trapping potential gives

$$V(r) = e \,/\, k_o \int_r^\infty p_i(r')\, dr'$$

$p_i(r')$ being the radial component of the polarization vector.

Once a description of the polarization field has been assigned, this potential is substituted into the usual radial Schrodinger equation

$$\left\{ \tfrac{1}{2}\, d^2/dr^2 + \ell(\ell+1)/2r^2 + V(r) \right\} P_i(r) = W_i\, P_i(r) \qquad (1)$$

and this solved for the single-particle energies W_i. $P_i(r)$, the radial wave-function, is related to the usual solution $\psi_i(r)$ through (2)

$$r\,\psi_i(r) = P_i(r)\, S_m(\theta,\phi). \qquad (2)$$

To compute the total energy of the system, another quantity , the medium polarization energy, must be defined. This is the energy required to deform the medium due to the presence of the polarization field exerted by the excess electron. If $\underline{D}$ is the dielectric displacement in equilibrium with this polarization

$$\Pi = \tfrac{1}{2}\, k_o^{-1} \int \underline{P}_i \cdot \underline{D}\, dr + \tfrac{1}{2}\, k_o^{-1}\, k_{st}^{-2} \int \partial(Tk_{st})/\partial T \underline{D}^2 dv.$$

The second factor, the entropy contribution, has generally been omitted in the current theory and will be neglected here also. It should be

noted that the remaining term strictly represents the free energy of polarization.

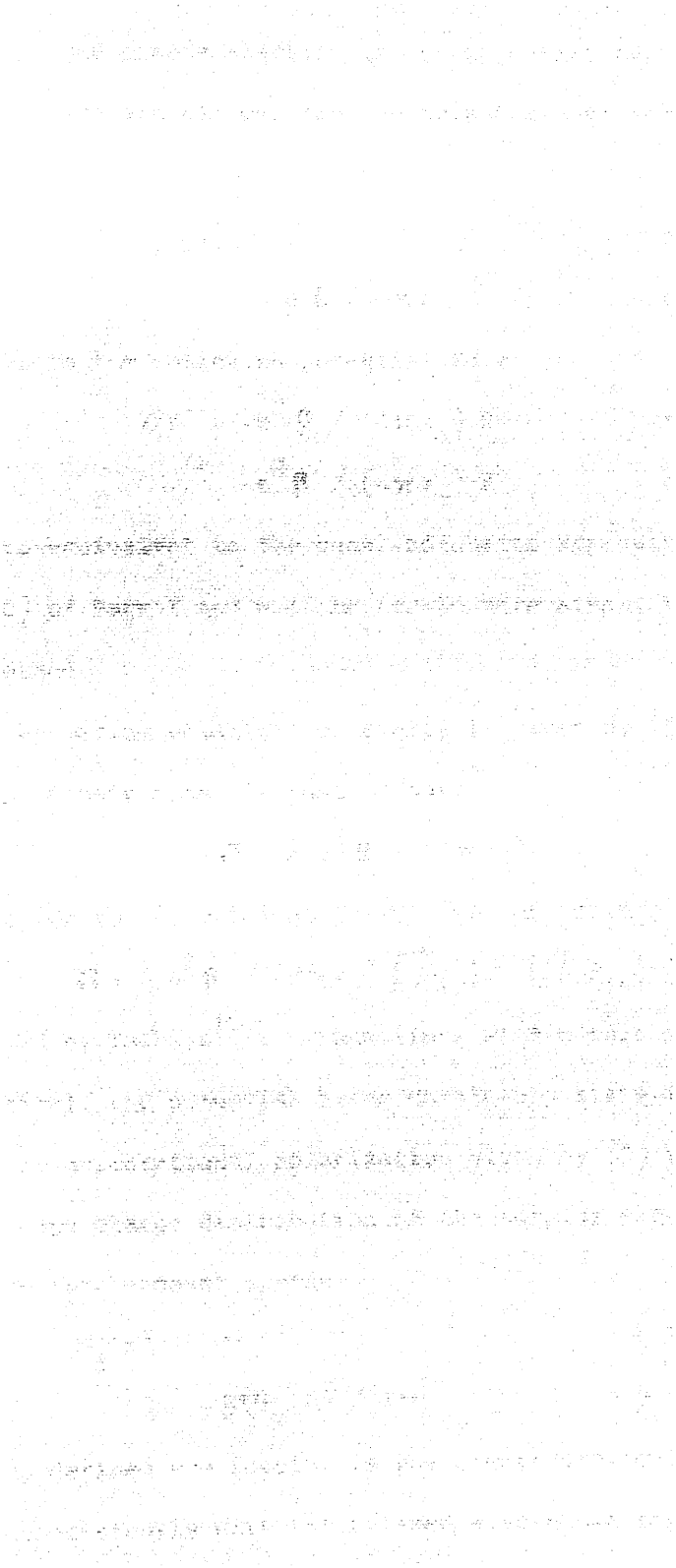

b) Inertial Polarization Effects.

Jortner[103] has assumed that the optical polarization of the medium due to the excess electron is not primarily responsible for electron trapping and has written the orientational polarization, p_{st}, as

$$p_{st}(r) = \begin{cases} 0 & r < R \\ -e\beta / 4\pi r^2 & r > R \end{cases} \tag{3}$$

thus leading to the following potential form

$$V(r) = \begin{cases} -e^2\beta / (4\pi k_o) R & r > R \\ -e^2\beta / (4\pi k_o) r & r < R, \end{cases} \tag{4}$$

This form is equivalent to the quasi-adiabatic approach discussed in Section 1(e) of Part I and will be termed here simply the adiabatic solution method.

The medium polarization energy is given by (5) since the displacement $\underline{D}$ in this model is just $-e/4\pi r^2$

$$\Pi = \tfrac{1}{2} e^2\beta / (4\pi k_o) R \tag{5}$$

This correction to the original formulation of Jortner which specified

$$\Pi = \tfrac{1}{2} e^2\beta / (4\pi k_o) \int_R^\infty P_{1s}(r)\, r^{-1}\, P_{1s}(r)\, dr$$

was suggested by Tachiya[107]. Transitions within this model are of course vertical, the potential being completely state-independent.

The orientational polarization given by (3) is not in equilibrium with the charge distribution of the surplus electron. Taking this balance into account yields

$$p_i(r) = \begin{cases} 0 & r < R \\ -\beta\nabla f_r(r) / 4\pi & r > R \end{cases} \tag{6}$$

where $f_i(r)$, defined previously, is the electrostatic potential associated self-consistently with the relaxed electronic state, r. Straightforward integration yields

$$V(r) = \begin{cases} -\beta e\, \nabla f_r(R) / 4\pi k_o & r < R \\ -\beta e\, \nabla f_r(r) / 4\pi k_o & r > R \end{cases} \tag{7}$$

for the corresponding potential form and leads to an inertial medium polarization energy of

$$\Pi = \tfrac{1}{2}\, e\, \beta \,/\, (4\pi k_o) \left\{ f_i(R) \int_o^R P_i^2(r)dr + \int_R^\infty P_i^2(r)\, f_i(r)\, dr \right\} \quad (8)$$

This is equivalent to an amendment suggested by Land and O'Reilly[106] to Jortner's original adiabatic model and is seen to be, instead, apposite to an scf treatment of inertial polarization effects. It has, however, been carried through into the adiabatic semi-continuum calculation of Kestner, Jortner and coworkers.

Calculations within this model appear not to have been reported, although Jortner[108] has shown the above potential form, (7), to follow from his analysis of dielectric effects on loosely-bound electrons. The potential should be taken, as written, to be governed by the charge distribution pertaining to the relaxed electronic state and a few numerical solutions with this constraint are reported later

c) Optical Polarization Effects.

So far no mention has been made of electronic polarization effects. In Jortner's[103] adiabatic treatment these are included by complementing the single-particle electronic energy, W_i, with a term

$$S_i^e = \tfrac{1}{2}\, e \,/\, (4\pi k_o) \int_r^\infty p_{op}(r)\, r^{-2}\, dv$$

appropriate to this effect. Noting that $p_{op}(r) = -e\gamma/4\pi r^2$ and taking the lower limit in the integration to be $\bar{r}_i$, the mean radius of the i^{th} electronic state charge distribution gives

$$S_i^e = \tfrac{1}{2}\, e^2 \gamma / (4\pi k_o)\, \bar{r} \qquad (9)$$

as an approximate electronic polar energy.

The total electronic energy within this model is then

$$E_i^e = W_i + S_i^e \,,$$

and correlation with the experimental heat of solvation is attempted by setting

$$-\Delta H = E_i^e + \Pi \,.$$

An alternative scf solution scheme deployed by Jortner[109] and later by Fueki, Feng and Kevan[110], who also incorporated it into a semicontinuum approach, implicitly involves the optical polarization in electron binding.

In this picture the total polarization p_t is given by

$$\begin{aligned} p_t(r) &= p_{st}(r) + p_{op}(r) \\ &= 0 && r < R \\ &= -\beta e \nabla f_r(r) / 4\pi - \gamma e \nabla f_i(r) / 4\pi && r > R \end{aligned} \qquad (10)$$

which gives rise to a potential, $V_i(r)$, of

$$\begin{aligned} 4\pi k_o V_i(r) &= -\beta e \nabla f_r(R) - \gamma e \nabla f_i(R) && r < R \\ &\quad -\beta e \nabla f_r(r) - \gamma e \nabla f_i(r) && r > R \end{aligned} \qquad (11)$$

and a medium polarization energy, U_i, of

$$\begin{aligned} 4\pi k_o\, U_i = {} & \tfrac{1}{2}\ \beta e \left\{ f_r(R) \int_o^R P_r^2(s)\, ds + \int_R^\infty P_r^2(s)\, f_r(s)\, ds \right\} \\ & + \tfrac{1}{2}\ \gamma e \left\{ f_i(R) \int_o^R P_i(s)\, ds + \int_R^\infty P_i^2(s)\, f_i(s)\, ds \right\} \end{aligned} \qquad (12)$$

due to both inertial and optical effects. r is written to represent the relaxed state in contrast to i which is the instantaneous state under consideration. The potential is now strongly state-dependent. The total energy of the system, medium + electron, may be obtained as

$$E_i = W_i + U_i$$

which implies that the heat of solvation is simply given by the negative of the total ground state energy. It is important to realize that transitions, vertical in the Franck-Condon sense, are now accompanied by a change in optical polarization.

Along with Jortner's adiabatic model this scf method has been incorporated into the mainstream of theoretical development of the semicontinuum models.

d) A Comparison and One Refinement.

As already mentioned, the scf approximation, which sets all the electrons on an equal footing, neglects the capabilty of the medium electrons to follow the detailed motion of the trapped species. On the other hand, the adiabatic treatment asserts this possibility to its full extent in assuming that the trapped potential is solely derived from inertial effects.

Since the binding energies of excess electrons, solvated or trapped, in polar substances is of the order of a few eV, the scf approach seems more justifiable. The criterion for the applicability of the adiabatic model, namely the large binding energy difference required between the medium and the surplus electrons, is scarcely satisfied. The ultra-violet edge of absorption is around 5 eV in these materials. Thus, while the adiabatic model undoubtedly overestimates the screening of the electronic polarization, the scf scheme precludes the existence of any correlated motion. Some more sophisticated technique designed to probe beyond the Hartree-Fock limit in an effort to include the effect of electronic polarization in a reasonable fashion is clearly required.

Tachiya et al.[111] have suggested that these polarized cavity models in fact also misjudge the effect of orientational polarization. Neither the adiabatic nor the scf approach account for the situation of inertial polarization in the vicinity of the elctron. In an attempt to allow for this, these workers have introduced a proportionality constant not equal to β between the orientational polarization and its equilibrium electric displacement.

Before the development of the theory required for the semi-continuum approach, one important modification of the simple polarized cavity models was investigated. This is the addition to the potential of a constant term, V_o, outwith the cavity, the energy of the so-called

quasi-free electron in the medium. This appears entirely analogous to the referral of the energy within the cavity, in the corresponding colour centre theory, to the bottom of the conduction band as zero. Experimental estimates of this quantiy in polar liquids are not at present available, though it does seem amenable to measurement. Reliable estimates do exist for rare-gas liquids[112] and liquid hydrocarbons.[113]

Theoretically, Springett et al.[114] have shown that a constant value of V_o (not varying with radius) usually provides a satisfactory description of the electron-medium interaction in the continuum. In the simple polarized cavity model it is taken to account for electronic polarization interactions within the bulk medium in addition to a kinetic energy term including scattering by medium molecules. It is therefore a very sensitive quantity strongly dependent on the delicate balance between long-range attractive and short-range repulsive forces. Some rather crude calculations of V_o have been performed[115] by applying the Wigner-Seitz sphere model to an electron in a dense polarizable fluid. The result for ammonia, $V_o = 0.2 + 1.0$ eV[116], is clearly most unsatisfactory and further clarification of this quantity is undoubtedly necessary.

Jortner and Kestner[116] have performed calculations for a variety of values of V_o added to Jortner's adiabatic model. However, any attempt to embellish the scf potential with this same term must be viewed with suspicion. Some of the factors it was introduced to handle have already been taken care of in this different formulation.

e) Results and Discussion.

In an effort to gain insight into the structure of the ammoniated electron, Jortner[103] has performed a variational solution of the simple adiabatic polarized cavity model using the potential given in the equation (3), with $k_{op} = 1.756$ and $k_{st} = 22.0$ appropriate to a temperature of 240°K. Employing the cavity radius as an adjustable parameter he attempted to match the peak of the observed absorption spectrum. With values of between 3.0 Å and 3.45 Å for the radius, 3.2 Å being the point of match, reasonable estimates of other experimental observables were obtained. Computing, for example, 1.67 eV for the heat of solution, which agrees very favourably with the derived value 1.7 ± 0.7 eV presented in this same paper as following from experiment. Happily, the existence of a cavity of radius in the region of 3.0 Å also offers a satisfactory account of the bulk volume expansion which accompanies the dissolution of metals in liquid ammonia. Various semi-empirical estimates of the "radius" of the ammoniated electron have been suggested[117]. These turn out to be mainly in the region of 4.5 Å. Taking the mean radius of the surplus electron in its ground state as a measure of this effective radius again provides a nice fit to the observed data.

Unfortunately, not only is the treatment in terms of an empirical radius, chosen to fit some observable rather suspect, but also the description of the electron-medium interactions implicit in this model is hopelessly naive. This latter deficiency has been, to some extent, screened by the use of an approximate solution technique. Namely, the Schrodinger equation incorporating the adiabatic potential has been solved variationally using one-parameter, single-exponential trial functions

$$P_{1s}(r) = N_1 \, r \exp(-ar)$$
$$P_{2p}(r) = N_2 \, r^2 \exp(-br). \qquad (13)$$

Tables II.1 and II.2 present a comparison of Jortner's variational results with the corresponding values obtained by the present numerical method. The agreement, at 3.2 Å, with the optical transition energy is at once spoiled, a cavity size of 3.69 Å being required to regain the concurrence. The heat of solvation is altered from 1.67 eV to 1.818 eV on accurate solution and to 1.085 eV by including the medium polarization energy (4) of Tachiya which is consistent with the simple potential form chosen.

In detail, it is evident that the numerical solution method lowers the derived 1s energy by between 8 and 10%, while having a considerably smaller effect on the 2p level, affording only a 3% improvement. This is in marked contrast with the large amelioration of the 2p energy arising from a similarly improved calculation scheme in the polarized cavity models solved in Part I relating to colour centres. Differences in the respective forms of trapping potential are the cause. The single-exponential 2p function employed in both cases offers a much better fit to the exact solution of the truncated coulombic potential arising here than to the square-well like form apposite to the F-centre problem. This difference is further evidenced in Figure II.4 which depicts the numerical and variational ground and first-excited state functions for the ammoniated electron in a cavity of 3.0 Å. The numerical 1s function is noticeably more compact than its variational counterpart while the 2p functions are much less disparate. The extent of the differences is not made clear by merely stating the magnitude of the discrepancies in the mean radii of these functions; 11% for the 1s case and 7% for the 2p functions. This quantity is insufficiently sensitive to the precise nature of the functions.

A much better guide is offered by the ratio, t_f, of the dipole-velocity and dipole-length oscillator strengths. As before

$$t_f = f_{vel} / f_{len}.$$

Scrutiny of Table II.2 reveals that even the t_f values of the numerically obtained functions are very far from unity. This in no way reflects the badness of the solution accomplished. It arises, rather, from the effect of the ad hoc inclusion of the electronic polarization energies into the transition energy required to compute the oscillator strengths. Neglecting this contribution to the electronic energy gives a transition energy at R = 3.0 Å of 0.585 eV whence the oscillator strengths of $f^v_{len} = 1.17$, $f^v_{vel} = 0.92$, $f^n_{len} = 0.941 = f^n_{vel}$ may be computed. The variational values were computed, using the optimum 1s and 2p exponents a and b respectively, from

$$f^v_{len} = 2^{11}\, a^3\, b^5 \,/\, (a+b)^{10}\, E(a)$$
$$f^v_{vel} = 2^7\, a^5\, b^5 \,/\, (a+b)^8\, E(a)^{-1}. \qquad (14)$$

Employing these improved f-values yields a t_f ratio of 0.78 for the variational functions and 1.000 for those derived numerically. This is now in much better accord with corresponding results secured in Part I. Clearly the inclusion of electronic polarization effects in the transition energy must be supplemented by the incorporation of the long range medium polar modes in the wave-functions bracketing the dipole-moment operator in the computation of the transition matrix elements. Otherwise really poor velocity-length concurrence results, the latter predicting values well in excess of unity.

Rusch et al.[118] have carried out an extensive program of variational solution within this model for cavities in ammonia ranging from 1.0 Å to 10.0 Å in radius. Figure II.2 displays their results, again obtained by employing an inflexible single-parameter trial function to describe both the ground (1s) and first excited (2p) states. The 1s lowering achieved by the present method persists over all cavity radii studied as does the 2p improvement, though as mentioned it is not so distinct. Also included in this diagram are the numerically obtained 2s and 3p functions. Assuming vertical transitions, as indicated

by the vertical line at 3.69 Å, a 1s - 2p transition energy of 0.800 eV is obtained at this radius, which mimics the observed peak value. The 1s - 2s transition, which is symmetrically forbidden, would occur at 1.24 eV; inside the envelope of the absorption band. The 1s - 3p transition would be peaked at 1.47 eV very far out into the high energy tail of the band.

One interesting feature concerned in this graph is the similarity in the behaviour of the s function energies at small R, steadily decreasing up to R = 0. Contrast the flattening observed in the p functions. Such likenesses are again demonstrated in Figure II.3 which plots the mean radii of the numerical functions and variational ones where available against cavity radius. The p functions are linear in R for large R only, while the s functions are approximately linear for all R. This reflects the differences inherent in the short-range nature of s and p functions. The discrepancies in the mean radii between the numerical and variational representations of both 1s and 2p functions are quite significant and similar to that in the cavity range studied by Jortner. They tend to become more pronounced at large R, this tendency being greater for the 2p function and to become less noticeable for small R. This is just what should be expected since the single-exponential functions should provide a good fit in the limit of zero-cavity radius, where the potential will become hydrogenic, falling off as βr^{-1}. The variational one-parameter 1s function loses this agreement quickly being more sensitive to the short-range (near r = o) behavior of the potential which changes drastically on defining a cavity of any size. The 2p function is governed to a greater extent by the nature of the coulomb tail and is somewhat insensitive to the potential at small r. Following this reasoning the single-exponential 3p energy is expected to be in close agreement with the numerical value. This is borne out by the slight dependence of the

3p energy on cavity radius shown in Figure II.1 and by the likeness of the scaled hydrogenic 3p energy to that derived numerically; these being coincident at 0.668 eV for zero cavity radius and differing by only about .07 eV at R = 3.2 Å.

Figure II.2 depicts the variation of transition properties with cavity radius. Both the variational results computed from the work of Rusch et al. and the present numerical values are included. It is seen that the alterations in the dipole matrix elements and the transition energies, obtained numerically, combine to exaggerate the discrepancies in the dipole-length oscillator strength. In the dipole-velocity case the effect of the changes has been cancelled to an appreciable extent.

Jortner[119] has essayed a matching of the optical properties of the hydrated electron using this same model potential and employing an identical variational solution technique. 1.45 Å is the chosen cavity radius. This is the average O - O distance in liquid water and stronger hydrogen bonding, larger surface tension and a smaller pressure effect on the spectrum than in ammonia, all suggest the presence of a smaller cavity in the former medium.

Tables II.3 and II.4 outline the comparison of these results with those secured numerically. The numerical 1s energy shows the expected magnitude of improvement but the variational 2p energy is, most surprisingly, lower than its numerical counterpart. The reason for this is unclear, Jortner not having reported any other data associated with this excited state. It is also somewhat disheartening to find that the numerical medium polarization energy, computed by the original Jortner formula is lower than the corresponding variational result. This is contrary to what was discovered in ammonia where the numerically derived values were consistently 5 - 6% below the variational value. However, a fresh computation of this quantity from

Jortner's original formula, using a 1s exponent of 0.284 au^{-1}, which reproduces the reported mean radius of this state, gave the value Π = 1.152 eV in much closer accord with the calculated trends in ammonia. It is not stated whether Jortner perhaps used some other formula to obtain his medium energy, e.g. the Land and O'Reilly amendment (7) though this would seem to yield but 1.28 eV with the above exponent. The results presented by Jortner suggest a heat of solution of around 1.85 eV, neglecting the cavity creation energy which is assumed to be small and was not included in the original formulation of the model potential. An optical transition energy of 1.65 eV was also computed. Both of these values are reasonably close to the experimental 1.72 eV and 1.70 eV respectively.

Numerical solution at 1.45 Å damages this agreement considerably. The new transition energy is placed at 2.089 eV and the heat of solvation at 2.488 eV using Jortner's formula or 0.994 eV assuming Tachiya's equation for consistency. The tables also include the numerical results at 1.84 Å cavity radius which reproduces the experimental absorption band maximum. However, the heat of solution is still badly overestimated (and underestimated by Tachiya's method). Jortner's comment that the (variationally obtained) "agreement should not be taken too seriously, as the theory is semi-empirical" certainly requires amplification for the case of hydrated electrons in the light of the present findings.

Application of the adiabatic treatment of the polarized cavity model in the context of a variational solution method has also been attempted in an investigation of the properties of crystalline ice[120] at 77°K. Using a "realistic" value for the dielectric function at low frequencies, k_{st} = 3.0, which implies orientational polarization is frozen in, no parametric fit to the observed band peak can be obtained. In the limit of zero-cavity radius, the relative permittivities

used imply a transition energy of only 1.20 eV, much too low to agree with experiment. Employing a static relative permittivity of 75.0, i.e. assuming free rotation of ice dipoles, which is unrealistic in view of the long relaxation time[121] allows a correlation of the maximum in the optical spectrum at a cavity radius of 1.37 Å.

Figure I.5 charts the variational solutions as a function of cavity radius for both the above parameterizations. Numerical calculations also presented in this figure show similar amelioration to those discussed in connection with water and ammonia. The alteration of k_{st} increases the orientational polarization contribution in the latter model and the effect of the improved solution technique is to move the optimum radius from the variationally obtained value of 1.38 Å out to 1.62 Å where a photoelectric threhold of 3.67 eV is now predicted. Julienne and Gary conclude that, since the correct dielectric function is unable to reproduce the band parameters, the surplus electron is most likely trapped in a region of physical defect. Clearly the failure of the simple polaron model here should not be taken too seriously, though, and more realistic attempts to compute the properties of electrons trapped in ice must be evaluated before such a conclusion is substantiated.

While it has been asserted that the scf formulation of the polarized cavity model is theoretically preferable to the approach just discussed, only a few calculations of the properties of excess electrons have been completed within this framework. Jortner's original application of this scheme[109] attempted to explain the observed optical and thermochemical properties of the hydrated electron. Columns 1 of Tables II.5 and II.6 contain these original results, as usual determined by recourse to an inflexible, one-parameter, variational trial function.

One disquieting finding was that, even in the limit of zero-

cavity radius, the prediction of this model of a 1s -2p transition energy of 1.33 eV is only beginning to approach the experimental value. This limit, of course, supplies the highest possible 1s -2p energy separation given by the model, since the quantity decreases steadily with increase in cavity radius. The heat of solution, at 1.30 eV, was also somewhat lower than would be desired. It should be noted that the original value of the total 1s state energy quoted in ref. 109 and repeatedly cited in subsequent reports is, in fact, in error. It appears that a factor of δ has inadvertently been omitted. The revised value, 1.30 eV replacing the old 1.32 eV, follows from the formula of the original source. Though this slight amendment is in no way serious, the properties computed by the variational approach of Jortner have been reestimated assuming that the error was not typographical. Thus the values reported here differ marginally from those of the initial work. The failure to replicate a reasonable transition energy for the hydrated electron has led to some concern over this use of the scf model.

In an attempt to alleviate the uncertainty surrounding the application of the scf treatment to this problem, Fueki, Feng and Kevan[122] endeavoured to enhance the accuracy of the variational solution by employing a much more flexible three-parameter trial function for the ground state of the form

$$P_s = N(P_{1s} + cP_{2s})$$

where $$P_{1s} = \left\{(2a)^3/2\right\}^{\frac{1}{2}} r \exp(-ar)$$

and $$P_{2s} = \left\{(2b)^3/2\right\}^{\frac{1}{2}} r\,(ur-1)\exp(-br).$$

A one-parameter representation of the 2p excited state was maintained and a cavity of zero radius was chosen for simplicity. Treating a,b and c as independent variational parameters yielded a massive, greater than 30%, lowering of the 1s energy with respect to Jortner's one-parameter work. The new transition energy was evaluated as 2.18 eV and the heat of solution placed at 1.81 eV. Consequently these workers

were able to assert that the observed band maximum could be fitted at a finite cavity radius. However, due to the complexity of this calculation, no attempt was made to further verify this statement by actually deriving this radius.

Tables II.5 and II.6 also include these new results together with the corresponding numbers secured employing the present finite-difference technique. The current numerical results fail to reproduce the vast improvement apparently obtained by the three-parameter work. Instead, the magnitude of the amelioration on Jortner's results is quite comparable to that obtained in the adiabatic treatment. The numerical ground state energies are again about 10% better. The mean radii are up to 12% more compact. No direct comparison of the total excited state energy is permissible since this quantity depends implicitly on the ground state inertial polarization energy. A more compact 1s function increases U_{st}, which governs the static polarization of all unrelaxed states. This tends to make the 2p energy more positive and hence conceals any improvement in the single-particle energy obtained.

The mean radii of Fueki et al. lie, quite reasonably, between the crude single-exponential and the accurate numerical values. Figures II.6 and II.7 tell a differnt story. While all three excited state functions are rather similar (Fig.II.7) the multi-parameter ground state function is markedly inappropriate (Fig.II.6). Further support for the veracity of the numerical function is provided by a comparison with a relatively flexible variational function employed by Pekar[100] in an unwitting solution of this self-same scf problem. Using a function of the form

$$P_{1s} = N\, r\, (1+dr+er^2)\, \exp(-dr),$$

Pekar obtained, with optimum parameters $d = .65$ au^{-1} and $e = d^2$, a total ground state energy of 1.45 eV, almost identical to that given

by the current work. A plot of this function is almost indistinguishable from the present numerical function and is not included in Figure II.6. Pekar's transition energy can not, however, be taken over for comparison as the altered effect of electronic polarization on the excited state was neglected in his work.

The total excited state energy computed by Fueki, Feng and Kevan is considerably more positive than the pertinent values of the other treatments. This is presumably due to the large inertial polarization developed through the nature of the ground state function of the former approach. In conclusion, it is apparent that the simple polarized cavity model, solved within the scf approximation, is incapable of reproducing the observed optical properties of the hydrated electron.

Table II.7 presents a comparison of one other set of calculations within this approach on the surplus electron in water. The one-parameter variational results of Jortner and the current numerical solutions again follow similar trends as in the adiabatic case. The numerical ground state energy is now almost 18% improved, a consequence of the gradual deterioration of the quality of the single-exponential fit to the true function for large cavities. The poorness of the match is evidenced in Figure II.9 which plots the ground state functions resulting from both treatments. Clearly, stating that the mean radii of these functions differ by 11% again conceals the extent of the disparity.

Since the permittivities of ammonia and water are somewhat similar, it is reasonable to expect that the scf solution will be capable of replicating the experimental absorption maximum in the former medium. This was found to be the case and Table II.8 sets the variational work of Jortner[123] with one-parameter variational functions as usual, alongside the numerical properties derived here. The trends in

the differences exhibited are, once more, entirely analogous to those found previously, both in the scf treatment of water and in the results obtained in the adiabatic approach. Also included are the values relevant to a cavity of radius 2.93 Å, at which the computed transition energy matches the absorption peak. The heat of solution, 1.09 eV, and the photoelectric threshold, 2.871 eV, are both somewhat at variance with experiment.

Figure II.9 reproduces the numerical results obtained here over a range of cavity sizes from 0.0- 5.0 Å, the vertical line indicates the point of match with the optical spectrum. The change in these energies with cavity radius is noticeably dissimilar to that observed on adiabatic solution (see Fig. II. 1). The s and p type energies behave here in a like fashion especially for small cavity size. At large R the 1s energy is rather more sensitive to variations in the cavity dimensions. The transition energy is seen to decrease monotonically with R as expected. This scf treatment of the ammoniated electron also underestimates the observed dependence of the absorption peak on temperature unless the coefficient of temperature expansion of the cavity is taken to be much in excess of 3.0×10^{-3} Å/deg.

The reasons underlying the differences in behaviour with R of the adiabatic versus the scf solution are evident from Figure II.10. This depicts the effective potentials experinced by the electron in these models as a function of cavity radius. All the adiabatic states are supported by the potential ϕ_a which drops off precipitously to $-\infty$ as R tends to zero. The scf potentials are, of course, state dependent but, in general, tend to some relatively small negative value as the cavity shrinks.

To complete this section, results within the scf formulation of the polarized cavity model, but neglecting all electronic polarization effects, equation (6), are listed as a function of cavity radius in Table II.9. The parameters employed in the numerical derivation of

these solutions are relevant to the ammoniated electron. The importance of the optical contributions to the scf scheme is at once demonstrated. In their absence the total ground state energies are very small and the upper limit on the predicted transition energy is but 0.504 eV. One comment is in order. It will be seen from this table that the concurrence of the dipole-length and dipole-velocity oscillators strengths has been regained in this formulation. The two values are identical for the 1s- 3p transition. The t_f values for the inertial + optical scf treatment were markedly different from unity. the reason is obvious. Again, as in the adiabatic approach the inclusion of state-dependent electronic polarization effects in the transition energy mars the length/velocity agreement. In the scf model this implies that the inclusion of some type of medium mode is again necessary if an accurate oscillator strength is required.

f) Conclusion.

The present numerical solution technique is seen to afford about a 10% improvement on the single-particle energies computed in the one-parameter variational work reported previously for both the adiabatic and scf formulations of the polarized cavity model. Derived properties are altered by a corresponding amount.This improvement in the accuracy of the obtained solution brings a number of results into question.

In the adiabatic treatment of the ammoniated electron the inclusion of a consistent form of medium polarization energy leads, when the potential is parameterized to fit the maximum in the optical absorption band, to a heat of solution which substantially underestimates the experimental value. Also, the predicted photoelectric threshold is somewhat higher than would be hoped. Application of this model to the hydrated electron, with the same matching criterion, yields a similarly disparate heat of solution. Attempts to correlate the observed properties of trapped electrons in ice by this approach require the inclusion of an unrealistically large low-frequency relative permittivity. The resulting increased inertial polarization is necessary to produce a potential well sufficiently deep to support electronic levels which would give rise to the experimental absorption band.

More critically, the hopefully superior scheme fails to give account of the optical properties of surplus electrons in water, despite a recent claim to the contrary. In actuality an early work of Pekar (1946!) is supported. For the ammoniated electron a parametric fit to the absorption peak may be achieved, but only at the expense of an unsatisfactorily low heat of solution and high photoelectric threshold. In addition, the sensitivity of the energy levels to variations in cavity size are insufficient to reproduce the observed temperature dependence of the spectrum. Efforts to reproduce the optical absorption spectrum of electrons in ice at $77^{o}K$, though not

reported here, using the scf approximation again fail. Even the incorporation of the artificially enlarged static dielectric function mentioned above was inadequate to allow prediction of a reasonable transition energy.

In both approximate formulations the computation of transition moments from purely electronic wave-functions and from state energies determined in part by the effect of electronic polarization generates some doubt as to the validity of the derived oscillator strengths. Though several theoretically reasonable methods exist[124] for computing the entire line-shape expected in both models, such a calculation was not pursued. The conceptual content of the polarized cavity models presented above was judged too naive to make this worthwhile. Instead, such a construction has been reserved for the semicontinuum models which are discussed in subsequent sections. It is expected that ameliorations in the single-exponential variational solutions of these models, performed to date, will be entirely analogous to those disclosed here.

The failure of the polarized cavity models, formulated within either the adiabatic or the scf approach, to take account of the structure of the medium may be overcome in an entirely different manner. This is demonstrated in the work of Dogonadze and Kornyshev[125] who have developed a many-body description of polar fluids in terms of the so-called electrodynamics of media with spatial dispersion. The underlying idea of this approach is the replacement of the local relation for the total polarization

$$\underline{P}_t(\underline{r}) = (1 - k_{st}^{-1})\underline{D}(\underline{r})$$

by a nonlocal equivalence of the type

$$\underline{P}_t^a(\underline{r}) = \Sigma_b \int c_{ab}(\underline{r},\underline{r}')\, \underline{D}^b(\underline{r}')\, d\underline{r}' \qquad (15)$$

where $c_{ab}(\underline{r},\underline{r}')$ depends on the static permittivity tensor $k_{st}^{ab}(\underline{r},\underline{r}')$, hence the term"spatial dispersion", through

$$c_{ab}(\underline{r},\underline{r}') = \delta_{ab}\,\delta(\underline{r}-\underline{r}') - \left\{k_{st}^{ab}(\underline{r},\underline{r}')\right\}^{-1}.$$

The mean dipole orientation in the bulk medium will now depend on the displacement at every point, thus allowing for the correlated motion of the medium molecules, which must surely exist. It is hoped to explore this promising avenue.

Tables IIa

Properties of surplus electrons derived from polarized cavity models.

Tables 1-4 contain results from adiabatic calculations, 1 and 2 in ammonia, 3 and 4 in water. The numbers obtained from the scf solution scheme are in Tables 5-9. 5 and 6 are for water with zero cavity radius, 7 in a void of 3.3 Å. 8 and 9 present results for ammonia.

All energies are in eV, distances in Å.

Table II.1

R	3.0^{v}	3.0^{n}	3.2^{v}	3.2^{n}	3.69^{n}
-W(1s)	1.415	1.501	1.356	1.440	1.310
-S(1s)	0.745	0.842	0.717	0.809	0.740
-E(1s)	2.160	2.344	2.073	2.249	2.050
-W(2p)	0.826	0.823	0.790	0.810	0.771
-S(2p)	0.484	0.518	0.472	0.507	0.479
-E(2p)	1.306	1.342	1.262	1.317	1.250
Π^{T}	1.258	1.258	1.179	1.179	1.022
Π^{J}	0.494	0.525	0.475	0.484	0.403
ΔH^{T}	-	1.085	-	1.070	1.028
ΔH^{J}	1.67	1.818	1.60	1.765	1.647

n present numerical results

v one-parameter solution [103].

Table II.2

R	3.0^{v}	3.0^{n}	3.2^{v}	3.2^{n}	3.69^{n}
$\bar{r}(1s)$	4.17	3.679	4.32	3.825	4.162
$\bar{r}(2p)$	6.42	6.004	6.56	6.122	6.487
E(a)	0.85	1.002	0.81	0.932	0.800
$f_{len}(a)$	1.70[a]	1.392	1.74[a]	1.406	1.435
$f_{vel}(a)$	0.63[a]	0.637	0.62	0.642	0.651
t_f	0.37	0.457	0.36	0.456	0.454
E(a')	-	1.738	-	1.652	1.471
$f_{len}(a')$	-	0.055	-	0.047	0.034

a computed from reported exponents[103]

n present numerical solution

v one-parameter variational solution[103]

Table II.3

R	1.45^{v}	1.45^{n}	1.84^{n}
$-W(1s)$	2.34	2.413	2.152
$-S(1s)$	1.11	1.308	1.150
$-E(1s)$	3.45	3.721	3.302
$-W(2p)$	-	1.002	0.980
$-S(2p)$	-	0.632	0.610
$-E(2p)$	1.80	1.634	1.590
Π^{T}	-	2.727	2.149
Π^{J}	1.60	1.233	0.962
ΔH^{T}	-	0.944	1.153
ΔH^{J}	1.85	2.488	2.340

n present numerical work

v one-parameter variational solution[119]

Table II.4

R	1.45^{v}	1.45^{n}	1.84^{n}
$\bar{r}(1s)$	2.8	2.402	2.730
$\bar{r}(2p)$	-	4.752	5.014
E(a)	1.65	2.089	1.700
$f_{len}(a)$	-	1.165	1.253
$f_{vel}(a)$	-	0.529	0.584
t_f	-	0.463	0.466
E(a')	-	3.008	2.623
$f_{len}(a')$	-	0.053	0.103

n present numerical work

v one-parameter variational solution[119]

Table II.5

W(1s)	-3.92[a]	-4.319[n]	-
E(1s)	-1.30	-1.440	-1.81[b]
U_{st}	1.46	1.602	-
$U_{Op}(1s)$	1.16	1.278	-
W(2p)	-2.01	-2.175	-
E(2p)	0.03	0.088	0.37
$U_{op}(2p)$	0.59	0.661	-

a one-parameter variational work, corrected from ref. 109

b three-parameter variational work[122]

n present numerical solution.

Table II.6

$\bar{r}(1s)$	2.55[a]	2.250[n]	2.4[b]
$\bar{r}(2p)$	4.9	4.292	4.6
E(a)	1.33	1.529	2.18
$f_{len}(a)$	0.98	0.714	0.88[c]
$f_{vel}(a)$	0.84	0.917	-
t_f	0.86	1.284	-
E(a')	-	2.375	-
$f_{len}(a')$	-	0.146	-
$f_{vel}(a')$	-	0.101	-

a one-parameter variational solution[109]

b three-parameter results[122]

c computed here

n numerical work.

Table II.7

$E(1s)$	-0.91^{v}	-1.101^{n}
$E(2p)$	0.02	-0.358
$\bar{r}(1s)$	3.95	3.514
$\bar{r}(2p)$	-	5.254
$E(a)$	0.93	0.743
$f_{len}(a)$	-	0.916
$f_{vel}(a)$	-	1.029
t_f	-	0.890
$E(a')$	-	1.425
$f_{len}(a')$	-	0.125
$f_{vel}(a')$	-	0.050

n present numerical work

v one-parameter variational solution[109]

Table II.8

R	0.0	1.0	2.0	3,0	4.0
$-E(1s)$	0.404	0.406	0.401	0.385	0.362
U	0.811	0.810	0.782	0.709	0.624
$\bar{r}(1s)$	4.232	4.238	4.364	4.734	5.257
$\bar{r}(2p)$	7.021	7.012	7.105	7.390	7.851
E(a)	0.504	0.504	0.479	0.414	0.341
$f_{len}(a)$	0.933	0.936	0.943	0.962	0.978
$f_{vel}(a)$	0.934	0.935	0.944	0.963	0.978
t_f	1.001	0.999	1.001	1.000	1.000
E(a')	0.879	0.866	0.840	0.769	0.663
$f_{len}(a')$	0.037	0.043	0.034	0.028	0.016

Table II.9

R	0.0^{v}	0.0^{n}	3.2^{v}	3.2^{n}	2.93^{n}
W(1s)	-	-4.407	-	-2.706	-2.871
E(1s)	-1.21	-1.349	-0.92	-1.053	-1.092
W(2p)	-	-2.030	-	-1.756	-1.792
E(2p)	0.05	0.077	0.01	-0.320	-.292
$\bar{r}$(1s)	2.67	2.320	3.96	3.490	3.326
$\bar{r}$(2p)	-	4.472	-	5.345	5.206
E(a)	1.26	1.426	0.93	0.732	0.800
$f_{len}(a)$	1.0	0.709	0.7	0.904	0.889
$f_{vel}(a)$	-	0.916	-	1.026	1.021
t_f	-	0.744	-	0.881	0.871

n present numerical solution

v one-parameter variational work[109]

Figures IIa

Figures 1-9 contain results from polarized cavity models of surplus electrons.

Adiabatic energy levels for ammonia at 240°K are in 1, 2 has the derived transition properties, 3 the mean radii and 4 the wavefunctions in a 4.0 Å cavity. Adiabatic results for water and ice (dashed quantities) are in 5.

6 and 7 have scf ground and excited state functions for the hydrated electron at zero cavity radius respectively. 9 is this in a 3.3 Å void. An scf treatment of ammonia yields 8.

Everywhere (a) is the ground 1s state, (b) the excited 2p, (c) 2s, (d) 3p. Except in 2 where (a) is the 1s-2p transition, (b) is $f_{len}(1s\text{-}2p)$, (c) is $f_{vel}(1s\text{-}2p)$ and (d) is the 1s-3p energy. Full-line is variational result except in 8 where these are circled points. Broken-line is numerical work (in 8 its full). The chain-line in 6 and 7 is a three-parameter solution[122].

Figure 10 compares the adiabatic and scf potentials experienced by the ammoniated. ϕ_i are the scf state-dependent potentials, ϕ_a is the common adiabatic well.

Figure II.1

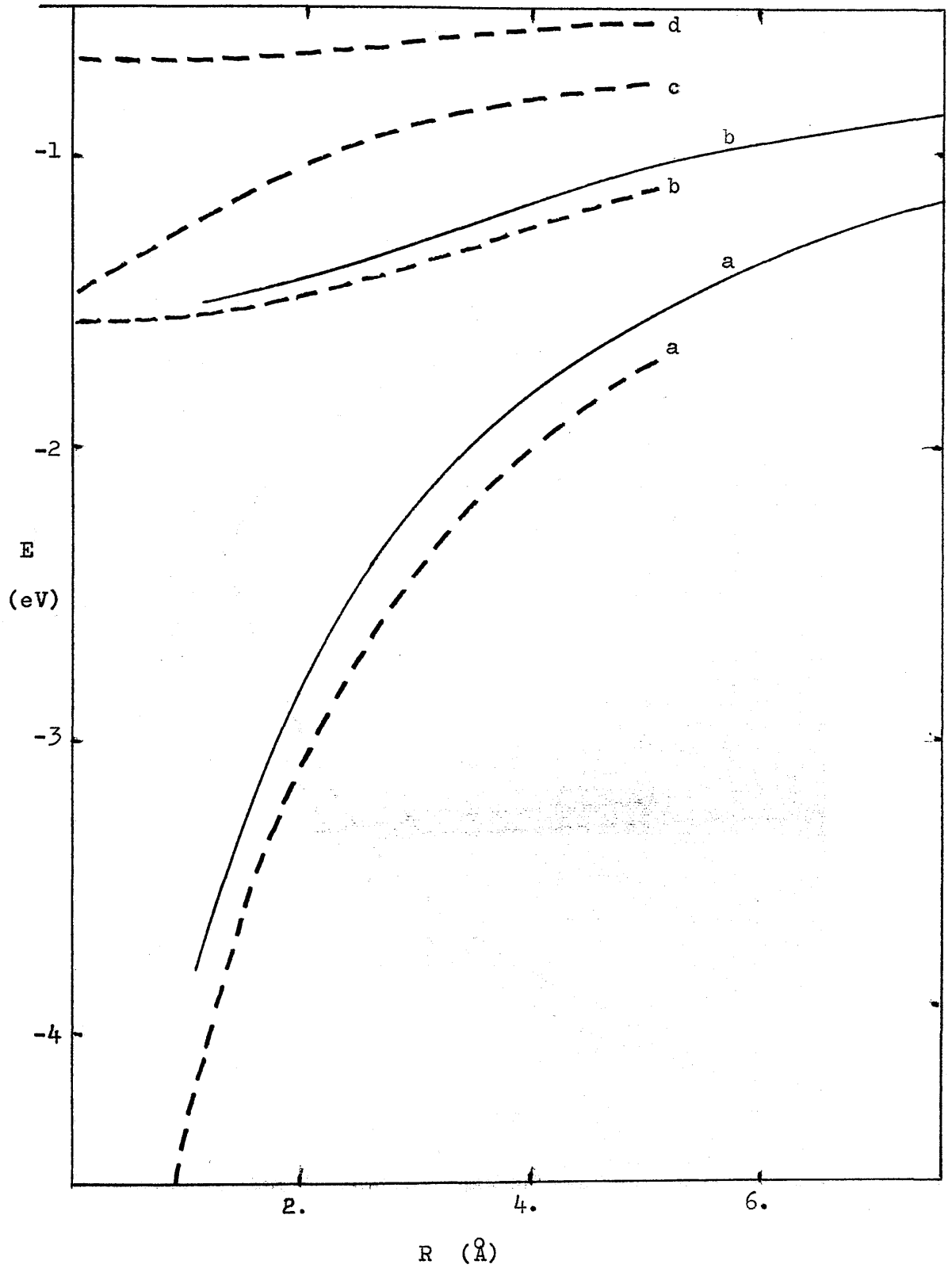

Figure II.2

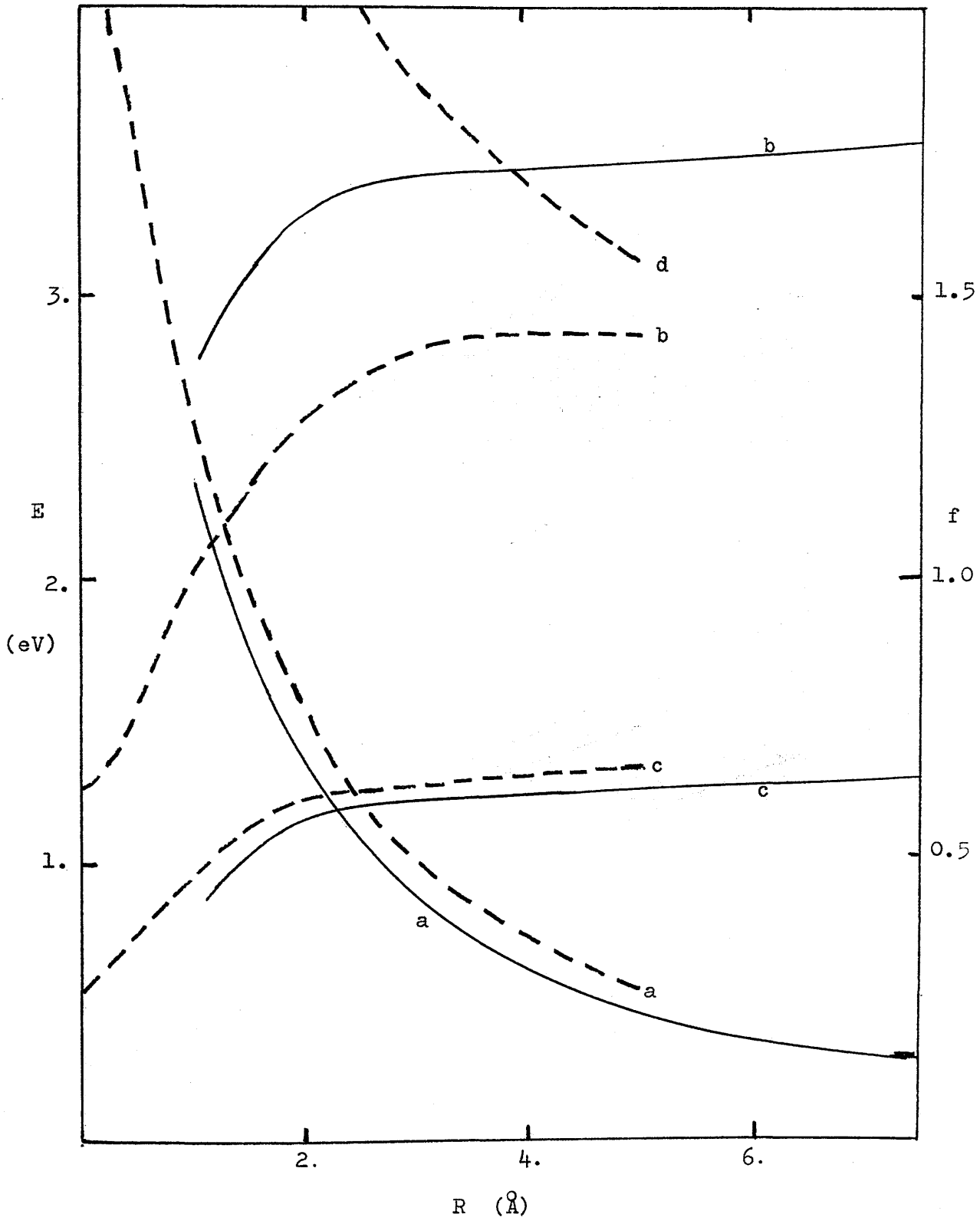

Figure II.3

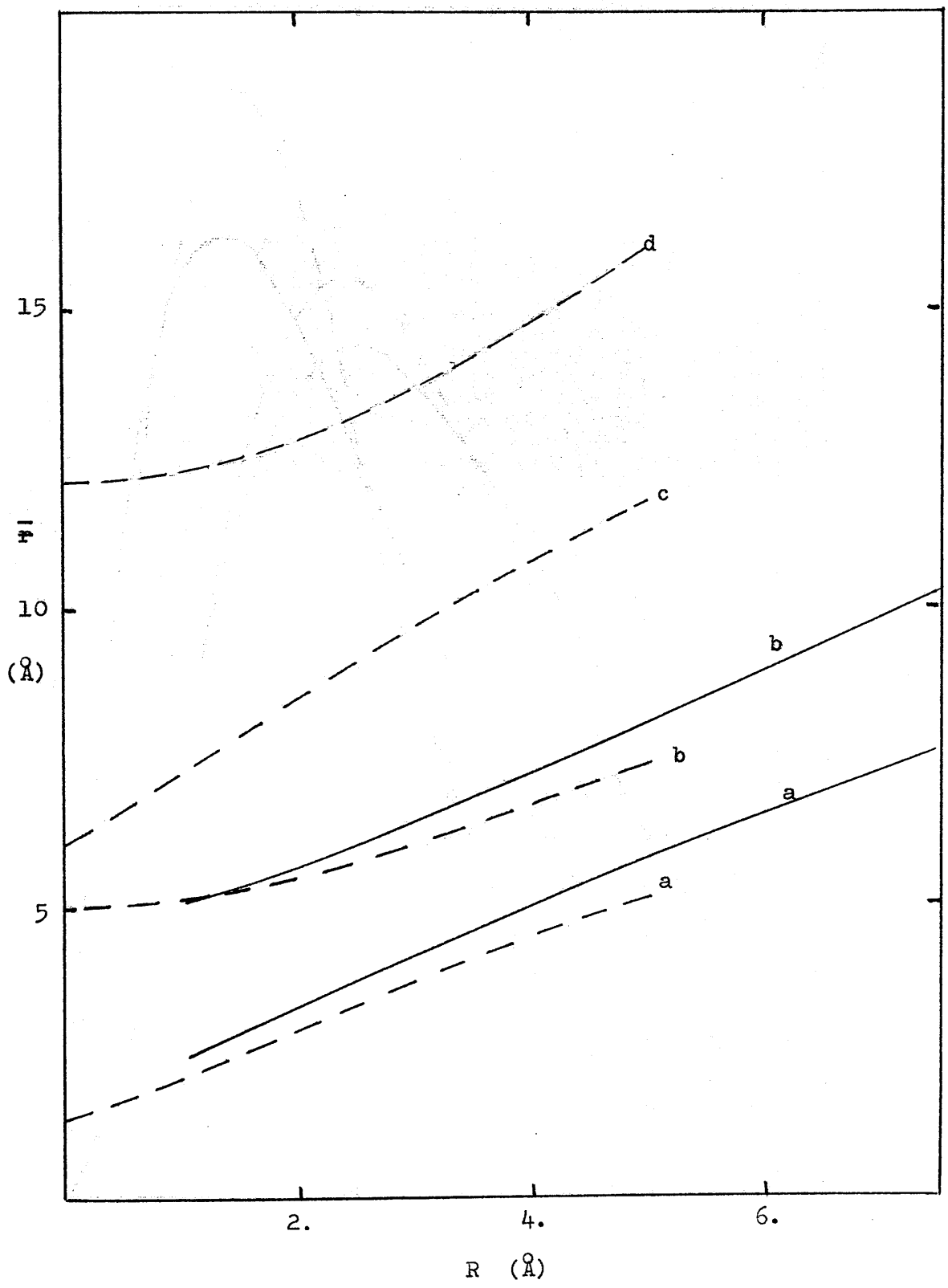

Figure II.4

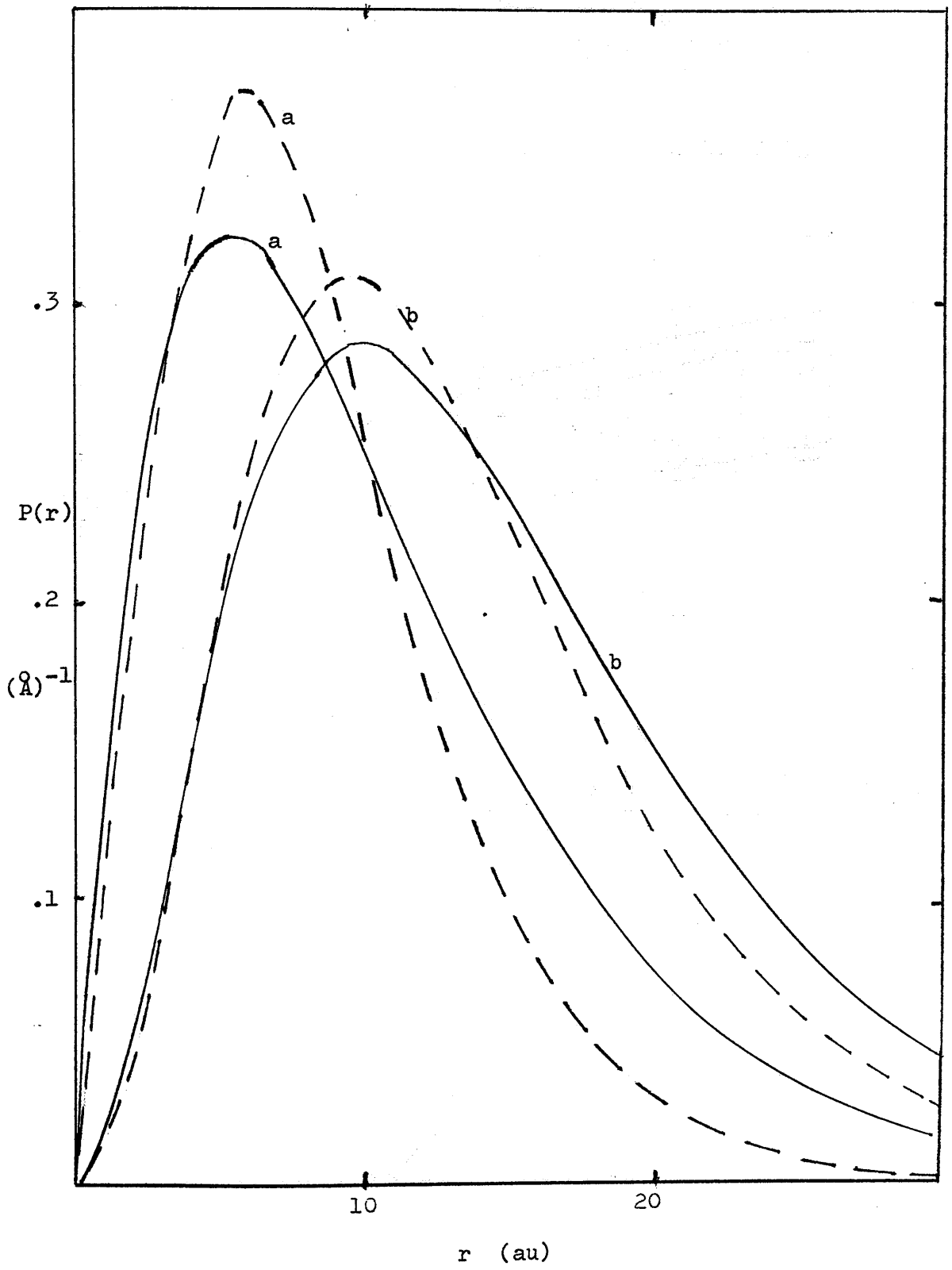

Figure II.5

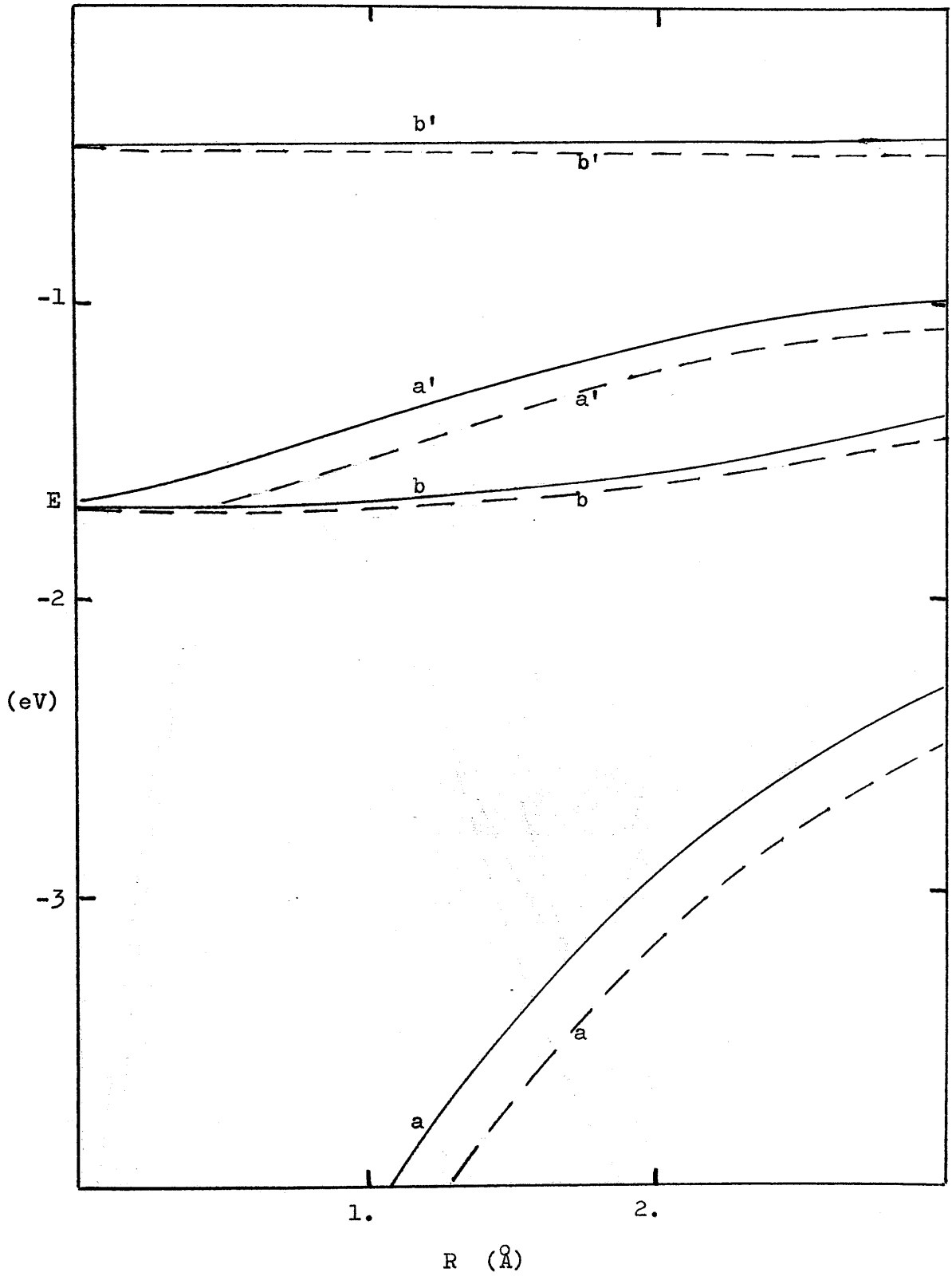

Figure II.6

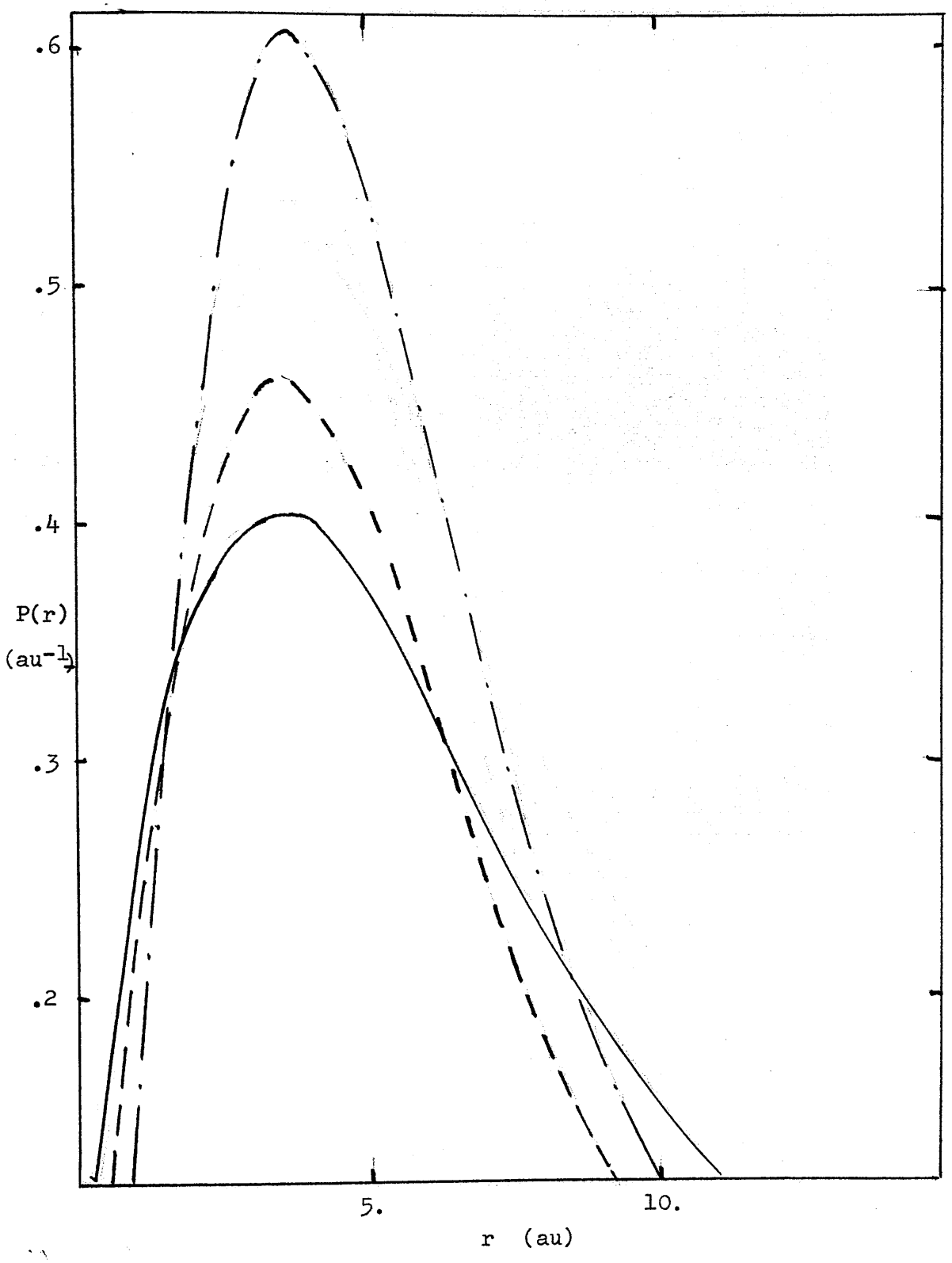

Figure II.7

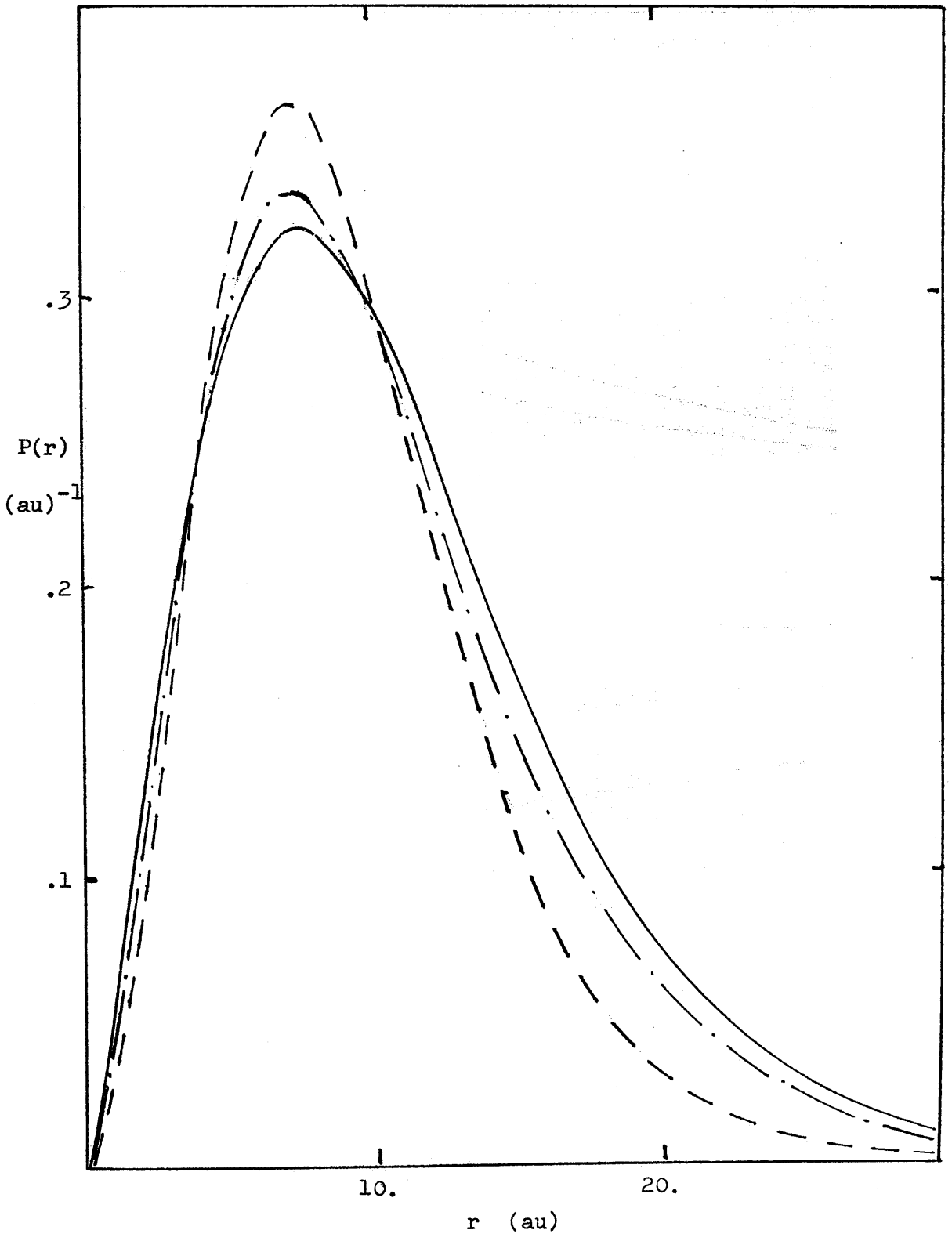

Figure II.8

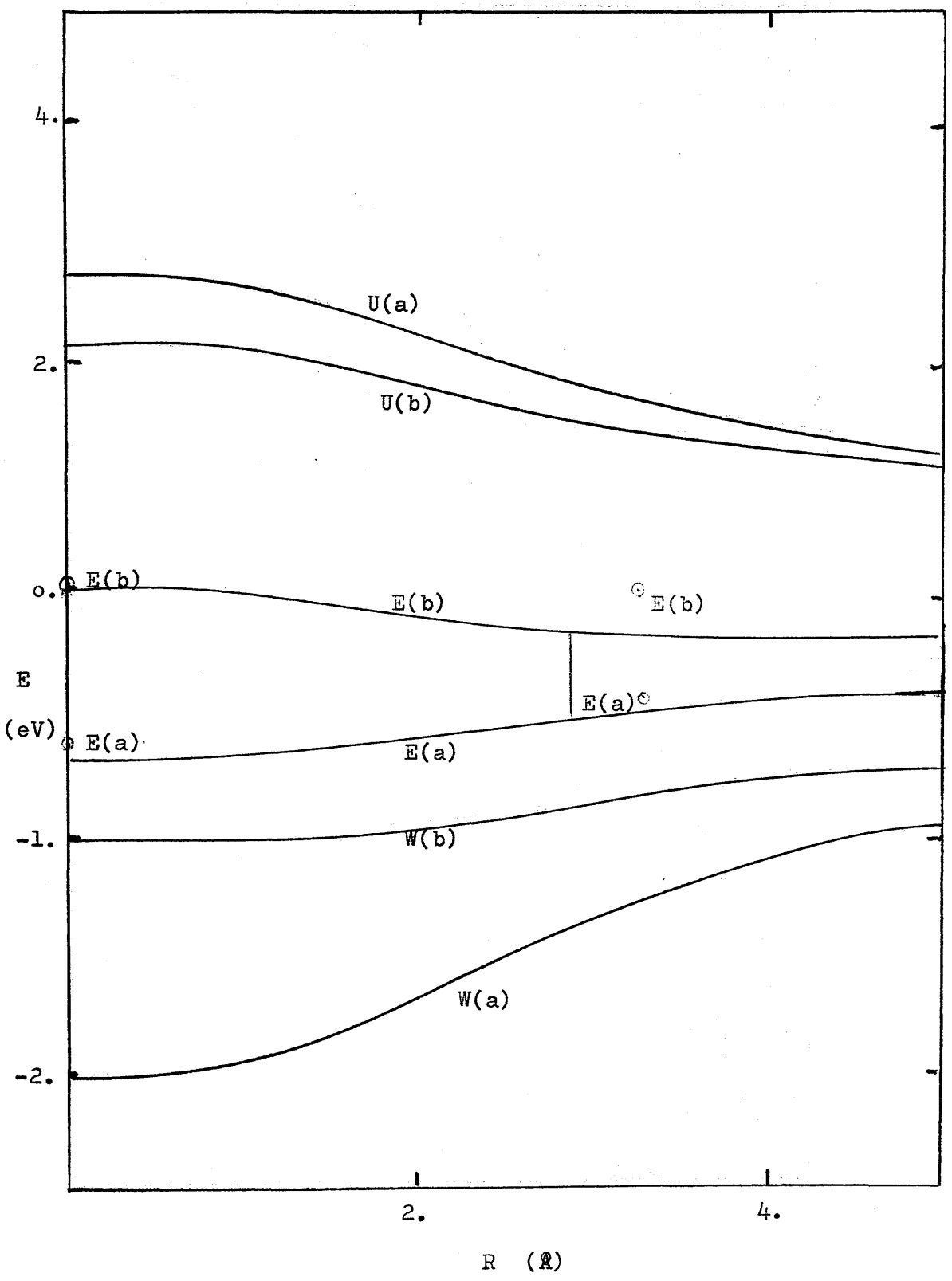

Figure II.9

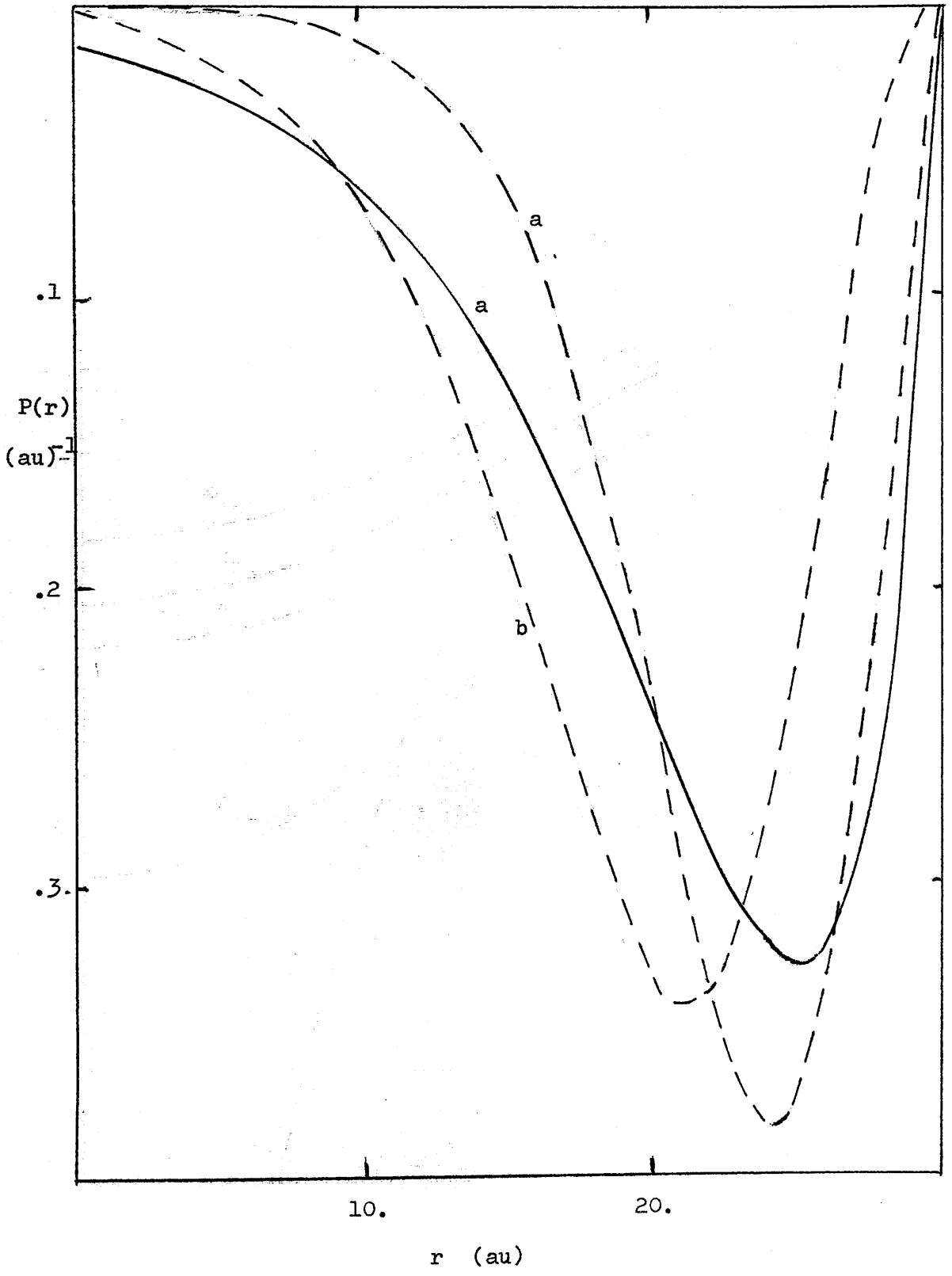

Figure II.10

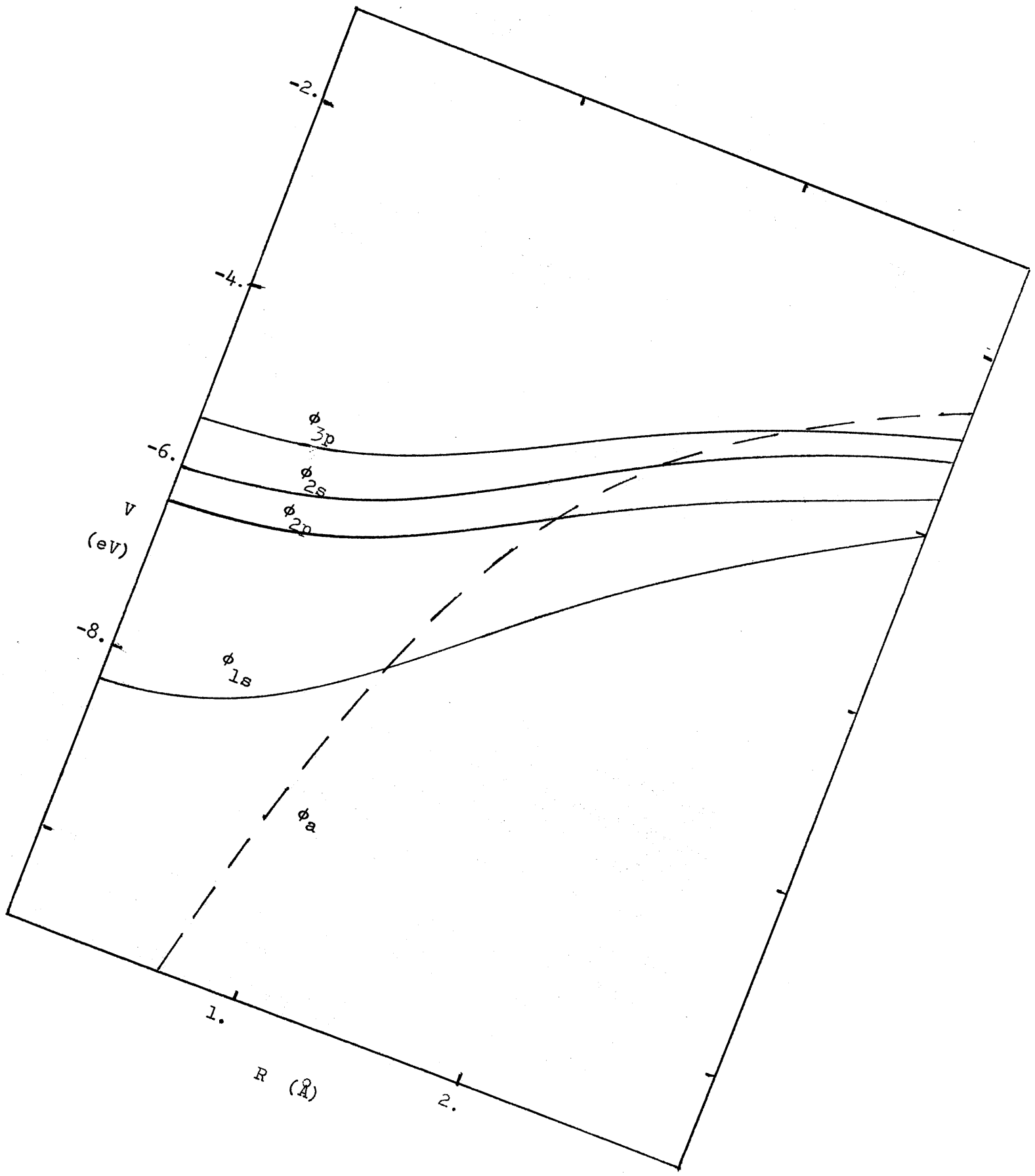

Section 3

Semicontinuum Models.

a) In an effort to allow for dielectric saturation in the vicinity of the trapped electron and to handle the short-range electron-medium interactions in a hopefully more realistic manner, the inclusion of discrete molecular structure in a surrounding solvation shell is a natural step.

O'Reilly[105] first introduced this approach, representing the molecules in the first coordination layer as non-polarizable point-multipoles. In this work, however, O'Reilly and later Land and O'Reilly[106] have employed the void radius in a parametric fashion. An obvious extension of these ideas involves the incorporation of repulsive interactions amongst the neighbouring molecules. This, coupled with cross-cavity interactions, should inhibit cavity collapse and allow the prediction of configuration stability of the system at some derived cavity radius.

This treatment has been followed in the works discussed here. Multipolar and induced interactions are introduced between the molecules of the solvating sheath. The short-range electron-medium interactions are determined principally by charge-oriented dipole energies, the latter component being crudely thermally averaged. Since the models were originally proposed to give account of the properties of hydrated and ammoniated electrons some estimate of the extent of hydrogen-hydrogen interference on molecular reorientation has generally been included, especially in the latter system.

The long-range electron-medium interactions have been carried through from the polarized cavity approach, in terms of an averaged bulk polarization. Both the scf and adiabatic formulations have been

maintained in alternative solution schemes. One further quantity must be specified to allow the computation of the total energy of the system; the cavity creation energy. This has been assumed to comprise a surface-tensional component and a pressure-volume work term. A minimum in the total energy of the system is sought and the properties of the solvated species are calculated at this derived optimum configuration. These concepts are next presented in detail.

b) The Semicontinuum Potential.

Work within the adiabatic approximation has been extended to a semicontinuum level under the guidance of Kestner and Jortner[126,127] and will be discussed first.

The surplus electron is assumed surrounded by a small number, N, of symmetrically distributed molecules of radius r_s with a "hard-core", $2a_s$ in diameter. These molecules are represented as polarizable point dipoles situated at a distance r_d from the centre of the cavity. The dipole moment, μ_o, is taken to be the gas phase value and the polarizability, α, is assumed isotropic. A void radius, r_v, is defined such that $r_d = r_v + r_s$ locates the dipoles, $R = r_d - a_s$ is the distance from the origin to the start of the hard-cores and $r_c = r_d + r_s$ measures the onset of the continuum.

If $\underline{F}_e$ is the field exerted by the solvated electron, then these dipoles may be assumed to experience an interaction described by the potential energy $K = -\underline{F}_e \cdot \underline{\mu}$ where $\underline{\mu} = \mu_o \cos\theta$ and θ is the angle between the moment vector and the radius vector from the origin to the dipole centre. The tendency of the enclosed electronic charge to orient the surrounding dipoles will be counteracted by the thermal agitation of the molecules in the medium. To account for this, a Boltzmann distribution of orientations is assumed such that, if dN is the number of dipoles with energies between K and K+dK, then dN is proportional to $\exp(-K/kT)\, dK$. The total effective moment is then given by

$$\mu = \mu_o / N \int_o^{\pi} \cos\theta \, dN$$

$$= \mu_o \coth(X) - X^{-1} \qquad (16)$$

where $X = \mu_o F_e(r_d) / kT$. Thus the temperature average of the direction cosine is included by way of the Langevin function[128] $L(x) = \coth(x) - x^{-1}$.

If the electron is assumed to experience a spherical polarization field created by the alignment of the adjacent dipoles a return

to the methods of the polarized cavity model is effected. This approach has been adopted in the work of Iguchi[129] and will not be pursued here. Alternatively the electron may be assumed to interact with the first solvation layer of molecules via the potential generated by direct charge-multipole interactions. The effective field, due to the excess electron, acting at the molecules may now be written as

$$F_e(r_d) = eC_i \,/\, (4\pi k_o)\, r_d^2 \qquad (17)$$

where C_i is that fraction of the electronic charge distribution, assumed spherically symmetric, enclosed up to the hard-core of the molecules. Since multipole orientation is assumed slow with respect to electronic processes, this charge distribution will always be that of the relaxed state under consideration,

$$C_r = \int_o^R P_r^2(s)\, ds$$

where P_r describes the radial variation of the relaxed state wave-function. In Land and O'Reilly's original treatment the expansion of the multipole potential was broken off to give a superposition of charge-dipole and charge-quadrupole interactions only. The latter term, however, proved to be rather insignificant and has been neglected in the formulations employed by Jortner and Kestner.

The electron is taken to interact with the bulk medium beyond the first discrete shell as in the adiabatic polarized cavity model. This leads to a single-particle electronic energy, W_i, which is a solution of the adiabatic potential, written in atomic units,

$$\left\{-\tfrac{1}{2}\, d^2 / dr^2 + \tfrac{1}{2}\, \ell_i(\ell_i+1) / r^2 + V(r)\right\} P_i(r) = W_i\, P_i(r) \qquad (18)$$

$$V(r) = \begin{cases} -N\mu/r_d^2 - \beta/r_c & 0 < r > R, \\ -N\mu/r_d^2 - \beta/r_c + V_o & R < r > r_d, \\ -\beta/r + V_o & r > r_d. \end{cases} \qquad (19)$$

V_o is again the energy of a quasi-free electron in the medium. Since no definite experimental values of this quantity for strongly polar liquids are available, it has been treated here as a parameter being

allowed to vary between $\pm$ 1.0 eV. Some simplistic calculations presented earlier suggest that this range will encompass the true value. Care is necessary, however, in adapting the eventual experimental value to this type of semicontinuum calculation. As it is used above, V_o is supposed to contain a representation of any interactions between the electron and the first coordination layer other than those explicitly accounted for in the dipole term. A measured value certainly will not include this contribution.

The total electronic energy, E_i, is obtained as a sum of W_i and a small term, S_i, due to interaction with the electronic polarization of the medium (reverting to S.I. units)

$$4\pi k_o S_i = - N\alpha e^2 C_i^2 / r_d^4 - \gamma e^2 C_i^2 / 2 r_c \qquad (20)$$

This definition of the term will be adopted here to facilitate comparison with the most recently reported variational results[130]. Since its original introduction it has undergone several slight modifications. Even in this final form the latter component would appear to be already counted in the usual usage of V_o.

The alternative line of attack, incorporating the scf formulation of the long-range electron-medium polarization interactions has been extensively employed in the work of Fueki, Feng and Kevan[131]. In this approach the short-range interactions are determined in a somewhat similar fashion to the method discussed previously. Some important modifications have, however, been made. The solvating molecules no longer possess hard-cores and are now entirely characterized by their radius, r_s. The defining measurements in this treatment for a void of radius r_v are $r_d = r_s + r_v$, the location of the dipoles and $R = r_d + r_s$, the distance to the start of the continuum. In addition to the charge-dipole interaction included before, the short-range electron-medium interactions are now supposed to comprise a charge-induced dipole contribution. The potential experienced by the surplus

electron in this scf scheme is, in au,

$$V_i(r) = -N\mu / r_d^2 - N\alpha C_i / 2 r_d^4 - \beta f_r(R) - \gamma f_i(R) \qquad 0 < r > r_d$$
$$- \beta f_r(R) - \gamma f_i(R) + V_o \qquad r_d < r > R \qquad (21)$$
$$- \beta f_r(r) - \gamma f_i(r) + V_o \qquad R < r.$$

is again $\mu_o \langle \cos\theta \rangle_r$, the subscripted r implying that the value of the average cosine apposite to the relaxed state is employed. Notice that the potential is now, as expected, state-dependent.

Choice of an appropriate value for V_o in this model must proceed with caution, the electron-electronic polarization interaction having already been accounted for in the long-range part of the scf potential. Substitution of this potential form into the relevant radial Schrodinger equation produces, on solution, single-particle electronic energies as before.

Clearly the electron-multipole interactions presented in both these methods are attractive in nature. Contraction of the void will thus increase the electronic energy term. To achieve the desired configurational stability, a medium rearrangement energy must now be introduced.

c) The Medium Rearrangement Energy.

As outlined in the introduction, the reorganization of the medium to accommodate both a cavity and an excess electron requires that energy be expended. The decomposition of this energy into its contributory parts has been performed in an identical way in both adiabatic and scf treatments of the semicontinuum model. It comprises a cavity creation energy, a bulk medium polarization component and a term depending on dipolar and induced dipolar interactions amongst the molecules of the first solvation shell. The detailed computation of these quantities is, however, slightly dissimilar in the alternative approximate solution schemes.

Jortner and Kestner have written the surface tension energy as

$$E_{ST} = 4 \pi \lambda R^2$$

where λ is the plane surface tension. Fueki, Feng and Kevan have chosen

$$E_{ST} = 4 \pi \lambda (r_d^2 - r_s^2)$$

to represent this term. Some conceptual difficulty is associated with the use of a plane-surface tensional parameter to describe cavity formation in the bulk of a dielectric medium. However, the term is not of crucial importance and the present method seems to be the most reasonable available. The other contribution to the cavity creation requirements is a measure of the work which must be done in expanding a volume against an ambient pressure p'. Both formulations cite this component as

$$E_{PV} = \tfrac{4}{3} \pi R^3 \, p'$$

This term is entirely negligible, except for large cavities under great pressures.

The dipole-dipole repulsion energy has also been incorporated into both treatments in an identical fashion

$$E_{dd}(i) = D_N \mu_T^2 / (4 \pi k_o) \, r_d^3.$$

The total effective moment includes a contribution from dipole-induced dipole interaction and is given by

$$\mu_T = \mu_o \langle \cos\theta \rangle_r + e\alpha C_i / r_d^2$$

Notice that the "permanent" contribution is governed by the relaxed state charge distribution while the induced term is influenced by the instantaneous electronic state under consideration. The constants D_N were first derived by Buckingham[132] and are presented in Table II.10.

Naturally the medium polarization energies have been handled in different manners in the alternative approaches. The scf formulation of this quantity, U_i, follows directly from the polarized cavity model and is simply

$$(4\pi k_o)\, U(i) = \tfrac{1}{2}\beta \left\{ f_r(R) \int_o^R P_r^2(s)\, ds + \int_R^\infty P_r^2(s)\, f_r(s)\, ds \right\} + \tfrac{1}{2}\gamma \left\{ f_i(R) \int_o^R P_i^2(s)\, ds + \int_R^\infty P_i^2(s)\, f_i(s)\, ds \right\} \qquad (22)$$

the former, inertial, component being determined by the relaxed state and the latter, optical, contribution responding to the instantaneous charge distribution of the surplus electron. In the adiabatic scheme the representation employed is open to question. The form actually included is the so-called correction of the original Jortner expression, presented in equation (4) and is due to Land and O'Reilly. See equation (7). The effect of this change is to include the interaction of that fraction of the electronic charge within the cavity with the static polarization of the bulk medium. However, as written,

$$\Pi = \tfrac{1}{2} e^2 \beta / (4\pi k_o) \left\{ f_r(r_c) \int_o^{r_c} P_r^2(s)\, ds + \int_{r_c}^\infty P_r^2(s)\, f_r(s)\, ds \right\} \qquad (23)$$

this expression appears apposite to an scf treatment of the inertial polarization; equation (5). Though Jortner has defended its application here[133] it is suggested in this present work that Tachiya's form, equation (4), is more consistent internally with the adiabatic treatment of this model.

As mentioned in the introduction, rupturing of the hydrogen-bonded structure of water and ammonia must take place to allow molecular rotation during electron trapping. In addition, the required orientation of the molecular dipoles in the formed solvating centre

must lead to steric interference of the hydrogen atoms attached to adjacent molecules. Little is known of the extent of the former process. However, several empirical estimates of the excess repulsion energy lost to the latter interactions on rearrangement exist. For ammonia these have been evaluated by a formula developed byEisenberg and Kauzmann[134] from studies on water(!), and adapted here as

$$E_{HH} = C_N \exp -4.6(A_N R - B_N) \quad \langle \cos\theta \rangle_r \qquad (24)$$

where the constants A_N, B_N and C_N are listed in Table II.10. In water the fewer hydrogens are generally presumed to be able to avoid one another better and this contribution has been largely neglected. Kamb's empirical equation[135]

$$E'_{HH} = I_N A \, (\sigma / C_N r_d), \qquad (25)$$

where σ= 2.8 Å, A = 4Kcal/mole, I_N is the number of interacting pairs and C_N is a distance scaling factor, has been applied by Jortner and Gaathon in a study of localized states in dense polar vapours[136].

These diverse components combine to give a state-dependent medium reorganization energy

$$E_m(i) = E_{ST} + E_{PV} + E_{dd}(i) + \Pi$$

for the adiabatic treatment, coupled with some form of hydrogen-hydrogen interaction, without which a sensible cavity radius cannot be established.In the scf approach

$$E_m(i) = E_{ST} + E_{PV} + E_{dd}(i) + U(i)$$

with the additional hydrogen-hydrogen term being partly optional.

Both approaches introduce a vertically obtained continuum state, treated as a delocalized unrelaxed state consistent with the relaxed state inertial polarization. Therefore, in the adiabatic treatment

$$E(CS) = E_{ST} + E_{PV} + E_{dd}(r) + \Pi + (E_{HH}) + V_0 \qquad (26)$$

while in the scf formulation

$$E(cs) = E_{ST} + E_{PV} + E'_{dd}(r) + U'(r) + V_o. \qquad (27)$$

The dash signifies the omission of optical components;

$$E'_{dd}(r) = D_N \left\{ \mu_o \langle \cos\theta \rangle_r \right\}^2 / (4\pi k_o)\, r_d^3$$

$$(4\pi k_o)\, U'(r) = \tfrac{1}{2}\beta \left\{ f_r(R) \int_o^R P_r^2(s)\, ds + \int_R^\infty P_r^2(s)\, f_r(s)\, ds \right\}$$

In the expression relevant to the adiabatic approximation it appears that the charge-induced term of the dipole-dipole contribution has been retained. It has, therefore, been included in the present work to allow comparison, but it is recognized to be redundant.

d) Correlation with Experiment.

The results of calculations, within the framework of the above semicontinuum models, on the properties of excess electrons in polar media are presented in terms of much simplified configuration coordinate diagrams, quite analogous to those applied to colour centres. The single configurational coordinate chosen in this system is again the void radius and only the effect of the toally symmetric breathing mode is considered. Thus, it is at once implied that the dependence of electronic energy on non-totally symmetric vibrations is weak and that the degeneracy of the excited state will not be resolved by the wholly radial mode. Jahn-Teller splitting of the excited state should lead to a temperature dependence of the half-width proportional to $T^{\frac{1}{2}}$, [137] which is contrary to observation.

To interpret these configuration coordinate diagrams, in particular to calculate the expected line-shapes, several assumptions are necessary. Firstly it is assumed that the classical high-temperature limit for the absorption line-shape can be safely used. This is certainly justifiable in the liquid ammonia and water calculations performed but must be viewed with some suspicion in ice at $77^{o}K$. In this latter case an effective temperature

$$T^{*} = \left\{E(a) \,/\, 2k\right\} \left\{\coth(E(a) \,/\, 2kT)\right\}$$

is introduced to account for quantum effects[138]. Next, the electronic transition moment, M, is again supposed independent of the coordinate. This appears reasonable over the range of values of the coordinate which contribute significantly to the spectrum.

With these assumptions a line shape function may be written

$$L(E) = M^{2}/Z \int \exp\left\{-E_{t}(r)_{x}/kT\right\} \delta\left\{E+E_{t}(r)_{x}-E_{t}(i)_{x}\right\} dx \qquad (28)$$

at each value of the distortion $x = r_{v}-r_{v}^{o}$, r_{v}^{o} is the void radius at the minimum in the total energy curve relevant to the relaxed state and the subscripted x indicates the configuration dependence of the

energies of the relaxed initial state, r, and the instantaneous final state, i. Z is the ground state partition function. The line shape is thus determined by the thermal population of the initial relaxed state and the x-dependence of the vertical transition energy.

Substitution of

$$A(x) = E_t(r)_{r_v} - E_t(r)_{r_v^o}$$

into (28), furnishes (29) on integration;

$$L(E) = M^2/Z\left\{\exp -A(x)/kT\right\}\left\{dx/dE\right\} \qquad (29)$$

from which all quoted line shapes and half-widths are deduced

The transition energy, E(a), is defined as

$$E(a) = E_t(i)_o - E_t(r)_o. \qquad (30)$$

This is distinct from the maximum in the predicted absorption band, $E(a)_{max}$, as derived from (29). Equality will hold only at low temperatures, but, in the temperature range considered here, deviations are of slight importance, being of the order of a few tenths of one percent.

The force constant of the totally symmetric vibration, K, follows simply from

$$K = \left\{\partial^2 E_t(r)_x / \partial x^2\right\}_{x=o}$$

from which the breathing frequency of the cavity, ν_c, may be obtained as

$$\nu_c^2 = K / 8\pi^2 \mu_M \qquad (31)$$

where $\mu_M = N\,m'$, m' being the mass of a medium molecule.

Other properties depending on the energy of the relaxed ground state are obtained from the configuration coordinate diagram in the limit of zero distortion. The heat of solution is given by

$$\Delta H = -E_t(r)_o \qquad (32)$$

and the photoconductivity threshold is

$$I = E_t(i)_o - E_t(r)_o \qquad (33)$$

where, in this case, i represents the vertically attained conduction state (see equations (26) and (127)). Since differences in the optical polarization to these states are small it may be expected that

$$I = V_o - E_e(r)_o.$$

The photoelectric threshold, the energy required to release electrons of zero kinetic energy from the bulk liquid, is given by

$$P = -E_e(r)_o \tag{34}$$

provided the surface potential and various other small effects are neglected. The thermal activation energy of any relaxed state is

$$E_t(r) = V_o - E_t(r)_o. \tag{35}$$

Thermal population of the low-lying vibrational levels associated with these relaxed states will tend to smear all these values toward lower energy.

As mentioned previously, the experimentalist, when measuring the change in absorption maximum of an optical band with temperature, generally works under a constant ambient pressure, p. Calculations employing the above temperature-dependent configuration coordinate diagrams, (the effect of temperature is mainly incorporated via the Langevin function), offer an estimate of this quantity under conditions of constant density, ρ. The two are simply related

$$\left\{\partial E(a)/\partial T\right\}_{\rho} = \left\{\partial E(a)/\partial T\right\}_{p} - \left\{\partial E(a)/\partial \rho\right\}_{T}\left\{\partial \rho/\partial T\right\}_{p}$$

Since values of the density coefficient at constant temperature are now available[139] and the variation of density with temperature at constant pressure has long been known[140] for the systems studied here the quantities may be readily compared.

e) Results and Discussion.

Computations of the properties of excess electrons within the semicontinuum approach require the specification of a number of parameters which describe the properties of the host media. Most of these are presented in Tables II.10 and II.11. The remaining two, N and V_o, are treated as unknown quantities and calculations have been performed employing reasonable values of these.

Within the adiabatic approximation, Kestner and Jortner[130] have obtained a solution on the semicontinuum level for a range of those parameters utilizing the potential form expressed in (19). A single-exponential, one-parameter trial function (13) has been supposed to be a sufficient representation of both the ground (1s) and first excited (2p) state charge distributions. By minimizing the single-particle electronic ground state energy, at each void radius, with respect to the variational parameter, a series of optimum exponents were derived. Employing these values the total electronic energy at each configuration was computed and combined with the corresponding medium rearrangement energy. The resulting variation of the total energy with cavity radius for the ammoniated electron at a temperature of 203°K is depicted in Figure II.11 for a choice of parameters N=4, V_o= 0.0 eV.

With the above parameters, the existence of a stable localized state of the surplus electron in ammonia is at once predicted. $E_t(1s)_o$ is less than the energy of the quasi-free electron in this medium and the second derivative of this total ground state energy with respect to the configurational parameter is positive. The optimum configuration lies at a void radius of 1.20 Å which allows the prediction of a heat of solution at 0.909 eV and a photoconductivity threshold of 1.95 eV. The onset of photoelectric emission is also placed at 1.95 eV in this model since the contributions to the energy of the quasi-free

state have been assumed to exactly cancel. The peak of the optical absorption band is calculated at 1.03 eV and the associated dipole-length oscillator strength is 0.66. All of the above numbers are in reasonable quantitative agreement with the previously reported experimental data.

To obtain some estimate of the bulk volume expansion arising from this cavity radius the effect of the structure breaking caused by reorientation of the ammonia molecules adjacent to the localized electron must be estimated. Copeland et al.[127] have suggested one way of achieving this. An effective radius of the cavity is defined by

$$R_e^3 = (r_v + 2r_s)^3 - Nr_s^3 ,$$

which is just apposite to the volume enclosed by the void and first solvation shell minus the volume of the molecules in this layer. For the above parameters, this turns out to be just above 3.0 Å, in close agreement with the value of 3.2 Å interpreted from the observed volume expansion data.

The numerical results secured in the present work offer no substantial change in this effective radius. The optimum void is found to be only a few hundredths of an Å more compact. Figure II.11 also contains the numerically constructed configuration curves for these parameters. A salient feature is the marked lowering of the total ground state energy on accurate solution. The amelioration, of the order of 12%, is but slightly greater than obtained in the polarized cavity models. The numerically derived unrelaxed excited states are, in fact, higher than their variational counterparts. However, no direct comparison of these total energies is possible. The improvement effected in the ground state charge distribution has increased the inertial polarization provided by this state, which all others experience. Hence the apparent anomaly.

Table II.12 holds a detailed comparison of the energies derived from the one-parameter variational solution and the present numerical method at the optimum void radius. In addition some results obtained variationally[145], employing a more flexible three-parameter optimization technique to represent the electronic ground state are exhibited. The 2s function of Figure II.11 derives from this work. The single-exponential single-particle ground state energy is 0.2 eV above the accurate solution, about 9% too high. The discrepancies in the pertinent charge distributions are magnified when the medium rearrangement energies are included. The total energy obtained variationally now deviates by 13% from the true value. It is also evident from this table that the numerically predicted heat of solution (32) is 1.05 eV, just on the lower limit of the experimental estimate and slightly better than the variational 0.91 eV. The photoconductivity threshold (33) lies at 2.22 eV and the onset of photoelectric emission (34) is expected at 2.21 eV, somewhat higher than would be desired. These estimates push the variationally obtained 1.95 eV (for both) further out of agreement with observation.

Unfortunately, the variational wave-functions for the above solution are not available for comparison. However, results from a similarly parameterized potential form, (36), are known

$$4\pi k_o V(r) = \begin{cases} -N\mu / r_d^2 - \beta / r_c & r < R \\ -\beta / r + V_o & R > r, \end{cases} \qquad (36)$$

and these are set alongside those derived by the finite difference method in Figure II.14. The variational 1s function is considerably too diffuse while the 2p functions are less discordant. A situation which is more reminiscent of polarized cavity models than the colour centre semicontinuum treatment. Numerical computation of the energy levels relevant to (36) reveals trends similar to those disclosed in the more complex potential form studied above. The variational single-

particle energy, 1.842 eV, is 8% above the accurate value, the total ground state electronic energy, 2.547 eV, differs by 12% and the numerical heat of solution is 15% greater. These are entirely analogous to the improvements secured above and it is expected that the functions depicted in Figure II.14 provide a good indication of the inadequacy of the single exponential functions as employed in the more complex potential. The optimum values of the three-parameter variational function, which involves a linear combination of 1s-, 2s- and 3s- like wavefunctions, are also not reported, hence a comparison is again precluded. The total relaxed ground state energy computed from this approach is almost indistinguihable from that obtained here. Thus, this function presumably affords a good representation of the true charge distribution of the ground state.

By analogy with the experimental findings in F-centres, it may be supposed that, if the 2p state exists long enough to allow the medium to accommodate its charge distribution, an emission band corresponding to a radiative transition to an unrelaxed ground state may possibly be observed. In this model the accommodation proceeds by relaxation of the short-range orientational polarization, the long-range inertial polarization remaining inflexible in an adiabatic treatment.

Figure II.12 contains the configurational coordinate diagram pertaining after matrix relaxation. The numerical relaxed excited state is virtually identical to the one-parameter variational curve. The 1s states, however, differ to an appreciable extent. Table II.13 details the comparison at the optimum configuration for emission. Also presented are the 3d and continuum state energies, computed numerically, transitions to which could presumably be induced by some excited-state spectroscopic technique involving optical pumping. Transitions to the former state account for almost all the available absorption oscillator strength from the relaxed excited state. The numerically deduced 2s

state is included to illustrate that no 2s - 2p mixing effects are likely in this system, even after relaxation. In absorption the two states differ by 0.27 eV and this separation is seen to have been maintained. It is interesting also that, within the framework of this approach, lattice relaxation, described in terms of molecular reorientation, is accompanied by a cavity shrinkage, to 1.05 Å with the above parameters. This is in marked contrast to the observations in similar models of the F-centre.

The optical absorption and emission properties derived from the above calculations, employing the present solution method are tabulated in Tables II.14 and II.15. These also include the few available variational data. Accurate solution has effected a substantial change in the peak energy of the 1s -2p absorptive transition, unfortunately to the detriment of concurrence with experiment. The calculated 1s -3p band is peaked far into the high-energy tail of the observed spectrum. The line shapes expected from the above configuration coordinate diagrams have been computed utilizing equation (29). The results for absorption are depicted in Figure II.15, unnormalized line shapes being presented. When weighted with the appropriate transition moments the 1s - 2s band disappears, being symmetry-forbidden. The 1s -3p and 1s -cs (the photoionization) are reduced by a factor of twenty. Thus, they are predicted, from the above model, to be too weak and too narrow to reproduce the observed tail. The 1s - 2p band, in itself, is obviously incapable of matching the experimental spectrum. While it is slightly asymmetrical, the deviation occurs on the low energy side. The numerically obtained half-widths are somewhat narrower than their variational counterparts both in absorption and emission. This is due to the slight enhancement in the curvature of the numerical relaxed state lines. The emission band is predicted to be Stokes shifted by about 0.65 eV from the peak of the optical absorption.

Two-photon absorption spectroscopy could perhaps reveal the presence of the 1s -2s transition, implied to be around 1.5 eV in this model. This, however, would require a single-photon energy of 0.75 eV which falls in a region of relatively broad intrinsic absorption bands in liquid NH_3. Perhaps the experiment would be better performed in deuteroammonia, ND_3, which possesses noticeably sharper lines in this spectral domain.

Table II.16 compares the properties determined by both variational (one-parameter) and numerical techniques for the same adiabatic potential created now by six solvating ammonia molecules. The usual comparative trends are observed on numerical solution. Increasing the number of solvent molecules in the model has tended to shift the computed properties out of agreement with experiment. The absorption bands have broadened slightly but it is obvious that this adiabatic treatment of the semicontinuum model fails to produce the observed half-width by a factor of 3 or 4 when the band is attributed to a single 1s - 2p transition derived from a single configurational coordinate, no matter the choice of parameters.

An attempt to reproduce the spectral properties of the hydrated electron with this model is presented in Table II.17. Similar numerical versus variational improvements are evident. The parameters chosen here are V_o = 0.0 eV, N = 4 and T = 298°K. The transition energy is much out of alignment with the observed value, though the heat of solution is quite reasonable. The predicted line-widths are again much too narrow. Though the transition energy can be suitably modified by altering the value of V_o to -1.3 eV, no betterment of the line-shapes can be obtained.

The total energies computed here, for the hydrated electron, have been derived without the inclusion of a hydrogen-hydrogen repulsive interaction term in the medium rearrangement energy. This omission

leads to tiny cavities, a void radius of 0.16 eV in the optimum for the above parameterization on absorption. Similar results would pertain in ammonia were the same contribution neglected. The dominant effect of this component in locating the configurational minimum is shown in Figure II.13, where the many contributions to the medium reorganization energy are plotted as a function of void radius. In addition to the values derived here, the long-range medium polarization from Tachiya's formula is included. Since the radius to the continuum onset is always greater than $2r_s$ no considerable alterations in the foregoing calculations are expected on inclusion of this term. This contrasts the situation in the polarized cavity models where the Tachiya formulation of this energy contribution led to very significant differences.

It is interesting to note that, without hydrogen-hydrogen repulsions, no stable emission configuration is disclosed, the total relaxed state energy decreases monotonically to a cavity of zero radius. This statement is also relevant in ammonia. The previous prediction of an emission possibility is totally dependent on the somewhat arbitrary inclusion of the precipitous E_{HH} term. Clearly, this unsatisfactory situation warrants further attention.

In contrast to the reported calculations within the adiabatic treatment of the semicontinuum model, which have been almost exclusively devoted to the properties of the surplus electron in ammonia, a few token calculations in water being available, Fueki, Feng and Kevan[131] have employed the alternative scf solution scheme to elucidate the structure of localized excess electron states in a large number of media, characterized by a wide range of polarity.

In these polar host matrices, the scf semicontinuum model has proved very capable of reproducing quantitative estimates of various experimental properties. In ice at $77^{o}K$, with parameters N=4 and V_o=-1.0 eV fixed, the predicted transition energy, 1.84 eV, the oscillator strength, 0.33, and the photoconductivity threshold, 2.36 eV, are in excellent accord with observation. While an identical choice of parameters affords close agreement with the oscillator strength in water at $298^{o}K$, both the heat of solution and the position of the band maximum are overestimated. Bringing these more into line with the experimental values, by, for instance, increasing N or making V_o more negative spoils the initial transition moment match. The heat of solution, photoconductivity threshold and absorption peak of the ammoniated electron are all reasonably estimated, again utilizing the above parameters. These latter results are obtained subject to the inclusion of hydrogen-hydrogen interactions which are neglected in the other media studied.

However, this work has again been advanced in the context of the variation principle employing, as usual, inadequate single-exponential trial functions. This is somewhat surprising, since these workers first reported the supposed massive enhancement in the accuracy of the scf solution to the polarized cavity model, for the hydrated electron in a cavity of zero radius, obtained by merely improving the flexibility of the variational trial functions. This effect can only be increased in transferring such calculations to a semicontinuum level.

The smooth, modified-coulomb potential apposite to the polarized cavity model has become a discontinuous square-well-like potential in the semicontinuum approach. In the polarized cavity calculations, the present numerical solution technique called the three-parameter variational solution into question. In the adiabatic semicontinuum model some considerable improvement on the original one-parameter variational work was effected on increasing the accuracy of the solution method. The variational solution scheme of Fueki, Feng and Kevan differs from that used in the adiabatic approach only in that the variations in the total energy were employed to judge the optimum exponent rather than the electronic component alone, which served as a criterion in the latter treatment. In view of these statements a thorough numerical investigation of the scf semicontinuum model was performed.

The configuration coordinate diagrams obtained by numerical solution of Fueki, Feng and Kevan's scf formulation of the semicontinuum model are set beside the original one-parameter variational results in Figures II.16,17 and 18 for the surplus electron in water at 298^{o}K, in ammonia at 203^{o}K and in ice at 77^{o}K, respectively. Four oriented molecules were included in the first shell and the energy of the quasi-free electron was specified at -1.0 eV outwith this layer in each system. The degree of accord between the approximate variational ground-state energy and the accurate solution is very poor for ice, where the respective values are some 20% disparate, improves slightly in water but is substantially better in ammonia, the difference in this medium being only 10%.

Figures II.19 and 20 illustrate part of the variational 1s- and 2p- like functions obtained at the respective total ground state minima in ice and water. The numerically derived functions are also shown. An examination of these figures reveals the reason for the large discrepancies in the configurational diagrams in these media.

Both the ground and first excited state one-parameter variational functions are markedly inappropriate, badly underestimating the compactness of the true charge distributions.

Figure II.23 depicts the potential wells sustaining the ground state charge distribution in water, ice and ammonia at this same optimum void radius. Figure II.24 contains the corresponding wells for the vertically attained excited (2p) state. The hydrated electron and the trapped electron in ice are constrained to move in relatively deep, narrow wells, that apposite to ice indicating stronger positive deviations from a coulombic tail in this matrix. These observations rationalize the noted amelioration in the 1s and 2p charge distributions. The single-exponential functions are inherently unable to provide a satisfactory representation of the true solution in such wells. A shallower, wider well pertains in ammonia and it may thus be expected that the originally employed approximate functions will prove somewhat more adequate in this system. Unfortunately, no variational functions are available for this model of the ammoniated electron, hence the direct comparison can not be made. However, some support of this expectation is evident in the smaller deviations exhibited in the relevant configuration coordinate diagram.

A detailed comparison of the numerical versus variational energy contributions to the ground and first excited states of the excess electron in the above media, at the void radius pertinent to the minima in the total ground state energy curves, is given in Table II.18. The true minima obtained in the present work deviate by a few hundredths of an $\mathring{A}$ from those presented here, but this was ignored in order to allow a direct match. The discrepancies in the ground state electronic energy are very substantial in ice and water. The quantity $[1 - C(i)]V_o$ should be added to the variational value, where C is the charge enclosed up to r_d^o, to realize an exact comparison but the difference remains of

the order of 15%. This effect is more noticeable for the 2p state energies which, uncorrected, are vastly disparate. The increased compactness, evidenced in the C(i) values, of the accurate wave-functions lead to an enhancement of the polarization and dipole-dipole terms which tends to cancel some of the disagreement in the total system energies, $E_t(i)$. In the 2p state, the variational 2p energy is actually below the present numerical value. It also produces stronger orientation in the solvating dipoles and tends to push up the energy of the conduction state.

The corresponding numerical results for two other excited states in these media are documented in Table II.19. One interesting feature is the near-degeneracy of the 2s and 2p states at the absorption coordinate in ice.

Completely analogous improvements were revealed in a similar study employing N=6 but this will not be detailed here.

Table II.20 lists the properties derived from these above energy values which may be compared with experiment. In general, increasing the accuracy of the solution tends to mar any claimed concurrence with observation. Though this agreement may be reintroduced, for a specific property, by a judicious manipulation of the input data, such an exercise was not deemed worthwhile. In any case, those most amenable to alteration, N and V_o, are, as used above, quite reasonable. In water the peak in the experimental absorption band may be matched with N=4 and V_o= -2.08 eV, but only at the expense of a discordant heat of solution and oscillator strength.

More importantly, the scf semicontinuum model again appears incapable of reproducing a reasonable half-width for the optical absorption band, considered as a 1s - 2p transition and derived using a single configurational coordinate. No reasonable choice of parameters was found in water which could produce a half-width greater than 0.25 eV,

a factor of 4 below the experimental value. Transitions to higher excited states are also relatively narrow and lie too far into the high-energy tails of the observed spectra to account for much of its intensity. They are, however, accompanied by somewhat larger oscillator strengths than those computed within the adiabatic approach.

Extensive numerical tests on the scf semicontinuum model were performed in the course of this work. These support the original claim of the insensitivity of predictions to such parameters as r_s, λ and p, the first two of which can only be guessed. The general trends reported with changes in the other variables were also followed on accurate solution. For example, the dominant role of long-range polarization interactions in water, especially in determining the ground state minimum is maintained. Contrast the more important effect of the short-range interactions in ice. In general, however, these trends are rather obvious by inspection of the input parameters in light of the scf potential form. The extremely small β value in ice accounts for the above difference. A somewhat extreme example of this is the prediction by Fueki, Feng and Kevan of the presence of no bound excited state for alkaline ice, employing the above model. As this is a glassy matrix, the result was obtained by merely "turning off" the long-range polarization. By this expedient a square-well is produced which is insufficiently deep to bind in a p state. The prediction is thus hardly surprising.

Figures II.21 and 22 illustrate the numerical search for a stable relaxed excited state in ice and water. None was found. The energy levels are seen to decrease monotonically to a void of zero radius. In the context of this approximate model this may be taken to imply the absence of radiative emission. The excited state presumably decays by some other radiationless process.

f) Conclusion.

As expected, application of the finite-difference numerical solution technique to the semicontinuum models, framed both within the adiabatic and scf approximation schemes, is capable of producing sizeable improvements in the energy levels derived by recourse to the variation theorem utilizing single-exponential trial functions. Such approximate functions are inherently unsuited to represent the true charge distributions apposite to the form of the model potentials. Correlation with experiment secured using the latter treatment of these models must be viewed with suspicion, particularly if some delicately balanced quantity is being tested.

However, both the adiabatic and scf approaches to the semicontinuum model are capable of producing qualitative agreement with most experimental observables for some choice of parameters. The latter appears more widely applicable and is certainly more consistent with the theoretical requirements of a model of the excess $e$lctron in polar media. The former is, to some extent, limited in scope and is incapable of producing sensible results without the inclusion of some arbitrary solvent-specific interactions, e.g. the hydrogen-hydrogen term in ammonia. In their absence, configurational stability is only established for vanishingly small cavity radii.

It is of the utmost importance that neither model, within its present formulation, is capable of estimating the observed absorption line-shapes, so characteristic of surplus electrons. This deficiency persists whether the band is assumed due to a single 1s - 2p transition or if this is supposed accompanied by a series of 1s-- np transitions extending to a continuum. One attempt to alleviate this difficulty has been essayed by Kestner and Jortner, who incorporated broadening due to medium polar modes and to some extent of non-totally symmetric cavity vibrations. These additions left the computed line-width still

far out of touch with experiment.

Numerical solution reveals that this inadequacy in prediction is not a function of the use of insufficiently accurate representations of the true charge distribution, an important result. Neither does accurate solution of the semicontinuum model shed any light on the recent suggestion that the observed absorptions in polar liquids are entirely due to bound-to-free transitions[148]. The present results predict a strongly-bound excited state in these media precluding this possibility.

From these observations, it might be supposed that some gross modification of the above models is required. The many-body theory of polar liquids mentioned previously in Section 2(f) provides such a modification. In effect it allows the consideration of all possible orientations of the adjacent solvent molecules, appropriately weighted, rather than just the optimum configuration pictured here with the limitation of a fixed number of molecules in the solvating sheath. It is hoped that this statistical approach, toward which the work of Tachiya is leaning, will prove fruitful in providing fresh insight into the properties of the solvated and trapped electron species.

Tables IIb

Properties of surplus electrons derived from semicontinuum models.

Tables 10 and 11 list the necessary input data for these models. The results of adiabatic calculations are in Tables 12-17 12 and 14 are for AMMONIA on absorption with N = 4, V_o = 0.0 eV, T = 203°K at an optimum void radius of 1.20 Å. 13 and 15 are for emission in this system with r_v = 1.05 Å. 16 has results for N = 6 in ammonia, for absorption with r_v = 1.65 Å and for emission, r_v = 1.55 Å. The data in Table 17 are for water with N = 4, T = 298°K, V_o = -1.0 eV. In absorption r_v = 0.16 Å.

Scf results for ammonia,water and ice on absorption are in Tables 18-20. All have N = 4, V_o = -1.0 eV.

All energies are in eV. Distances are in Å, except in Table 19 where the mean radii are in au.

Table II.10

N	4	6	8	12
A_N [b]	1.633	1.414	1.155	1.000
B_N [b]	0.471	0.600	0.752	0.843
C_N [b]	2602.4	5204.7	6940.0	10416.
D_N [a]	2.2964	7.1140	12.820	41.074

a ref. 132

b ref. 127

Table II.11

Medium	water	ammonia	ice
k_{op}	1.78[a]	1.76[a]	1.78[a]
k_{st}	80.0[a]	21.3[a]	3.00[d]
μ	1.85[a]	1.47[a]	1.85[a]
n	1.51[b]	2.00[b]	1.51[b]
λ	72.0[q]	40.0[e]	100.[d]
r_s	1.40[c]	1.50[e]	1.40[c]
a_s	0.90[e]	1.00[e]	-
T	298	203	77
$\left[\partial E(a)/\partial \rho\right]_T$	2.5[f]	1.0[f]	-
$\left[\partial \rho / \partial T\right]_p$	5.5[f]	1.3[g]	

a ref. 141; b ref. 142; c ref. 143; d ref. 144;

e ref.127; f ref. 139 ; g ref. 140.

Table II.12

$E_e(1s)$	-2.010^a	-	-2.205^n
$E_t(1s)$	-0.909	-1.053	-1.051
$E_e(2p)$	- --	-	-0.936
$E_t(2p)$	0.121	0.147	0.186
$E_e(2s)$	-	-	-0.637
$E_t(2s)$	-	0.394	0.454
$E_e(3p)$	-	-	-0.441
$E_t(3p)$	-	-	0.708
$E(cs)$	-	-	1.172

a one-parameter variational[130]

b three-parameter variational[145]

n numerical

Table II.13

$E_e(2p)$	-	-0.815^{n}
$E_t(2p)$	-0.183^{v}	-0.185
$E_e(1s)$	-	-1.408
$E_t(1s)$	-0.730	-0.774
$E_e(2s)$	-	-0.549
$E_t(2s)$	-	0.088
$E_e(3d)$	-	-0.371
$E_t(3d)$	-	0.261
$E_t(cs)$	-	0.632

n numerical

v one-parameter variational[130]

Table II.14

$E(a)$	1.03[a]	1.20[b]	1.237[n]
$f_{len}(a)$	0.66	-	0.930
$f_{vel}(a)$	0.44	-	0.827
$W(a)$	0.10	0.12	0.084
$E(a')$	1.6[c]	-	1.759
$f_{len}(a')$	-	-	0.056
$f_{vel}(a')$	-	-	0.052
$W(a')$	-	-	0.096
$E(cs)$	1.9	-	2.223
$W(cs)$	-	-	0.105

a one-parameter variational[130]

b three-parameter variational[145]

c estimated

n numerical

Table II.15

E(e)	0.548[v]	0.589[n]
$f_{len}(e)$	-	0.975
W(e)	-	0.090
E(2p-2s)	-	0.273
E(2p-3d)	-	0.446
$f_1(2p-3d)$	-	0.049
E(cs)	-	0.817

n numerical work

v variational solution[130]

Table II.16

$E(a)$	1.15[a]	1.369[b]	1.385[n]
$f_{vel}(a)$	-	-	0.824
$W(a)$	0.132	-	0.109
$E(a')$	1.6[c]	-	1.903
$f_{vel}(a')$	-	-	0.050
$W(a')$	-	-	0.117
ΔH_s	0.973	1.156	1,154
I	2.326	-	2.601
$E(e)$	0.535	-	0.572
$f_{len}(e)$	-	-	0.962
$W(e)$	-	-	0.107
$\varepsilon_t(1)$	0.113	-	0.117

a one-parameter variational[130]

b three-parameter variational[145]

c estimated

n numerical

Table II.17

ΔH	1.658^{v}	1.889^{n}
I	4.096	4.492
E(a)	2.70	3.167
$f_{len}(a)$	0.99^{a}	1.121
$f_{vel}(a)$	0.70^{a}	0.854
W(a)	-	0.112
E(a')	-	4.061
$f_{len}(a')$	-	0.046
$f_{vel}(a')$	-	0.042
W(a')	-	0.123

a Jortner and Gaathon[146]

n present numerical work

v one-parameter solution[72]

Table II.18

	Water		Ammonia		Ice	
r_v^o	0.53		1.16		0.53	
$-E_e(1s)$	6.158[v]	7.606[n]	-	4.437[n]	4.873[v]	6.307[n]
$U(1s)$	2.049	2.134	-	1.616	1.380	1.440
$-E_t(1s)$	2.752	3.282	1.942[v]	2.114	2.076	2.589
$E_{dd}(1s)$	1.687	2.091	-	0.427	1.716	2.139
$-E_e(2p)$	2.215	3.423	-	2.841	1.003	2.112
$U(2p)$	1,762	1.912	-	1.433	0.912	1.022
$-E_t(2p)$	0.601	0.365	0.981	0.936	0.237	0.205
$E_{dd}(2p)$	0.743	0.847	-	0.192	0.698	0.746
$C(1s)$	0.571	0.735	-	0.574	0.563	0.738
$C(2p)$	0.070	0.131	-	0.092	0.018	0.049
$\langle \cos\theta \rangle$	0.970	0.977	-	0.952	0.992	0.994
$E_t(cs)$	0.878	0.938	0.125	0.327	0.284	0.306

n numerical

v variational[131,167]

Table II.19

Medium	water	ammonia	ice
$E_e(2s)$	-2.825	-2.333	-1.938
$U(2s)$	1.671	1.151	0.867
$E_t(2s)$	-0.309	-0.735	-0.208
$Edd(2s)$	0.746	0.302	0.724
$E_e(3p)$	-2.071	-1.829	-1.390
$U(3p)$	1.482	1.129	0.665
$E_t(3p)$	0.272	-0.389	0.101
$E_{dd}(3p)$	0.707	0.170	0.687
$C(2s)$	0.066	0.133	0.034
$C(3p)$	0.039	0.033	0.009
$\bar{r}(2s)$	10.909	14.914	14.284
$\bar{r}(3p)$	17.986	21.650	31.325

Table II.20

	Water		Ammonia		Ice	
$E(a)$	2.15^{v}	2.717^{n}	0.961^{v}	1.178^{n}	1.84^{v}	2.385^{n}
$f_I(a)$	-	0.515	-	0.725	-	0.251
$f_v(a)$	-	0.814	-	0.905	0.39	0.452
$W(a)$	-	0.226	-	0.091	-	0.071
$E(a')$	-	3.554	-	1.863	-	2.690
$f_l(a')$	-	0.129	-	0.152	-	0.055
$f_v(a')$	-	0.142	-	0.104	-	0.078
$W(a')$	-	0.207	-	0.1028	-	0.066
ΔH	2.75	3.282	1.942	2.114	2.08	2.589
I	3.63	4.220	2.067	2.441	2.36	2.896
P	4.6	5.2	3.1	3.4	3.4	3.9

n numerical work

v variational solution[131,167]

Figures IIb

Figures 11-24 derive from semicontinuummodels of excess electrons in water at 298°K, ammonia at 203°K and ice at 77°K.

With N = 4 and V_o = 0.0 eV, the adiabatic approach in ammonia gives 11 on absorption and 12 on emission. 14 presents the resulting functions from a similar calculation at the optimum absorption void.

With N = 4 and V_o = -1.0 eV, the scf treatment of absorption in ammonia , water and ice gives 17,16 and 18, the functions at the optimum void radii being plotted in 19 for ice and 20 for water. Scf emission results are in 21 for ice and 22 for water.

In the above full-line is variational result and broken-line is present numerical work except for 16,17 and18 where this is reversed. (a) is 1s state, (b) is 2p, (c) is 2s, (d) is 3p, (e) is the vertical continuum level.

13 shows the various contributions to the adiabatic medium rearrangemant energy which gives 11. (a) is the total relaxed ground state energy. (b) is Jortner's polarization energy (broken-line is Tachiya's value). (c) is the vertical continuum level, (d) is the dipole-dipole repulsion term and (e) is the H-H interaction energy. (f) is the surface tensional component.

15 presents unnormalized line-shapes derived from 11. (a) is 1s-2p, (b) is 1s-2s, (c) is 1s-3p and (d) is 1s-cs.

23 and 24 depict the scf potentials supporting the ground 1s state and excited 2p state respectively. Full-line, water; broken-line, ice; Chain-line, ammonia.

Figure II.11

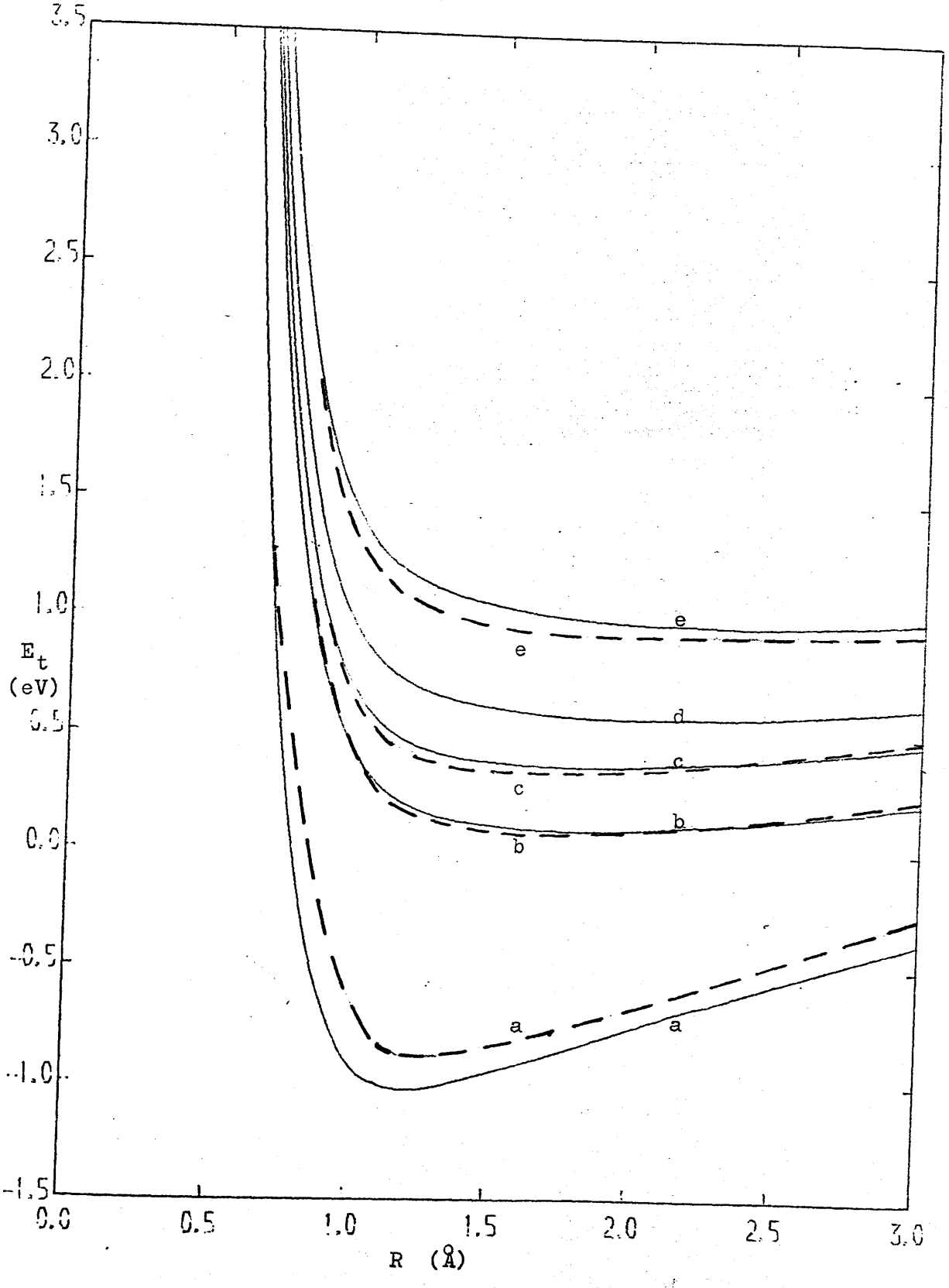
3.5
3.0
2.5
2.0
1.5
1.0
0.5
0.0
-0.5
-1.0
-1.5
E_t (eV)
0.0
0.5
1.0
1.5
2.0
2.5
3.0
R (Å)
a
a
b
b
c
c
d
e
e

Figure II.12

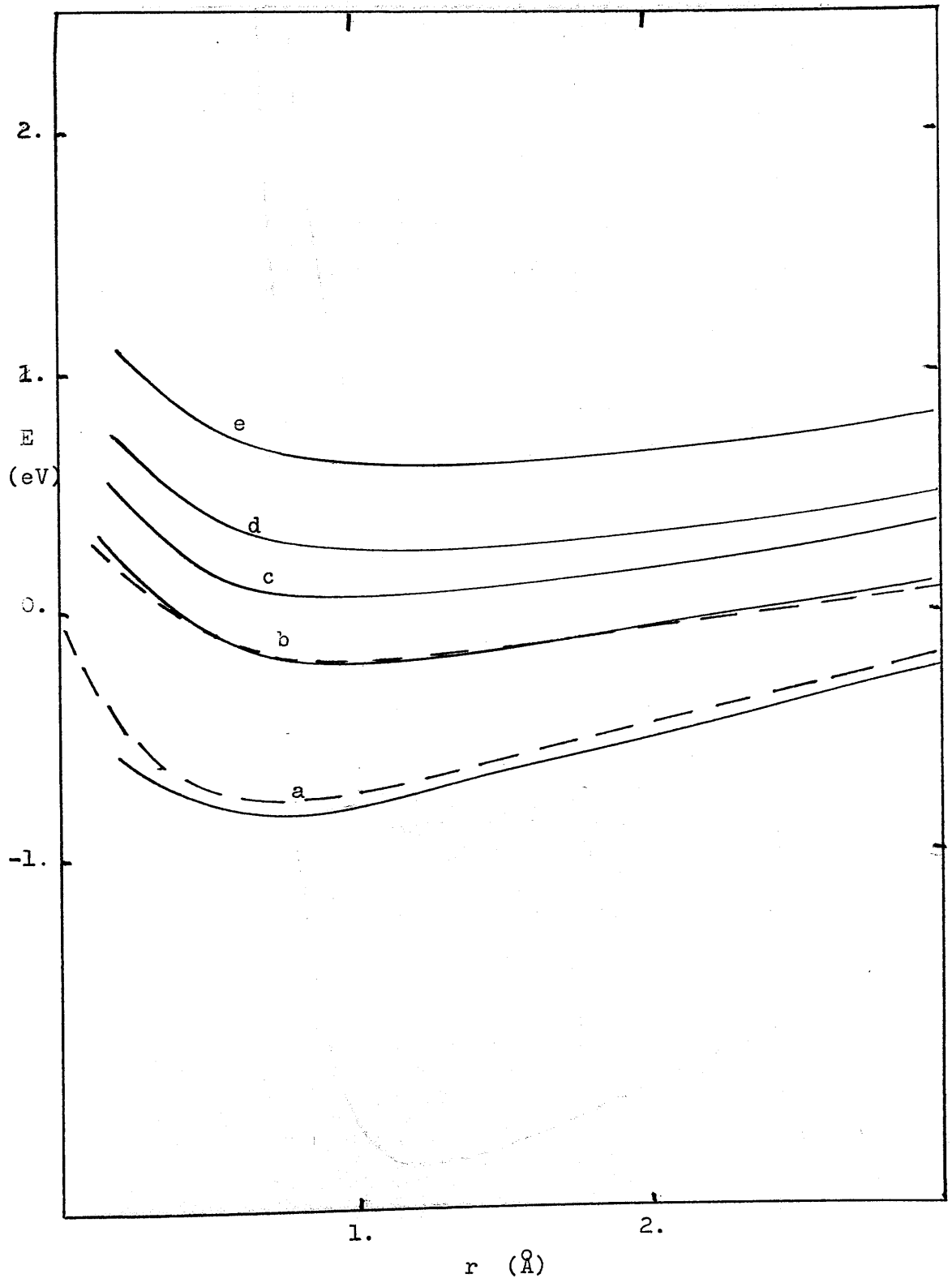

Figure II.13

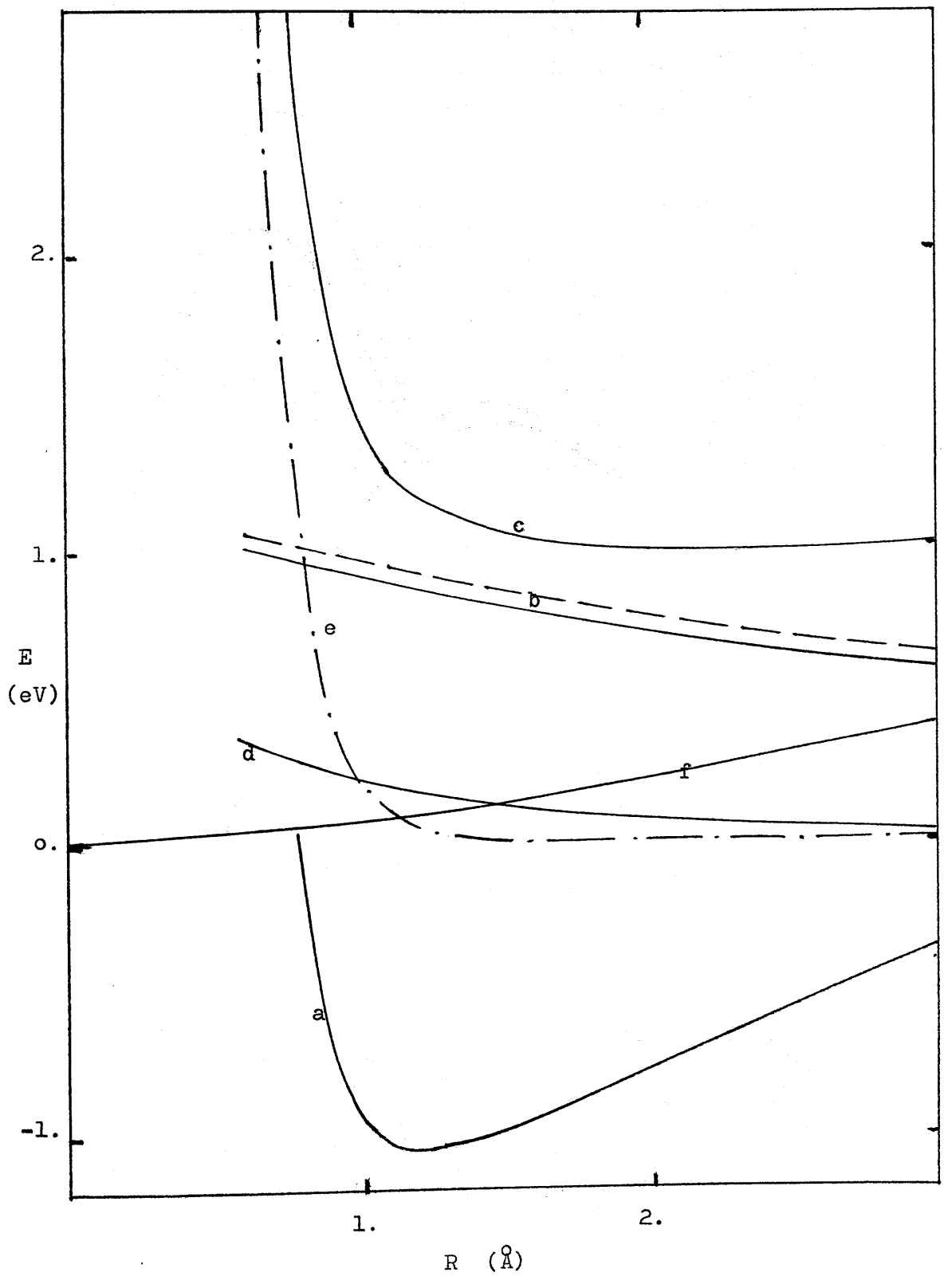

Figure II.14

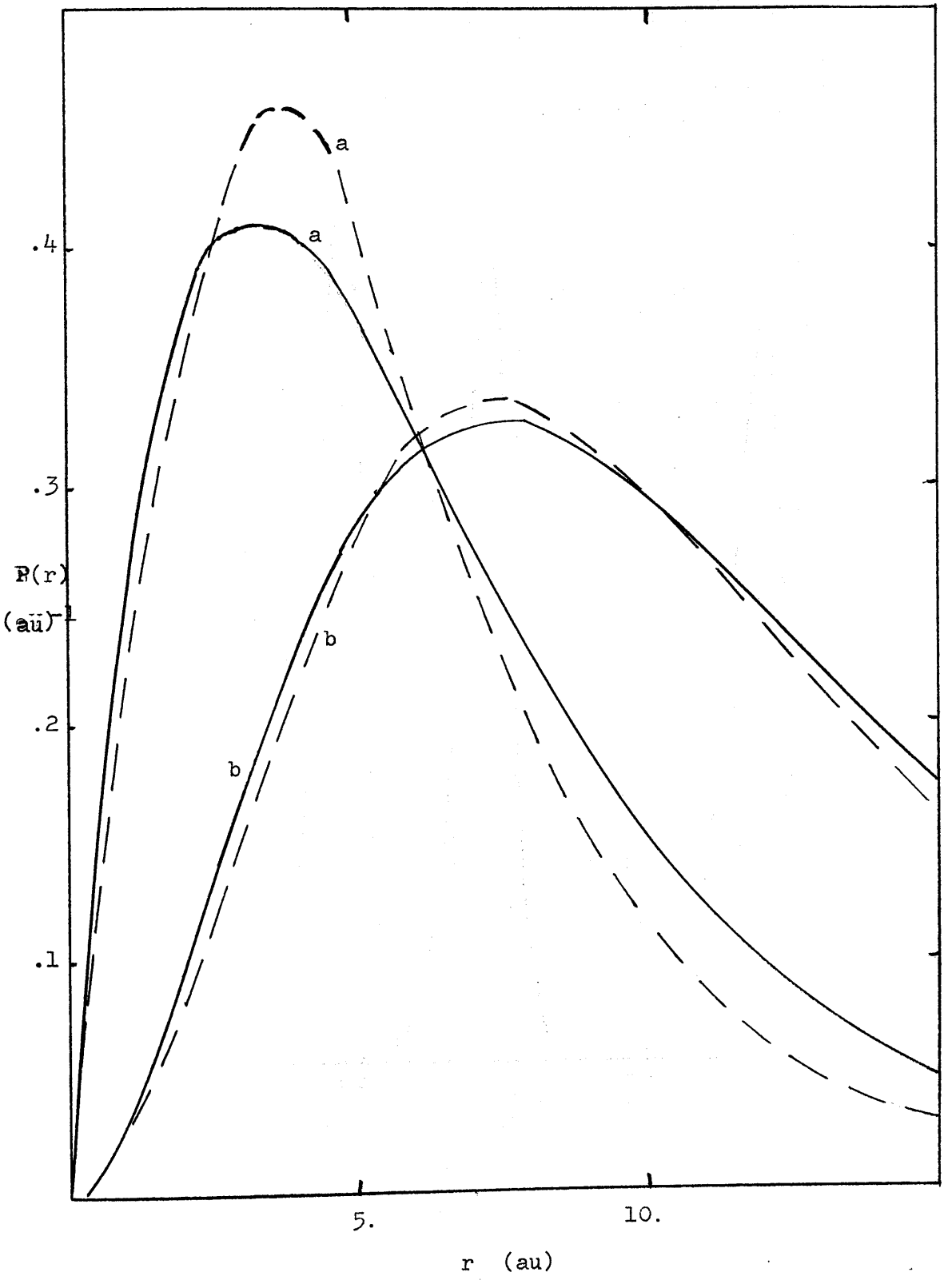

Figure II.15

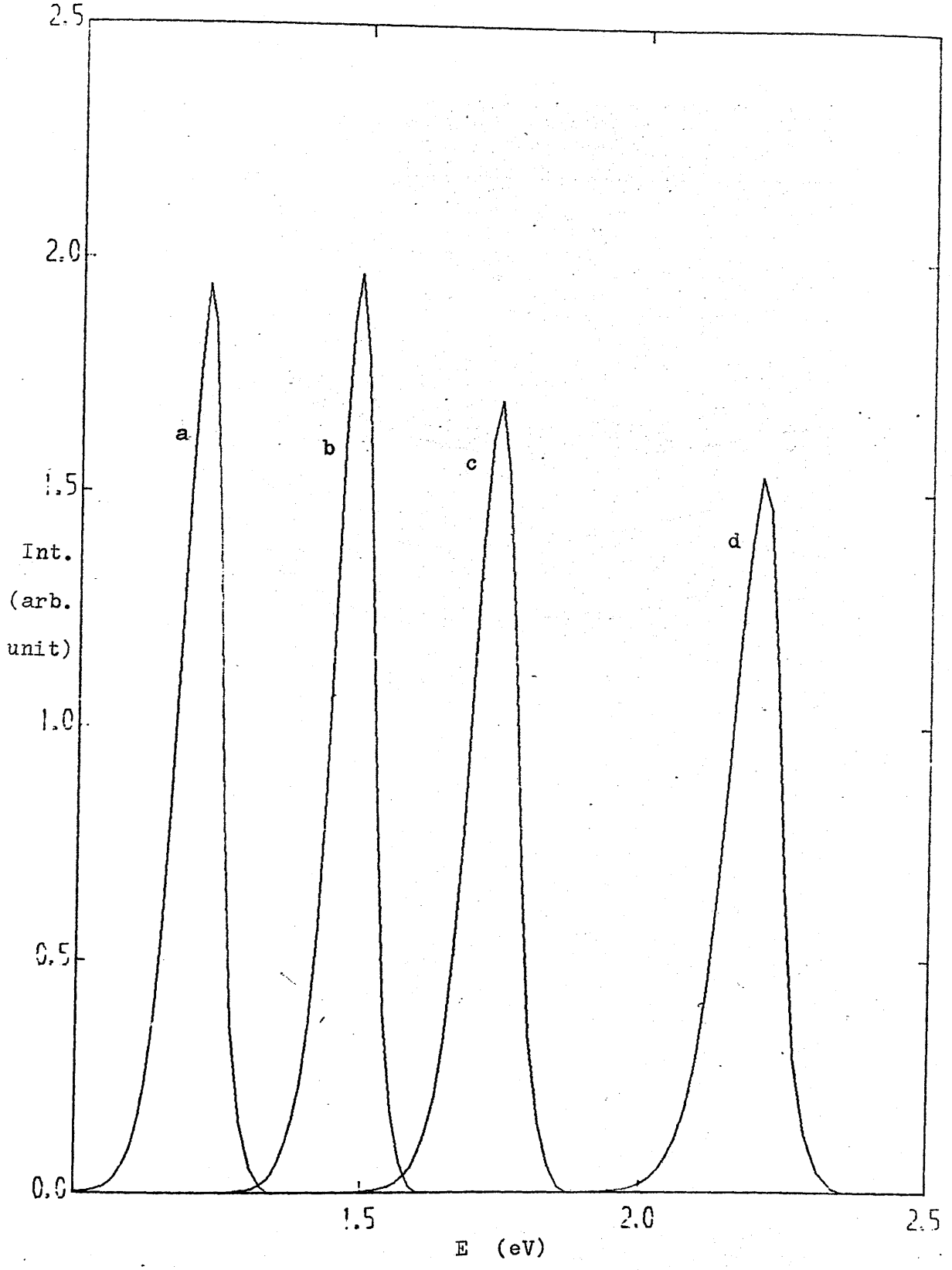

Figure II.16

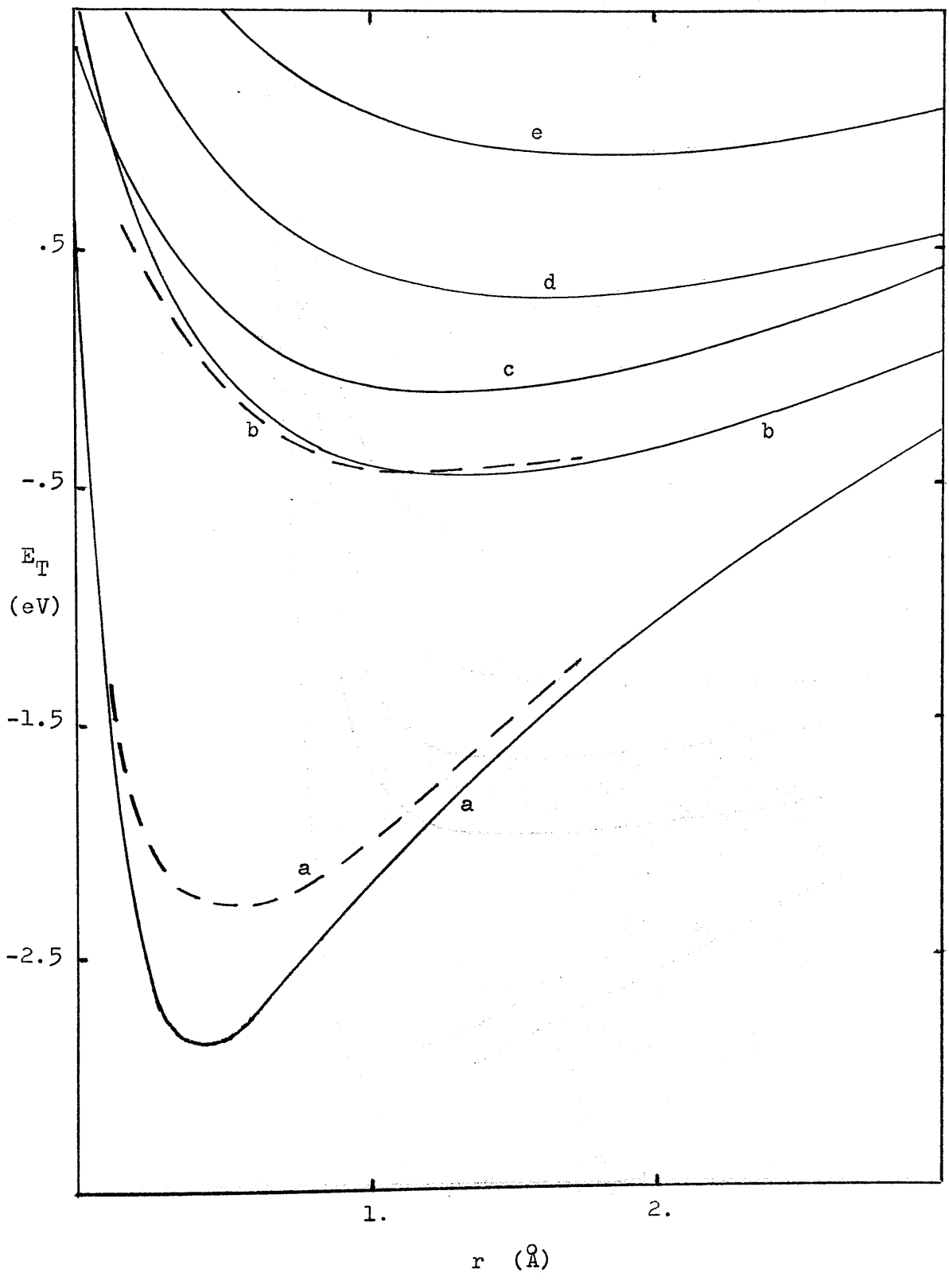

Figure II.17

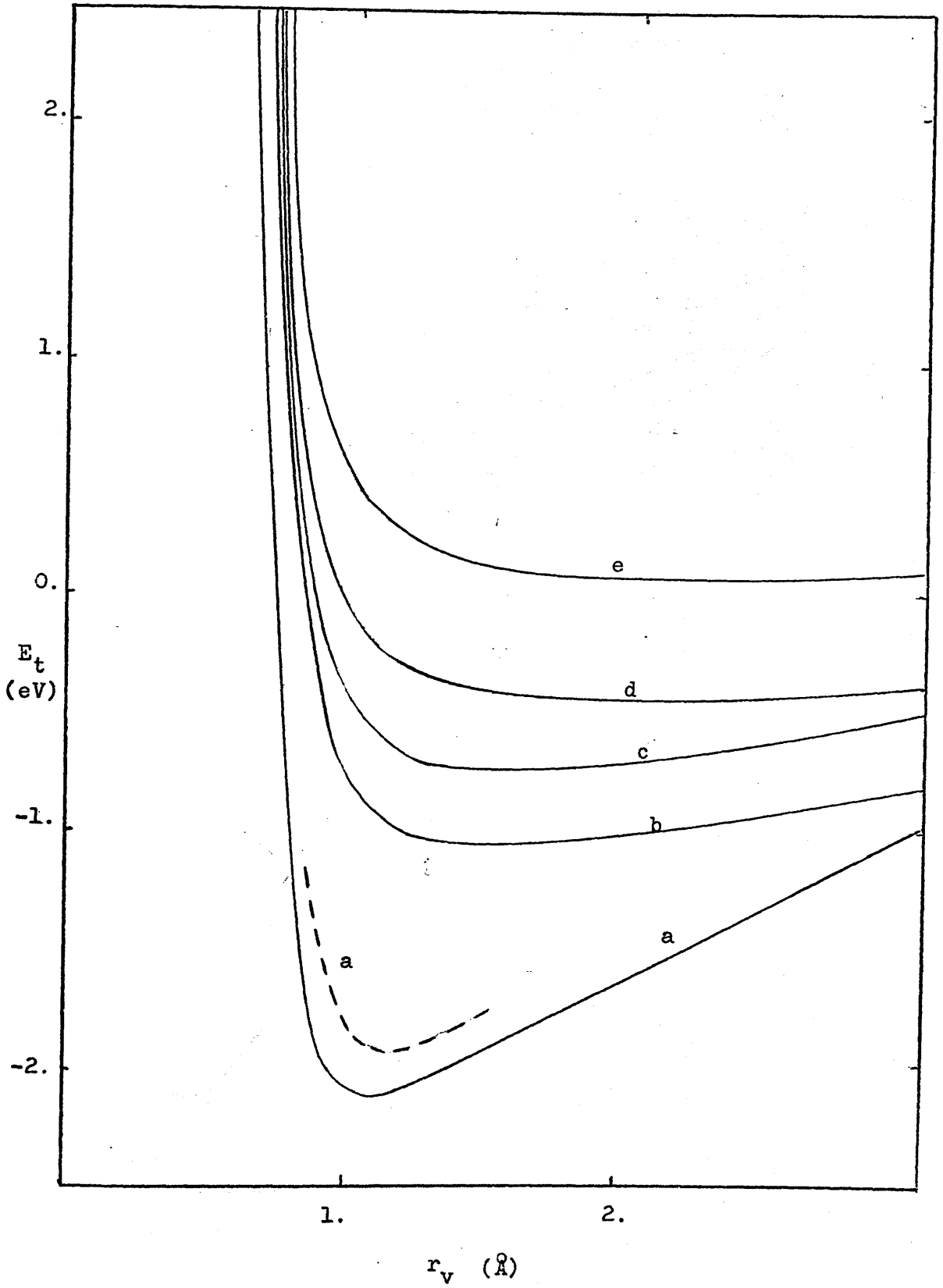

Figure II.18

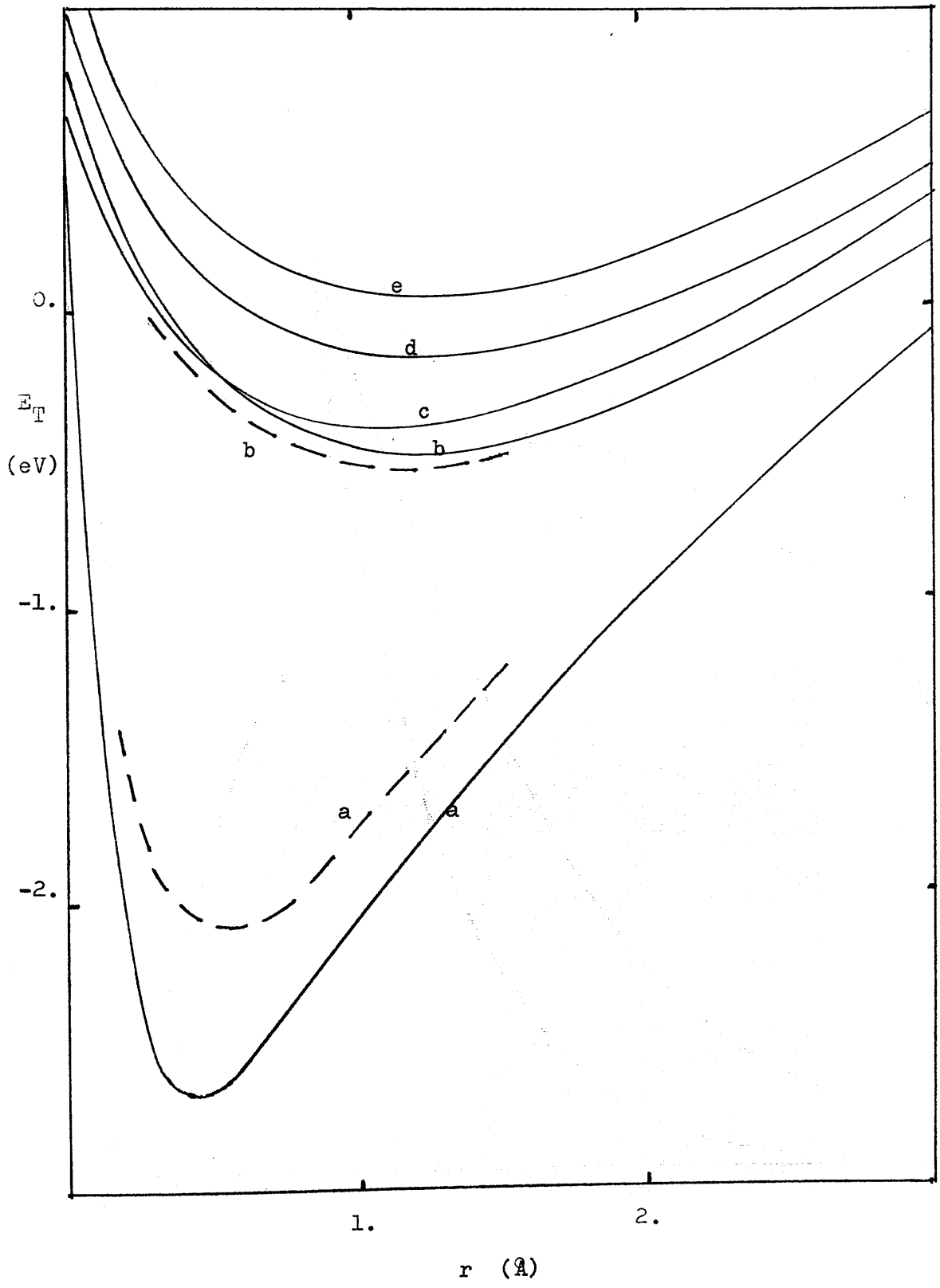

Figure II.19

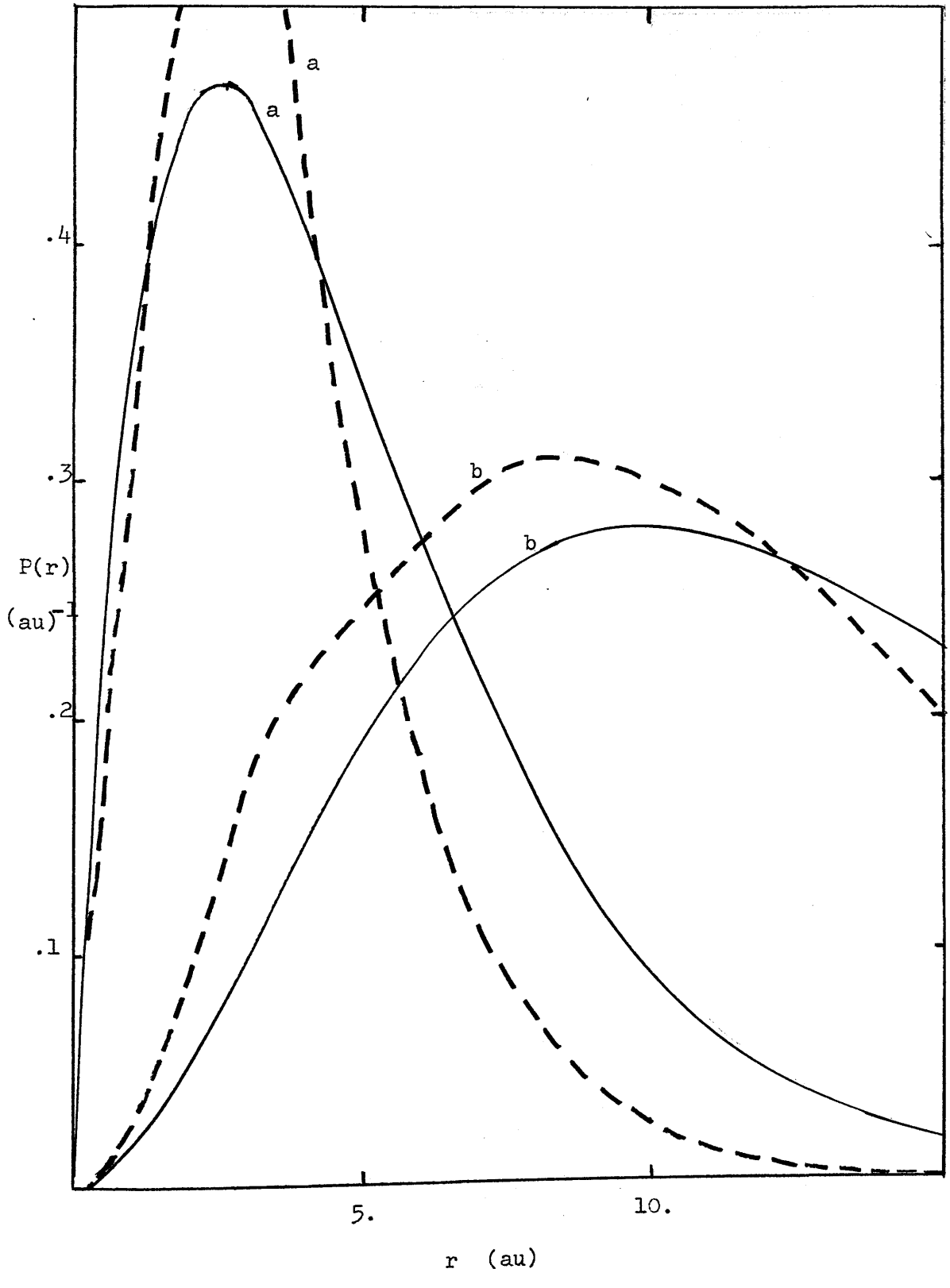

Figure II.20

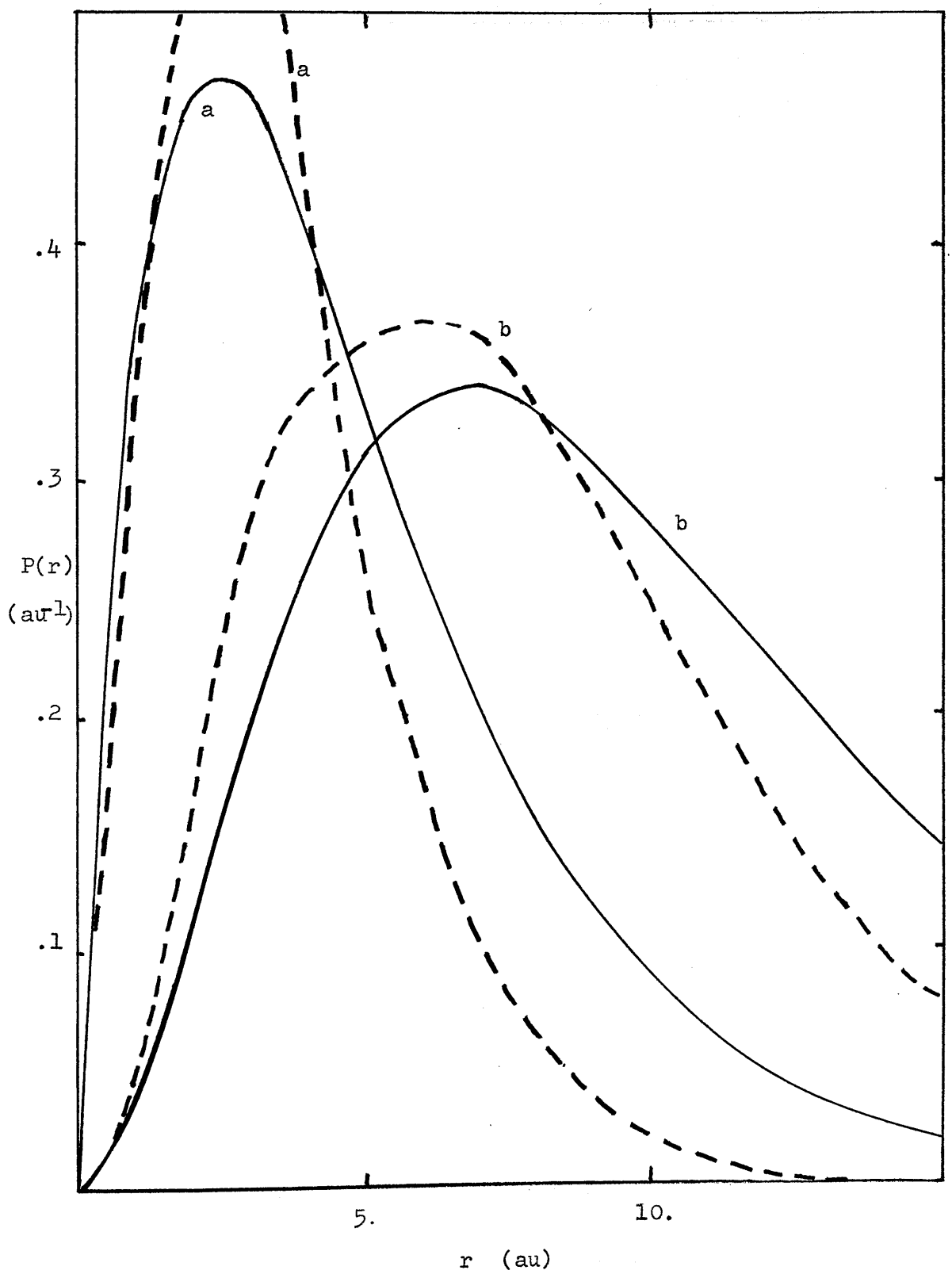

Figure II.21

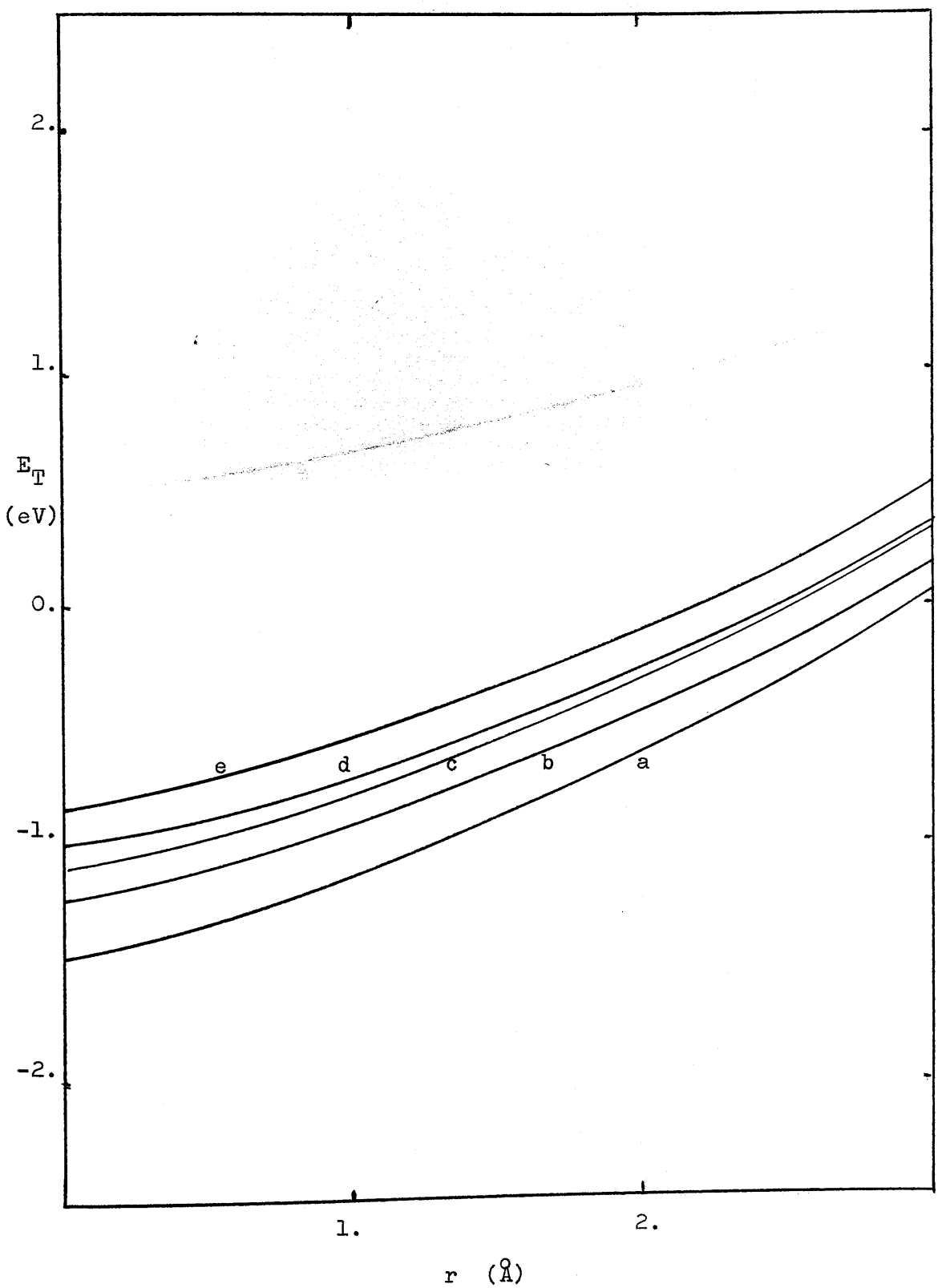

Figure II.22

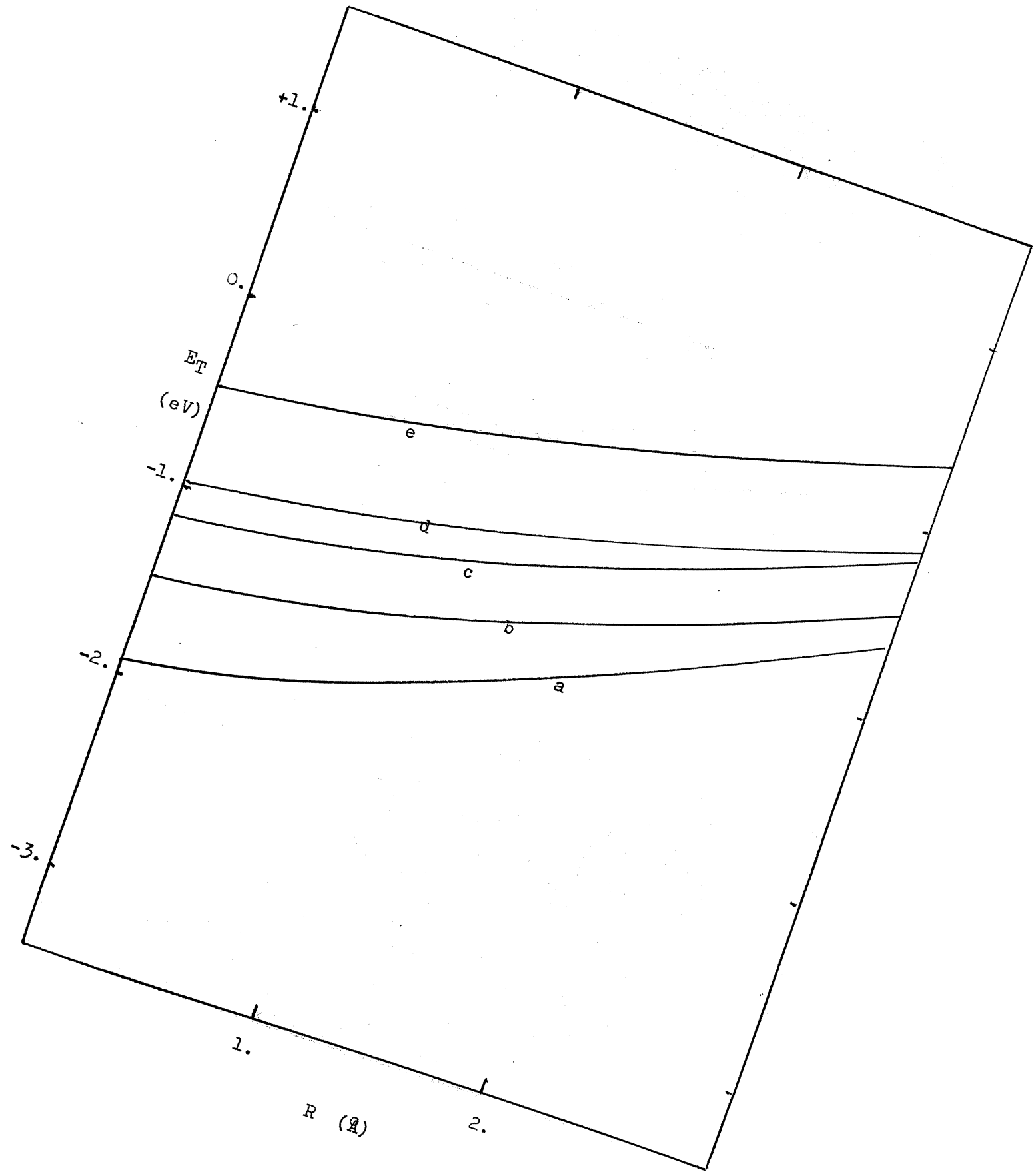

Figure II.23

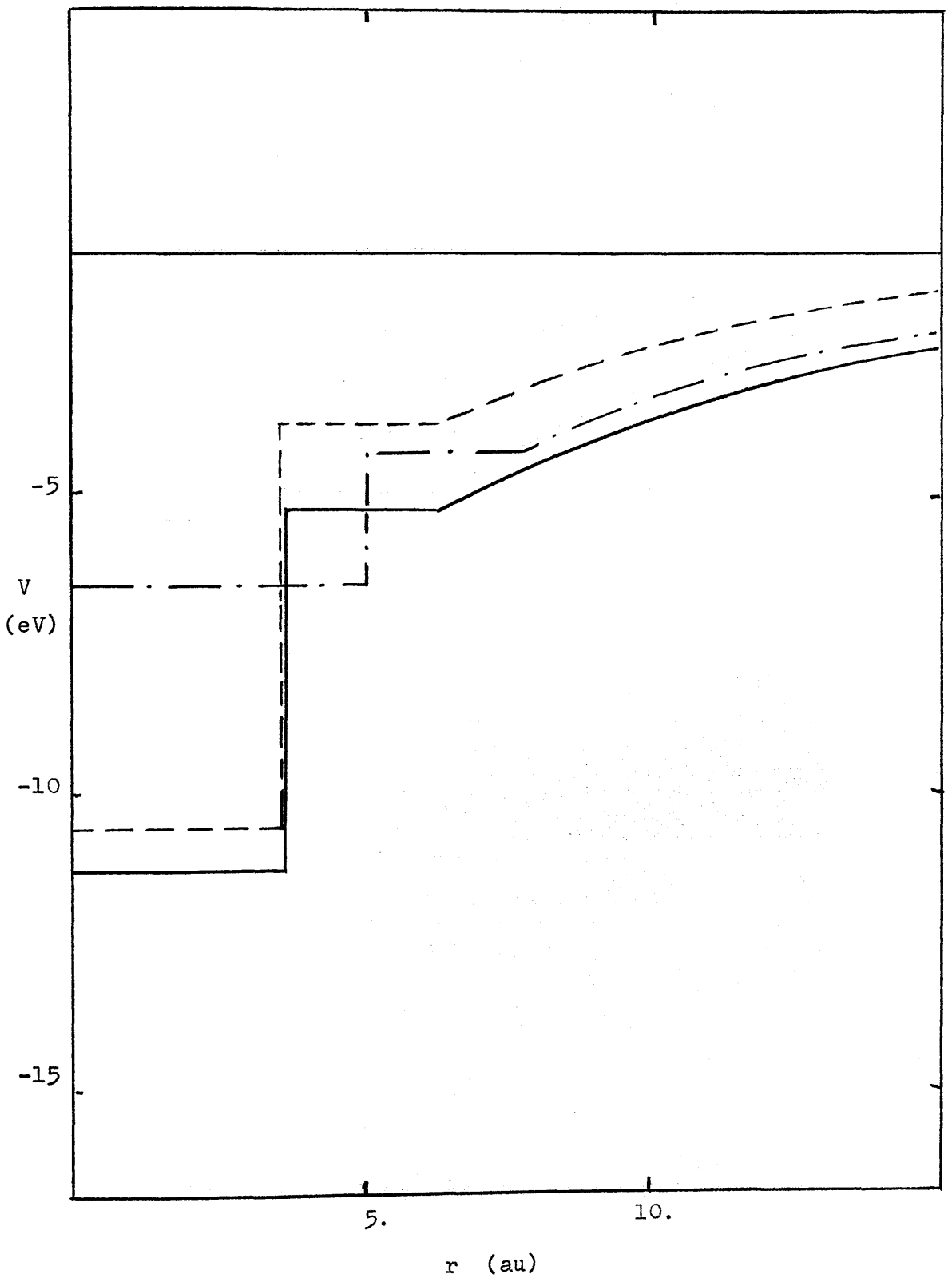

Figure II.24

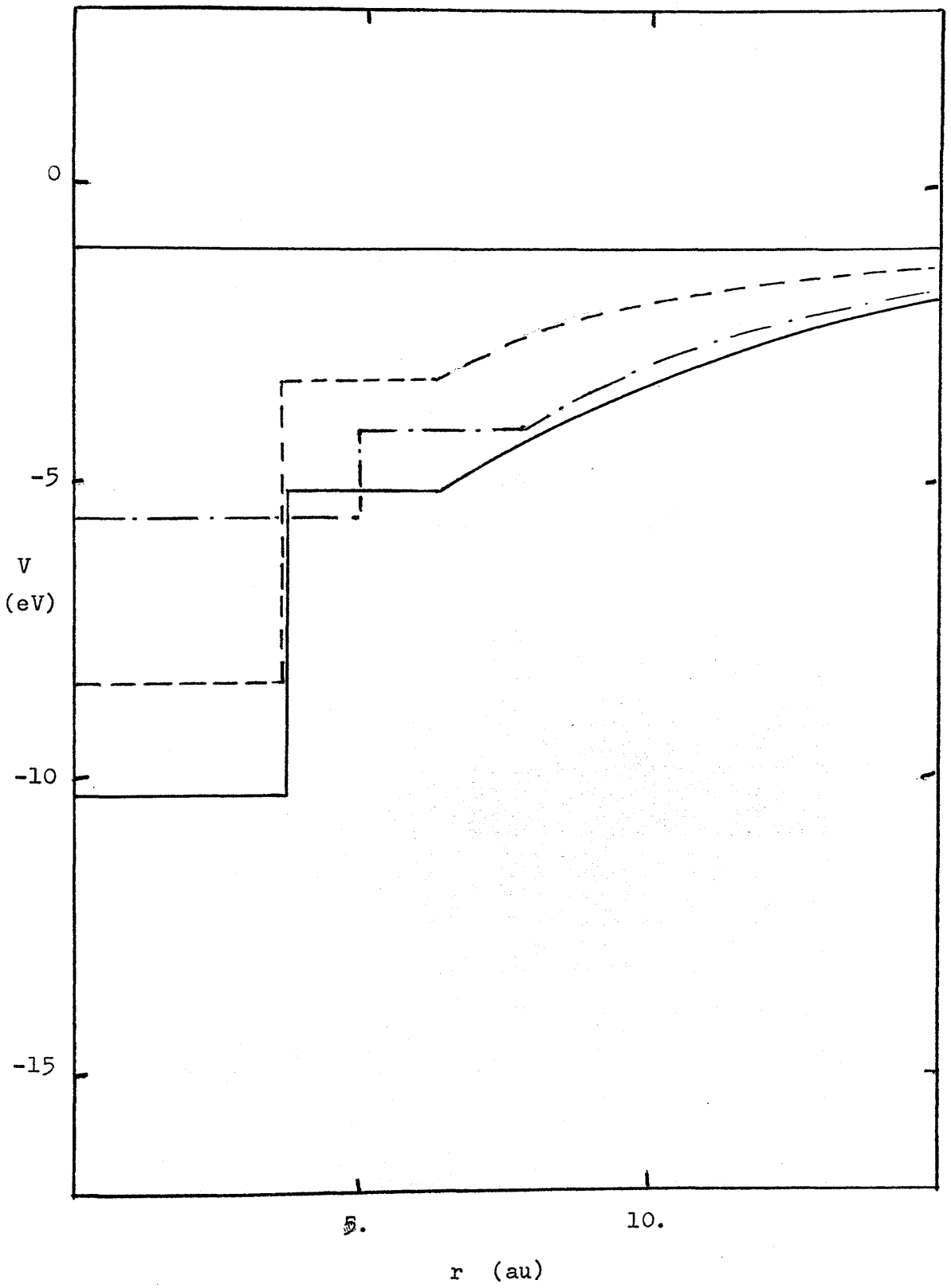

PART III

Surplus Dielectron Species in Polar Media.

Section 1

Introduction.

a) Experimental Findings.

In marked contrast to the vast body of experimental observations relating to the properties of surplus electrons in polar media, very little firm knowledge, but much speculation, exists as to the properties of the corresponding dielectron species. In crystalline solids the existence of such a species which comprises two electrons trapped at a single anion defect, the F'-centre, is well accepted. More recently, accrued experimental evidence has been interpreted in terms of the trapped dielectron in glasses and liquids.

In γ-irradiated glassy alkaline ice at $77^{o}K$ the species appears to be characterized by a broad optical absorption band peaking near 1.24 eV[148], to the red of the known one-electron band. Several kinetic decay results have been rationalized in terms of thermal and optical dissociation of the dielectron to produce the single-electron species[149]. In water flash-photolysis studies, under certain conditions, indicate the presence of a long-lived precursor of the hydrated electron[150], which has been suggested to be the hydrated dielectron[151]. The necessary pervading conditions, in particular that the lifetime of the hydrated single-electron species with respect to all other reactions must be greater than about 0.2 msec will, unfortunately, probably hinder its detection in pulse-radiolytic experiments.

Various models proposed for the observed increase in spin-pairing with increase in metal concentration in metal-ammonia solutions include the postulate of an ammoniated dielectron[152]. This was suggested as possessing an absorption band peaked at 0.81 eV. The spectral shift concomitant with increase in concentration has been suggested to

arise from the overlapping of the absorption bands due to the presence of both one and two-electron species in the dilute region[156]. At least one alternative explanation of this observation has been aired, in terms of an ionic cluster model of these solutions, which implies that the changes are merely due to some modification of the bulk structure of the medium at increased concentrations[153]. One attempt to resolve the absorption envelope to its components has failed,[154] one is deemed successful[155]. The high mobility of the electron solvated in both water and ammonia, especially the latter, must depend on the existence of some special transfer mechanism. A transition from one to two-electron cavities has been proposed[157]. On the other hand, detailed equilibrium constant studies[158] and pressure variation experiments[159] have failed to indicate the presence of the species in metal-ammonia solutions.

Clearly, much remains to be done to elucidate the properties and establish the existence of the solvated dielectron species. Perhaps it will be seen eventually to occupy a position of importance, similar to its ubiquitous single-electron counterpart.

b) Theoretical Developments.

Theoretically, the existence of the dielectron species in metal-ammonia solutions was first proposed by Ogg[97] and later by Freed and Sugarman[160]. In Ogg's calculation the dielectron was assumed constrained by an infinitely high-walled square-well potential of radius R_v and depth $2\delta e^2/4\pi k_o R_v$. The electron-electron interaction term was guessed at $e^2/4\pi k_o R_v$. Hill[161] demonstrated that the correct repulsion term was 1.79 times this estimated value, which made the trapped dielectron an improbable species in the limit of zero concentration and at zero temperature. However, by neglecting the presence of any equilibria, other than that involving a one-electron to two-electron cavity balance, at finite concentrations and at reasonable (liquid ammonia) temperatures the two-electron species was found to be preferred. The extremely large excitation energies derived in these infinite-walled models for the single ammoniated electron species was evidence of the need to consider a less rigidly constrained charge distribution.

This approach was adopted in the work of Land and O'Reilly, previosly mentioned in connection with computations on properties of the ammoniated electron. A particle in a finite box model was employed, the height of the walls being estimated from charge-dipole and charge-quadrupole contributions. With a few other adjustments, such as the inclusion of optical polarization terms, reasonable accord with the empirically suggested 0.81 eV was attained. The cavity was assumed surrounded by a rather large number of solvent molecules and its size, for the single-electron species, chosen to fit the observed volume expansion data. For the dielectron a void of exactly double this volume was selected. A crude medium reorganization energy was computed which placed the one-electron transition at 1.14 eV and that due to the dielectron at 0.64 eV. The latter species was revealed as unstable with respect to dissociation into two separate single-electron cavities, an

energy change of about 0.9 eV accompanying this reaction. The above formulation neglected any correlation in the motion of the electrons in the doubly occupied cavity.

O'Reilly[162] has recently improved the approximations involved in this approach to some extent by including the actual dipole-dipole interactions among the neighbouring solvent molecules, twenty-three(!) in all, and reversed the above stability criterion. An attempt to treat the electron correlation problem by an iterative perturbation technique did not converge, but an estimate of this contribution enhances the predicted relative stability of the dielectron.

A more realistic appraisal of the potential experienced by the electrons in the doubly-occupied well was felt necessary and the semicontinuum models presented previously were the obvious candidates. As an introduction to the problem and to gauge the effects of electron-electron correlation in these systems, a thorough study of the foregoing polarized cavity models was first undertaken.

At the time of initiation of this work, the only dielectron studies available, within these models, were those of Fueki[163], who considered the scf polarized cavity model, but only in the limit of zero cavity radius, for trapped dielectrons in aqueous systems, Fueki and Noda[164], who performed an adiabatic calculation within the polarized cavity approach on the ammoniated dielectron and Kestner and Copeland[165], who used an early form of the adiabatic semicontinuum treatment employing large numbers (12 and 18) of first layer molecules coordinating the electron pair in ammonia.

The two, first mentioned, calculations were based on a variational Hartree solution technique using the usual inflexible one-parameter representations of the single-particle functions. All aspects of instantaneous correlated motion of the electrons were neglected. The last involved a detailed determination of the ground (^1S) state properties

only, but employed more flexible variational functions and attempted to include correlation by means of a two-term configuration interaction scheme. While this predicted a stable two-electron cavity should exist, it was indicated that two one-electron voids were to be preferred.

However, during the course of the present study, calculations on the semicontinuum level, an adiabatic treatment by Copeland and Kestner[166] and an scf approach by Feng, Fueki and Kevan[167] have been published. While this detracts from any originality in the present work, it offers a further area of evidence for the necessity of at least solving for the properties of these approximate models in a rigorous fashion. Both the above semicontinuum calculations have been pursued employing the limited variational technique demonstrated here as insufficient. Once the accurate solutions of a given model potential are known, statements about the essential physical content of the model can be made with more certainty.

c) Treatment of Correlation in Dielectron Species.

The Hamiltonian operators relevant to all the polarized cavity and semicontinuum models discussed here for the solvated dielectron may be written as a sum of two single-particle contributions and, of course, the electron-electron interaction term. In an endeavour to gain some insight into the effect of instantaneous correlation of surplus electron motion in these systems, some way of going beyond the usual Hartree-Fock treatment of electron-electron coupling is necessary. A perturbation scheme which involved a combination of numerical techniques and the conventional variational approach was chosen as most satisfactory.

The simplest possible perturbation scheme was chosen namely

$$H^{o} = \Sigma_{i=1}^{2} h^{o}(i) = -\tfrac{1}{2}\nabla_1^2 + V(r_1) - \tfrac{1}{2}\nabla_2^2 + V(r_2)$$

$$\psi^{o} = \phi_{1s}(1)\,\phi_{1s}(2)\,2^{-\frac{1}{2}}\left[\alpha(1)\beta(2) - \alpha(2)\beta(1)\right]$$

$$H^{1} = r_{12}^{-1}$$

i.e. a hydrogenic form for the zeroth Hamiltonian and the electron-electron interaction as the perturbation.

This leads to the perturbation equation

$$(H^{o} - E^{o})\,\psi^{1} = (E^{1} - H^{1})\,\psi^{o} \qquad (1)$$

where

$$E^{1} = (\psi^{o} \mid H^{1} \mid \psi^{o})$$

But the solution of (1) involves six different electron coordinates. Clearly some simplifications are necessary. Immediate integration over the Euler angles leaves equations in r_1, r_2, and r_{12}, i.e. a three-dimensional problem. Such an approach has been attempted by Barraclough and Mooney[168] for the ground state of the helium atom, but requires massive computational effort.

Alternatively, the first-order wave-function may be expanded in a series of Legendre polynomials in $x = \cos\theta_{12}$ which yields

$$\psi^{1} = \Sigma_{\ell=o}(4\pi)^{-1}\,U_{\ell}(r_1,r_2)\,P_{\ell}(x)$$

whereupon substitution into the perturbation equation (1) and integration

out of the angular variables leaves an infinite series of two-dimensional equations which prove much more tractable.

This results in the solution of an elliptical partial differential equation for each component of separate value

$$\left[-\tfrac{1}{2}\left\{r_1^{-2}\,\partial/\partial r_1\,(r_1^2\,\partial/\partial r_1) + r_2^{-2}\,\partial/\partial r_2\,(r_2^2\,\partial/\partial r_2)\right\}\right.$$
$$\left. + \tfrac{1}{2}\ell(\ell+1)\,(r_1^{-2}+r_2^{-2}) + V(r_1) + V(r_2) + 0.5 + 0.5\right] U_\ell(r_1,r_2)$$
$$= (0.625\,\delta_{\ell o} - r_a^\ell / r_b^{\ell+1})\,R_{1s}(r_1)\,R_{1s}(r_2) \qquad (2)$$

where r_b is the greater, and r_a the lesser, of r_1 and r_2. This leaves the second order perturbation energy, E^2, as a simple sum of partial-wave contributions, it being diagonal in the U_ℓ.

$$E^2 = \Sigma_\ell\,\varepsilon^2(\ell)$$
$$= \Sigma_\ell\,(2\ell+1)^{-1}\int U_\ell(r_1,r_2)\,(r_a^\ell / r_b^{\ell+1} - 0.625\,\delta_{\ell o})$$
$$R_{1s}(r_1)\,R_{1s}(r_2)\,r_1^2\,r_2^2\,dr_1\,dr_2$$

Radial equations such as (2) were conventionally solved by variational methods. McKoy and Winter have indicated that finite-difference techniques could be profitably employed[169]. Whereas solutions for $\ell=0$ were found readily by a simple Gauss-Seidel iteration technique, it was discovered that the S-wave ($\ell=0$) apparently did not have a sufficiently diagonally-dominant coefficient matrix on the left-hand side[170]. A direct method, Gaussian-elimination, was employed for the S-wave to obviate the above convergence difficulties.

To this end it was noted[171] that the $\ell=0$ component of the first-order wave-function can be satisfactorily represented by a configuration interaction type function

$$\chi = (r_1^m\,r_2^n + r_1^n\,r_2^m)\;\exp(-\alpha r_1 - \beta r_2) + \exp(-\beta r_1 - \alpha r_2)$$

A 54-term function of this kind was found adequate to reproduce the Winter and McKoy results exactly. This method was, however, found unsuitable for higher partial-waves due to extreme difficulties in maintaining precision[172]. An iterative technique was therefore retained for the $\ell=o$ solutions of the linear equations resulting on finite-difference

discretization of (2). Successive over-relaxation was employed. Although it was not possible to determine any prescription for the optimum value of the relaxation parameter, , substantial improvements on the Gauss-Seidel method =1 could generally be found.

One simple example indicates the power of this method in obtaining both the coulomb and instantaneous radial correlation energy. For a simple hydrogenic potential $V(r) = r^{-1}$, the correction to the energy obtained in the S-limit (L=0,only) was -3.4101 eV. The contribution from L=1, the P-limit, gave an additional -0.7210 eV, the D-limit, -0.1063 eV. The total second-order energy in the limit of L=20 was found to be -4.2896 eV and the S-wave is seen to give almost 80% of the radial correlation energy. Including the total second-order energy obtained above provided an estimate of the total energy of the $1s^2$ electron pair in helium of -78.9976 eV, very close to the exact value of -79.0096 eV reported by Pekeris[174] and Pekeris et al.[173]

An alternative perturbation scheme may be developed choosing the Hartree-Hamiltonian in the zeroth order equation.

$$\left[-\tfrac{1}{2}\boldsymbol{\nabla}_1^2 + V(r_1) + J(r_1) - \boldsymbol{\varepsilon}^{o}_{1s}\right]\boldsymbol{\phi}_{1s}(r_1) = 0$$

is then the equation satisfied by the zero-order one-electron orbitals in $\boldsymbol{\psi}^{o}$, where

$$J(r_1) = \int \boldsymbol{\phi}_{1s}(r_2)\, r_{12}^{-1}\, \boldsymbol{\phi}_{1s}(r_2)\, dv_2.$$

Expanding the first-order pair function leads to [175]

$$\left[-\tfrac{1}{2}\left[r_1^2\,\partial/\partial r_1\,(r_1^2\,\partial/\partial r_1) + r_2^{-2}\,\partial/\partial r_2\,(r_2^2\,\partial/\partial r_1)\right]\right.$$
$$+ \tfrac{1}{2}\boldsymbol{\ell}(\boldsymbol{\ell}+1)\,(r_1^{-2}+r_2^{-2}) + V(r_1) + V(r_2)$$
$$\left. + J(r_1) + J(r_2) - 2\,\boldsymbol{\varepsilon}^{o}_{1s}\right] U_{\boldsymbol{\ell}}(r_1,r_2)$$
$$= \left[\left[E^1 + J(r_1) + J(r_2)\right]\boldsymbol{\delta}_{\boldsymbol{\ell}o} - r_a^{\boldsymbol{\ell}}/r_b^{\boldsymbol{\ell}+1}\right]$$
$$R_{1s}(r_1)\,R_{1s}(r_2),$$

with $E^1 = -(1s1s\left|r_{12}^{-1}\right|1s1s)$,

and $E^2 = \Sigma_{\boldsymbol{\ell}}\,(2\boldsymbol{\ell}+1)^{-1}\int R_{1s}(r_1)\,R_{1s}(r_2)\left[r_a^{\boldsymbol{\ell}}/r_b^{\boldsymbol{\ell}+1}\right.$
$$\left. - \boldsymbol{\delta}_{\boldsymbol{\ell}o}\left[E^1 + J(r_1) + J(r_2)\right]\right] U_{\boldsymbol{\ell}}(r_1,r_2)\, r_1^2\, r_2^2\, dr_1\, dr_2.$$

This approach, using the scf single-particle functions as zero-order orbitals was also tested but found to give no difference in accuracy and no substantial improvement in convergence with L.

Section 2

Polarized Cavity Models.

a) Theory.

Both the adiabatic and the scf formulations of the polarized cavity models for single-electron species may be readily modified to accommodate the presence of an additional electron.

If a relaxed state function is written (st), a combination of two single particle orbitals, and a general instantaneous state as (ij) then, assuming spherical symmetry as before, the i^{th} one-electron orbital in the state under consideration satisfies the usual radial equation (3). In atomic units

$$\left\{-\tfrac{1}{2}\, d^2/dr^2 + \ell_i(\ell_i+1)/2r^2 + V^i_{pol}(r) + V^{(i)}_{int}(r)\right\} P_i(r) = W_i\, P_i(r), \qquad (3)$$

where V_{pol} is the trapping polarization potential and V_{int} describes the effect of electron-electron interaction. The superscripted i indicates that these potentials may be state-dependent.

In the adiabatic approach the previous, one-electron inertial trapping potential is merely doubled to give

$$(4\pi k_o)\, V_{pol}(r) = \begin{cases} -2e^2\beta / R & r < R \\ -2e^2\beta / r & r > R. \end{cases} \qquad (4)$$

The indexed i has now been dropped since this same potential is assumed to sustain all states in the adiabatic approximation.

The electronic and medium-inertial polarization terms are altered in an exactly analogous fashion. Thus the single particle energies, W(i) and W(j), obtained as solutions of (3) are augmented by the identical electronic polarization terms

$$S^e(k) = -\tfrac{1}{2}\gamma e^2 / (4\pi k_o)\, F(k)$$

to give a total electronic energy of the state (ij) as

$$E^e(ij) = W(i) + W(j) + S^e(i) + S^e(j) - E_{int}$$

where $E_{int} = (k|V^k_{int}|k)$ and k is i or j. This last term must be subtracted to cancel the double-counting of the electron-electron interactions in the single particle energies. Tachiya's form of the medium polarization energy was carried through here becoming simply

$$\Pi^T = 2\beta e^2 / (4\pi k_o) R \qquad (5)$$

This is four times the corresponding value in the one-electron case; twice the induced polarization and twice the number of electrons interacting with it.

In the scf scheme, the orientational contribution to the polarization is influenced by the charge distributions of both relaxed state electrons, while the optical contribution responds only to the instantaneous state, i.e.

$$(4\pi k_o) V^i_{pol}(r) = \begin{cases} -\beta\{p_s(R) + p_t(R)\} - \gamma\{p_i(R) + p_j(R)\} & r < R \\ -\beta\{p_s(r) + p_t(r)\} - \gamma\{p_i(r) + p_j(r)\} & r > R \end{cases} \qquad (6)$$

with $p_k(r)$ as $r^{-1}Y_o(k,k;r)$. As before the total system energy is obtained by combining, with the resulting electronic energy, a medium polarization term

$$\begin{aligned}(4\pi k_o) U(ij) = \beta\{ & p_s(R)\int_o^R P_s(r)\,dr + \int_R^\infty P_s(r)\,p_s(r)\,dr \\ & + p_t(R)\int_o^R P_t(r)\,dr + \int_R^\infty P_t(r)\,p_t(r)\,dr\} \\ +\gamma\{ & p_i(R)\int_o^R P_i(r)\,dr + \int_R^\infty P_i(r)\,p_i(r)\,dr \\ & + p_j(R)\int_o^R P_j(r)\,dr + \int_R^\infty P_j(r)\,p_j(r)\,dr\} \end{aligned} \qquad (7)$$

The electron-electron interactions are introduced into both treatments in an identical way. They are artificially separated, as in (8), to be the sum of a coulomb term, F, and an exchange term, G.

$$V^i_{int}(r) = F_i(r) + G_i(r) \qquad (8)$$

The coulomb term in the presence of a surrounding dielectric medium is adopted from the work of Land and O'Reilly. Namely

$$(4\pi k_o) F_i(r) = \begin{cases} f_i(r) - \gamma f_i(R) & r < R \\ k_{op}^{-1} f_i(r) & r > R \end{cases}$$

where $f_i(r) = r^{-1}Y_o(j,j;r)$. That is, they depend on the average charge

distribution of the other electron in the configuration under consideration. The presence of the medium is seen to reduce the electron-electron interaction outwith the cavity and to merely add a constant contribution within it. The exchange term may not be evaluated in this simple manner but is simply approximated here as

$$G_i(r) = k_{op}^{-1}\, g_i(r)$$

for all values of r, where

$$g_i(r) = c_{ij}\, r^{-1} Y_1(i,j;r)\, P_j(r)\, P_i^{-1}(r)$$

The c_{ij} are the usual constants resulting on the integration over the angular coordinates. The Y_k are defined in Part I.

b) Results and Discussion.

Fueki and Noda[164] employed the simple adiabatic potential, (4), to investigate the properties of the ammoniated dielectron within a polarized cavity model. Single-exponential variational, one-electron orbitals were used throughout. Thus the ground state, assumed singlet S, is given as a product of two identical one-parameter 1s functions and the first excited state, ^1P, is the usual antisymmetrized product of 1s and 2p orbitals.

The electron-electron interaction in the ground state was treated in the way presented above but, for the excited state, it was assumed to be reduced by the optical relative permittivity for all values of r. This procedure was justified in terms of a diffuse excited state function reducing the probability of both electrons being inside the cavity simultaneously.

The results of these workers, obtained by minimizing the sums of the ground and excited state single-particle energies respectively, to derive optimum exponents, are in Table III.1. This also contains the present numerical results. The accurate solution has, once again, revealed the inadequacy of the variational approach, affording rather less than a 10% lowering in the total electronic energies. The electronic polarization energies are about 15% different. Figure III.2 indicates the cause. The variational functions are markedly too diffuse. The extent of the disagreement with the accurate functions is not revealed here by merely comparing the electronic energies since, to obtain these, the coulomb repulsion term must be added. The compactness of the numerical charge distributions has pushed up the value of this contribution, thus cancelling some of the previous gain. Quite similar improvements are noticed in the excited state charge distribution and energy components.

In Figure III.1 a comparison of the numerical and variational

energy terms over a range of cavity sizes is illustrated. The amelioration is, of course, maintained.

The treatment of correlation discussed earlier afforded another 10% drop in the energy of the ground state $1s^2$ pair. In the limit deployed, contributions from partial-waves up to L=15 were included, it is hoped that all radial correlation has been accounted for.

Assuming that the volume expnsion data, supposed to be 65-93 ml/mole for the ammoniated dielectron[176], can be interpreted in terms of a doubly-occupied cavity of about 4.0 Å in radius, Fueki and Noda compute a peak absorption energy of 0.46 eV for the ^1S to ^1P transition and an oscillator strength of 1.1. They suggest that a proper inclusion of the coulomb term for the excited state may increase this energy to about 0.6 eV, in better accord with the empirical suggestion of 0.81 eV. However, as indicated in Table III.2 this hope was in vain. Accurate numerical solution, together with a consistent treatment of electron-electron interaction, placed the transition energy at 0.475 eV, very little different from the variational value.

The pair-function approach to the instantaneous correlation problem, as developed here, could not be used to gauge the extent of this effect in the excited state. Assuming the magnitude of the correlation interaction in this state to be negligible a new estimate of the absorption peak is 1.0? eV, the ground state energy having been lowered by 0.54 eV on the inclusion of correlation.

An idea of the relative stability of the ammoniated dielectron with respect to dissociation into two single electrons may be obtained by merely comparing the heats of solution of the respective species. Fueki and Noda attempted this and derived the solution heat by augmenting the total ground state energy with a medium polarization contribution, Jortner's original expression for the one-electron species was employed, and a small surface tensional energy, computed just as in

the adiabatic semicontinuum approach. Making the further assumption that the volume occupied by the dielectron is approximately twice as great as that filled by the single solvated particle, for the sake of comparing cavity radii, Fueki and Noda place the heat of the associated reaction at -0.15 eV per electron. This value was obtained by employing Jortner's "optimum" one-electron cavity, 3.2 Å, to give the heat of solvation of the single species, and the present 4.0 Å void for the dielectron.

Following a similar matching procedure here, the new best fit to the one-electron band is at 3.69 Å which gives a heat of solution of 0.686 eV, incorporating both Tachiya's polarization term and the above surface tensional component. To be consistent a similar parameterization of the dielectron cavity, assuming the suggestion of 0.81 eV as the absorption peak, was carried out. Neglecting, for the moment, the effect of correlation on the ground state, this results in a cavity of 2.8 Å for the dielectron and a heat of solvation of 0.732 eV per electron. This implies a heat of association of -0.05 eV and thus a slightly stable dielectron. Including the properly correlated two-electron ground state relocates the optimum cavity at 4.6 Å, giving a heat of solvation of but 0.460 eV per electron, much favouring unpairing.

Table III.3 contains some properties of the hydrated dielectron computed within the above framework. In compiling this tabulation the correlated ground state energy was employed. It was neglected in Table III.2. No experimental hint as to the position of the dielectron absorption is presently available in this medium and no comparison with observation is possible. However, assuming that the commonly observed band happens to overlay the dielectron peak, entirely without justification, then the heat of association may be evaluated to be in the neighbourhood of -0.1 eV by the above method. The numerical match to the single-electron absorption within the same model-potential approach,

as derived in Part II, was used to estimate the heat of hydration of the single-electron species, i.e. a one-electron cavity of 1.84 Å was assumed and a heat of hydration of 0.723 eV, computed using Tachiya's medium polarization as here, resulted. The surface tensional contribution employed the plane-surface tension of water at $7.2 \times 10^{-3} Jm^{-2}$.

Viewed in terms of the above model, the position of the spectral band maximum of the dielectron species, in both aqueous and ammoniacal media, is expected to exhibit slightly enhanced red shifts with increasing temperature and blue shifts with increase of ambient pressure relative to the corresponding one-electron absorption peak. This is attributable to the stronger variation with cavity radius computed in the ground state of the doubly-occupied void.

In metal-ammonia solutions, if it is assumed that the apparent molar extinction coefficient at the band maximum of the dielectron absorption is less than twice the corresponding peak value in the single-electron species, then following Catterall and Symons[152] the temperature variation of the observed band may be explained. Such an assumption is supported in the variational work of Fueki and Noda, who obtain a dipole-velocity oscillator strength of 1.1 for the doubly-filled cavity transition at a radius of 4.0 Å. This is compared with a value of 0.62, computed in the dipole-velocity form, from Jortner's original single-electron wave functions in a void of 3.2 Å. Proceeding, as before, to make the comparison at the parametrically-matched, numerically-obtained cavity radii, gives a dipole-velocity oscillator strength of 0.651 for the one-electron transition in the 3.69 Å cavity and of 1.489 in a 2.8 Å void and 1.762 in a 4.6 Å void, first neglecting, then including, the effect of electron-electron correlation in the ground state energy. The inequality obtained is contrary to the original assumption in both cases and to the prediction of the variational principle.

Fueki has investigated the properties of dielectrons in aqueous

media within the confines of the self-consistent field treatment of the polarized cavity model.

A variational approach was employed and a two-parameter, Hylleras-type function (9), was chosen to represent the ground-(^1S) state charge distribution, in the hope of including some of the correlation energy.

$$\Psi(^1S) = N\left[\exp(-ar_1)\exp(-br_2) + \exp(-br_1)\exp(-ar_2)\right]. \quad (9)$$

However, the minimization procedure, designed to discover the best total ground state energy, revealed that the optimum exponents were identical. Thus a return to the Hartree approximation of electron-electron interaction was effected. The excited (^1P) state was expressed, as above, in an antisymmetrized product form. All aspects of instantaneous correlation were ignored.

Calculations were performed over a range of static dielectric functions from 80.0, apposite to water at room-temperatures, down to 3.0, found in low-temperature crystalline ice, at 88^oK.[177] Results were obtained only in the limit of zero cavity radius for two reasons. Firstly, this expedient greatly simplifies the required computational effort. Secondly, based on early studies of the effect of pressure on the spectra derived from the single-electron species in water[178,179], the associated cavity could be assumed very small. A stability criterion for dielectron dissociation was readily derivable since the model chosen is capable of analytical solution. Provided $(1-k_{op}^{-1})k_{st}$ was greater than unity, then, assuming that no important reactions which would remove the hydrated single-electron species prior to pairing were present and that entropy effects could be neglected, the dielectron was energetically more favourable than two separated, solvated particles. It was thus implied that in aqueous media a static relative permittivity greater than 2.28 would be sufficient to allow the existence of a stable, doubly-occupied cavity.

The experimentally observed absorption band attributed to the dielectron in glassy alkaline ice was compared to the variationally obtained transition energies and rough agreement could be found if the low-frequency dielectric function lay between the values of 4.0 and 5.0.

Table III.4 analyses the difference computed in the energy contributions to the ground and first excited state obtained by employing the present accurate solution technique. The variational ground state components have been secured using the reported value of the mean radius of this state to calculate the optimum 1s-orbital exponents. A substantial, 10 to 12%, increment is disclosed in each term, contributory to the total ground state energy, for both values of the relative permittivity listed. Indeed, the trend is, of course, reproduced over all values of this parameter. Direct comparison of the corresponding ameliorations achieved in the singlet P excited state properties is precluded, no variational data other than the total system energy for this state having been reported. These data can not now be obtained from the mean radii of the excited state since this is a function of the optimized variational parameters of both component one-electron orbitals, which were not individually quoted. As usual, in the scf scheme, the total energy comprises various contributions from the orientational polarization of the relaxed ground state. The disparity in the total excited state energy is thus not a meaningful guide to the accuracy of the original solution.

However, Figures III.3 and III.4 do indicate the inadequacy of the single-exponential functions. They again underestimate the compactness of the true charge distributions. This effect is particularly pronounced in the variational excited (^{1}P) state for a small value of the low-frequency dielectric function. Decreasing this parameter allows percolation of the electron-pair out into the bulk surrounding medium

to a large extent. Compare the mean radii for k_{st}= 80.0 and k_{st}= 3.0 in Table III.4. The variationally obtained approximate representation of the charge distribution, used by Fueki, considerably overestimates the magnitude of this effect.

The quantiy $E_t(^1S)$, specified in Table III.4, is the total system energy with the electron in a relaxed ground state in which the instantaneous correlations in the motion of the bound electron pair have been included by means of the method discussed earlier. The application of this technique to the scf problem involved here(self-consistent in the trapping polarization field) was discovered to be computationally hazardous. Coding requirements became tricky and convergence was generally poor if direct iterative attempts were employed. Fortunately, the simple Aitken "del-squared" process proved to give satisfactory stabilization in the majority of cases studied.[180] The expended effort resulted in a further lowering of the order of 6% in the total ground state energy.

Carrying through this correlated ground state energy, the properties listed in Table III.5 are obtained. The uncorrelated variational and numerical properties are also tabulated here. With a dielectric function appropriate to water the similar improvements, secured numerically, in both the ground and excited states have left the variationally predicted value of the transition energy, 2.04 eV, virtually unaltered. Inclusion of correlation effects in the ground state, as mentioned previously, no effort was made to include an estimate of this contribution in the excited state, gives about a 0.4 eV increase in this quantity. On the other hand, for k_{st}= 3.0 the larger magnitude of the apparent improvement in the ^1P energy has halved the variational absorption energy. The correlation correction, of the order of 0.15 eV here, does not renew the agreement.

If a parametric match, in this limit of zero cavity radius, to

the observed dielectron spectrum in alkaline ice is desired, then a value of k_{st} in the region of 8.0 must be deployed with the present numerical method. The oscillator strength of the transition is then 0.764 or 0.951 in this model, depending whether the dipole-length or dipole-velocity expression for this quantity is selected. The manner of inclusion of polarization in the scf approach is the reason for the disparity. This value of the dielectric function, considerably larger than that suggested by Fueki, may not be at all inappropriate in such a glassy disordered medium as alkaline ice. Presumably large fluctuations in the local short-range microscopic structure of the material could induce such an effect. In a system like this the usefulness of a bulk parameter such as the relative permittivity in characterizing the detailed properties observed is doubtful. As indeed is the application of the above model which relies on the existence of long-range polarization potentials to provide a stabilizing potential.

It is interesting to note that, within the scf formulation of the polarized cavity model and in the adiabatic approximation discussed above, the excited singlet-P state is predicted to be strongly bound in all systems studied. This is in marked contrast to the situation in the F'-centre in crystalline solids where the very broad spectral band attributed to this species is assigned to be due to a bound-to-free transition.

Variationally, the dielectron was predicted stable with respect to dissociation into two singly-occupied cavities in water and ice. The numerically derived heats of hydration, presented in Table III.4 for both dielectron and one-electron species, confirm this prediction. (If ΔH_{12} is positive, then the paired species will be preferred.) When the effect of correlation is included in the ground state dielectron energy this stability is, of course, enhanced. Interestingly, accurate numerical solution has not detracted from the simple stability

criterion of Fueki.

The finite-difference technique was employed to investigate the behaviour of the solutions of the scf polarized cavity model at finite void radii. Parameters apposite to ammonia were selected since the dielectron could be assumed to produce an absorption band peaking at 0.81 eV in this medium. A cavity radius of 4.48 Å gave the point of match and yielded a heat of solution of 1.284 eV per electron. This estimate, when compared with the analogously determined value of 1.092 eV for single-electron ammoniation in a cavity of 2.93 Å, as derived in Part II, indicates that, within this model, the ammoniated dielectron is predicted to be stable by about 0.2 eV per electron. In the finite cavity the ^1P state remained strongly bound.

The computed transition energy, in this approach, was again found to be more strongly dependent on variations in cavity size than the corresponding one-electron quantity in ammonia. Thus, somewhat larger spectral changes, of the order of 10-15% greater, might be expected, concomitant with increase in temperature and pressure, in the dielectron absorption.

Of course, such predictions should not be taken too seriously, considering the many limitations inherent in such a naive model. To consider such refinements as the effect of entropy changes, which must surely accompany electron pairing, the above polarized cavity models, with their conceptually elementary potential forms are most unsuitable. Any assertion of the importance of such effects is best left to a model which takes some account of the microscopic structure of the dielectric medium in which the electron and electron-pair are imbedded. Such is the goal of the semicontinuum approach.

Section 3

Semicontinuum Models.

a) Theory.

Again, both self-consistent field and adiabatic treatments of this model system may be easily adapted to describe the presence of the additional electron.

Assuming, as before, a relaxed state (st), an instantaneous state (ij) and the necessary spherical symmetry, the customary radial Schrodinger equations may be written for each of the single-particle functions in the state under consideration.

In both approaches the requisite potential forms may be decomposed into a long-range polarization contribution, a short-range charge-multipole interaction, a constant repulsive term and the electron-electron interaction energy. The constant repulsive term in both models is just V_o, the energy of the quasi-free state. It acts outwith R, the hard-core radius, in the adiabatic case and r_d, the radius to the dipole-centres in the scf scheme. It should be noted that, in the dielectron system, V_o is effectively included twice, once for each electron. (This will lead to further obscurities in attempting to take over the relevant experimental parameter to this treatment when it is eventually obtained.) Thus all total energies should be referred to twice V_o if some estimate of the absolute stability of the state under consideration is required.

Similarly, an identical description of the electron-electron interaction is employed in both of these semicontinuum approaches. It is just as in equation (8) above, see Section 2(a). However, the discontinuity in the coulomb potential is again set at R in the adiabatic model and at r_d in the scf treatment.

As observed in the solvated single-electron calculations within the semicontinuum approximation, the other contributions differ substantially.

Jortner's form of the long-range inertial polarization potential is maintained in the adiabatic formulation, but the truncation is now set at r_c, the onset of the continuous medium. Thus

$$(4\pi k_o)\, V^{adb}_{pol}(r) = 2\beta e^2 / r_c \qquad r < r_d$$
$$2\beta e^2 / r \qquad r > r_d.$$

In the scf scheme, this contribution is as in equation (6) for the scf polarized cavity model of the dielectron. R in the scf semicontinuum model also measures the beginning of the continuum.

Handled adiabatically, the short-range"molecular" potential, $V_{mol}(r)$, arising from the orientation of the neighbouring solvating dipoles is completely governed by the relaxed state charge distribution

$$(4\pi k_o)\, V^{adb}_{mol}(r) = N e \mu / r_d^2 \qquad r < r_d$$
$$0 \qquad r > r_d$$

where is now $_o \cos _{st}$, the average value of the cosine being influenced by the relaxed state of both trapped electrons. The orienting field due to the electron pair is now

$$F(r_d) = e(C_s+C_t) / (4\pi k_o)\, r_d^2 ,$$

C_k being the charge enclosed in the k^{th} relaxed state up to the hard-cores of the surrounding molecules. In the scf approach this charge-oriented dipole interaction is supplemented with a charge-induced dipole term. Here, this is simply a sum of contributions from the charge distributions of both particles in the instantaneous state under consideration. Thus, in total

$$(4\pi k_o)\, V^{scf}_{mol}(r) = -N\mu e / r_d^2 - N\alpha e^2 (C_i + C_j) / 2r_d^4$$

and this acts only within r_d.

The total adiabatic electronic energy may now be written as

$$E^e(ij) = W(i) + W(j) + S^e(i) + S^e(j) - E_{int}$$

where $S^e(k)$ is the electronic polarization amendment defined as in Part II. In the adiabatic work of Copeland and Kestner[166] a simpler form,

$$(4\pi k_o)\, S^e(k) = -N \alpha e^2\, C(k) / r_d^4 ,$$

was employed but this results in no great disparity with the expression utilized here. The incorporation of $C(k)$ in the above formula as opposed to the square of this quantity employed here, partially compensates the neglect of the latter term in equation (20) of Part II.

The various contributions to the medium rearrangement energy also reflect the presence of the additional electron. The cavity creation terms remain unchanged. The medium long-range polarization energies may be carried through fom the respective treatments in the corresping polarized cavity models, provided they are still assumed discontinuous at the continuum onset outwith the first coordination layer. Tachiya's expression for the medium orientational polarization in the adiabatic approach was maintained here for consistency. It is four times the corresponding value in the one-electron semicontinuum model. The use of this expression to estimate the inertial polarization work done on the medium, as opposed to Land and O'Reilly's correction to Jortner's original formula, produces no crucial differences here, due to the large values of r_c employed. Notice also that, in the computation of the scf polarization contribution to the medium energy, the factor of $\frac{1}{2}$ which occurred in the corresponding one-electron treatment has been dropped. In addition, the polarization fields of both electrons have, of course, been included. Thus, for the same effective polarizing potential, the dielectron cavity requires four times the amount of work to be performed on the medium than does the single electron species to accomodate their respective charge distributions.

The dipole-dipole repulsion energies amongst the first-layer molecules, which were identical in the alternative solution schemes of

the one-electron problem remain the same. Here they are

$$E_{dd}(ij) = D_N \mu_T^2 / (4\pi k_o) r_d^3 ,$$

where $_T$ is now a sum of the averaged cosine value, governed by the relaxed state distributions of both electrons, times the gas-phase dipole moment and a polarization contribution $e^2\alpha[C(i) + C(j)]/r_d^2$ depending on the instantaneous state of the two particles.

The hydrogen-hydrogen repulsive term, if included, remains just as before, except that the exponential term is modified by the new value of the average cosine, now appropriate. This completes the various contributions to the medium reorganization energy and represents the total work which must be done on the medium to accept the presence of the localized dielectron.

The energy of the optically excited conduction state may be obtained by making several assumptions. Firstly, after promotion of one electron into the conduction band, all interaction of this particle, via coulomb repulsive and exchange attractive forces, with the member of the pair remaining bound, is neglected. The ionized electron is assumed, as in the one-electron case, to possess zero kinetic energy. All electronic polarization effects are determined by the field of the still-trapped electron. This particle experiences a short-range potential which is unchanged in the adiabatic formulation since this includes only inertial effects. However, in the scf treatment the induced component becomes reduced by the subtraction of the contribution originally due to the excited electron. Similarly in this solution scheme the long-range, optical polarization potential must not include a contribution from the ionized particle. Other contributions, such as the electronic medium polarization energy on the induced component of the multipole repulsion term in the first layer must also neglect the presence of the excited electron. This last contribution is the only one to change in the adiabatic approach to calculating the same state.

b) Results and Discussion.

Copeland and Kestner[166] have pursued a study of the localized dielectron species solvated in metal-ammonia solutions. This work has been performed in the context of a semicontinuum model, solved within the electronic adiabatic approximation. It forms, essentially, an extension of a previous investigation into the properties of solvated electron pairs in this medium which employed an early form of the currently used adiabatic semicontinuum model. The model was refined to its present state through calculations of the properties of single surplus electrons by Copeland, Kestner and Jortner[127].

In their original two-electron work, Copeland and Kestner[165], assuming one- and two-electron cavities surrounded by rather large numbers, twelve and eighteen, of solvating ammonia molecules, optimum cavity radii, establihed by minimizing electronic energies, were obtained For the one-electron species, inclusion of twelve solvent molecules yielded a void of 1.82 Å in radius, whereupon a transition energy of 1.54 eV and a heat of solution of 1.68 eV were computed. Solvation of the dielectron by a similar number of ammonia molecules produced a transition energy of 0.88 eV and a heat of solution of 3.3 eV per electron. Thus, the relative stability of the dielectron with respect to dissociation into two singly-occupied voids was placed at 0.81 eV per electron. This value was computed neglecting entropy and other contributions. (For example, the two-electron cavity had contracted to 1.5 Å) Incorporating eighteen solvent molecules changed the numbers slightly but did not substantially effect the predictions.

In the more recent work, these authors have employed the full adiabatic potential described above and compounded the resulting electronic energies with the well-tested expression for the medium rearrangement energy, as used in the single-electron systems. A variational approach was adopted but no mention was made of the form of the one-

electron orbitals selected. In the original work the ground (^1S) state had been written as a product of two relatively flexible single-particle 1s functions and it was hoped that this procedure had been followed here. However, only one orbital parameter was reported to describe the entire ground state charge distribution. It was therefore assumed that the usual simple product of single-exponential Slater functions had been deployed to estimate the combination of one-electron orbitals. This assumption is supported by a simple calculation of the charge up to the hard-cores, a value for which was also reported.

In an endeavour to obtain some optimum value for the variational parameter, the minimization of several combinations of energy contributions was investigated. No substantial difference in the derived cavity radii or total energies was disclosed. This is an important result. Previously, in the one-electron studies, only the electronic single-particle energy had been optimized and the best exponent thus obtained had been used to compute all other state-dependent quantities. The results presented here derive from a minimization of the total electronic energy, including the electronic polarization component, compounded with the long-range medium inertial polarization energy. While this removes the need to assume an adiabatic following of the electron charge distribution by this latter term, it seems a somewhat inconsistent procedure. Preferably the total energy should be optimized.

Assuming a first coordination layer comprising twelve molecules for the dielectron in ammonia, the computed variation of the total ground state energy with cavity radius revealed a minimum of 0.3687 eV. The energy of the quasi-free state had been set to zero. Thus, in the limit of an scf treatment of electron-electron interaction, which is what the above Hartree approximation provides, the ground state, being greater in energy than the quasi-free state, should be unstable with respect to delocalization.

In an effort to alleviate this difficulty, the effect of angular correlations in the motion of the electron pair was inserted into the ground state charge distribution by a simple configuration interaction method. The basic Hartree scf function was mixed with a linear combination of excited state 2p orbitals. The correlation energy thus recovered, of the order of 0.4 eV, 12% of the total electronic energy, proved sufficient to depress the total ground state energy below the reference zero. Thus predicting localization of the dielectron to be favoured. Similar results were obtained on the inclusion of correlation for two other choices of V_o. In both cases, a positive total energy was lowered below the effective energy zero of the system.

A comparison of this calculation, which estimated a very small heat of solvation for the doubly-occupied cavity, 0.031 eV per two electrons with V_o=0.0 eV, (the heat of solvation is defined here to be the negative of the total system energy) with results on the single-electron species in voids lined by four and six molecules, predicted that the dielectron would be very unstable towards dissociation; by almost 1.0 eV per electron.

Table III.8 presents these variational results for comparison withthose obtained numerically. About a 10% gain has been effected in the electronic ground state energy on accurate solution. This is carried through to the total energies, these being 0.35 eV disparate. It is clear that, even with the accurate numerical solution, the chosen model just fails to predict a localized state. The numerically-obtained optimum cavity radius was, in this case, coincident with Copeland and Kestner's value of 2.95 Å. Including, by the method discussed above, the effect of instantaneous correlation in the ground state charge distribution affords a further drop in the energy, about 7% the total electronic energy, around 0.3 eV.

As a comparison with the numerically secured properties of the single-electron species within this model will reveal, (see Part II), the final, correlated heat of solution of the ammoniated dielectron, placed here at 0.14 eV per electron, is still well short of indicating associative stability. The dissociation reaction is predicted here to favour two uncoupled singly-occupied cavities by an amount of 1.01 eV per electron. This computation involved a consideration of the numerically obtained heat of solution of the heat of ammoniation of the single electron in a six molecule system with an identical V_o value (see Table II.16). This consideration is analogous to the comparison employed by Copeland and Kestner but it must be viewed with suspicion. While the entropy change, as regards the number of solvant molecules irrotationally bound per solvated electron, is accounted for by merely doubling the number of coordinating molecules, the volume occupied by the effective dielectron cluster has increased fivefold in going from the singly- to the doubly-occupied void.

The reason for the marked amelioration in the ground state energy on accurate solution is evident by inspection of Figure III.9. This reveals that the numerically derived ^1S function is much more compact than its variational counterpart. As explained earlier the approximate function was constructed assuming a simple Hartree product of two identical Slater ^1S functions was employed in the variational treatment. It should be noted that the correlated function was not obtained in a form suitable for graphical presentation. Thus, Figure III.9 holds only the accurately derived numerical functions treating the electron-electron interaction by an scf scheme. This remark also applies to the ^1P function plotted.

Difficulties in convergence were again encountered in applying the correlation method developed previously. This time the problem was the self-consistent treatment of the short-range dipole orientation

term. However, these were overcome in a manner identical to that mentioned in the discussion of the numerical work on the scf polarized cavity model but only at the expense of rather large amounts of computer time. The fully correlated solution technique, in the limit of L=12, was therefore employed only for a small range of cavity sizes in the neighbourhood of the numerically derived minimum.

Figure III.10 illustrates the variation of the numerical total ground and excited state energies with cavity radius. The two available variational data are also included. No approximate excited state calculations were reported. As is obvious, the first excited state, supposed ^1P, is very much unbound with respect to V_o. The ^1S to ^1P transition energy at the optimum void radius turned out to be 0.809 eV. The coincidence of this value with Catterall and Symons' suggestion is, of course, entirely fortuitous, depending completely on the parameterization of the model chosen. For example, setting V_o= -0.5 eV yields a transition energy of 0.64 eV while V_o= 0.5 eV provides 0.95 eV as a measure of the position of the absorption band maximum. The computed oscillator strengths and full-width at half-height of the expected band are presented in Table III.8, for the sake of completeness. The band is observed to be somewhat narrower than that due to the single electron transition as computed in Part II, for cavities comprising four and six molecules. It is interesting to note that Catterall and Symons' constraint of inequality in the apparent molar extinction coefficients is reproduced here. The oscillator strength for the optimum singly-occupied cavity with six molecules and V_o= 0.0 eV is 0.854, while that due to the dielectron species discussed above is but 0.764. The dipole-velocity oscillator strengths have been selected for the comparison. Thus twice the one-electron band peak will be much higher than that of the dielectron (account having been taken of the relative half-widths).

Within the terms of the adiabatic semicontinuum model the

computed dielectron transition half-width on absorption appears too narrow to contribute much to the width of the observed spectral band, even allowing for a slightly displaced overlap with that due to the one-electron species. Various attempts to arbitrarily overlay the derived line-shapes resulting in a smooth band of maximum width 0.15 eV. It is thus obvious that assuming such a spectral coincidence will not alleviate the fundamental difficulty, the prediction of narrow half-widths, besets the semicontinuum theories.

The vertically obtained continuum state, derived applying the considerations of Section 3(a) is also pictured in Figure III.10. At the configurational minimum a photon energy of 1.468 eV would be required to excite an electron into this state.

Some investigations into the application of the adiabatic semicontinuum model to the structure of the hydrated electron were effected in the course of the present work by merely adjusting the required input parameters, relative permittivities, etc. and neglecting the hydrogen-hydrogen interactions. Calculations performed employing four solvating molecules disclosed no configurational minimum, the total ground state energy simply decreased smoothly to a void of zero radius. Altering the value of V_o incorporated, between the limits of +1.5 eV and -1.0 eV did not change this finding. Similarly stepping up the number of surrounding water molecules to six produced no significant difference. With N=8 and V_o= -0.5 eV perhaps a slight hint of the presence of a minimum very close to the origin was obtained. For twelve oriented dipoles this minimum was definitely observable but was located at a void radius of but 0.12 Å. An electronic energy of -6.46? eV was computed and the total ground state energy evaluated to be -0.621 eV. This value was secured without the inclusion of correlation effects and lies well above the reference quasi-free state, $2V_o$= -1.0 eV. Recomputation of the total ground state energy by the technique available

to include instantaneous correlation was again performed only in the region of the numerically derived minimum for N=12. On the incorporation of correlation effects a lowering of 0.392 eV in the total ground state energy was produced. Thus, the heat of solvation of the hydrated dielectron, in this adiabatic semicontinuum model, was placed -1.013 eV per two electrons. This is only marginally below the reference zero and predicts that the doubly-filled cavity will be very unstable with respect to dissociation into two single-electron species. Compare Table II.17, which indicates a hydration energy of the order of 1.6 eV for the single surplus electron with four coordinating molecules in a void of 0.16 Å.

The results of the above calculation are expected to be applicable to dielectrons in low temperature ice, if the properties of this system are obtained with the framework of the electronic adiabatic approximation. This study was not pursued but in the absence of hydrogen-hydrogen interactions, very little difference from water is expected in ice, the latter medium being distinguishable mainly by a much lower β value. A qualitative inspection of the appropriate potential terms, in the light of the medium reorganization contributions, suggest that the above model will also indicate dissociative instability of the dielectron in this system.

Based on the results of their finding in metal-ammonia solutions, Copeland and Kestner felt able to assert that some alternative spin-pairing mechanism, other than dielectron formation, must be responsible for the observed decrease in paramagnetic susceptibility with increase of metal concentration in this medium. The results of the present work show that an accurate solution of the potential form employed does not change this conclusion and that, within the limitations of the model, dielectrons are unstable in ammonia, water and probably ice with respect to single solvated particles.

In direct contrast to the somewhat gloomy predictions of the non-existence of solvated dielectron species, at least in polar liquids, made by the above adiabatic treatment of the semicontinuum approach, a self-consistent field solution scheme on an identical approximation level has evidenced the apparent stability of the dielectron with respect to dissociation in all media studied.

Feng, Fueki and Kevan have extended their scf semicontinuum model to treat the localized dielectron species in various media characterized by a wide range of polarity. In each system studied, water and ammonia at their respective liquid temperatures, crystalline ice at 77°K and low-temperature methyltetrahydrofuran and amine glasses, it proved possible both to establish the configurational stability of the doubly-occupied cavity, by requiring that the second derivative of the total ground state energy with respect to the configurational coordinate, at the minimum value of this energy, was positive and to provide an indication of the relative stability of the paired species with respect to two separated trapped particles, by estimating a positive heat of dissociation. As defined here this quantity, H_{12}, is simply the difference in the respective heats of solution per electron for the doubly-and singly-occupied cavities, i.e.

$$\Delta H_{12} = \tfrac{1}{2}\Delta H_2 - \Delta H_1 .$$

ΔH_2 is the heat given out on solvation of the dielectron; it is simply the negative of the computed total system energy. It is interesting to observe that, again in each case, the minimum in the total energy was considerably negative with respect to the effective energy zero, selected as the energy of the quasi-free state in the system.

These comprehensive calculations were performed by applying the theory outlined in Section III.(a). Unfortunately, recourse was again made to a variational solution technique. An antisymmetrized ground state wave-finction, assumed ^1S, was chosen and the antisymmetric

spin part promptly factored out in the absence of any spin-dependent operators. This left the usual Hartree product form for the ground state charge distribution. The product was assumed to comprise a pair of identical, hydrogenic, single-exponential, one-particle functions. The variational procedure was applied to the total energy of the system in an effort to secure the optimum value of the one independent variable coefficient. This was repeated for each value of the cavity radius studied and a configurational coordinate diagram was constructed in terms of a void radius r_v. An excited P-type state was assumed to be lowest optically attained level and this was represented as a properly antisymmetrized product of two linear combinations of one-parameter hydrogenic s- and p-type functions. Minimization of the total nergy of the system, with the electronic structure described by this charge distribution, produced optimum values of the two variational exponents involved. Thus, these workers were able to compute the relative separation of the spin-allowed $^1S - {}^1P$ transition in addition to the spin-forbidden $^1S - {}^3P$ promotion. An optically obtainable conduction state was computed, again in accordance with the considerations of Section 3(a).

The treatment of electron-electron interaction was carried through in the spirit of the Land and O'Reilly formulation. The excited state exchange term was reduced by the high-frequency dielectric function for all radii as before. The latter approximation was justified by estimating the relative importance of the exchange and coulomb contributions to the electron-electron interaction in the light of the computed results. Exchange energies were of the order of 25% of the coulomb repulsion throughout. While this approach, thus offers a reasonable estimate of the interelectronic forces within the limited context of the inflexible variational system employed, it neglects any aspect of instantaneous correlation in the motion of the trapped electron pair. The effect of this correlation, included in the present work, is, in some cases,

comparable to the magnitude of the exchange interaction and therefore, is of substantial importance.

Feng, Fueki and Kevan have experimented with models containing from four to twelve surrounding molecules and have employed various values of V_o, mainly selected on the basis of providing good fits to the one-electron spectra. As evidenced in Part II, accurate numerical solution has destroyed the apparent match obtained in both cases and this above procedure is not wholly justifiable. While, in each system, configurational stability was achieved for each value of N chosen, a result duplicated here numerically, detailed values were reported only for N=4, which provided the deepest minimum in every case. Increasing the number of solvating molecules has been found, here, to markedly decrease the predicted transition energy and the heat of solution (it exerts a major effect on the ground state), but even in the limit of N=18, all dielectrons studied in the present work, in water, ammonia and ice proved stable with respect to dissociation. Results are also detailed here only for N=4.

Table III.6 presents a comparison of the numerical versus variational contributions to the singlet P excited states, for the dielectron in water, ammonia and ice. Parameters chosen were N=4 and V_o= -1.0 eV in each case. The now customary, improvements were observed on numerical solution. In the ground state, the total, variationally-derived, electronic energy was between 8% and 12% too high. It was disclosed in the corresponding one-electron studies in these media that the variational results for ammonia were considerably more appropriate to the true charge distribution than those in the other systems. A similar observation is pertinent here. Figures III.7 and III.8 illustrate the numerical and variational wave-functions for both ground and first excited states in ammonia and ice respectively. Those appropriate to ice are again seen to be more disparate. This may, again, be attributed to the

fundamentally different nature of the potential experienced by the electron pair between ice or water and ammonia. The reason for the marked difference is, of course, due to the inclusion of hydrogen-hydrogen interactions in the latter media. Even in this scf treatment, in the form incorporated, hydrogen-hydrogen repulsions dominate the factors which govern the position of the optimum configuration. If this term is neglected the configuration coordinate diagram relevant to ammonia becomes extremely similar to that applying in aqueous systems. A similar picture was presented in the adiabatic semicontinuum treatment of the ammoniated dielectron. Here, the hydrogen-hydrogen interaction term, very significant for the twelve molecule systems studied, was primarily responsible for placing the minimum in the configuration curve at such a large radius, and incidentally, in making the ground state so delicately bound. Even with N=4, as here, this contribution to the medium rearrangement energy still pushes the optimum void out to 1.0 Å as compared to 0.35 Å in both water and ice. Accurate numerical solution has, as usual, not changed the location of these minima by more than a few hundredths of an angstrom.

The other contributions to the total ground state energy are ameliorated in a corresponding fashion. The long-range polarization contribution has become considerably more positive, reflecting the more compact nature of the numerical ground state charge distribution. The short-range dipole-dipole repulsion term is also rather greater, largely due to the increase in the induced component. Similar statements are applicable in all three media studied but the effects are again less pronounced in the case of the ammoniated dielectron. It is interesting to observe that the ground state properties in ice are determined by an almost equal balance of long- and short-range components. In the other media long-range polarization forces predominate. In terms of the applied model potential, this is rationalized by the low inertial contributions

to the polarization developed by the dielectron trapped in ice and to the greater extent of the orientation of the molecules in the first coordination layer for this species. The low temperature used leads to little thermal disarrangement.

The inclusion of correlation effects into the ground state wave-function proved to provide almost insurmountable difficulties. The potential is now self-consistent in the enclosed charge, the average cosine, the induced dipole term and the long-range polarization. Convergence difficulties proliferated and oscillatory solutions were commonplace. Solutions including the effect of correlation on the electronic energy alone were eventually accepted as the best that could be obtained in the time available. The other contributions to the total system energy were assumed to remain unchanged from the accurate numerical solution and the correlation on the electronic energy carried through to the total energy unaltered. Based on work in the adiabatic approximation, where fully correlated total energies were eventually obtained, it is estimated that the maximum change in the values reported here for the total energy, including correlation, will not exceed +0.1 eV. Copeland and Kestner have also carried through the electronic improvement unaltered in their adiabatic calculations Thus, it is expected that in the limit chosen, partial waves up to L=9 were included in the expansion, a fair estimate of the instantaneous correlation effect in the ground state charge distribution was obtained here. The estimate ranged from 0.3 eV to 0.5 eV in the systems studied and was again only computed in the neighbourhood of the numerically derived relaxed state minima.

Figures III.5 and III.6 provide a representation of the numerically obtained improvements on the single-exponential variational results in the configurational coordinate diagrams for ammonia and ice respectively. The parameters chosen in both cases were N=4 and V_o= -1.0 eV.

The charge distributions illustrated in Figures III.7 and III.8 were obtained at the appropriate ground state configurational minimum for this parameter set. As is expected the ground state configurational curve for ice shows a substantial improvement, which is less marked in ammonia. As was discovered in the scf treatment of the simple solvated species within the semicontinuum model, the improvements effected in the representation of the ground state charge distributions have pushed the numerically derived excited states above their variational counterparts. This reflects the strong dependence of the vertically reached excited states on the inertial polarizations influenced by the relaxed ground state. Table III.6 indicates this finding, illustrating that, although the numerical electronic energies are markedly lower than the corresponding variationally obtained values, the amelioration has been completely concealed in the total energy, having been cancelled by concomitant alterations in the other terms, contributory to the total excited state energy. This remark also evidently applies to the vertically obtained conduction state.

Table III.7 lists the properties secured in the present numerical study of the electronic structure of the localized dielectron in water, ammonia and ice. The numbers presented pertain to N=4 and $V_o = -1.0$ eV in each case and were computed from the values displayed in Table III.6. It is particularly interesting to note that the marked decrease in the ground state energy, especially on the inclusion of correlation, (all dashed quantities have this incorporation), when set against the effective positive shift in the excited state total energies, leads to a very large increase in the predicted transition energies for the dielectron species studied. The variational value of 2.296 eV for dielectron absorption in water has been almost doubled. The freshly computed peak of the optical spectrum of the hydrated dielectron is placed at 4.35 eV. Similar discrepancies occur in ammonia and, to a

lesser extent, ice. The oscillator strengths for the 1s - 2p transition in the singly-occupied cavity are seen to be approximately half those due to the two-electron void absorption when computed using either the dipole-length or the dipole-velocity expressions. As before, it is not possible to say which of these values is the more accurate here for the reasons explained earlier. A significant observation is that the half-widths of the dielectron bands are of the same order of magnitude as those deriving from transition involving the one-electron species. Compare Table II.20. In the accurate numerical solution, with the parameters as chosen above, none of the dielectron spectra overlap those due to the single-solvated particle. This coincidence could, no doubt, be enforced by a suitable manipulation of N and V_o. This was not attempted here. Again, in contrast to the broad, bound-to-free F'-band observed in the alkali-halide crystals, the dielectron transitions in the polar media studied are very much bound-to-bound. The ^1P states are substantially below the reference zero in each material and as stated, the absorption bands are, comparatively, extremely narrow.

The photoconductivity threshold, when secured numerically, is placed at very high values, ranging from 4.6 eV in ice to 9.1 eV in water, the latter being inside the ultraviolet absorption edge. The onset of the photoelectric emission is predicted to occur from solvated dielectron species at 11.1 eV in water, 7.2 eV in ammonia and 6.6 eV in ice. This again neglects such contributions as the surface potential and electron back-scattering from the surrounding vapour.

Accurate numerical solution has not altered the variationally asserted statement of stability of the dielectron species. It has, rather, lent further support to it. The heat of solution per electron in water for the doubly-charged void is 4.85 eV, which within the same model, and the same solution method, a heat of 3.28 eV was predicted for hydration of a single electron. The heat of the dissociation reaction

is thus placed at 1.57 eV per electron in aqueous systems, making it very improbable. The above has, of course, neglected any entropy contributions which, since four molecules are assumed surrounding each cavity, will be of some importance. On electron unpairing, four extra molecules per electron will become effectively immobilized. An accurate estimate of the extent of this contribution is out of the question. Many problems concerning the amount of rupturing of the hydrogen-bonded structure of the aqueous medium must first be resolved. Based on the heat of fusion of water, it is expected that the quantity will not exceed 0.4 eV and hence will not alter the above stability conclusion.

An extensive investigation into the properties of the ammoniated dielectron, for various values of N and V_o, was undertaken in an effort to explain the contradictory claims of the alternative semicontinuum models as to its relative stability. The disparity remained unresolved. Even with N≅12 and V_o=+1.0 eV the scf solution scheme preferred a doubly-occupied void to a single solvated particle, the solvation energy of which was computed using half the number of solvating molecules and a quasi-free state of 0.5 eV. This seems to be the optimum type of comparison.

It appears, then, that some fundamental difference in the formulation of the scf and adiabatic potentials or medium reorganization energies is responsible for the contrary predictions. In the course of the present work the conclusion was reached that the responsibility could be almost equally divided between two sources. Firstly, the manner of the incorporation of the long-range polarization forces in the scf treatment leads to much more pronounced polarization contributions to the potential tail, especially in the dielectron studies. Secondly, the inclusion of short-range charge-induced dipole interactions in the scf scheme provides a marked difference in the depth of the trapping well. An attempt made to alleviate the first-mentioned problem will be

discussed briefly in the subsequent section. It should also be stressed that inclusion of V_o as an identical parameter in both theories is not allowable. Contrast the increase in electronic energy with more positive V_o in the adiabatic formulation with the decrease observed on similarly altering this component in the scf scheme. In omitting the induced interaction, the adiabatic approximation treats the solvent molecules as non-polarizable with respect to producing a localization field. Thus this is likely to lead to noticeable differences when the solvent molecules under consideration are characterized by a high polarizability, as is the ammonia molecule.

Subsequent to the completion of this thesis, further work, initiated primarily as an investigation of a more suitable description of the hydrogen-hydrogen repulsive interaction, has revealed the need for substantial alterations in the adiabatic semicontinuum results on the dielectron species. The revised values have been inserted in column "c" of Table III.8. Figure III.10, also being outdated, needs redrawing. Since this involves a lowering of the entire ^1S and ^1P curves by about 3.0 eV, sensible comparison with the currently reported variational results is lost. The revised figure has thus not been included.

Most importantly, the adiabatic formulation is now seen to be capable of supporting, in ammonia, a dielectron, stable with respect to dissociation.

Section 4

A Second Solvation Shell.

In an effort to resolve the contradictory predictions of the adiabatic and scf treatments of the semicontinuum model as to the relative stability of the localized dielectron species in ammonia with respect to dissociation into two separately solvated electrons, a second solvation shell was introduced. It was hoped that this modification would remove the dominating effects of long-range polarization forces which could now be assumed to act only outwith the second discrete molecular sheath. At such large distances the differences in the two alternative treatments of this quantity should prove negligible.

The incorporation was effected in a manner entirely analogous to the development of the original single-solvation shell model. A small number, N_2, of solvent molecules, represented as polarizable point dipoles, were introduced outwith the original coordinating layer. These were again symmetrically placed and, for computational convenience, their number was generally taken to be twice that of the inner shell, N_1. The molecules in this second coordination sphere were assumed characterizable by parameters, identical to those employed to represent the inner molecules. The incorporation was effected in both the scf and adiabatic approaches and was tested first for one-electron systems.

In the adiabatic approximation the electron was assumed to experience a multiply discontinuous potential constructed just as for the one-shell case but now possessing several more "shelves". Thus

$$
(4\pi k_o)\, V(r) = \begin{cases}
-\Sigma_i N_i \mu_i / r_{di}^2 - \beta e / r_{c2} & r < R_1 \\
-\Sigma_i N_i \mu_i / r_{di}^2 - \beta e / r_{c2} + V_1 & r < r_{d1} \\
-N_2 \mu_2 / r_{d2}^2 - \beta e / r_{c2} + V_1 & r < r_q \\
-N_2 \mu_2 / r_{d2}^2 - \beta e / r_{c2} + V_2 & r < r_{d2}
\end{cases}
$$

$$-\beta e / r + V_2 \qquad r < r_{d2}$$

where an obvious notation distinguishes the contributions from the separate shells and r_q is the munimum of r_{c1} and R_2. The electronic polarization terms and medium reorganization contributions were computed in an obvious manner, assuming that the continuum began outwith r_{c2}.

As a first approximation all intershell effects were neglected and a configurational coordinate diagram in terms of r_{v1} and r_{v2} was constructed. In the absence of intershell interactions, for N_1=4, N_2=8, V_1=0.0 eV=V_2 in ammonia, one smoothly obtained minimum was disclosed at the values r^o_{v1} = 1.21 Å and r^o_{v2} = 2.23 Å. This was somewhat surprising since on the inclusion of only one discrete molecular layer the appropriate diagram also possesses a minimum at 1.21 Å. However, some substantial drop in the total system energy was afforded; from the single-shell value of -1.051 eV to -2.661 eV. The fresh value of the computed 1s -2p transition lay at 3.15 eV and possessed a dipole-velocity oscillator strength of 0.622. The dipole-length expression yielded 1.391. While the transition energy has moved in the wrong direction the marked lowering of the total relaxed state energy was promising.

The inclusion of intershell interactions was effected by "switching-on" the interlayer hydrogen-hydrogen and dipole-dipole contributions. The latter were computed by a rather laborious, pairwise summation technique, the former from considerations similar to the one-shell studies. This resulted in an energy surface pock-marked by shallow local minima. Much computational effort was expended to obtain the true minimum and the method of steepest descents proved to be the most suited optimization technique. For the ammoniated electron, with parameters as specified above, the coordinates of the absolute minimum were found at r^o_{v1} = 1.18 Å and r^o_{v2} = 2.46 Å, not much different from their previous values. The total system energy was obtained as

-1.048 eV and the 1s - 2p transition placed at 2.83 eV. It was thus observed that the inclusion of a second solvation shell was unlikely to increase the predicted heats of solution computed within the adiabatic approximation.

In the scf scheme a similar multiply discontinuous potential was introduced;

$$(4\pi k_o)\, V(r) = \begin{cases} -\Sigma_j (N_j \boldsymbol{\mu}_j / r_{dj}^2 - N_j \boldsymbol{\alpha} e C_j / 2r_{dj}^4) - V_{pol}(R_2) & r < r_{d1} \\ -N_2 \boldsymbol{\mu}_2 / r_{d2}^2 - N_2 \boldsymbol{\alpha} e C_2 / 2r_{d2}^4 - V_{pol}(R_2) + V_1 & r < r_{d2} \\ -V_{pol}(R_2) + V_2 & r < R_2 \\ -V_{pol}(r) + V_2 & r < R_2 \end{cases}$$

with $V_{pol}(r)$ as before and the sum over j encompassing both shells.

In ice, with N_1=4, N_2= 8, V_1= -1.0 eV = V_2, again assuming only intashell effects the following results were obtained

$$r_{v1}^o = 0.50\ \text{Å},\ r_{v2}^o = 1.81\ \text{Å};\ E_t(1s) = -4.578\ \text{eV},\ E(a) = 4.131\ \text{eV}$$

These should be compared with the corresponding single-shell values

$$r_{v1}^o = 0.51\ \text{Å};\ E_t(1s) = -2.591\ \text{eV},\ E(a) = 1.939\ \text{eV}$$

Again a considerable lowering of the total ground state energy was observed concomitant with a large increase in the derived transition energy. The inclusion of intershell interactions, no hydrogen-hydrogen repulsion was supposed present in ice, pushed the inner void inward fractionally and expanded the outer layer more markedly to give

$$r_{v1}^o = 0.48\ \text{Å},\ r_{v2}^o = 1.99\ \text{Å};\ E_t(1s) = -3.210\ \text{eV},\ E(a) = 2.562\ \text{eV}$$

Thus it was expected that applying the above modification to an scf semicontinuum calculation could produce higher heats of solvation.

The contradictory predictions of the two solution schemes were tested over a range of N_1, N_2, V_1 and V_2 for the one-electron species and found to be, disappointingly, verified in most cases. However, the calculations were tentatively applied to the dielectron species. The results are not encouraging. With an scf solution scheme and two interacting shells, the ammoniated dielectron, with N_1= 4, N_2= 8,

$V_1 = -1.0$ eV $= V_2$, was found, after a rather long search of a dimpled energy surface, to possess a total ground state energy of -5.897 eV at a location given by $r^o_{v1} = 0.92$ Å and $r^o_{v2} = 2.64$ Å. A similarly tedious hunt for the deepest minimum in the adiabatic treatment of this species yielded, with $N_1 = 6$, $N_2 = 12$ and $V_1 = 0.0$ eV $= V_2$,

$$r^o_{v1} = 1.04 \text{ Å}, \; r^o_{v2} = 2.26 \text{ Å}; \; E_t(^1S) = -0.211 \text{ eV}$$

Instantaneous electronic correlation effects were not included in either of these treatments but their magnitudes are expected to be similar in both. It thus seems that the inclusion of a second solvation shell is incapable of producing agreement between the alternative formulations of the semicontinuum model as to the dissociative stability of the ammoniated dielectron.

Fresh computations within the adiabatic approach now predict a stable dielectron species, in accord with the scf studies. This conclusion will not be invalidated on insertion of a second solvation shell.

General Conclusions.

The need for an accurate solution tehnique to derive the properties of the model potentials, suggested as representative of the structure of localized excess electron states in polar media has been clearly demonstrated.

Just such a method was thoroughly tested in one-electron colour-centre calculations in crystalline solids on both the polarized cavity and semicontinuum approximation levels. In these systems the finite-difference technique applied here was illustrated to be capable of efficiently reproducing known accurate solutions and of substantially ameliorating existing variational treatments, especially if these had been performed utilizing crude single-exponential trial functions.

Almost without exception, the study of the electronic structure of the surplus electron and dielectron species in polar liquids, ices and glasses on both model levels has been carried out within the framework of this inadequate, approximate solution method. Here, the proven numerical technique is shown to provide sizeable alterations in previous variational work. A number of results have been called into question.

In the adiabatic formulation of the simple polarized cavity model, accurate solution has revealed that, if the cavity radius is selected to fit one observable property, then concurrence of prediction with other measureables is not to be, in general, expected. In the scf polarized cavity model, a variational result which apparently removed early doubts as to the applicability of this model to the hydrated electron has been shown to be misleading. Numerical solution has revealed that, even in the limit of zero cavity radius, the predicted transition energy for the hydrated electron does not approach the experimental value.

More generally, it is suggested that these models represent two extremes, between which the correct formulation of a polarized cavity model of excess electrons in polar media lies. The work of Tachiya is

recognized as a step toward the correct path. The inclusion of a similar statistical treatment of electronic polarization interactions, perhaps via field-theoretic arguments should provide a more realistic formulation.

On the semicontinuum level, the predictions of one-electron models obtained by variational solution of suitably parameterized scf treatments, for water, ice and ammonia have been pushed considerably out of accord with experiment. Undoubtedly a fresh parameterization could be developed, in the light of the numerically obtained results, to renew the concurrence but, in general, attempts to do this for one specific property will be to the detriment of another. While it is recognized that this scf formulation of the semicontinuum approach is more consistent with the theoretical requirements inherent in the excess electron problem in polar liquids, it is asserted that in this scheme an accurate numerical solution is essential. The marked alterations in the energy level structure from that obtained using single-parameter variational techniques lead to crucial differences in computed properties, especially if these are delicately balanced quantities. It is felt that the adiabatic approach to the semicontinuum model is somewhat inconsistent with the demands of the situation. In particular, the need to introduce, rather arbitrarily, such dominating terms as the hydrogen-hydrogen repulsions in ammonia is disconcerting. Clearly, some estimate of this effect is desirable, but it is thought that it is not amenable to such a simple treatment as is envisaged here.

The failure of both versions of the semicontinuum theory to predict sufficiently large half-widths for the absorption bands due to trapped and solvated electrons is revealed not to be a function of the approximate nature of the previously employed solution techniques. If anything, accurate solution narrows the predicted bands. Within the framework of these models, contributions of transitions to higher excited

states to the observed absorption band has been shown to be unlikely. These peak at energies too high, have oscillator strengths too low, and are too narrow to produce the substantially asymmetric tail observed. In addition, speculation as to the nature of the first excited state of surplus electrons in ammonia, water and ice cannot hinge on the results of these semicontinuum calculations. They consistently predict strongly-bound final levels in the above media. The lifetime of the excited state of the hydrated electron has recently been suggested to be of the order of 1 psec. Based on a lattice relaxation process the adiabatic semicontinuum model predicts a radiative lifetime of the order of 10 nsec. The supposed emission band, which is predicted intense, has not been observed. It appears the model is again at fault. Interestingly the scf formulation of the semicontinuum model provides no indication of stable relaxed excited states.

More generally, the idea of computing the properties of a dynamic species from a fixed configuration of solvent molecules is believed to be dubious. Instead, a statistical approach founded in the theory of electrodynamics with spatial dispersion is felt preferable. This method seems infinitely more suitable to allow consideration of the really interesting presolvation and decay processes occurring in polar media than do the static pictures presented above. It is hoped to investigate this promising avenue at a future date.

For tw-electron species, numerically obtained results reveal that the approximate variational solutions of both polarized cavity and semicontinuum models are substantially in error. If the effect of the instantaneous correlated motion of the electron pair is to be included, surely it must be based on a sound knowledge of the actual charge distributions pertaining to the model applied. The absence of much definite experimental data on dielectron species renders the polarized cavity models virtually useless. Few values are available for parameterizing

variables, such as the cavity radius, and then, little or no comparison with other observables is possible. On a semicontinuum level, numerical solution of an scf treatment supports the variational prediction of configurational and relative dissociative stabilities of the dielectron species in water, ice and ammonia. It also supports the opposite conclusion, the preference of two separated singly-occupied cavities, as obtained in an adiabatic calculation.

One attempt to remove this contradiction has been investigated. A second solvation shell was included in the hope of reducing some of the major computational difference encountered in the alternative solution schemes. The exercise has proved fruitless. The contrasting predictions remain.

From the derived half-widths and peak positions of the dielectron transitions in ammonia, water and ice, it is felt unlikely that these species are responsible for any part of the observed spectrum. In particular, they are incapable of adding much to the previously mentioned, inadequate single-electron transition half-widths predicted. Thus it seems that some major modification of the semicontinuum theory is necessary.

The opinion developed during the course of this work is that a detailed understanding of the properties of excess electrons and dielectrons solvated or trapped in polar media awaits the development of a much more refined theoretical approach than is at present employed. In particular the neglect of a detailed investigation of spin-dependent properties should be rectified. Such methods as currently used are thought to contain much of the essential physical content of the situation but no hope is seen in continual piecemeal modifications to the pervading concepts. In this context, the idea of an electron, or a pair of electrons, located in a void in the medium is clearly an artifact. No such cavities can surely exist. While the cavity concept has been

of fundamental importance in illuminating just which effects must necessarily be included, it is thought to have become largely superfluous. Hopefully, some new theory can bypass this "open-block" and lead to a deeper understanding of the structure of such systems.

In conclusion, I thank the many experimentalists who have provided such a steady flow of intriguing observations on the properties of surplus electrons as to make this field one of continuing lively debate and much inherent interest.

Further research, performed subsequent to the completion of this thesis, has resolved the discord. The adiabatic formulation now supports a stable dielectron.

Tables III

Properties of dielectrons in polar media from polarized cavity models and semicontinuum approaches.

Tables 1 and 2 list the adiabatic polarized cavity model results in ammonia, 3 in water. Predictions of the scf polarized cavity model for water and ice are in Tables 4 and 5. Tables 6 and 7 contain the scf semicontinuum results for water, ammonia and ice, each with N=4 and V_o=-1.0 eV. Table 8 has adiabatic semicontinuum results for ammonia with N = 12 and V_o= 0.0 eV.

All energies are in eV, distances in Å.

Table III.1

R	3.0		4.0		5.0	
$-W(1s)$	-	1.469^{n}	-	1.161^{n}	-	0.961^{n}
$-S(1s)$	0.722^{v}	0.836	0.566^{v}	0.666	0.477^{v}	0.554
$-E(1s)$	-	2.305	-	1.827	-	1.515
$-W(^{1}S)$	4.679	4.997	3.713	3.983	3.069	3.366
$-S(^{1}S)$	1.444	1.672	1.132	1.332	0.953	1.108
$-E(^{1}S)$	6.123	6.669	4.845	5.316	4.021	4.424
$-W(1s)$	-	2.177	-	1.643	-	1.318
$-S(1s)$	-	1.014	-	0.808	-	0.673
$-E(1s)$	-	3.190	-	2.451	-	1.992
$-W(2p)$	-	0.724	-	0.654	-	0.590
$-S(2p)$	-	0.498	-	0.437	-	0.385
$-E(2p)$	-	1.222	-	1.090	-	0.975
$-W(^{1}P)$	4.028	4.932	3.267	3.575	-	3.091
$-S(^{1}P)$	1,345	1.512	1.119	1.245	-	1.058
$-E(^{1}P)$	5.373	5.905	4.368	4.820	-	4.078

n numreical, v variational[164]

Table III.2

R	3.0		4.0		5.0	
$\bar{r}(^1S)$	4.30^v	3.719^n	5.47^v	4.667^n	6.52^v	5.614^n
$\bar{r}(^1P)$	5.65	4.654	6.67	5.485	-	6.352
$C(^1S)$	-	0.726	-	0.800	-	0.850
$C(^1P)$	-	0.529	-	0.677	-	0.741
Π^J	2.002	-	1.471	-	1.146	-
Π^T	-	5.031	-	3.774	-	3.018
ΔH_2	3.895	1.412	2.972	1.140	2.247	0.779
E(a)	0.75	0.763	0.46	0.475	-	0.318
$f_1(a)$	-	1.973	-	1.956	-	1.886
$f_v(a)$	-	1.529	-	1.689	-	1.815

n numerical

v variational[164]

Table III.3

R	1.0	2.0	3.0	4.0
$\bar{r}(^1S)$	1.742	2.639	3.634	4.570
$\bar{r}(^1P)$	3.088	3.656	4.434	5.274
$C(^1S)$	0.402	0.634	0.756	0.831
$C(^1P)$	0.291	0.486	0.612	0.701
Π^T	15.819	7.909	5.273	3.955
ΔH	0.560	0.941	1.376	1.623
$E(a)$	3.138	1.455	0.807	0.500
$f_{len}(a)$	1.358	1.927	2.035	2.001
$f_{vel}(a)$	0.872	1.366	1.588	1.727
$-E_t(^1P)$	12.054	8.251	6.340	5.165

Table III.4

	$k_{st} = 80.0$		$k_{st} = 3.00$	
$W(^1S)$	-15.91^v	-17.692^n	-4.75^v	-5.273^n
$U(^1S)$	14.81	16.484	5.47	6.075
$E(^1S)$	-1.10	-1.208	0.72	0.802
$G(^1S)$	4.21	4.689	2.30	2.560
$E_t(^1S)$	-5.31	-5.897	-1.58	-1.758
$\bar{r}(^1S)$	1.80	1.569	3.29	2.876
$W(^1P)$	-	-10.590	-	-3.961
$U(^1P)$	-	9.172	-	4.014
$E(^1P)$	-	-1.418	-	0.053
$G(^1P)$	-	2.392	-	1.404
$E_t(^1P)$	-3.29	-3.810	-0.74	-1.351
$\bar{r}(^1P)$	3.43	2.667	6.95	4.452

n present numerical work

v variational solution[163]

Table III.5

	k_{st} = 80.0		k_{st} = 3.00	
E(a)	2.02[v]	2.070[n]	0.84[v]	0.407[n]
E(a)'	-	2.459	-	0.515
$f_{len}(a)'$	-	0.928	-	0.702
$f_{vel}(a)'$	-	1.333	-	0.916
ΔH_1	1.30	1.440	0.590	0.651
ΔH_2	5.31	5.897	1.58	1.758
ΔH_{12}	1.355	1.509	0.20	0.228
$\Delta H_2'$	-	6.269	-	1.866
$\Delta H_{12}'$	-	1.695	-	0.282

n numerical

v variational[163]

Table III.6

	Water		Ammonia		Ice	
r_v^o	0.35		1.0		0.35	
$E_e(^1S)$	-21.88^v	-24.83^n	-12.56^v	-13.38^n	$-16,09^v$	-18.15^n
$U(^1S)$	8.671	9.245	6.158	6.375	5.832	6.269
$-E_t(^1S)$	7.926	9.271	5.186	5.632	5.125	5.758
$E_{dd}(^1S)$	5.220	6.253	0.802	0.961	5.053	6.057
$-E_{cr}(^1S)$	-	9.749	-	6.001	-	6.051
$-E_e(^1P)$	17.40	18.27	11.02	11.243	10.92	11.62
$U(^1P)$	7.942	8.593	5.627	6.056	4.573	4.970
$-E_t(^1P)$	5.630	5.399	4.275	4.072	3.023	2.906
$E_{dd}(^1P)$	3.761	4.217	0.699	0.770	3.240	3.681
$C(^1S)$	1.094	1.328	0.910	1.078	1.057	1.333
$C(^1P)$	0.812	0.998	0.793	0.932	0.691	0.838
$-E_t(cs)$	0.738	0.638	0.883	0.801	1.505	1.452

Table III.7

	Water		Ammonia		Ice	
E(a)	2.296[v]	3.873[n]	0.912[v]	1.560[n]	2.102[v]	2.852[n]
E(a)'	-	4.350	-	1.929	-	3.145
$f_1(a)'$	-	1.106	-	1.317	-	0.613
$f_v(a)'$	-	1.418	-	1.682	-	0.874
W(a)'	-	0,208	-	0.118	-	0.109
ΔH_2	7.926	9.271	5.186	5.632	5.152	5.758
$\Delta H_2'$	-	9.749	-	6.001	-	6.051
I	7.188	8.626	4.303	4.831	3.620	4.306
I'	-	9.101	-	5,200	-	4.599
P'	9,2	11.1	6.3	7.2	5.6	6.6
ΔH_1	2.752	3.282	1.942	2.114	2.076	2,589
$\Delta H_{12}'$	1.211	1.593	0.651	0.887	0.487	0.437

n numerical

v variational[167]

Table III.8

$E_e(^1S)$	-3.440^v	-3.774^n	-6.733^c
$E_t(^1S)$	0.369	0.011	-2.948
$E_c(^1S)$	-0.031	-0.277	-3.236
$E_e(^1P)$	-	-2.984	-5.548
$E_t(^1P)$	-	0.532	-2.032
$E(a)'$	-	0.809	1.204
$f_{len}(a)'$	-	0.989	1.472
$f_{vel}(a)'$	-	0.764	0.514
$W(a)'$	-	0.080	0.083
$E(cs)$	-	1.468	4.427

n present numerical work

v variational[166]

c corrected

Figures III

Figures 1-4 have results from polarized cavity models for dielectrons. 1 is in ammonia with an adiabatic treatment for which 2 shows the derived functions in a 4.0 Å cavity. Charge distributions of the hydrated dielectron and that trapped in ice from the scf scheme are in 3 and 4.

Figures 5-10 pertain to semicontinuum models. 5 is an scf solution for ammonia at 203°K, 7 contains the derived functions at the optimum radius. 6 and 8 are similar, but for ice at 77°K. All four have N = 4, V_o = -1.0 eV. The configuration coordination diagram for ammonia within the adiabatic approximation is in 10 and 9 shows the corresponding wave-functions at the optimum radius.

Variational results are in full-line except in 10 where they are circled points. Broken-line indicates present numerical work (in 10 it is full). Chain-lines are correlated ground state properties(in 10 these are broken). (a) denotes ground (^{1}S) state, (b) excited (^{1}P) state and (c) the vertical continuum level.

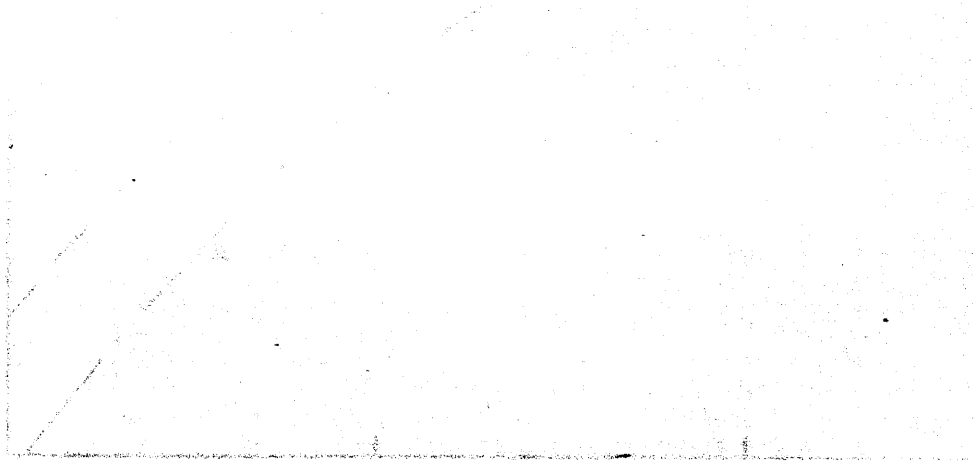

Figure III.1

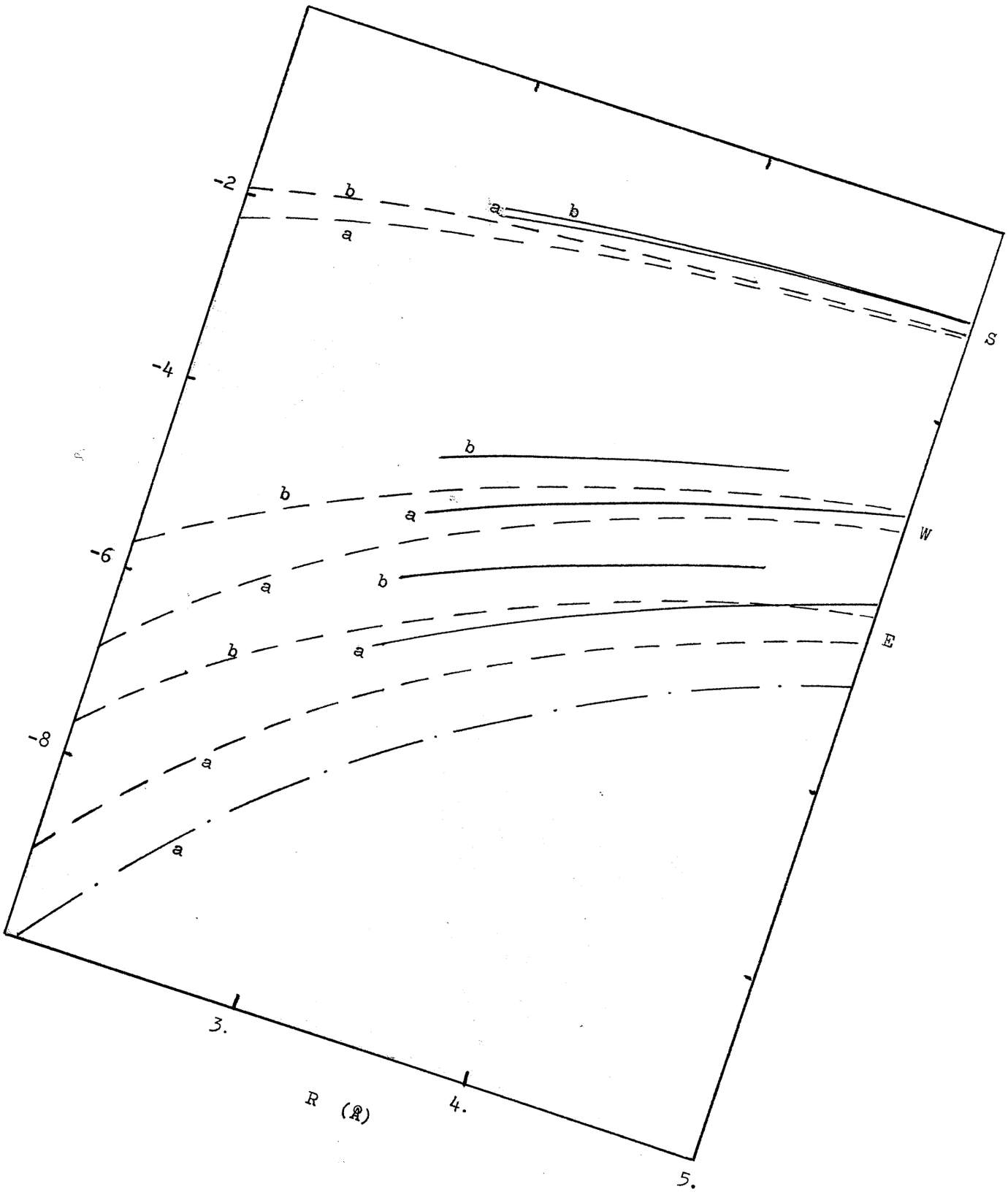

Figure III.2

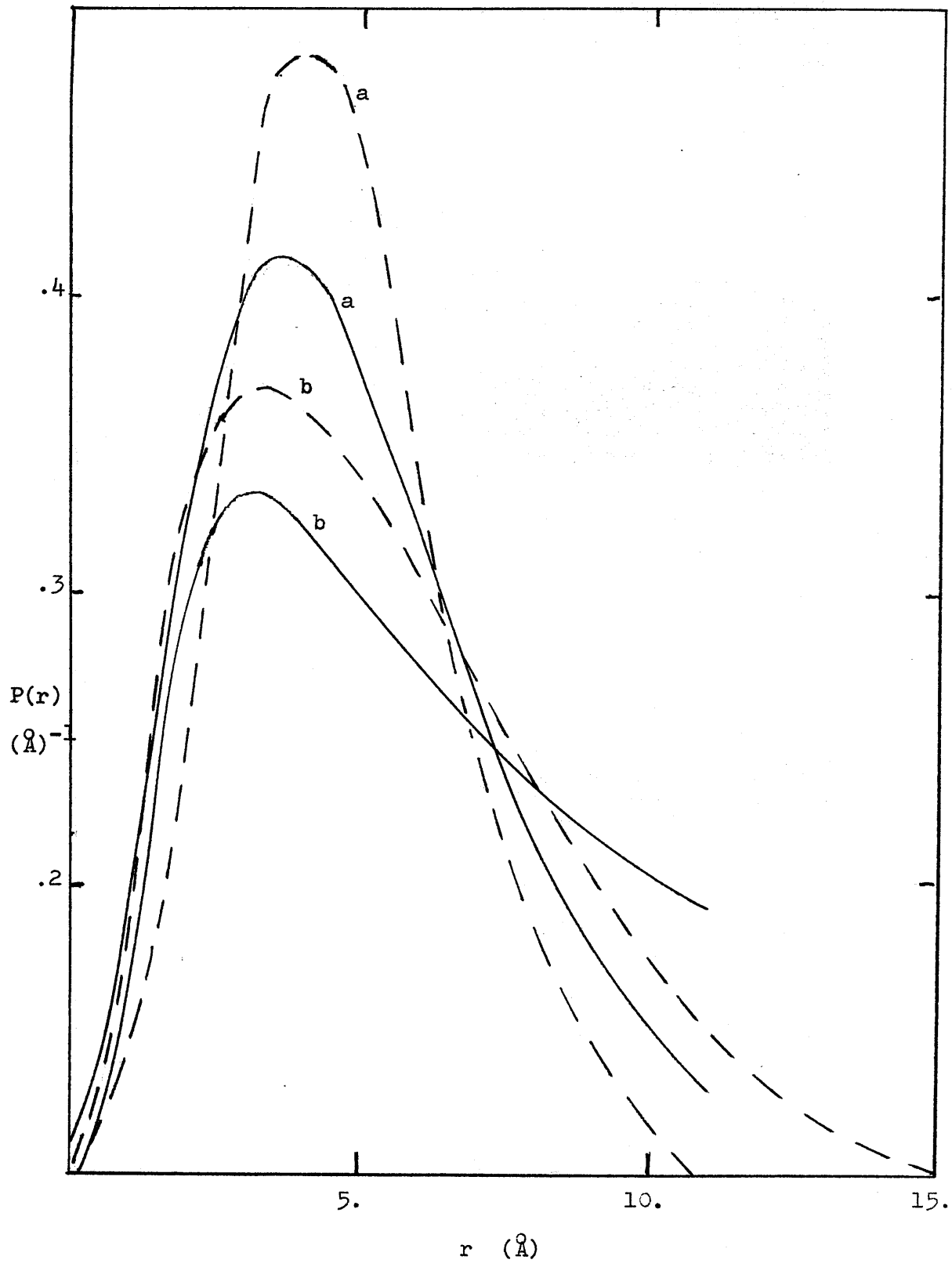

Figure III.3

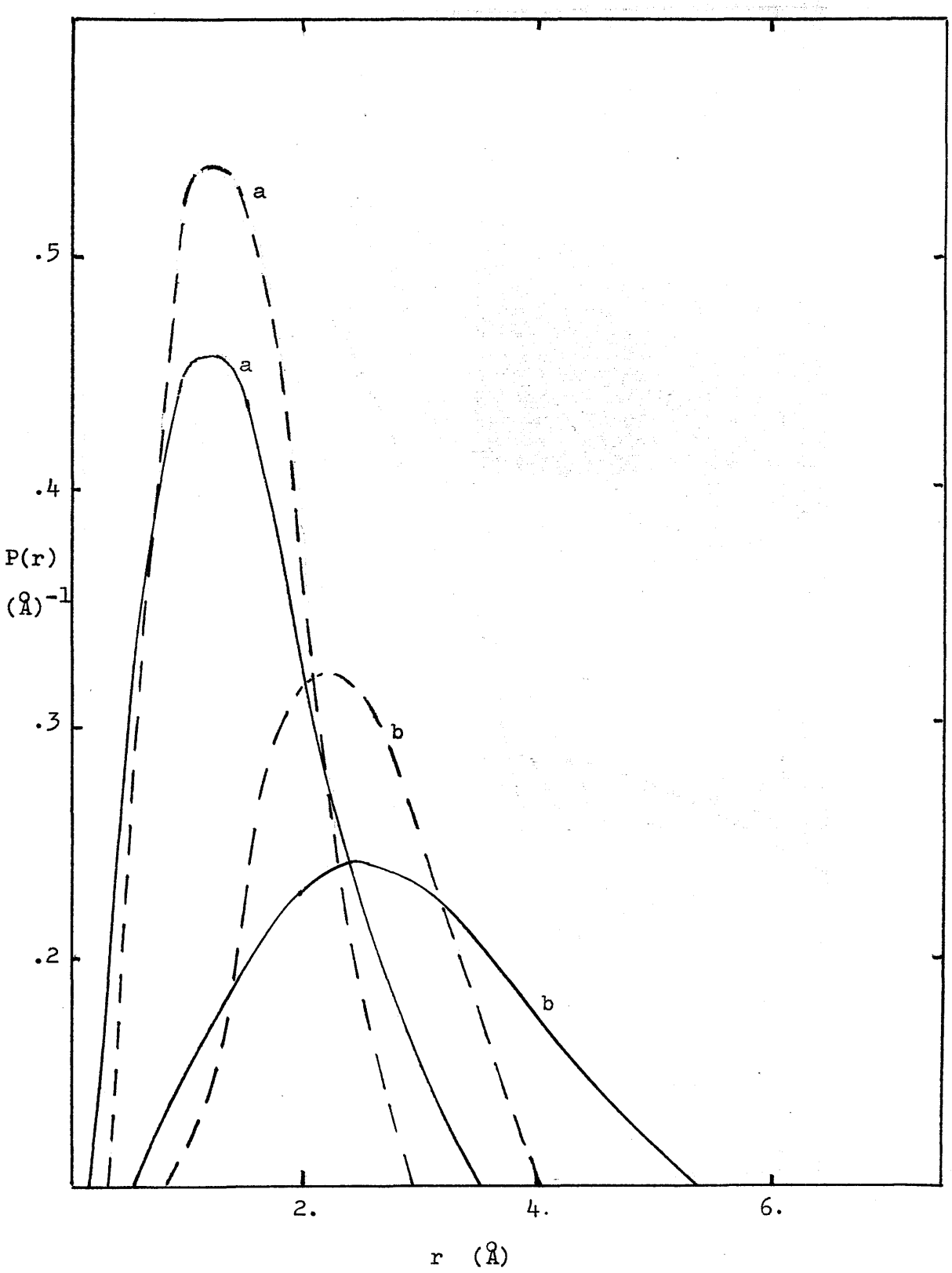

Figure III.4

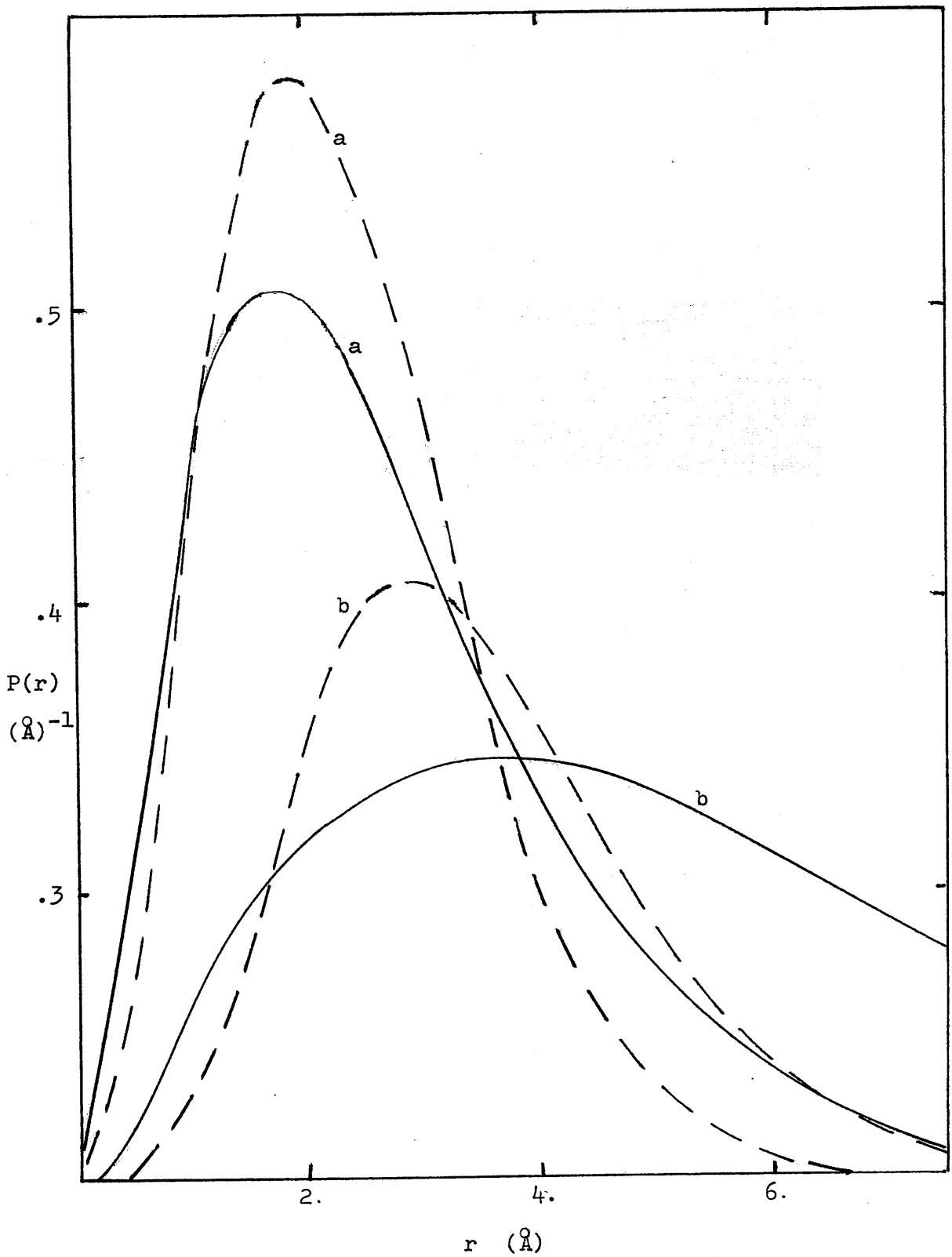

Figure III.5

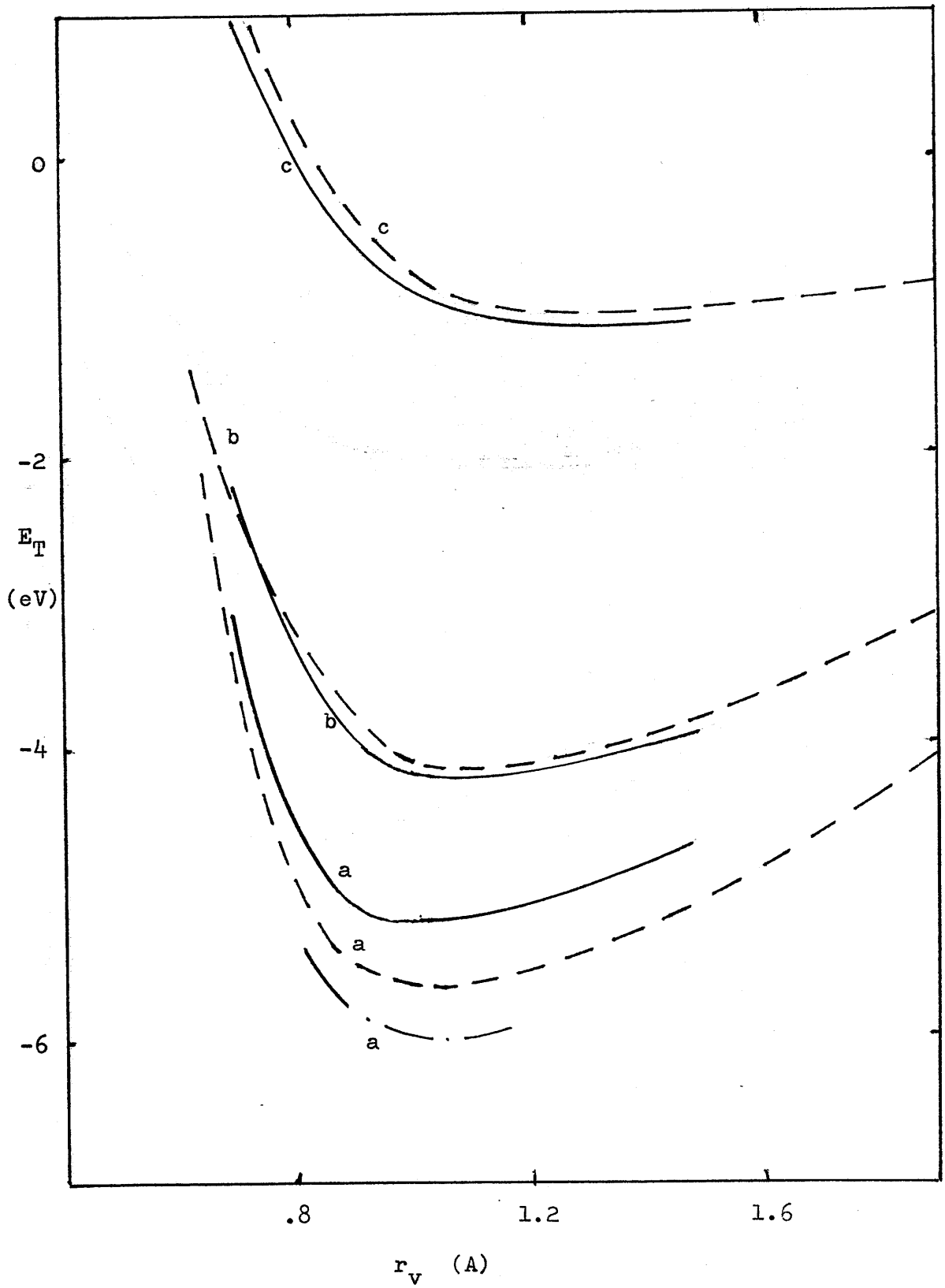

Figure III.6

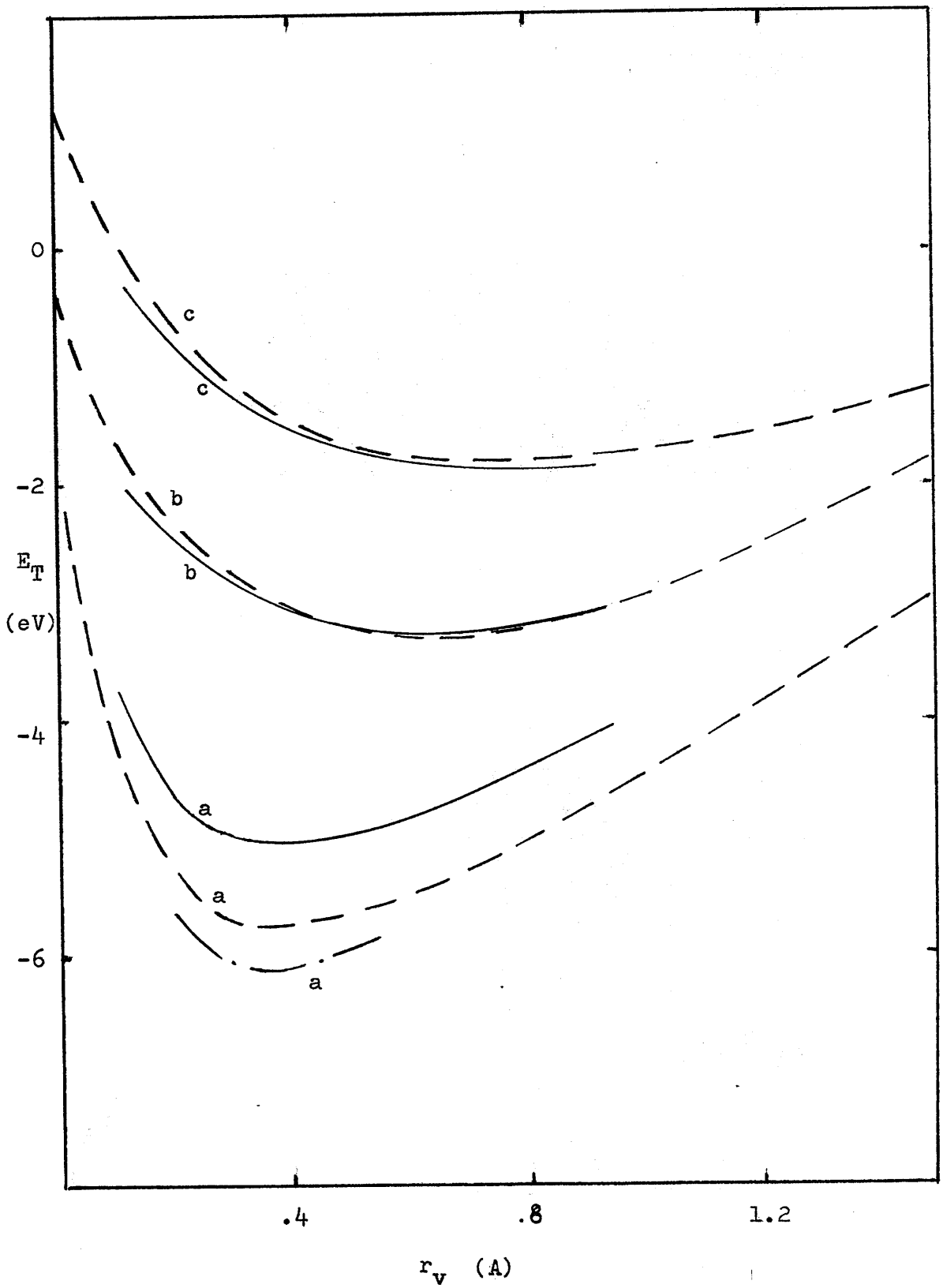

Figure III.7

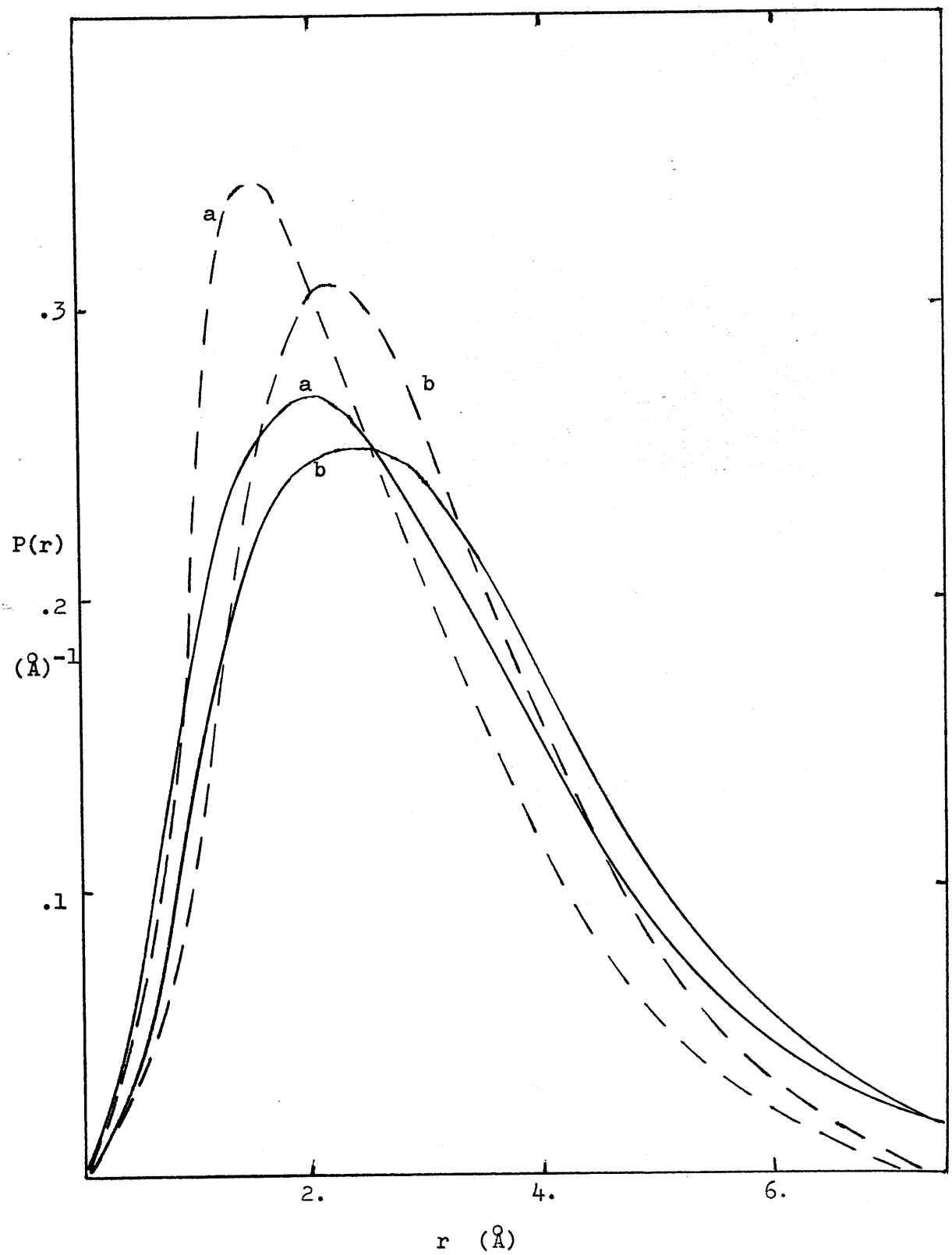

Figure III.8

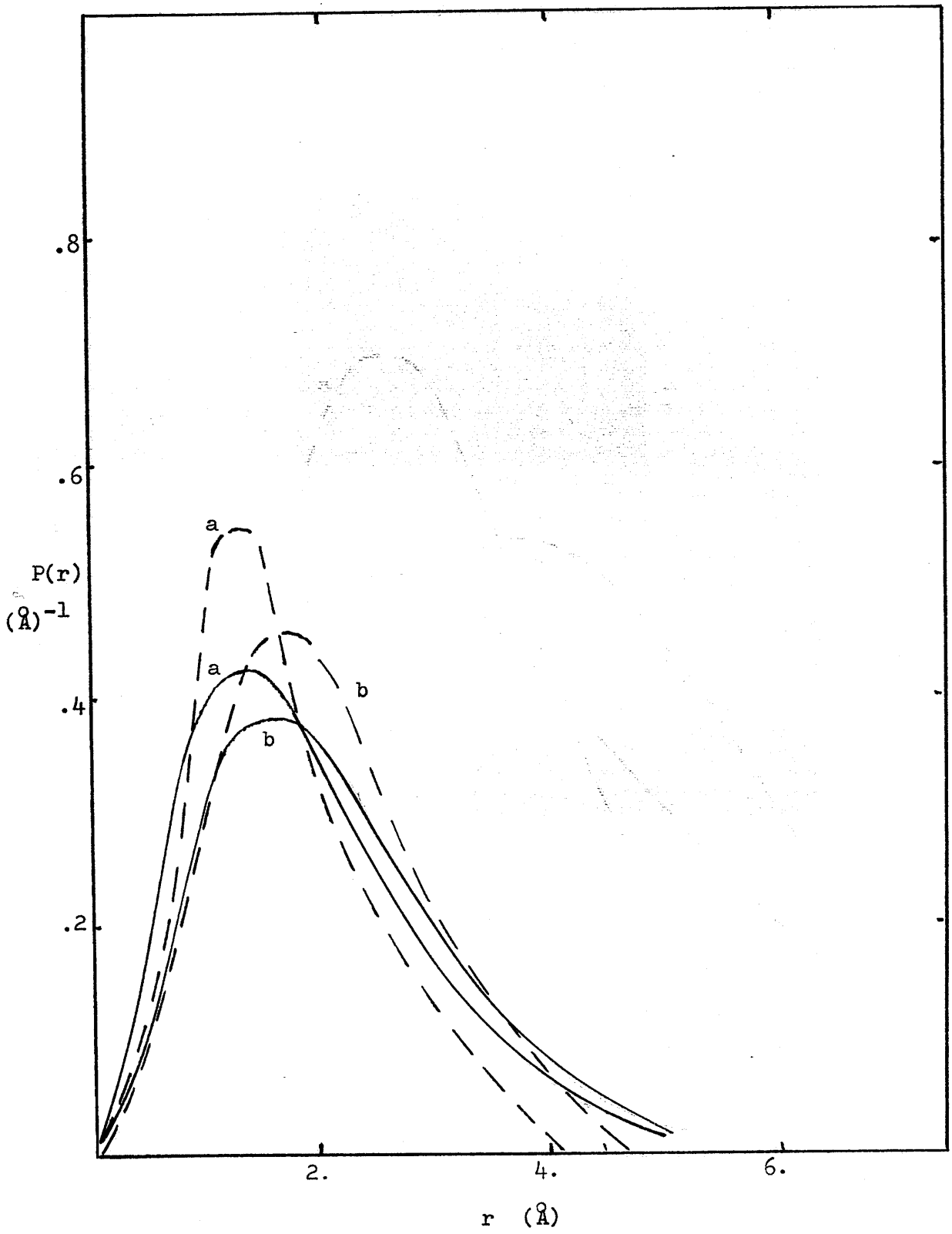

Figure III.9

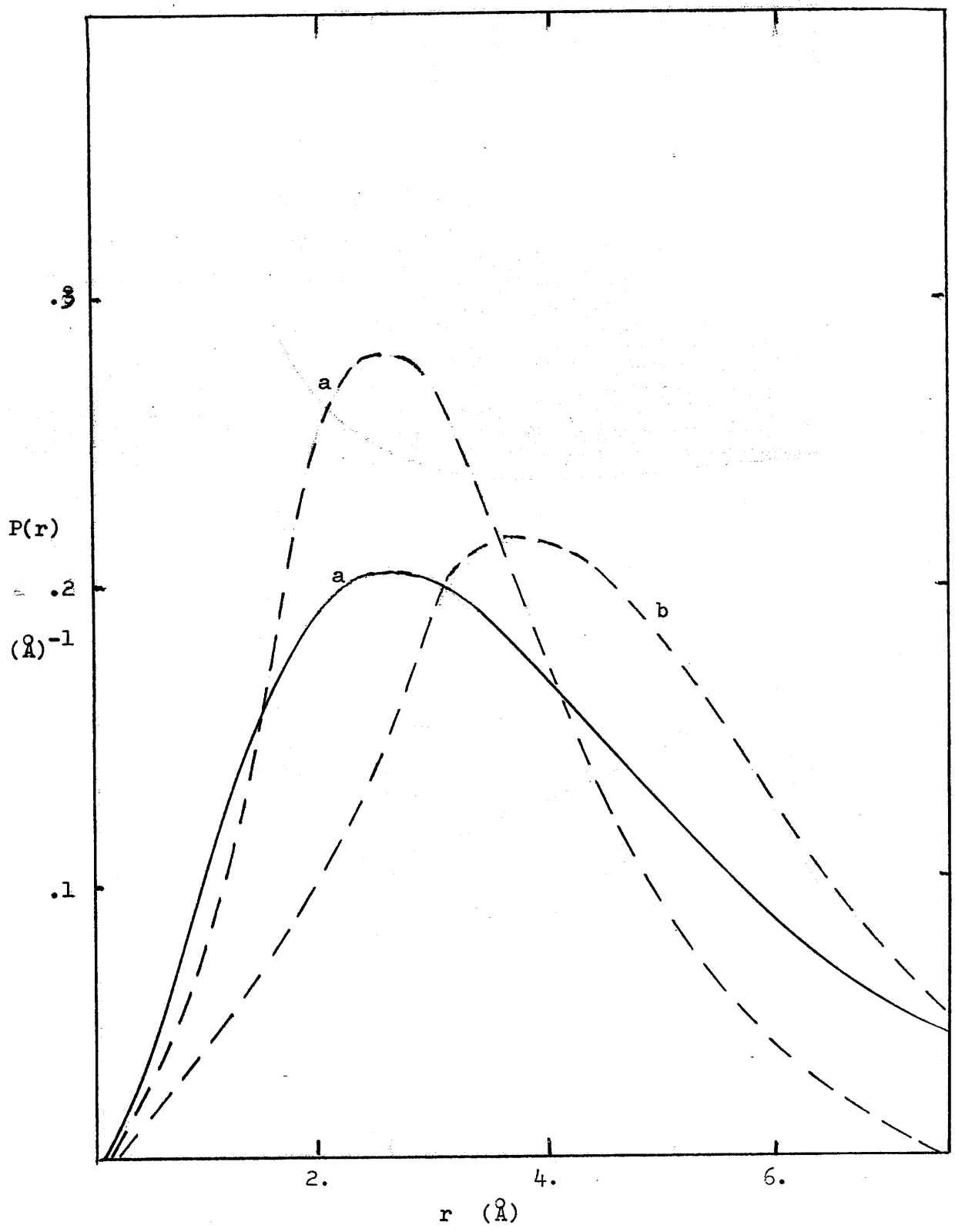

Figure III.10

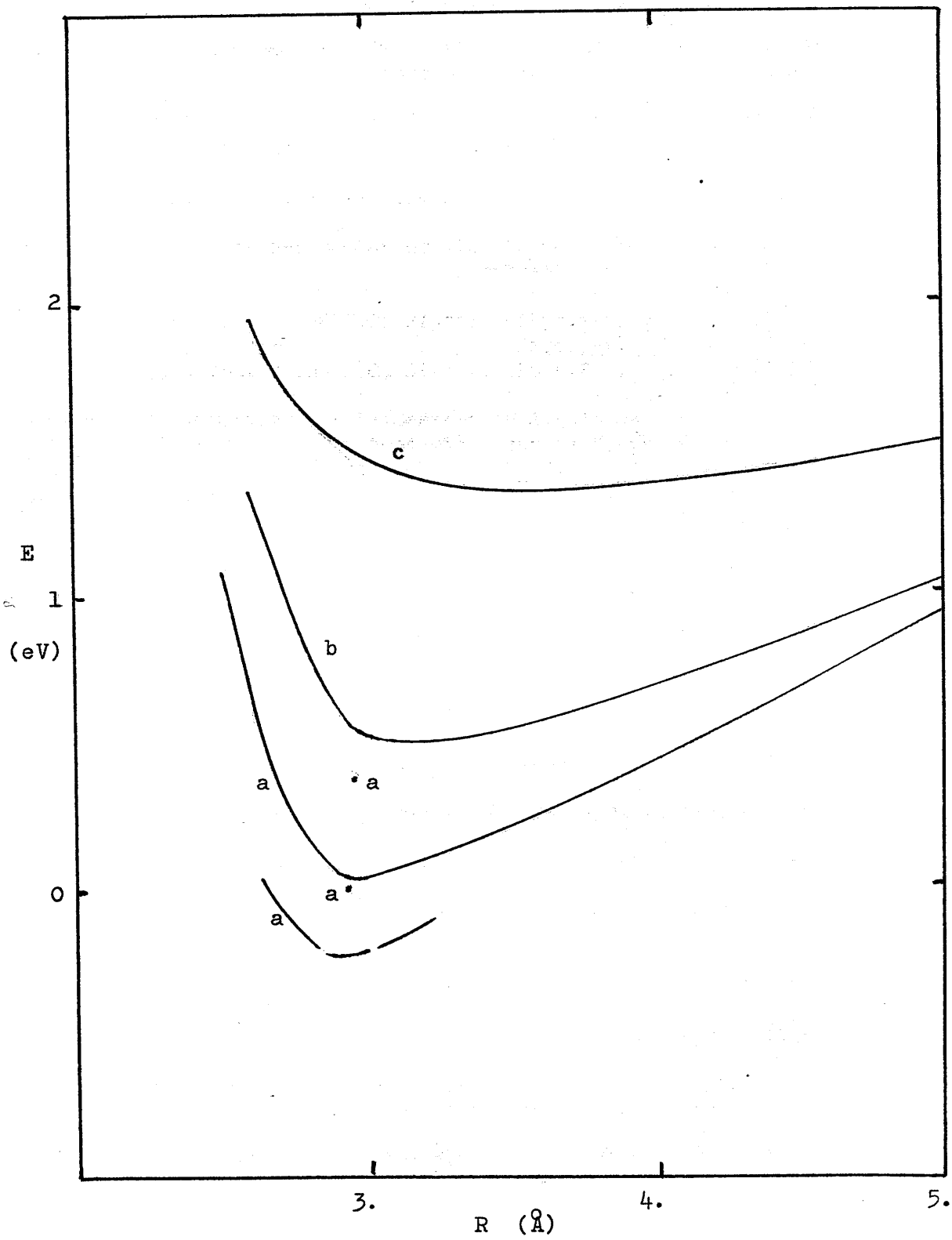

References

1. F. Seitz in "The Modern Theory of Solids", pp 470-473. McGraw-Hill, N.Y. (1940).

2. D.R. Hartree in "The Calculation of Atomic Structure", p 50. John Wiley and Sons, N.Y. (1957).

3. M. Born and K. Huang in "The Dynamical Theory of Crystal Lattices", p 166. Clarendon Press, Oxford (1954).

4. B.S. Gourary and F.J. Adrian, Solid State Physics 10, 12 (1960).

5. N.F. Mott and M. Gurney in "Electronic Processes in Ionic Crystals", p 81. O.U.P. London (1940).

6. G.F. Koster and J.C. Slater, Phys.Rev. 95, 1167 (1954),
G.F. Koster, Phys.Rev. 95, 1436 (1954),
G.F. Koster and J.C. Slater, Phys.Rev. 96, 1208 (1954).

7. J.J. Markham in "F-Centres in Alkali Halides", Academic Press, N.Y. (1966).

8. R.A. Smith in "Wave Mechanics of Crystalline Solids", p 348. Chapman and Hall, London (1961).

9. W. Kohn and J. Ouffroy, Phys.Rev. B8, 2485 (1973).

10. W. Kohn, Phys.Rev. B1, 4388 (1973).

11. J. des Cloizeaux, Phys.Rev. 135, A685, A698 (1964).

12. W.B. Fowler, Phys.Rev. 135, A1725 (1964).

13. W. Jost, J.Chem.Phys. 1,466 (1933).

14. N.F. Mott and M.J. Littleton, Trans.Farad.Soc. 34, 485 (1938).

15. E.S. Rittner, R.A. Hunter and F.K. du Pre, J.Chem.Phys. 17, 198 (1948),
F.K. du Pre, R.A. Hunter and E.S. Rittner, J.Chem.Phys. 18, 379 (1949).

16. W. Gebhardt and H. Kuhnert, Phys.Status Solidi 14, 157 (1966).

17. J.D. Zahrt and S.H. Lin, Theo.Chim.Acta. 12, 256 (1968).

18. J.J. Markham in "F-Centres in Alkali Halides", p 316. Academic Press, N.Y. (1966).

19. S.R. Tibbs, Trans.Farad.Soc. 35, 1471 (1939).

20. J.H. Simpson, Proc.Roy.Soc. A197, 269 (1949).

21. J.A. Krumhansl and N. Schwartz, Phys.Rev. 89, 1154 (1953).

22. D.L. Dexter, Phys.Rev. 83, 435 (1951),
" 93, 244 (1954).

23. J.A. Krumhansl, Phys.Rev. 93, 245 (1954).

24. W. Gebhardt and H. Kuhnert, Phys.Lett. 11, 15 (1964).

25. K. Lehovec, Phys.Rev. 92, 253 (1953).

26. R.K. Swank and F.C. Brown, Phys.Rev. 130, 34 (1963).

27. W.A. Smith, A.E.C. rept. KAPL-1720 (1957).

28. H.F. Ivey, Phys.Rev. 72, 341 (1947).

29. P. Podini and G. Spinolo, Solid State Comm. 4, 263 (1966).

30. D.Y. Smith and G. Spinolo, Phys.Rev. 140, A2121 (1965).

31. H.S. Bennett, Phys.Rev. 169, 729 (1968).

32. I.M. Boswarva and A.B. Lidiard, Phil.Mag. (1968).

33. M.P. Tosi, Solid State Physics 16, 52 (1964).

34. H.S. Bennett, Phys.Rev. B3, 2763 (1971).

35. Y. Toyozawa, Prog.Theor.Phys. (Kyoto) 12, 422 (1954).

36. R.F. Wood and U. Opik, Phys.Rev. 179, 783 (1969).

37. R.F. Wood and H.W. Joy, Phys.Rev. 136, A451 (1964).

38. S.-F. Wang, Phys.Rev. 132, 573 (1963),
" 153, 939 (1967).

39. R.K. Swank and F.C. Brown, Phys.Rev.Lett. 8, 10 (1962).

40. E.U. Condon and G.H. Shortley in "The Theory of Atomic Spectra", p 98. Cambridge Univ. Press (1970) - reprint.

41. M. Lax, J.Chem.Phys. 20, 1752 (1952).

42. R.H. Silsbee, Phys.Rev. 138, A180 (1965).

43. D. Pines in "Polarons and Excitons" eds. G.G. Kuper and G.D. Whitfield. Oliver and Boyd (1963) p 33.

44. "Physics of Color Centers" ed. W.B. Fowler. Academic Press, N.Y. (1968).

45. W.B. Fowler and D.L. Dexter, Phys.Rev. 128, 2154 (1962).

46. L.F. Stiles et al., Phys.Rev. B2, 2077 (1970).

47. H. Watts and G.A. Noble, J.Chem.Phys. 40, 2051 (1964).

48. W.B. Fowler, E. Calabrese and D.Y. Smith, Solid State Comm. 5, 569 (1967).

49. J.C. Kemp, Phys.Rev. 171, 1024 (1968).

50. P. Feltham and I. Anders, Phys.Stat.Solidi 10, 203 (1965).

51. G. Feher, Phys.Rev. 103, 834 (1956),
" 105, 1122 (1957).

52. J.H. de Boer, Rec.Trav.Chim. 56, 301 (1937).

53. J.M. Worlock and S.P.S. Porto, Phys.Rev.Lett. 15, 697 (1965).

54. S. Radhakrishna and H.K. Sehgal, Phys.Lett. 29A, 286 (1969).

55. E.J. Hart and J.W. Boag, J.Amer.Chem.Soc. 84, 4090 (1962).

56. E.J. Hart and M. Anbar in "The Hydrated Electron"
Wiley Interscience, N.Y. (1970).

57. W.C. Gottschull and E.J. Hart, J.Phys.Chem. 71, 2102 (1967).

58. E.M. Fielden and E.J. Hart, Rad.Res. 32, 564 (1967).

59. R.R. Hentz and D.W. Brazier, J.Chem.Phys. 54, 2777 (1971).

60. R.R. Hentz, Farhataziz and E.M. Hansen, J.Chem.Phys. 55, 4974 (1971).

61. M.G. Robinson, K.N. Jha and G.R.Freeman, J.Chem.Phys. 55,4953 (1971).

62. R.D. Hentz, Farhataziz and E.M. Hansen, J.Chem.Phys. 57, 2959 (1972).

63. B.D. Michael, E.J. Hart and K. Schmidt, J.Phys.Chem. 75, 2798 (1971).

64. J.W. Hunt and J.K. Thomas, Rad.Res. 32, 149 (1967).

65. M.J. Bronskill, R.K. Wolff and J.W. Hunt, J.Phys.Chem. 73, 1175 (1969).

66. M.J. Bronskill, R.K. Wolff and J.W. Hunt, J.Chem.Phys. 53, 4201 (1970).

67. G.A. Kenney-Wallace and P.C. Walker, J.Chem.Phys. 55, 447 (1971).

68. J.M. Baxendale, Rad.Res.Suppl. 4, 139 (1964).

69. K. Schmidt and S. Anbar, J.Phys.Chem. 73, 2846 (1969).

70. "Solutions Metal-Ammoniac" eds. G. Lepoutre and M.J. Sienko
Benjamin, N.Y. (1964).

71. "Metal-Ammonia Solutions" eds. J.J. Lagowski and M.J. Sienko
Butterworths, London (1970).

72. "Electrons in Fluids" eds. J. Jortner and N.R. Kestner
Springer-Verlag, Berlin (1973).

73. R.R. Dewald and J.H. Roberts, J.Phys.Chem. 72, 4224 (1968).

74. J.J. Lagowski in ref. 72, p 32.

75. R. Catterall in ref. 71, p 105.

76. M.H. Cohen and J.C. Thompson, Adv.Phys. 17, 857 (1968).

77. R.K. Quinn and J.J. Lagowski, J.Phys.Chem. 73, 2326 (1969).

78. R.C. Douthit and J.L. Dye, J.Amer.Chem.Soc. 82, 4472 (1960).

79. H. Blades and J.W. Hodgkins, Can.J.Chem. 33, 411 (1955).

80. Farhataziz, L.M. Perkey and R.R. Hentz, J.Chem.Phys. 60, 4383 (1974).

81. S.A. Al'tshuler and B.M. Kozyrev in "Electron Paramagnetic Resonance", Acad.Press, N.Y. (1964).

82. D.E. O'Reilly, J.Chem.Phys. 50, 5378 (1969).

83. C.A. Hutchinson and D.E. O'Reilly, J.Chem.Phys. 52, 4400 (1970).

84. B.L. Smith and W.H. Koelher in ref. 72 p 139.

85. P.F. Rusch and J.J. Lagowski in ref. 72 p 169.

86. J. Jortner, J.Chem.Phys. 30, 839 (1959).

87. G.V. Teal, Phys,Rev. 71, 138 (1948).

88. P. Delahay, J.Chem.Phys. 55, 4188 (1971).

89. K. Eiben and I.A. Taub, Nature 212, 1002 (1966).

90. O.F. Khodzhaev, B.G. Ershov and A.K. Pikaev, Izv.Akad.Nauk. SSSR. Otd.Khim.Nauk. 246 (1968).

91. I.A. Taub and K. Eiben, J.Chem.Phys. 49, 2499 (1968).

92. K. Kawabata, J.Chem.Phys. 55, 3672 (1971).

93. K. Kawabata, S. Okabe and S. Taniguchi, J.Chem.Phys. 57, 2855 (1972).

94. H. Hase and L. Kevan, J.Chem.Phys. 54, 908 (1971).

95. I. Eisele and L. Kevan, J.Chem.Phys. 53, 1867 (1970).

96. I. Eisele, R. Lapele and L. Kevan, J.Amer.Chem.Soc. 91, 6504 (1969).

97. R.A. Ogg, J.Amer.Chem.Soc. 68, 155 (1940),
J.Chem.Phys. 14, 114,295 (1946),
Phys.rev. 69, 243,668 (1946).

98. W.N. Lipscomb, J.Chem.Phys. 21, 52 (1953).

99. R.A. Stairs, J.Chem.Phys. 27, 1431 (1957).

100. S. Pekar, J.Phys.(USSR) 10, 341,347 (1946).

101. S. Pekar and M.F. Diegen, Zh.Eksp.Teor.Fiz. 18, 481 (1948).

102. L. Landau, Sov.Phys. 3, 664 (1933).
A.C. Davydov, Zh.Eksp.Teor.Fiz. 18, 913 (1948).

103. J. Jortner, J.Chem.Phys. 30, 839 (1959).

104. M.D. Newton, J.Chem.Phys. 58, 5833 (1973).

105. D.E. O'Reilly, J.Chem.Phys. 41, 3736 (1964).

106. R.H. Land and D.E. O'Reilly, J.Chem.Phys. 46, 4496 (1967).

107. M. Tachiya, J.Chem.Phys. 56 6269 (1972).

108. J. Jortner, Mol.Phys. 5, 257 (1962).

109. J. Jortner, Rad,Res.Suppl. 4, 24 (1964).

110. K. Fueki, D.-F. Feng and L. Kevan, Chem.Phys.Lett. 4, 313 (1969).

111. M. tachiya, Y. Tabata and K. Oshima, J.Phys.Chem. 77, 263, 2286 (1973).

112. B. Raz and J.Jortner in ref. 72 p 413.

113. R.A. Holroyd and M.J. Allen, J.Chem.Phys. 54, 5014 (1971).

114. B.E. Springett, M.H. cohen and J. Jortner, Phys.Rev. 159, 183 (1967).

115. B.E. Springett, M.H. Cohen and J. Jortner, J.Chem.Phys. 48, 2720 (1968).

116. J. Jortner and N.R. Kestner in ref. 71 p 49.

117. E.J. Hart and M. Anbar in ref. 56 p 60.

118. P.F. Rusch, W.H. Koelher and J.J. Lagowski in ref. 71 p 41.

119. J. Jortner in "The Radiation Chemistry of Aqueous Systems" ed. G. Stein.

120. P.S. Julienne and L.P.Gary, Mol.Cryst. 5, 135 (1968).

121. R.P. Auty and R.H. Cole, J.Chem.Phys. 20, 1309 (1952).

122. K. Fueki, D.-F. Feng and L. Kevan, Chem.Phys.Lett. 4, 313 (1969).

123. J. Jortner in "Modern Quantum Chemistry" ed. O. Sinanoglu Acad.Press. N.Y. (1965) Part II p 91.

124. K Huang and A. Rhys, Proc.Roy.Soc.(London) 204A, 406 (1950).

125. R.R. Dogonadze and A.A. Kornyshev, Phys.Stat.Sol. 53, 439 (1972)
" 55, 843 (1973).

126. J. Jortner and N.R. Kestner in ref, 71 p 49.

127. D.A. Copeland, N.R. Kestner and J. Jortner, J.Chem.Phys. 53, 1189 (1970).

128. P. Langevin, Ann,Chim.Phys. 5, 70 (1905).

129. K. Iguchi, J.Chem.Phys. 48, 1735 (1967).

130. N.R. Kesner and J. Jortner, J.Phys.Chem. 77, 1040 (1973).

131. K. Fueki, D.-F. Feng and L. Kevan, J.Chem.Phys. 56, 5351 (1972).
" J.Chem.Phys. 57, 1253 (1972)
" J,Amer.Chem.Soc. 95, 1398 (1973).

132. A.D. Buckingham, Disc.Farad.Soc. 24, 151 (1957).

133. J. Jortner, J.Chem.Phys. 57, 5452 (1972).

134. D. Eisenberg and W. Kauzmann in "The Structure and Properties of Water" p 46. O.U.P. London (1968).

135. B. Kamb, J.Chem.Phys. 43, 3917 (1965).

136. J. Jortner and A. Gaathon in ref. 72. p429.

137. Y. Toyozawa in "Dynamical Processes in Solid-State Optics", ed. R. Kubo. Benjamin, N.Y. (1969).

138. F.E. Williams and M.H. Hebb, Phys.Rev. 84, 1181 (1951).

139. U. Schindewolf in ref. 71. p 199.

140. Inter.Crit.Tables Vol. 3 ,p 23. McGraw-Hill, N.Y. (1933).

141. "Handbook of Chemistry and Physics" ed. R.C. Weast, 50th ed. C.R.C. (1969).

142. H.H. Landolt and R. Bornstein in "Atom und Moleculer Physik", p 509. Springer-Verlag, Berlin (1950).

143. G. Nemethy and H.A. Scheraga, J.Chem.Phys. 36, 3382 (1962).

144. N.H. Fletcher in "The Chemical of Ice", C.U.P., London (1970).

145. J. Logan and N.R. Kestner, J.Phys,Chem. 76, 2738 (1972).

146. N.R. Kestner, J. Jortner and A. Gaathon, Chem.Phys.Lett. 19, 328 (1973).

147. B.C. Webster and G. Howat, Rad.Res.Rev. 4, 259 (1972).

148. L. Kevan, D.R. Renneke and R.J. Friauf, Solid State Comm. 6, 469 (1968).

149. J. Zimbrick and L. Kevan, J.Amer.Chem.Soc. 89, 2483 (1967).

150. N. Basco, G.A. Kenney-Wallace and D.C. Walker, Chem.Comm. 917 (1969).

151. N. Basco, G.A. Kenney-Wallace, S.K. Vidyarthi and D.C. Walker, Can.J.Chem. 50, 2059 (1972).

153. M. Gold, W.L. Jolly and K.S. Pitzer, J.Amer.Chem.Soc. 84, 2264 (1962).

152. R. Catteral and M.R.C. Symons, J.Chem.Soc. A, 13 (1966).

154. W.H. Koehler and J.J. Lagowski, J.Phys.Chem. 73, 2329 (1969).

155. G. Rubinstein, T.R. Tuttle and S. Golden, J.Phys.Chem. 77, 2872 (1973).

156. T.R. Tuttle, G.Rubinstein and S. Golden, J.Chem.Phys. 44, 3791 (1966).

157. L. Onsager, Rev.Mod.Phys. 40, 710 (1968).

158. J.L. Dye in ref. 71, p 1.

159. U. Schindewolf, Angew.Chem. 81, 190 (1968).

160. S. Freed and N. Sugarman, J.Chem.Phys. 11, 354 (1947).

161. T.L. Hill, J.Chem.Phys. 16, 394 (1948).

162. D.E. O'Reilly, J.Chem.Phys. 55, 474 (1971).

163. K. Fueki, J.Chem.Phys. 50, 5381 (1969).

164. K. Fueki and S. Noda in ref 71, p 19.

165. N.R. Kestner and D.A. Copeland in ref. 71, p 27.

166. N.R. Kestner and D.A. Copeland, J.Chem.Phys. 58, 3500 (1973).

167. D.-F. Feng, K. Fueki and L. Kevan, J.Chem.Phys. 58, 3281 (1973).

168. C.G. Barraclough and J.R. Mooney, J.Chem.Phys. 54, 35 (1971).

169. V. McKoy and N.W. Winter, J.Chem.Phys. 48, 5514 (1968).

170. N.W. Winter and V. McKoy, Phys.Rev. A2, 2219 (1970).

171. F.W. Byron and C.J. Joachain, Phys.Rev. 157, 1 (1967).

172. C. Schwartz, Phys. Rev. 126, 1015 (1962).

173. Y. Accad, C.L. Pekeris and B. Schiff, Phys.Rev. A4, 516 (1971).

174. C.L. Pekeris, Phys.Rev. 127, 509 (1962).

175. N.W. Winter, V. McKoy and A. Laferriere, Chem.Phys.Lett. 6, 175 (1970).

176. U. Schindewolf, R. Vogelsgesang and K.W. Boddeker, Angew.Chem. 79, 1064 (1967).

177. N.E. Dorsey in "Properties of Ordinary Water Substance in All Its Phases", p 485. Rheinhold, N.Y. (1940).

178. R.R. Hentz, Farhataziz and D.J. Milner, J.Chem.Phys. 47, 5381 (1967).

179. U. Schindewolf, Adv.Chem.Ser. 81, 598 (1968).

180. M.H. Alexander and R.G. Gordon, J.Chem.Phys. 56, 3823 (1972).

181. W.E. Rudge, Phys.Rev. 181, 1020 (1968).

182. F.W. deWette and B.R.A. Nijboer, Physica 24, 1105 (1959).

183. R.F. Stewart, Mol.Phys. 24, 879 (1972).

184. L. Richardson and J. Gaunt, Phil.Trans.Roy.Soc. A226, 299 (1927).

Appendix A

Numerical Methods.

In each model potential studied, both on the semicontinuum and polarized cavity approximation levels and for both one- and two-electron species, the assumption of spherical symmetry results in the necessary solution of a wholly radial Schrodinger equation for the system. The general equation to be solved is thus

$$Du = Eu$$

where D involves a different operator, second order with respect to the radial coordinate,r. An iterative technique was selected for the solution of such a second order differential equation. A trial function u_o was guessed which differed from the correct function by an amount c_o thus

$$(D-E)\, c_o = -(D-E)\, u_o. \qquad (1)$$

A finite-difference representation was chosen to approximate derivative term, the operator being written in a simple three-point formula. Solving (1) for c_o,however, requires a knowledge of the exact eigenvalue E. This difficulty was overcome by introducing the Rayleigh mean, (2), at each cycle

$$E_{RM} = (u|D|u) \,/\, (u|u). \qquad (2)$$

The tridiagonal matrix resulting on the discretization of the differential operator in D by the three-point approximation formula was efficiently solved by a diagonal condensation technique[181] to give the correction c_o. Cycling was continued till the eigenfunctions obtained in adjacent passes did not differ by more than one part in 10^{-4}.

In general, it was found that a linear scale was unsatisfactory, especially for diffuse functions. A transformation to a "square-root" grid was thus effected in all cases.

In the solution of adiabatic potential problems strip-sizes of

100(100)500 were employed and accurate functions obtained by Richardson extrapolation[184]. In the scf treatments a similar extrapolation technique was utilized but the calculations were generally performed over strips of 300(100)500. In part, this was necessitated by the increased computational time required in the scf calculations where many convergence difficulties were encountered. Especially in the two-electron work. These were overcome by application of the Aitken δ^2-process which usually provided considerable enhancement in the convergence rate and was able to stabilize oscillatory solutions.

In calculations on two-electron species involving correlation a fourth-order difference formula was preferred

$$f''(r_o) = 1/12\ h^{-2}\ \ -f(r_o+2h) + 16f(r_o+h) - 30f(r_o) + 16f(r_o-h) - f(r_o-2h)$$

and strip-sizes of 150(50)300 were employed. Care was necessary at the boundaries and the simple expedient of switching to a second-order approximation was found to be adequate in this region.

Appendix B

Lattice Summations.

A relevant energy contribution to the medium reorganization work required to be performed on the bulk crystalline medium to accommodate the presence of an ionic defect and a surplus electron at a colour centre in a crystalline solid, is the change in electostatic energy developed when the nearest-neighbour cation moves in the background potential of the perfect point-ion lattice.

In Part I, this was expanded in a series in powers of the distortion, x, of the form

$$E_1 = -N/a\ (c_4x^4 + c_6x^6 + c_8x^8 + c_{10}x^{10} + \ldots)$$

The coefficients in this expansion are lattice sums, (1), over a perfect crystal structure excepting the missing anionic origin

$$S'_{l,m} = \sum'_j Y_{lm}(\theta_j, \phi_j) \exp(2\pi i q_j \underline{k}\, \underline{r}_j)\, r_j^{-l-1} \qquad (1)$$

Here, $Y_{l,m}$ is the usual normalized spherical harmonic, q_j is the charge on the j^{th} ion located at the point $\underline{r}_j = (r_j, \theta_j, \phi_j)$ in the direct lattice, and $\underline{k}$ is the vector of the reciprocal lattice given by

$$\underline{k} = \tfrac{1}{2}\underline{b}_1 - \tfrac{1}{2}\underline{b}_2 - \tfrac{1}{2}\underline{b}_3 .$$

The b's form the basis of the reciprocal lattice. The dash indicates that the point in the origin is omitted, and the inclusion of the exponential modulation term is just a functional way of depicting a set of discrete point charges.

A method of obtaining such sums as (1) was sought which would be both quickly convergent and readily programmable. Since the values relevant to two crystal structures only were desired, the latter need was strongly emphasized. The generalized Ewald θ-function technique[181] was discarded as being too highly sophisticated for the limited use required here and an alternative approach was adopted.

As usual the main difficulty with such infinite summations over arrays of point charges is their extremely slow convergence. In an effort to remedy this in some simple fashion (1) was transformed formally into an integral, utilizing the properties of the δ-function, which was split into two parts by the introduction of a damping function and its complement. The accelerating function chosen must be such that as its argument tends to infinity it tends to zero rapidly. Rapid convergence of the first component was thus assumed. The second term was transformed into reciprocal space where the first few terms of the infinite summation resulting on performing the integration were sufficient to provide fast accurate convergence. It was later discovered that this method was identical to a technique extensively studied by de Wette and Nijboer[182] and that their choice of an accelerating function, the incomplete gamma function, proved much more successful than the attempts investigated here. The error function and a sort of truncated Langevin function, 1- L(x), were employed. Since their choice of function also provided more readily performed integrals it was adopted here along with their treatment of the general lattice sums required. The method will not be detailed here, Table B1 merely lists the evaluated summations for reference.

Table B1

n	c_n(NaCl)	c_n(CaF_2)
4	3.578 582	1.846 871
6	0.989 499	0.573 329
8	2.942 159	3.259 293
10	1.010 713	1.009 224

Publication

A Numerical Study of the Continuum Model for Solvated Electrons.

Ian Carmichael and Brian Webster, J.Chem.Soc. Farad.Trans. (in press).